Structure-Function Studies of GABA-C receptor ligands

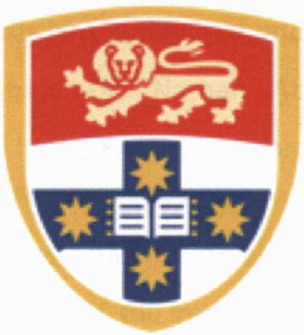

A thesis submitted for the fulfilment of the degree of
Doctor of Philosophy
Faculty of Pharmacy
The University of Sydney
Australia

Izumi Yamamoto

B.Sc. (Hons) *in* Pharmacology
University College London
United Kingdom

March 2012

Certificate of authorship and originality

The work described in this thesis was conducted under the supervision of Prof. Mary Chebib, A/Prof. Jane Hanrahan, Dr. Nathan Absalom and Dr. Jane Carland (Department of Pharmacology) in the Faculty of Pharmacy, The University of Sydney.

I certify that the work in this thesis has not previously been submitted for a degree nor has it been submitted as part of the requirements for a degree. In addition, I certify that all the information sources and literature used are indicated in the thesis.

Izumi Yamamoto
March 2012

Acknowledgements

It is with a great honor and joy that I use this opportunity to express my gratitude to Mary, Jane, Nathan and Jane; my supervisors as without them this thesis would not have been possible.

Mary, you provided an environment that allowed me to explore freely, while offering me guidance when required. I am grateful for the opportunity to be a part of your group and your continuous support throughout my PhD. Nathan and Jane, thank you for your valuable inputs in our research projects and for your constant encouragement to work in the lab. Nathan, your passion in research truly inspired me. Thank you for teaching me Science as well as Aussie sports terminologies during recordings (Cricket, Doggie Racing, Aussie Football etc...). Jane and Graham, your generous sharing of your knowledge in Medicinal Chemistry was valuable to complete this thesis. Our collaborators, David, Muni and Luke, working with you were priceless experience; thank you. The generous support from Mrs Dorothy Lamberton for providing 'John A Lamberton Scholarship' was greatly appreciated.

I am thankful for all my colleagues I met during my PhD; Elena, Taima, Tin, Hye-lim, Steve, Navnath (Suraj?), Gracia, Nasiara, Petrine, Tim, Katherine, Irene, Maja, Jetta, Ida, Clarissa, Michael, Alice, Gigi, Kelvin, Dyvia, Aileen, Petra, Ho-Joon, Laura, Nhu, Emilie, Steven, Chow, Andrew, Kathy and Thi Cam. I learnt a lot from you all, I wish all the best in the future. I am also grateful to Thomas's group; Thomas, Peta, Meryem, Rose, Prasad, Vishy and Otto for their help in the tissue culture room.

I also gained valuable friendships with Postdocs and people I shared the office with (S201); Melanie, Petra, Tristan, Angelina, Maryem and Shery. You guys made my university life exciting and fun!

A special thank you to Melanie, Taima, Petra, Elena, Tristan, Hye-lim, Tin, and Steve for their encouragements during my PhD and helping to format this thesis. You guys have been great listeners and I appreciate all the laughter we had together.

I am grateful to my family for their support to complete this degree. Mum, Dad, my grandfather Shinzaburo and Auntie Keiko; thank you very much for your support and have trust in me as always. Without you, my study abroad would not have been possible, and I cannot thank you enough for the amazing experiences I had during my studies. I would also like to send a special gratitude to my step-grandfather Karl and my late grandmothers, Motoko and Midori who always encouraged me to pursue my dream and passion.

I would like to thank my friends for their support and encouragement throughout my PhD. A special thank you to my first Aussie flat mate, Ali for welcoming me to the flat in Glebe. Whenever I had to make big decisions, I trusted my "gut" feelings. Still, as much my decision to live in Australia felt right, I felt nervous about it. In my first week in Sydney, I met Ali. I still remember her warm welcome to the flat when we met for the first time, which released my worriment. And now she is my life coach, and a very dear friend of mine! Thank you Ali for listening, guiding and supporting me at any time, wherever you are in the world. I also want to acknowledge UCL Pharmaholiday buddies for their support to initiate my PhD in Sydney. Eranthi, Diggie, Jon, Kaday and Jo, thank you for your encouragements and I always felt your continuous support from the other side of the world. Kaday, you were always enthusiastic about your future, which inspired me to pursue my own. I am always looking forward to hearing everyone's next steps of life, however, it seems impossible that there are no more steps for you. You have gone too soon, we miss you Xx.

Moving from UK to Australia was a huge adventure. It was challenging at times but I followed my decision to the end, cherishing every moment with my colleagues and friends here in Australia. So I thank you all again for being a part of my journey. Now I am ready to embark on a new journey again.

Lastly, thank you Australia for sharing your beautiful nature and fantastic food.

No worries, mate!

Table of contents

List of figures

List of tables

Abbreviations

Abbreviations	Full Name
(±)-ACPAM	(±)-4-aminocyclopent-1-enecarboxamide
5-HT_{3A} receptor	Serotonin type 3A receptor, 5-hydroxytryptamine type 3A receptor
ACh	Acetylcholine
AChBP	Acetylcholine-binding protein
ACPBPA	(Aminocyclopentanyl)butylphosphinic acid
(+)-4-ACPCA	(+)-4-aminocyclopent-1-ene-1-carboxylic acid
3-APMPA	3-Aminopropyl(methyl)phosphinic acid
3-APA	3-Aminopropylphosphonic acid
3-APPA	3-Aminopropylphosphinic acid
BSA	Bovine serum albumin
CACA	*cis*-4-Aminocrotonic acid
CAMP	*cis*-(aminomethyl)cyclopropanoic acid
cDNA	Complementary deoxyribonucleic acid
cRNA	Complementary ribonucleic acid
CGP36742/ SGS-742	3-Aminopropyl-*n*-butylphosphinic acid
CGP44532	*S*-(3-amino-2-hydroxypropyl)methylphosphinic acid
CGP44533	*R*-(3-amino-2-hydroxypropyl)methylphosphinic acid
Cl^- channel	Chloride channel
CNS	Central nervous system
C-terminal	Carboxy terminal
DAVA	5-Aminovaleric acid
dNTP	Deoxynucleotide triphosphate
DMSO	Dimethyl sulfoxide
EC_{50}	Agonist concentration that elicits 50% maximum response or antagonist concentration that inhibits 50% spontaneous current
E. coli	*Escherichia coli*
ELIC	*Erwinia chrysanthem* proton-gated ion channel
3F-GABA	3-fluoro-γ-aminobutyric acid
G-protein	GTP-binding protein
GABA	γ-Aminobutyric acid
$GABA_A$ receptor	γ-Aminobutyric acid-A receptor
$GABA_B$ receptor	γ-Aminobutyric acid-B receptor
$GABA_C$ receptor	γ-Aminobutyric acid-C receptor
GB1	$GABA_B$ receptor subunit 1

GB1a	$GABA_B$ receptor subunit 1, splice variant a
GB1b	$GABA_B$ receptor subunit 1, splice variant b
GB2	$GABA_B$ receptor subunit 2
GABOB	γ-Amino-β-hydroxybutyric acid
Gabazine or SR-95531	6-Imino-3-(4-methoxyphenyl)-1(6*H*)-pyridazinebutanoic acid
4-GBA	4-guanidinobutanoic acid
GIRK	G-protein-coupled inwardly-rectifying potassium channels
GLIC	*Gloebacter violaceus* proton-gated ion channel
GluCl	Glutamate-gated chloride channel
3-GOHP	3-[guanidine]-1-oxo-1-hydroxy-phospholane
GPCR	G-protein-coupled receptor
GDP	Guanine dinucleotide phosphate
GTP	Guanine trinucleotide phosphate
Gly	Glycine
HEK-293	Cell line 293 human embryonic kidney cells
HEPES	4-(2-Hydroxyethyl)-1-piperazineethanesulfonic acid
I4AA	Imidazole-4-acetic acid
IC_{50}	Antagonist concentration that inhibits 50% maximum response
I_M or I_{MAX}	Maximum current response
I/I_M	Intrinsic efficacy, percent maximum GABA response
K_B	Dissociation equilibrium constant for antagonist
LGIC	Ligand-gated ion channel
MA stretch	Membrane associated stretch
M1 domain	First transmembrane domain
M2 domain	Second transmembrane domain
M2 domain	Third transmembrane domain
M2 domain	Fourth transmembrane domain
M1-M2 loop	Intracellular loop between the first and second transmembrane domain
M3-M4 loop	Intracellular loop between the third and fourth transmembrane domain
2-MeTACA	*trans*-4-Amino-2-methylbut-2-enoic acid
nACh	Nicotinic acetylcholine
ND96	Frog ringer buffer
n_H	Hill coefficient
N-terminal	Amino terminal
OR2	Oocyte releasing buffer2
PCR	Polymerase chain reaction
REFER	Rate-equilibrium free energy relationship

SCAM	Substituted-cysteine accessibility methods
SEM	Standard error of the mean
TACA	*trans*-4-Aminocrotonic acid
THIP	4,5,6,7-Tetrahydroisoxazole[4,5-c]pyridine-3-ol
TPMPA	(1,2,5,6-Tetrahydropyridine-4-yl)methylphosphinic acid
ρ_1F124	ρ_1 Subunit with phenylalanine at the position 124
ρ_1F124X	ρ_1 Subunit with phenylalanine at the position 124 mutated to amino acid X
ρ_1T244	ρ_1 Subunit with threonine at the position 244
ρ_1T244X	ρ_1 Subunit with threonine at the position 244 mutated to amino acid X
ρ_1Y102	ρ_1 Subunit with tyrosine at the position 102
ρ_1Y102X	ρ_1 Subunit with tyrosine at the position 102 mutated to amino acid X
VFT	Venus flytrap
VCF	Voltage-clamp fluorometry
ZAPA	(*Z*)-3-[(aminoiminomethyl)thio] prop-2-enoic acid

Journal Publications and Conference Presentations

Journal Publications

Gavande N, Yamamoto I, Salam NK, Ai T-H, Burden PM, Johnston GAR, Hanrahan JR and Chebib M 'Novel cyclic phosphinic acids as $GABA_C$ ρ receptor antagonists: design, synthesis and pharmacology' *ACS Medicinal Chemistry Letters*, 2011, **2**, 11-16

Ng CL, Kim H-L, Gavande N, Yamamoto I, Kumar RJ, Mewett KN, Johnston GA, Hanrahan JR and Chebib M 'Medicinal chemistry of ρ $GABA_C$ receptors' *Future Medicinal Chemistry*, 2011, **3**, 197-209

Yamamoto I, Deniau GP, Gavande N, Chebib M, Johnston GAR and O'Hagan D 'Agonist responses of (*R*)- and (*S*)-3-fluoro-γ-aminobutyric acids suggest an enantiomeric fold for GABA binding to $GABA_C$ receptors' *Chemical Communication (Cambridge)*, 2011, **47**, 7956-7958

Yamamoto I, Jordan MJT, Gavande N, Doddareddy MR, Chebib M and Hunter L 'The enantiomers of *syn*-2,3-difluoro-4-aminobutyric acid elicit opposite responses at the $GABA_C$ receptor' *Chemical Communication (Cambridge)*, 2011, **48**, 829-931

Yamamoto I, Carland JE, Locock K, Gavande N, Absalom N, Hanrahan JR, Allan RD, Johnston GAR and Chebib M 'Structurally diverse GABA antagonists interact differently with open and closed conformational states of the ρ_1 $GABA_C$ receptor' *ACS Chemical Neuroscience*, 2012, DOI: 10.1021/cn200121r

Yamamoto I, Absalom N, Carland JE, Doddareddy MR, Gavande N, Johnston GAR, Hanrahan JR and Chebib M 'Differentiating enantioselective actions of GABOB: A possible role for threonine 244 in the binding site of $GABA_C$ ρ_1 receptors' *ACS Chemical Neuroscience*, 2012, DOI: 10.1021/cn3000229

Conference Presentations

Yamamoto I, Gavande N, Carland JE, Johnston GAR, Hanrahan JR, Chebib M 'The effect of novel gabazine analogues on GABA receptors' 45th Australian Society of Clinical and Experimental Pharmacologists and Toxicologists (ASCEPT) Annual Scientific Meeting, Perth, Australia, 4-9 December 2011

Yamamoto I, Gavande N, Carland JE, Johnston GAR, Hanrahan JR and Chebib M 'Threonine 244 determines the pharmacology of *S*- and *R*-GABOB at GABA *rho*$_1$ receptors' 41st Annual Meeting of the Society for Neuroscience, Washington, DC, USA 12-16 November 2011

Yamamoto I, Carland JE, Johnston GAR, Hanrahan JR and Chebib M 'Threonine 244 determines the pharmacology of (*R*)- and (*S*)-GABOB at $GABA_C$ *rho*$_1$ receptors' Gage Ion Channels & Transporters Conference, Canberra, Australia 18-20 April 2011

Yamamoto I, Gavande N, Absalom NL, Locock K, Mewette KN, Johnston GAR, Hanrahan, JR and Chebib M 'Interaction of $GABA_C$ antagonists with constitutively active receptors' Australian Neuroscience Scociety (ANS) Conference, Auckland, New Zealand 29 January - 1 February 2011

Yamamoto I, Carland JE, Habashy D, Abdel-Halim H, Absalom NL, Hanrahan JR and Chebib M 'Phenylalanine 124 at ρ_1 $GABA_C$ receptors influences the on-off rates for GABA' 43rd Australian Society of Clinical and Experimental Pharmacologists and Toxicologists (ASCEPT) Annual Scientific Meeting, Sydney, Australia, 29 November – 2 December 2009

Abstract

Throughout the central nervous system (CNS), the Cys-loop superfamily of ligand-gated ion channels (LGICs), including nicotinic acetylcholine, serotonin type-3A, strychnine-sensitive glycine and γ-aminobutyric acid A/C receptors, play important roles in synaptic transmission by converting chemical signals into electric signals. Designing potent and subtype-selective ligands with therapeutic value requires knowledge about how ligands interact with their binding sites.

γ-Aminobutyric acid (GABA) is the predominant inhibitory neurotransmitter in the mammalian CNS and its binding modes at GABA receptors have not been fully elucidated. $GABA_C$ receptors consist of ρ subunits (ρ_1-ρ_3) and they are known to form homomeric receptors. The five subunits are arranged around a central chloride selective ion channel pore. Each subunit contains a large extracellular N-terminal domain, four transmembrane domains (M1-M4) of which the second (M2) lines the channel pore and a large M3-M4 intracellular loop. The orthosteric binding site is located at the interface between two subunits in the N-terminal domain and the key residues for ligand binding are found at the five discontinuous loops (A-E).

This thesis describes how ligand binding and receptor gating are closely related and explores the effect of receptor conformational changes upon ligand binding. A series of point mutations in the N-terminal domain of the $GABA_C$ ρ_1 receptor were created and expressed in *Xenopus* oocytes. The mutant receptors were then examined using a range of pharmacological tools to probe function which was measured using the two-electrode voltage clamp method.

The GABA binding mode was explored at GABA receptors using the enantiomers of 3-fluoro-γ-aminobutyric acid (3F-GABA) and stereoisomers of 2,3-difluoro-4-aminobutyric acids as conformational probes. Both enantiomers of 3F-GABA were full agonists, with the *R*-3F-GABA being approximately 3-fold more potent than *S*-3F-GABA at $GABA_C$ receptors. In contrast, both enantiomers were partial agonists with similar efficacy and potency at $GABA_A$ receptors. These results suggest a

different GABA binding mode at $GABA_C$ receptors to that found in the related but pharmacologically distinct $GABA_A$ receptors. The effect of the different stereoisomers of 2,3-difluoro-4-aminobutyric acids were also examined at $GABA_A$, $GABA_B$ and $GABA_C$ receptors. In the study, two enantiomeric $GABA_C$ receptor ligands were identified, one of which is an agonist (2*S*,3*S*-2,3-difluoro-4-aminobutyric acid) while the other is an antagonist (2*R*,3*R*-2,3-difluoro-4-aminobutyric acid).

4-Amino-3-hydroxybutanoic acid (GABOB) is an endogenous ligand found in the CNS in mammals and a metabolite of GABA. Homology modeling of the $GABA_C$ ρ_1 receptor revealed a potential hydrogen (H-bond) interaction between the hydroxyl group of GABOB and threonine 244 (T244) located on loop C of the ligand binding site. Using site-directed mutagenesis, the effect of mutating T244 on the efficacy and pharmacology of GABOB and various ligands were examined. It was found that mutating T244 to amino acids that lacked a hydroxyl group in the side chain produced GABA insensitive receptors. Only by mutating ρ_1T244 to serine (ρ_1T244S) produced a GABA responsive receptor, albeit 39-fold less sensitive to GABA than ρ_1 wild-type. It was also found that this mutation also changed the activity of $GABA_C$ receptor partial agonists, muscimol and imidazole-4-acetic acid (I4AA). At the concentrations tested, both muscimol and I4AA antagonized the currents produced by GABA at ρ_1T244S mutant receptors (Muscimol: $\rho_1$wild-type, EC_{50} = 1.4 μM; ρ_1T244S, IC_{50} = 32.8 μM. I4AA: ρ_1 wild-type, EC_{50} = 8.6 μM; ρ_1T244S, IC_{50} = 21.4 μM). This indicates that T244 is predominantly involved in channel gating.

R-(–)-GABOB and *S*-(+)-GABOB are full agonists at ρ_1 wild-type receptors. In contrast, *R*-(–)-GABOB was a weak partial agonist at ρ_1T244S (1mM activates 26 % of the current produced by GABA EC_{50} versus ρ_1 wild-type, EC_{50} = 19 μM; I_{max} 100%), and *S*-(+)-GABOB was a competitive antagonist at ρ_1T244S receptors (ρ_1 wild-type, EC_{50} = 45 μM versus ρ_1T244S, IC_{50} = 417.4 μM, K_B = 204 μM). This highlights that the interaction of GABOB with T244 is enantioselective.

In contrast, the potencies of a range of antagonists tested, 3-aminopropyl(methyl)phosphinic acid (3-APMPA), 3-aminopropylphosphonic acid (3-

APA), *S*- and *R*-(3-amino-2-hydroxypropyl)methylphosphinic acid (*S*-(–)-CGP44532 and *R*-(+)-CGP44533), were not altered. This suggests that T244 is not critical for antagonist binding. Receptor gating is dynamic and this study highlights the role of loop C in agonist-evoked receptor activation, coupling agonist binding to channel gating.

Ligands acting on receptors are considered to induce a conformational change within the ligand-binding site by interacting with specific amino acids. In this study, tyrosine 102 (Y102) located in the GABA binding site of the ρ_1 subunit of the $GABA_C$ receptor was mutated to alanine (ρ_1Y102A), serine (ρ_1Y102S) and cysteine (ρ_1Y102C) to assess the role of this amino acid plays on the action of 12 known and 2 novel antagonists. Of the mutated receptors, ρ_1Y102S was constitutively active providing an opportunity to assess the activity of the antagonists on ρ_1 receptors with a proportion of receptors existing in the open conformational state compared to those existing predominantly in the closed conformational state (ρ_1 wild-type, ρ_1Y102C and ρ_1Y102A).

It was found that the majority of antagonists studied were able to inhibit the constitutive activity displayed by ρ_1Y102S, thus displaying inverse agonist activity. The exception was (±)-4-aminocyclopent-1-enecarboxamide ((±)-4-ACPAM) not exhibiting any inverse agonist activity, but acting explicitly on the closed conformational state of ρ_1 receptors.

It was also found that GABA antagonists were more potent at the closed compared to the open conformational states of ρ_1 receptors suggesting that they may act by stabilizing the closed conformational state and thus reducing activation by agonists. Furthermore, of the antagonists tested, Y102 was found to have the greatest influence on the antagonist activity of gabazine (SR-95531) and its analogue (SR-95813).

Our $GABA_C$ ρ_1 receptor homology model identified a novel cavity, which extended beyond the GABA binding site. The model predicted phenylalanine 124

(F124), one of the residues lining the cavity, was pointing towards the orthosteric binding site. In this study, F124 was mutated to various amino acids and only a modest effect on receptor pharmacology was observed. However, the mutations had a significant effect on the channel deactivation rate ($\tau_{Deactivation}$). This finding suggests that F124 may play a role in channel gating or stabilizing the open conformation of the receptor.

Designing potent selective agents are the key for the further understanding of the physiological roles of $GABA_C$ receptors. Gabazine (SR-95531) is a potent $GABA_A$ receptor competitive antagonist. In this study, a series of novel gabazine analogues were tested at $GABA_A$ and $GABA_C$ receptors. Of the compounds studied, (*p*)-methoxy analogue without the butyric acid side-chain was 20-fold more potent at $GABA_C$ over $GABA_A$ receptors. As there was no butyric acid side chain, it is suggested that the carboxylic acid is not important for gabazine activity at this receptor. Establishing the structure-activity relationship based on this analogue will facilitate the development of selective $GABA_C$ receptor antagonists with possible physiological effects including memory-enhancement.

Overall, our studies describe agonist and $GABA_C$ receptor antagonist induced conformational changes within the ligand binding site. Our findings also highlight the dynamic nature of receptor gating, initiated by ligand binding at a site physically distinct from the ion channel.

Chapter 1:

Receptor Structure and Function

Chapter 1: Receptor Structure and Function

1.1 Ligand-gated ion channels

In the central nervous system (CNS), the main inter-cellular communication is mediated by chemical signalling molecules, such as neurotransmitters. An imbalance between excitatory and inhibitory neurotransmissions leads to disorders of brain function. There are two classes of pharmacologically important cell-surface receptors for neurotransmission, the ligand-gated ion channels (LGICs), and the G-protein-coupled receptors (GPCRs). LGICs are also known as ionotropic receptors and they are oligomeric transmembrane proteins containing an ion channel pore. The classification of LGICs is determined by their pharmacological profiles and subunit structures.

1.2 Cys-loop LGICs

One of the LGIC superfamilies, the Cys-loop LGIC superfamily plays key roles in chemical synapses by converting chemical signals into electric signals throughout the nervous system. The interaction of neurotransmitter leads to the channel opening allowing ions to move across the membrane. The Cys-loop family includes nicotinic acetylcholine (nACh), serotonin type-3A (5-HT_{3A}), strychnine-sensitive glycine (Gly) and γ-aminobutyric acid A/C ($GABA_{A/C}$) receptors and invertebrate glutamate-gated chloride channels (GluCl) (Corringer *et al.*, 2010; Hilf *et al.*, 2009a; Miller *et al.*, 2010; Thompson *et al.*, 2010).

1.2.1 Receptor structure

Amongst the Cys-loop family, the structure of nACh receptors has been characterized in most detail. Early electron diffraction studies using the electric organ of *Torpedo Marmorata,* where nACh receptors are highly expressed, revealed a pentameric quaternary structure of the receptors (Unwin, 1993). Other experimental evidence confirms that all members of the family have an identical quaternary

pentameric structure (Chang *et al.*, 1996; Langosch *et al.*, 1988; Nayeem *et al.*, 1994). The schematic representation of how the five subunits are assembled is shown in Figure 1.1. A single subunit structure contains, a large extracellular N-terminal domain, four hydrophobic transmembrane domains (M1-M4) where M2 is known to form the channel pore, and a large cytoplasmic M3-M4 loop domain.

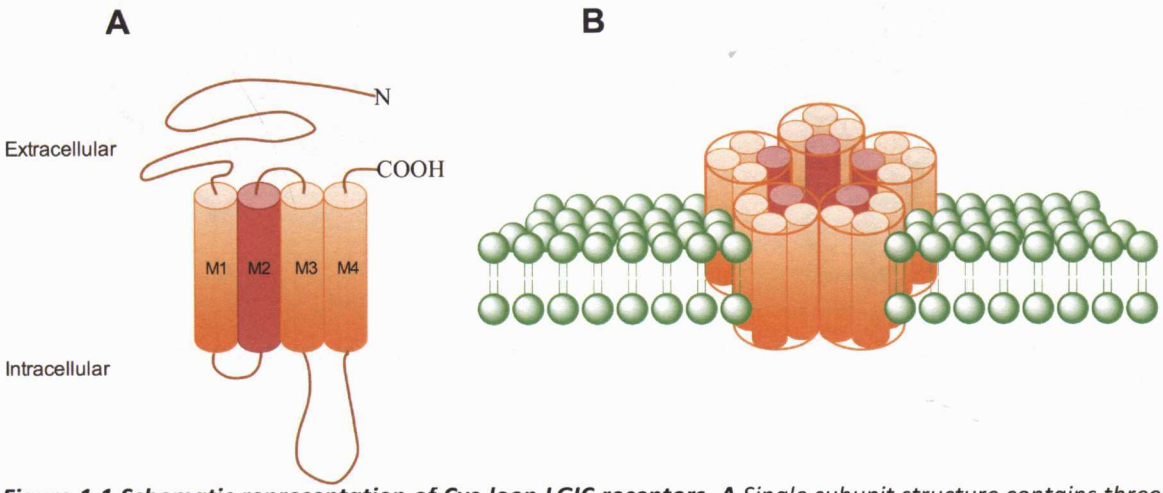

Figure 1.1 Schematic representation of Cys-loop LGIC receptors. A *Single subunit structure contains three main domains, a large extracellular N-terminal domain, four hydrophobic transmembrane domains labeled M1-M4, M2 in red forming the lining of channel wall, and a large cytoplasmic loop domain between M3 and M4.* ***B*** *Five subunits assembled to form a channel through plasma membranes.*

1.2.2 Receptor structure and function

As expected from their sequence similarities, all members of the Cys-loop family share similar tertiary and identical quaternary hetero- or homo-pentameric structures (Ortells *et al.*, 1995) (Figure 1.2). Functional, biochemical and electrophysiological evidence suggests that there are three main steps involved in chemical to electrical signal transduction: neurostansmitter binding, coupling between the binding site and the channel, and channel gating. In Cys-loop LGICs, agonist binding induces conformational changes in the N-terminal domain, and then transmits the signal *via* the coupling region to gate the ion-selective pore (Figure 1.3) (Unwin, 2005).

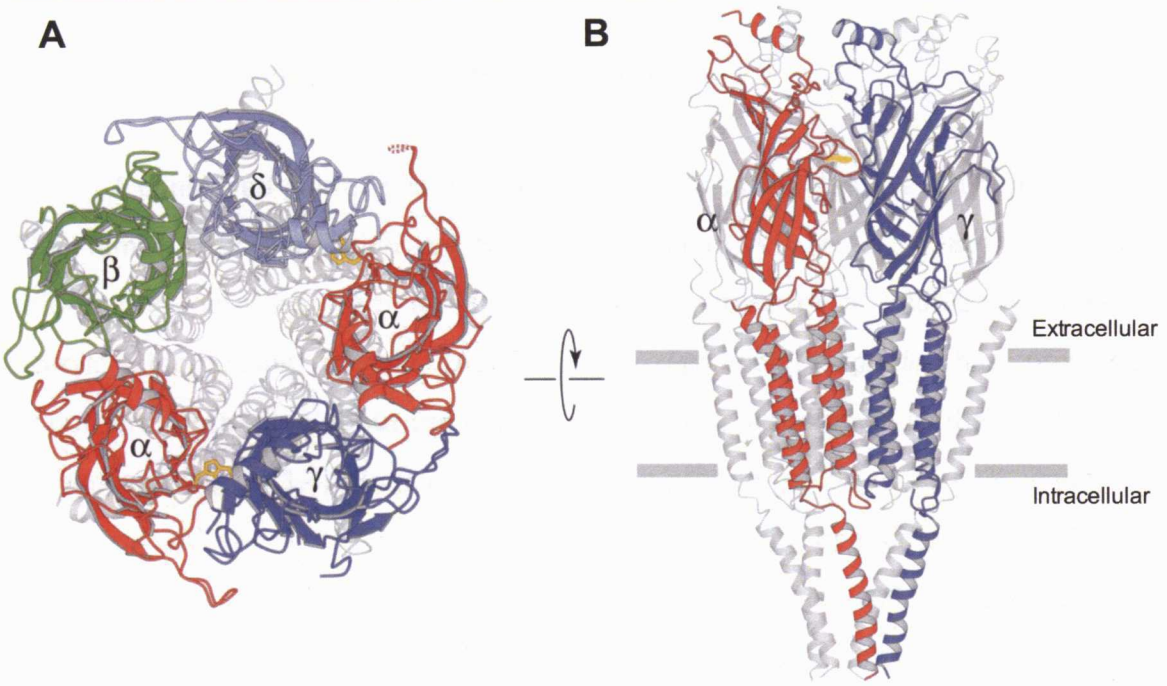

Figure 1.2 Quaternary structure of nACh receptor from Torpedo Mamorata. A *Top view of the quaternary structure. The orthosteric ligand binding site is located between the two ring structures.* ***B*** *View of the quaternary structure parallel with the membrane plane. Figure adapted from reference (Unwin, 2005).*

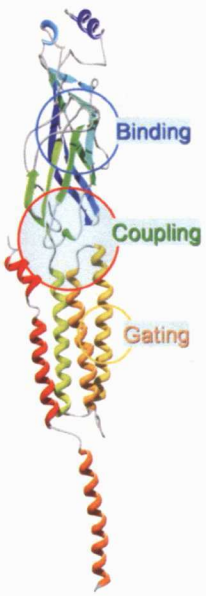

Figure 1.3 Ribbon diagram of a single subunit. *Important functional domains are highlighted; N-terminal domain in blue, forming the orthosteric binding site. Transmembrane domains in yellow, forming the gating machinery. The multiple loops between the two domains in green, forming the coupling region. Figure is the homology model of the human α_7 nACh receptor subunit, adapted from reference (Zhang et al., 2011).*

1.2.2.1 *Extracellular-N-terminal domain*

A conserved pair of cysteine residues, which is the signature structure in Cys-loop family, is found within the N-terminal domain (Kao *et al.*, 1986). Structural information obtained from an X-ray crystal structure of a soluble pentameric acetylcholine-binding protein (AChBP) from *Lymnaea stagnalis* has provided important information about the binding site for ACh, also known as the orthosteric binding site (Figure 1.4) (Brejc *et al.*, 2001). The protein has up to 15-24% sequence homology with the N-terminal of Cys-loop receptor family. For example, the nACh α_7 receptor subunit exhibits 24% sequence homology (Brejc *et al.*, 2001). The AChBP has the ability to bind to known nACh receptor agonists and antagonists, revealing information about the orthosteric ligand binding site. The binding site is located at the interface between two subunits, where one subunit contributes to the principal and the other contributes to the complementary side of the binding site (Figure 1.4) (Smit *et al.*, 2001). The key residues for ligand binding at the orthosteric binding site are formed by six discontinuous loops termed loops A-F. Loops A-C are from the principal subunit, and loops D-F are from the complementary subunit (Figure 1.5).

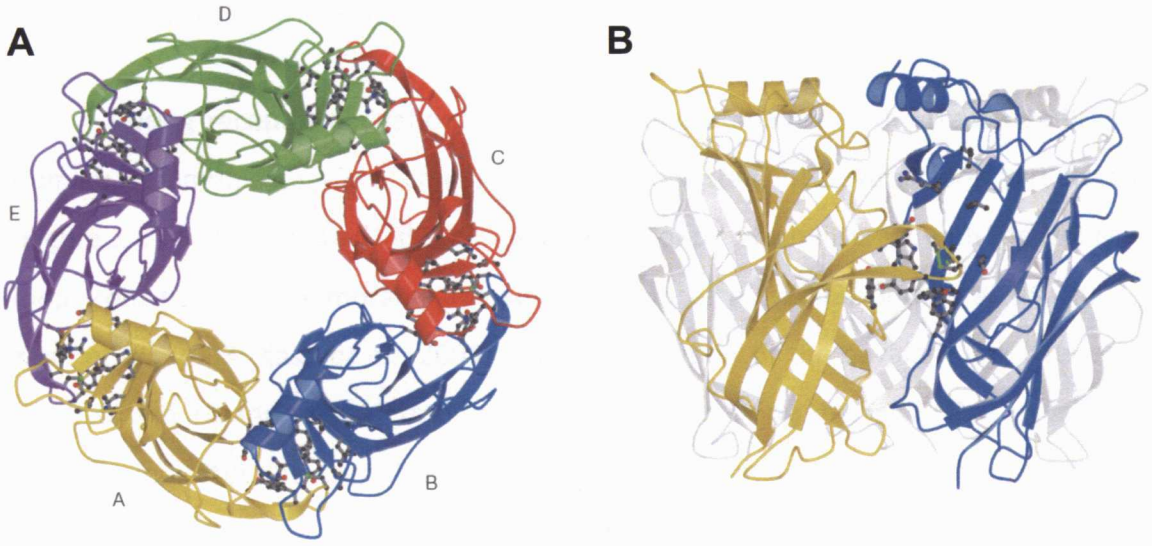

Figure 1.4 Ribbon diagram of AChBP. A *Top view of pentameric structure of AChBP.* ***B*** *Side view of AChBP showing orthosteric ligand binding site formed between two domains: yellow, principle subunit; blue, complementary subunit. Model adapted from reference (Brejc et al., 2001).*

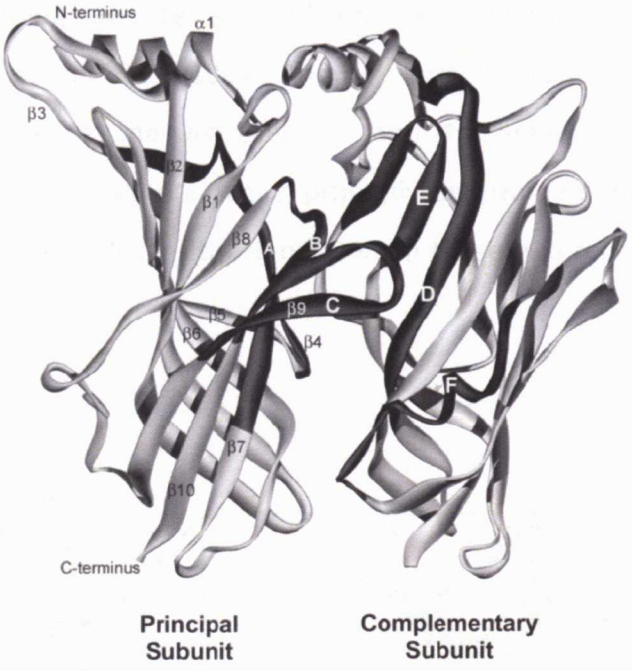

Figure 1.5 Ribbon diagram of AChBP, showing the principal and complementary subunits forming ligand binding site. *The principle subunits account for loops A-C and loops D-F are formed by the complementary subunit. Figure adapted from reference (Thompson et al., 2010).*

1.2.2.2 Coupling region

During receptor activation, the extracellular domain and the transmembrane domain communicate *via* a coupling region, consisting of several loop structures (Figure 1.6), including the β1-β2, Cys- and β8-β9 loops which interact with the M2-M3 loop from the transmembrane domain (Absalom *et al.*, 2003; Bouzat *et al.*, 2004; Kash *et al.*, 2003; Kash *et al.*, 2004). The investigation of the covalent link between the β-strand 10 and pre-M1 transmembrane domain using the rat $GABA_A$ α_1 and β_2 subunits indicates the contribution of this region in agonist induced channel gating (Mercado *et al.*, 2006). The recent work of Bouzat and co-workers, who applied the electrical fingerprinting strategy using the α_7-5-HT_{3A} chimeric receptors, provided us with new insights into the function of the coupling region during Cys-loop receptor activation (Andersen *et al.*, 2011; Bouzat, 2011; Bouzat *et al.*, 2008; Bouzat *et al.*, 2004; Rayes *et al.*, 2009). They identified three loops in the AChBP, which were the

links between the binding site interface and transmembrane domains that mediate the coupling process (Bouzat *et al.*, 2004). Another study found structural differences at the interface between the extracellular and transmembrane domains of homomeric α_7 and 5-HT_{3A} receptors, which primarily determine differences in open-channel lifetime and rate of desensitization between these two receptors (Bouzat *et al.*, 2008).

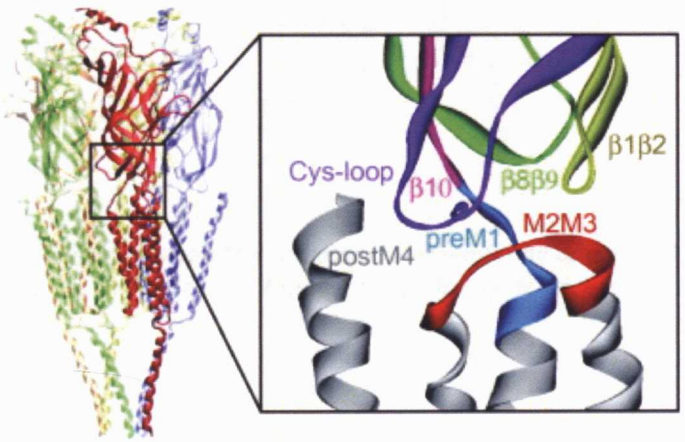

Figure 1.6 Structure of the coupling region. *Ribbon diagram of Torpedo nACh receptor, and a magnified window indicates the structures at the interface between extracellular and transmembrane domains. Each loop is color coded: yellow, β1-β2 loop; purple. Cys-loop; green, β8-β9 loop; pink, β-strand 10; blue, pre-M1 and red, M2-M3 loop. Figure adapted from reference (Bouzat, 2011).*

1.2.2.3 Four hydrophobic transmembrane domains (M1-M4)

Four membrane spanning α-helices in each subunit form the transmembrane domain of Cys-loop receptors. To date, the best available structural information of transmembrane domain comes from a 3.3 Å resolution X-ray crystal structure of the eukaryotic Cys-loop receptor, GluCl α from *Caenorhabditis elegans* (Hibbs *et al.*, 2011) and 4 Å resolution cryo-electron microscopy images from the nACh receptor from *Torpedo Marmorata* (Miyazawa *et al.*, 2003). Both structures agree that the α-helices from each subunit are arranged symmetrically with the five M2 helices lining

the channel pore, and M1, M3 and M4 helices stabilize the bundle arrangement (Figure 1.7).

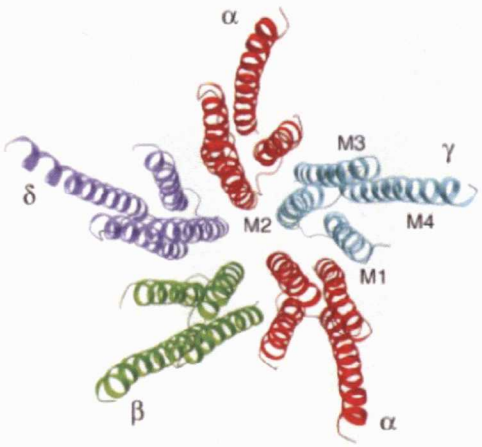

Figure 1.7 Structural arrangements of nACh receptor transmembrane domain (M1-M4). *Top view of the channel pore. M2 helices are lining the pore. Figure adapted from reference (Miyazawa et al., 2003).*

The channel pore structures differ between anion and cation selective receptors (Absalom *et al.*, 2009). When studying pore regions, the prime numbering system has been applied to compare M2 residues between family members, where lysine at position 242 of *Torpedo* nACh α_1 subunit is equivalent to the 0′ position. There is a conserved leucine residue (Leu 9′) and a flanking valine residue (Val 8′) in the middle of the helix. The anion selective channels mainly consist of polar residues, such as glycine, serine and threonine. In contrast, polar residues are clustered at the intracellular end of M2 at cation selective channels and the intracellular mouth has a net negative charge (Figure 1.8). Initially, it was reported that the ion selectivity of the channel was determined by three rings of charged amino acids in the M2 region of nACh receptors (Konno *et al.*, 1991). However, deletion of the proline residue (Pro-2′) located at the intracellular end of the M2 region in glycine α_1 receptors produced receptors with reduced anion selectivity and an increased pore diameter from 5.4 Å to 6.9 Å. This indicates that the size of channel pore is also important in ion selectivity (Lee *et al.*, 2003). Therefore, the ion selectivity at the M2 region is determined by

residue electrostatics at the selectivity filter region and the diameter of the channel pore (Keramidas *et al.*, 2004).

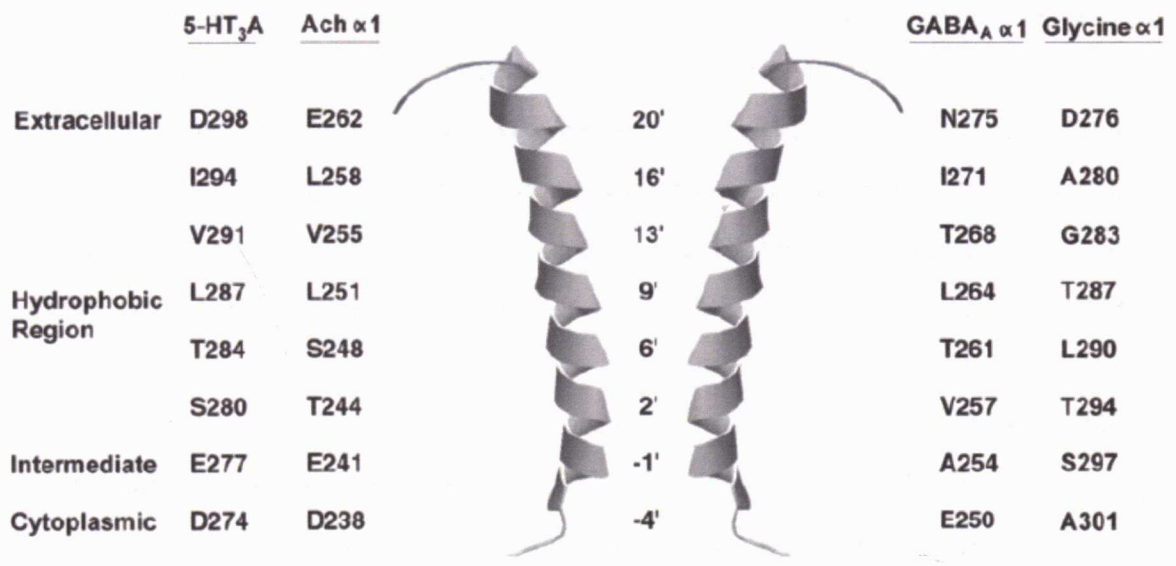

Figure 1.8 Residues in M2 terminal facing the water accessible surface. *Polar residues are found below conserved Leu 9´ at M2 helices of 5-HT$_{3A}$ and nACh α_1 subunits. At GABA$_A$ α_1 and glycine α_1 subunits, polar residues are found at entire length of M2 helices. Figure adapted from (Thompson et al., 2010).*

M1, M3 and M4 helices stabilizes the bundle arrangement (Figure 1.7). The outer ring which is in contact with the lipid bilayer, is formed by the M1 α-helix. Mutagenesis studies of the M1 α-helix demonstrated that these residues influence receptor desensitization, agonist efficacy and receptor assembly (Thompson *et al.*, 2010). Application of the substituted cysteine accessibility method (SCAM) at the intracellular end of GABA ρ_1 M1 α-helix and the M1-M2 loop found seven residues (A271, T272, L277, W279, V280, P290 and A291) were functionally modified by negatively charged sulfhydryl reagents and greater accessibility was achieved in the presence of agonist. This indicates that M1-M2 loop region is facing the ion permeation pathway and possibly influencing the ion selectivity of the channel (Filippova *et al.*, 2004).

M3 and M4 α-helices shield the M2 helix from the lipid environment (Figure 1.7) and mutation of these regions have significant effects on receptor function, such

as changes in whole-cell currents and single-channel kinetics of nACh and 5-HT_3 receptors (Thompson *et al.*, 2010). Recent studies provided experimental evidence suggesting that these regions also affect receptor expression. Serial deletions at the C-terminal and M4 α-helix of human $GABA_C$ ρ_1 receptors revealed that receptor functions are maintained up to a critical point, tryptophan (W) 475. Further deletion after W475 failed to form functional receptors, even though localization of the mutant receptors in the plasma membrane was observed (Reyes-Ruiz *et al.*, 2010). Mutation of C-terminal residues was also found to influence the cell surface expression of 5-HT_{3A} receptors (Butler *et al.*, 2009). Interestingly, non-assembly receptors, comprising the extracellular N-terminal domain and M1-M3 transmembrane domain, can be restored by co-expression with the M4 transmembrane α-helix (Haeger *et al.*, 2010; Villmann *et al.*, 2009). The evidence implies that the function of M3 and M4 α-helices may extend beyond simply stabilizing the bundle arrangement.

1.2.2.4 Cytoplasmic M3-M4 loop domain

There are passages (portals) for ions formed at the cytoplasmic domain in the nACh receptor, formed by amino acids located within the cytoplasmic M3-M4 loop domain, also known as the membrane associated (MA) stretch (Miyazawa *et al.*, 1999; Popot *et al.*, 1984) (Figure 1.9). The MA stretch at the majority of cation-selective subunits is lined by polar or negatively charged side chains, whereas anion selective subunits, such as GABA and glycine receptors, the MA stretch is lined by positively charged side chains (Peters *et al.*, 2010; Unwin, 2005). Recent studies using nACh and 5-HT_{3A} receptors have shown that the MA stretch is important for the interaction with intracellular proteins (Huebsch *et al.*, 2003; Jeanclos *et al.*, 2001), receptor targeting (Williams *et al.*, 1998) and channel conductance (Gee *et al.*, 2007; Hales *et al.*, 2006; Kelley *et al.*, 2003). In addition, there is experimental evidence suggesting that charged residues in the MA stretch in chloride-selective glycine α_1 receptors affect channel conductance (Carland *et al.*, 2009). One of the studies constructed a series of loop chimeras containing the cytoplasmic M3-M4 loop domain from different nACh receptor subunits (α_1-α_{10}, and β_1-β_4), to investigate the influence

of the domain on receptor assembly, surface expression and functional properties (Kracun *et al.*, 2008). The domain had no influence on the formation of subunit tertiary structures, however a significant influence on the formation of quaternary structures and cell surface expression was observed.

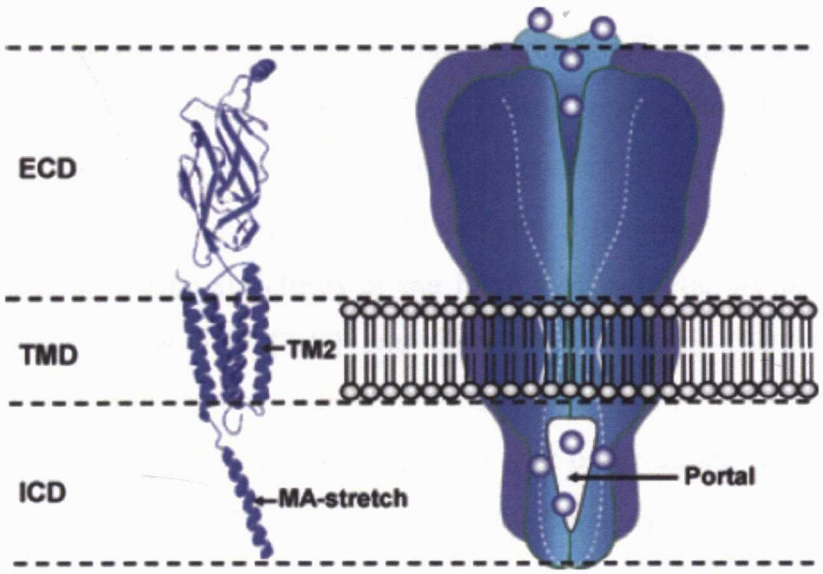

Figure 1.9 Schematic representation of Cys-loop family pentameric structure and the location of portal. *Left, ribbon diagram of a single subunit of human 5-HT_{3A} receptor. The channel lining transmembrane domain 2 (TM2) and MA-stretch are indicted. Right, Schematic representation showing the location of portal forming the permeation pathway in the receptor. Abbrebiations: ECD, extracellular domain; TMD, transmembrane domain; ICD, intracellular domain; MA, membrane-associated. Figure adapted from reference (Peters et al., 2010).*

1.2.3 Channel gating

To convert agonist binding into the channel gating, signals are mediated from the extracellular domain to the transmembrane domains *via* the coupling region, located at the interface between extracellular and transmembrane regions of Cys-loop receptors (Bouzat *et al.*, 2004). The understanding of how ligand binding initiates global conformational changes to activate a receptor is not fully understood due to the lack of X-ray crystal structures of either the open or closed conformational states of Cys-loop LGICs (Cederholm *et al.*, 2009). Nevertheless, the channel gating mechanism is probably "relatively" simple and interactions with low energy states are involved since the channel rapidly opens and closes in a reversible manner (Kash *et al.*, 2004). The X-ray crystal structures of the related prokaryotic proton-gated ion channels, *Erwinia chrysanthem* (ELIC) and *Gloebacter violaceus* (GLIC) represent closed and desensitized channel conformations (Figure 1.10), respectively. They provide information on structural rearrangements that occur during receptor gating (Hilf *et al.*, 2009a; Hilf *et al.*, 2009b; Hilf *et al.*, 2008). Recently, a crystal structure of the eukaryotic Cys-loop receptor, GluCl α from *Caenorhabditis elegans* has been reported (Hibbs *et al.*, 2011). The GluCl-Fab complex was co-crystalized with the allosteric agonist ivermectin and in additional with L-glutamate and the open-channel blocker picrotoxin. The open channel conformation was similar to the conformation found in GLIC.

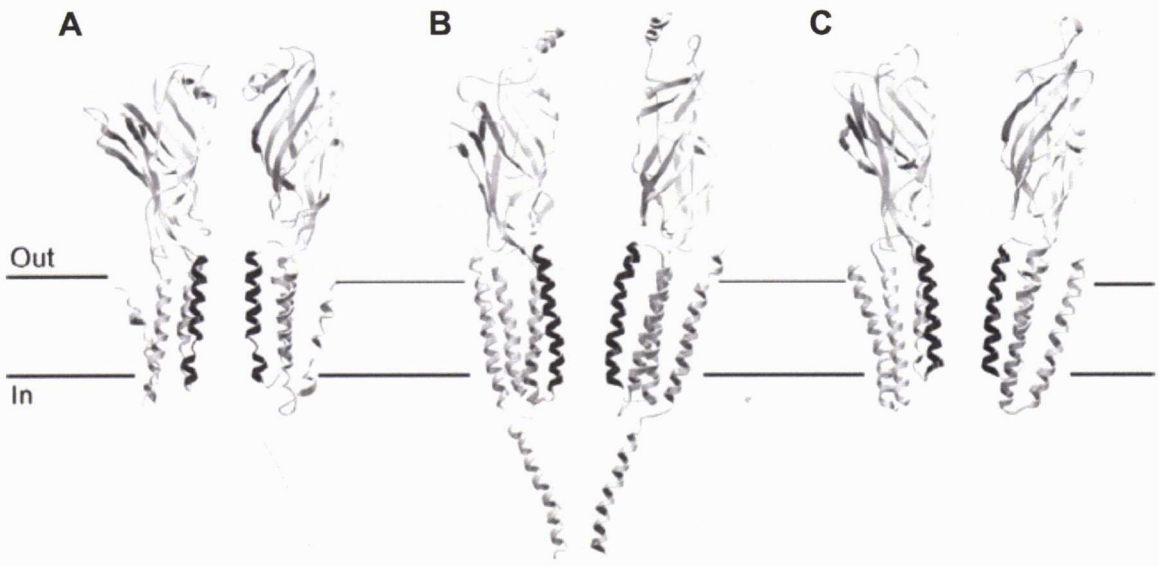

Figure 1.10 Comparison of structures. ***A*** *X-ray crystal structure from ELIC.* ***B*** *Electron micrograph structure from Torpedo marmorata.* ***C*** *X-ray crystal structure from GLIC. Figure adapted from reference (Absalom et al., 2009).*

The rate-equilibrium free energy relationships (REFER) approach has been widely used to analyze the sequence of conformational changes during nACh receptor channel gating (Chakrapani *et al.*, 2005; Chakrapani *et al.*, 2004; Chakrapani *et al.*, 2003; Cymes *et al.*, 2002; Grosman *et al.*, 2000a; Grosman *et al.*, 2000b; Jha *et al.*, 2007; Purohit *et al.*, 2007a; Purohit *et al.*, 2007c; Wang *et al.*, 2011; Zhou *et al.*, 2005). This method can characterize transition states of individual amino acids during channel gating by measuring single channel opening and closing rate constants of receptors with point mutations. The gating equilibrium constant is dependent upon the opening and closing rate constants. If the value of the gating equilibrium constant changes with the amino acid mutation, this implies that the opening and/or closing rate constants have been altered. The REFER method can determine which rate constant was altered. A REFER plot is a log-log plot of the closing rate constant versus the gating equilibrium constant and its slope is called ϕ. One interpretation, ϕ values give the relative timing of the movement of the amino acid residues during channel gating (Purohit *et al.*, 2007c). Higher values indicate that amino acid movement occurs earlier in a sequence of conformational changes, while similar values indicate that these amino acids move together. It was found that the sequence of

conformational changes that occur during gating can be divided into several clusters according to their ϕ values (Figure 1.11). This indicates that after agonist binding, the N-terminal domain moves in a stepwise manner before the channel opens. Combining information from studies using crystal structures and ϕ-value analysis gives great insights into how Cys-loop receptors work.

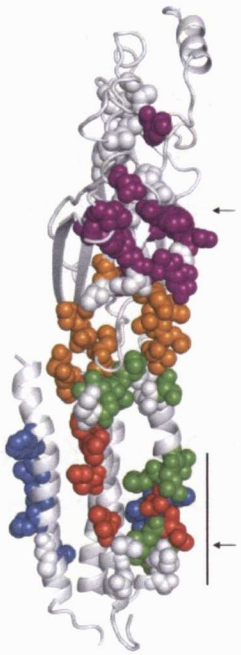

Figure 1.11 Map of ϕ-value in the nACh α subunit. *Residues with similar ϕ values are clustered, suggesting each cluster moves as a rigid body. Spheres represent the residues where ϕ value was measured and residues with similar ϕ-values are colour coded: purple, >0.90; orange, 0.75-0.85; green, 0.59-0.72; blue, 0.48-0.57; red, 0.26-0.35; white, no ϕ value. Upper and lower arrows indicate N-terminal and transmembrane domains. Figure adapted form reference (Purohit et al., 2007c).*

Kinetic studies of agonist induced channel gating reveals that there are three steps involved in receptor activation; agonist binding, sequential conformational change, and gating (Chang *et al.*, 2009). Traditionally, the relationship between agonist binding and receptor activation was explained by two equilibrium constants, the binding and gating constants (Del Castillo *et al.*, 1957). For the majority of Cys-loop receptors, at least two binding sites are required to initiate signal transduction from the extracellular domain before inducing conformational changes across the receptor to gate located within the M2 domain (Amin *et al.*, 1993). However, recent studies have shown that binding of a single agonist molecule is sufficient to activate

receptors (Andersen *et al.*, 2011; Jha *et al.*, 2010). The two constants, binding affinity and receptor gating, are coupled with mutual influence upon each other (Colquhoun, 1998). For example, the agonist binding affinity increased at the open conformation of $GABA_C$ ρ_1 receptors (Chang *et al.*, 1999). A new study comparing the effects of full and partial agonists on channel gating suggested that the coupling between binding and receptor gating was not a single step (Lape *et al.*, 2008). Instead, there was an intermediate state, termed the 'flip state', where a conformational change occurs at the ligand binding domain then leads to channel gating (Figure 1.12). This observation is supported by the findings from ϕ-value analysis (Purohit *et al.*, 2007c). Partial agonists were found to be less likely to induce the conformational change into the flip state, while the conformational changes for the flip to open state remain the same (Lape *et al.*, 2008).

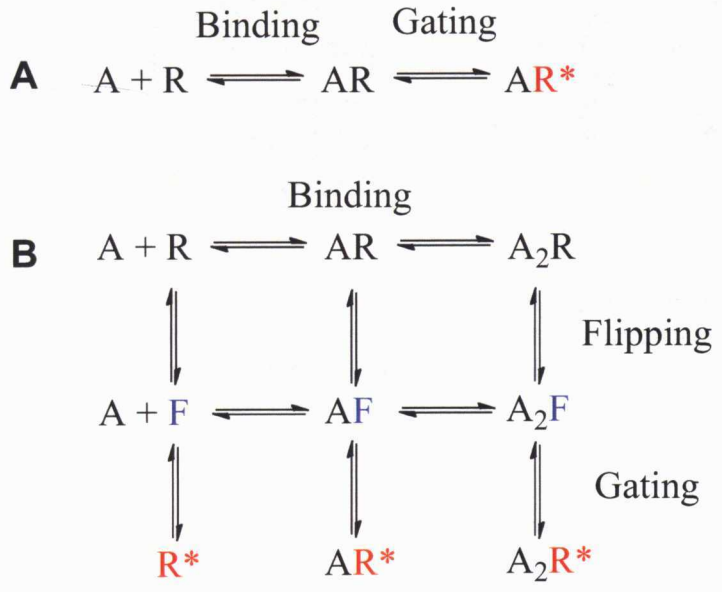

Figure 1.12 Activation Scheme. A *The del Castillo-Katz mechanism, adapted from reference (Del Castillo et al., 1957). Agonist (A) binds to a receptor (R). AR complex then isomerizes to open conformation (AR*).* ***B*** *Flip model with two binding steps, typical for all heteromeric Cys-loop receptors, adapted from reference (Lape et al., 2008). Flip state (F, AF or A_2F) represents the conformation entered after agonist binding (R, AR or A_2R) but before channel opening (R*, AR* or A_2R*).*

1.2.3.1 *Extracellular domain and gating*

Ligand binding induces a local conformational change at its binding site. Studies using AChBP crystal structures show that the binding of different ligands leads to different movements within the binding pocket (Celie *et al.*, 2004; Hansen *et al.*, 2005; Hibbs *et al.*, 2009). For example, structures of agonists and antagonists bound to *Aplysia* AChBP complexes revealed distinctive binding conformations (Hansen *et al.*, 2005). The binding of agonists evokes 'loop C closure', resulting in a constriction of the binding site, while antagonists push loop C away from the binding site (Figure 1.13). The conformational change in loop C appears to be one of the first steps that contributes to channel gating.

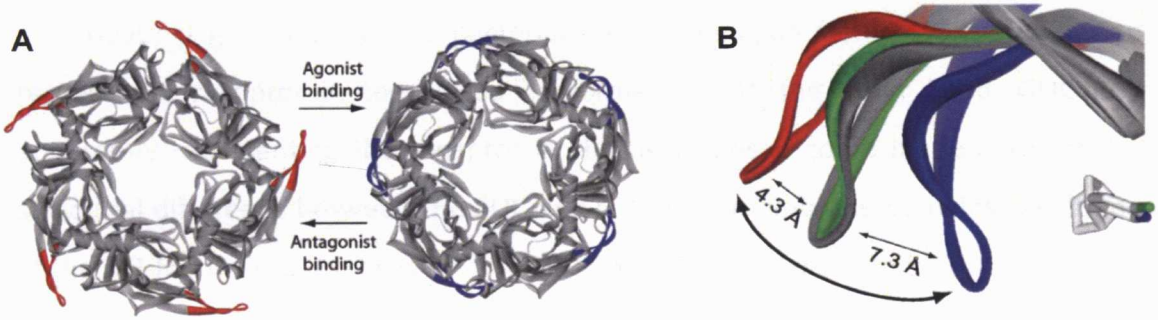

Figure 1.13 Conformational change of loop C. A *Top view of distinctive conformations of agonist (blue loop C) and antagonist (red loop C) bound Aplysia AChBP pentamers.* ***B*** *Overlay of loop C in apo Aplysia AChBP (gray), agonist (blue) and antagonist (red) bound complexes. The curve arrow illustrates loop C closure and opening upon ligand binding. Figure adapted from reference (Hansen et al., 2005).*

Changes in the Loop F conformation in the crystal structure of AChBP have also been observed (Celie *et al.*, 2004). The movement of loop F may be due to the movement of loop C. Loop C is linked to the bottom of loop F within the same subunit (Chang *et al.*, 2009). Moreover, an intersubunit hydrogen bond (H-bond) between loops C and F upon agonist binding in muscle nACh receptors has been reported (Gleitsman *et al.*, 2008). This H-bond has a potential to cause outward movement of loop F, mediating signals to coupling regions, β1-β2 loop and M2-M3 loop (Chang *et al.*, 2009).

1.2.3.2 *Transmembrane domain and gating*

The images from electron microscopy of the open conformation of nACh receptors of *Torpedo marmorata* indicate that channel opening involves a rotation of the pore forming transmembrane, M2 α-helix (Unwin, 1993). The gate of the pore is formed by hydrophobic interactions, and rotation most probably disrupts the interactions to widen the pore and allow ions to flow (Chang *et al.*, 2009) (Figure 1.14**A**). However, protonation scanning of M2 α-helix using single channel analysis suggests that the rotation of M2 in the open conformation is minimal (Cymes *et al.*, 2005). Studies of bacterial ELIC and GLIC structures raise a new gating mechanism termed the pore dilation mechanism. In these studies, it is suggested that the tilting of the M2 and M3 domain is the cause of pore dilation (Bocquet *et al.*, 2009; Hilf *et al.*, 2009b) (Figure 1.14**B**). The bacterial LGIC homologue from ELIC is thought to represent a receptor in the closed conformation. On the other hand, GLIC was apparently representing the receptor in the desensitised conformation. The major structural difference between the ELIC and GLIC transmembrane domains was found at the M2-M3 helices, which were tilted out in GLIC (Hilf *et al.*, 2009b).

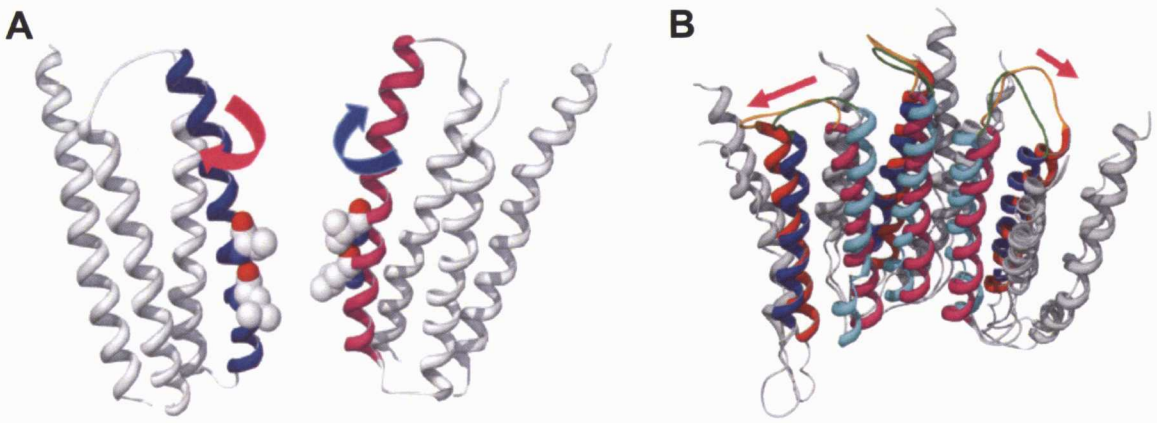

Figure 1.14 Channel pore gating. ***A*** *M2 terminal rotation hypothesis.* ***B*** *M2 terminal tilting and pore dilation hypothesis. Close conformation: cyan, M2 and blue M3. Open conformation: pink, M2 and red, M3. Arrows indicate the direction of M2-M3 tilting. Figure adapted from reference (Chang et al., 2009).*

1.3 Conclusion

The Cys-loop receptor structure and function has been extensively studied using a variety of biochemical techniques including cryo-electron microscopy, X-ray crystallography and mutagenesis. Gene studies revealed that member of this family share significant amino acid sequence homology. This led to the development of homology models, including homology models of $GABA_C$ ρ_1 receptor ligand binding site (Abdel-Halim *et al.*, 2008; Adamian *et al.*, 2009; Harrison *et al.*, 2006b; Osolodkin *et al.*, 2007). However, a detailed molecular knowledge of the sites of drug targets remains unclear due to the lack of X-ray crystal structures of Cys-loop receptors. The gating mechanism of Cys-loop receptors is still incompletely understood, although information from prokaryotic proton-gated ion channel (GLIC and ELIC) crystal structures gave a great insight into the structural rearrangement during channel gating. In addition, the REFER approach and kinetics studies have revealed that the sequence of conformational changes in the N-terminal domain occurs in clusters during agonist-evoked channel gating.

Chapter 2:

GABA receptors

Chapter 2: GABA receptors

γ-Aminobutyric acid (GABA) is the predominant inhibitory neurotransmitter in the mammalian central nervous system (CNS), acting via $GABA_A$, $GABA_B$ and $GABA_C$ receptors (Chebib et al., 2000; Farrant et al., 2007; Mody et al., 2004). The classifications of GABA receptors are according to their structural and pharmacological profiles. $GABA_A$ and $GABA_C$ receptors are ionotropic receptors, belonging to the Cys-loop family of LGICs. Chloride ions flow across the cell membrane via the chloride selective ion channel pore, and the direction of the ion flow is determined by the electrochemical gradient, the membrane potential difference across the cell and the intracellular and extracellular concentrations of chloride ions according to the Nernst equation. In most mature neurons, the opening of chloride channels leads to net inward flow of chloride ions, resulting in the hyperpolarization of neurons. However, GABA also has excitatory actions at particular cell types or immature neurons where the intracellular chloride ion concentration is high or the membrane is at a negative potential (Ben-Ari, 2001; Cherubini et al., 1991; Farrant et al., 2007). $GABA_B$ receptors are metabotropic receptors coupled to G-proteins. GABA binding at $GABA_B$ receptors activates $G_{i/o}$-proteins, propagating cell-signalling cascades to interact with various effectors including ion channels and other receptors to modify its cellular physiology (Emson, 2007).

In the adult brain, 17-20% of neurons are GABAergic (Somogyi et al., 1998). GABA generally mediates inhibition by hyperpolarizing the membrane increasing the sodium influx required to reach the threshold for an action potential. The balance between excitatory and inhibitory neurotransmission is fundamental for normal function of the CNS and disruptions cause disorders of the nervous system. GABA receptors are broadly expressed in the CNS and considered as therapeutic targets for a wide range of neuronal disorders including epilepsies, moods disorders, schizophrenia and sleep, cognitive and anxiety disorders (Johnston, 2005). For example, classical benzodiazepine drugs act via $GABA_A$ receptors by enhancing GABAergic neuronal inhibition in the CNS.

Ever since the presence of GABA in mammalian system was first reported in 1950 (Awapara *et al.*, 1950; Roberts *et al.*, 1950), numerous studies have been carried out to elucidate the role of GABA in the mammalian CNS. The understanding of the anatomical distribution of GABA receptors in the brain has been greatly enhanced using *in situ* hybridization and immunohistochemistry techniques, and the knock-in and knockout mice experiments have contributed to understanding the functional role of GABA receptors in the CNS. Selective ligands, such as bicuculline have also been used in research to elucidate the function of GABA receptors in mammalian CNS (Curtis *et al.*, 1970; Curtis *et al.*, 1971a; Curtis *et al.*, 1971b). The first GABA receptor subunits were cloned in 1987 (Schofield *et al.*, 1987) and their discovery led to multiple other related subunits by using complementary deoxyribonucleic acid homology hybridization screening methods. The cloning of GABA subunits has also enabled recombinant systems to express receptor subunit combinations in order to investigate the roles of individual subunits in receptor function and pharmacology.

2.1 $GABA_A$ receptors

$GABA_A$ receptors mediate fast synaptic inhibition predominantly in the adult CNS. GABA binding at this class of receptor opens chloride selective channels and typically result in hyperpolarization of neurons. They have several modulatory binding sites that bind known drugs including benzodiazepines, anesthetics, ethanol, barbiturates and neurosteroids.

2.1.1 $GABA_A$ receptor structure

To date, 16 human $GABA_A$ receptor subunits have been identified; α (α_1 - α_6), β (β_1 - β_3), γ (γ_1 - γ_3), δ, ε, π and θ (Whiting, 2003). Functional $GABA_A$ receptors are heteropentameric assemblies of five subunits. Each subunit contains a large extracellular domain, four transmembrane domains (M1-M4) and a large intracellular M3-M4 loop. The large number of subtypes allows a vast diversity of possible receptor combinations. However, only a small proportion of receptor combinations are relatively abundant (Sieghart, 2006). The majority of receptors are composed of two α, two β and one γ subunits combination (Chang *et al.*, 1996; Farrar *et al.*, 1999; Im *et al.*, 1995; Tretter *et al.*, 1997), while δ, ε and π subunits, thought to be substitute for the γ subunit form a minority of functional $GABA_A$ receptors (Sieghart, 2006). Of the vast number of $GABA_A$ receptor subtypes, the $\alpha_1\beta_2\gamma_2$ receptor combination is the most abundant receptor combination in the brain (Whiting, 2003). The GABA orthosteric binding site is located at the interface of the extracellular domains of α and β subunits (Smith *et al.*, 1995). The considerable heterogeneity in receptor combinations have generated distinctive pharmacological and physiological properties of $GABA_A$ receptors in the CNS (D'Hulst *et al.*, 2009).

2.1.2 $GABA_A$ receptor pharmacology

$GABA_A$ receptors were first classified as 'bicuculline-sensitive' receptors (Curtis *et al.*, 1970). Bicuculline (Figure 2.1) inhibited the fast-synaptic inhibition differentiating from the receptors mediating slow, long lasting inhibition in the CNS.

Later on, the receptors mediating fast-synaptic inhibition, blocked by bicuculline were classified as $GABA_A$ receptors introduced by Hill and Bowery (1981) (Bormann, 2000; Bowery, 1989; Chebib *et al.*, 1999)

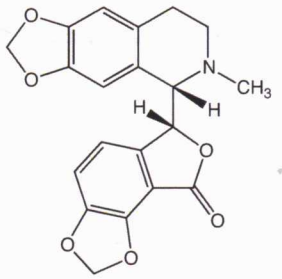

Bicuculline

Figure 2.1 Structure of bicuculline.

2.1.2.1 $GABA_A$ receptor agonists

GABA, imidazole-4-acetic acid (I-4AA) and γ-amino-β-hydroxybutyric acid (GABOB) (Figure 2.2) are endogenous agonists and activate $GABA_A$ receptors (Johnston, 1996a; Krogsgaard-Larsen *et al.*, 1994). GABA contains three rotatable bonds that give rise to multiple conformations. The GABA analogue, muscimol (Figure 2.2) is a natural product isolated from *Amanita muscaria* mushrooms. Muscimol is a potent agonist at $GABA_A$ receptors and it has a depressant effect similar to GABA in the CNS (Brehm *et al.*, 1972; Johnston *et al.*, 1968). An conformationally restricted analogue of muscimol, 4,5,6,7-tetrahydroisoxazolo[4,5-c]pyridin-3-ol (THIP) (Figure 2.2), also known as gaboxadol, is a partial agonist at $GABA_A$ receptors (Krogsgaard-Larsen *et al.*, 1994). It has analgesic and sedative properties in humans (Kjaer *et al.*, 1983). Interestingly, THIP is a superagonist at δ-containing receptor combinations ($\alpha_4\beta_3\delta$), and the ability to target these receptors suggests THIP may act as a potential hypnotic drug (Boehm *et al.*, 2006; Krogsgaard-Larsen *et al.*, 2006).

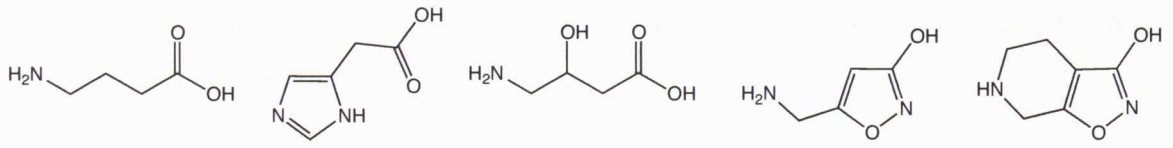

Figure 2.2 Structures of $GABA_A$ agonists.

2.1.2.2 $GABA_A$ receptor antagonists

Bicuculline and gabazine (SR-95531) (Figure 2.3) are classical $GABA_A$ receptor competitive antagonists. Gabazine (SR-95531) is a potent GABA antagonist and widely used as a pharmacological tool when studying GABA receptors *in vitro, in vivo* or *ex vivo* (Kitamura *et al.*, 2011; Meeks *et al.*, 2009; Vigh *et al.*, 2011). Furosemide (Figure 2.3) is a negative allosteric modulator of α_6 containing receptors (Jackel *et al.*, 1998).

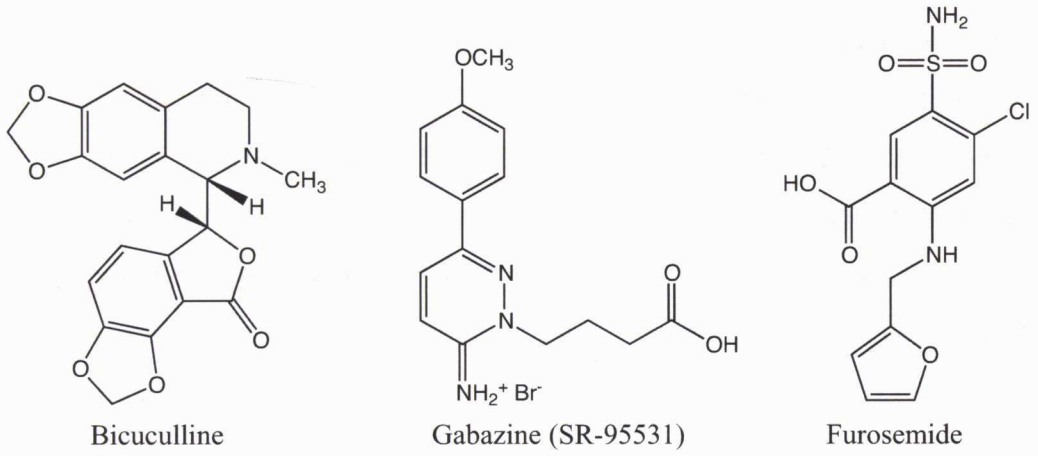

Figure 2.3 Structures of $GABA_A$ antagonists.

2.1.2.3 $GABA_A$ receptor modulators

The benzodiazepine (Figure 2.4) binding site is considered to be located between the α and γ interface, potentiating the effect of GABA at most $GABA_A$ receptors (Johnston, 2005). It acts only in the presence of GABA, increasing GABA's affinity for the $GABA_A$ receptor. Benzodiazepines affect the open channel probabilities to enhance chloride ion influx (Bianchi *et al.*, 2009; Costa *et al.*, 1979). Thus, it is known as a positive allosteric modulator. Diazepam, (Figure 2.4) an

analogue of benzodiazepine also known as valium, is a commercially available benzodiazepine (Martin *et al.*, 1999).

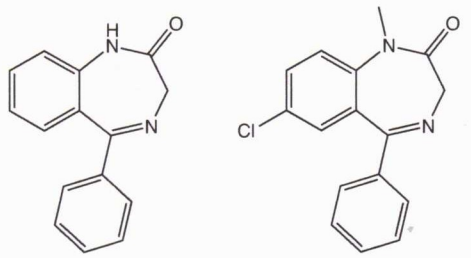

Benzodiazepine Diazepam

Figure 2.4 Structures of benzodiazepine and diazepam.

Flavonoids are also modulators at $GABA_A$ receptors (Hanrahan *et al.*, 2011). They are found in our food sources, such as fruits, vegetables and chocolate (Manach *et al.*, 2004). Flavone, flavanone, flavan-3-ol and isoflavone are the examples of different classes of flavonoids (Figure 2.5). Several studies suggest flavonoids bind to discrete sites, located independently from the flumazenil-sensitive benzodiazepine site (Gavande *et al.*, 2011; Karim *et al.*, 2011b; Mewett *et al.*, 2009), however, the exact location of the binding site is yet to be determined. Although flavonoids are generally thought to be positive modulators, recently the direct activation of $GABA_A$ receptors by 2'-methoxy-6-methylflavone in the absence of GABA has been reported (Karim *et al.*, 2011a).

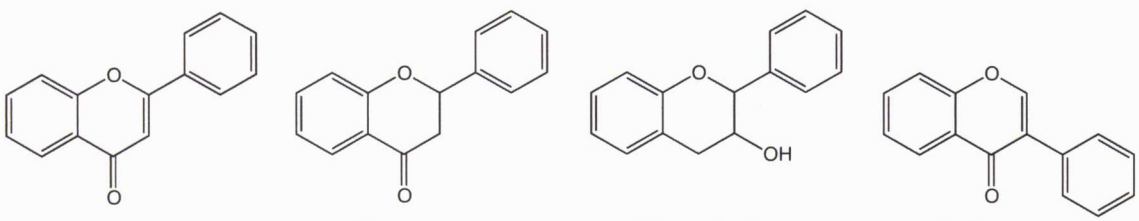

Flavone Flavanone Flavan-3-ol Isoflavone

Figure 2.5 Structures of flavone, flavanone, flavan-3-ol and isoflavone.

Neurosteroids such as pregnenolone and ganaxolone (Figure 2.6) are allosteric modulators of $GABA_A$ receptors (Belelli *et al.*, 2002). They enhance chloride influx via $GABA_A$ receptors by increasing the open channel probabilities (Lambert *et al.*, 1995). Studies using chimeras formed between subunits with high and low sensitivity for

potentiation by neurosteroids identified the neurosteroid binding sites to be located within the transmembrane domains of α and β subunits (Hosie *et al.*, 2007).

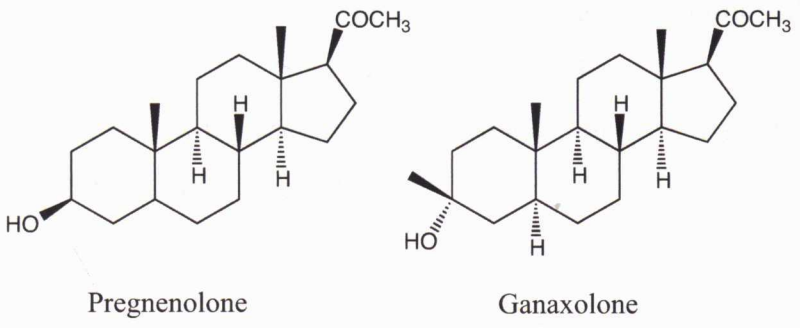

Pregnenolone Ganaxolone

Figure 2.6 Structures of pregnenolone and ganaxolone.

Barbiturates (Figure 2.7) have in the past been used clinically for the treatment of a variety of disorders, including sleep and anxiety disorder. Barbiturates enhance the action of GABA by increasing the open channel duration by up to five times (Mathers *et al.*, 1980; Parker *et al.*, 1986). The actions of barbiturates are concentration dependent, at > 50 μM, barbiturates act as agonists at $GABA_A$ receptors and in millimolar concentrations, they act as antagonists (Akk *et al.*, 2000; D'Hulst *et al.*, 2009). The β subunit is partly involved in barbiturate binding (Rudolph *et al.*, 2004) and the absence of a γ subunit does not affect the activity of barbiturate, suggesting their binding sites are independent from benzodiazepine sites (Akk *et al.*, 2000; Davies *et al.*, 1997).

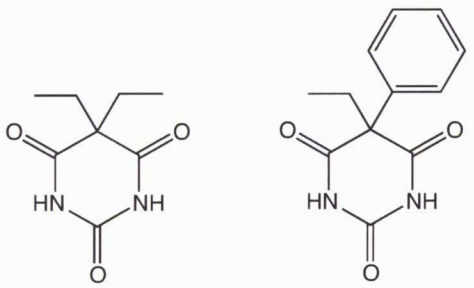

Barbitone Phenobarbitone

Figure 2.7 Structures of barbitone and phenobarbitone.

Anesthetics including propofol and etomidate (Figure 2.8) are known to potentiate the actions of GABA at $GABA_A$ receptors (Kopp Lugli *et al.*, 2009; Pistis *et al.*, 1997). Mutagenesis studies have revealed that the anesthetic binding sites are located in the M2 and M3 transmembrane domains of α and β subunits (Krasowski *et al.*, 1998; Mihic *et al.*, 1997; Siegwart *et al.*, 2002). It has been shown that residues in the β subunit play a crucial for propofol and etomidate binding (Belelli *et al.*, 1997; Krasowski *et al.*, 1998; Siegwart *et al.*, 2002).

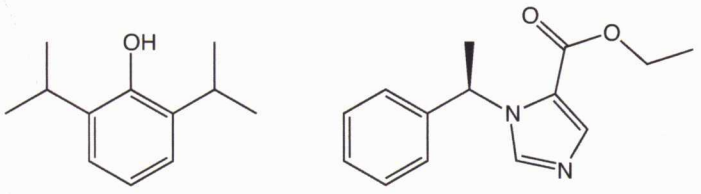

Propofol Etomidate

Figure 2.8 Structures of propofol and etomidate.

2.1.3 $GABA_A$ receptors as therapeutic targets

$GABA_A$ receptors are implicated directly or indirectly in many brain disorders including anxiety, mood, cognitive, epilepsies, schizophrenia and sleep disorders (Johnston, 2005). Studies using *in situ* hybridization (Laurie *et al.*, 1992; Persohn *et al.*, 1992; Wisden *et al.*, 1992) and immunohistochemistry (Fritschy *et al.*, 1992; Pirker *et al.*, 2000; Sperk *et al.*, 1997) have shown the anatomical localization of the $GABA_A$ receptor subunits, revealing that individual subunits have distinct distributions in the brain.

Activation of $GABA_A$ receptors leads to two types of inhibitory effects on the postsynaptic membrane, 'phasic' and 'tonic' inhibitions (Figure 2.9). Postsynaptic $GABA_A$ receptors are activated by millimolar concentrations of GABA released from presynaptic vesicles, mediating the fast inhibitory postsynaptic potential. This specific point inhibitory process is known as 'phasic' synaptic inhibition, which is mediated predominantly by most γ_2-containing receptors such as, $\alpha_1\beta_{2/3}\gamma_2$, $\alpha_2\beta_{2/3}\gamma_2$ and $\alpha_3\beta_{2/3}\gamma_2$ receptors (Farrant *et al.*, 2005; Nusser *et al.*, 1995; Nusser *et al.*, 1998). In contrast extrasynaptic $GABA_A$ receptors, including δ-containing receptors ($\alpha_6\beta_x\delta$, $\alpha_4\beta_x\delta$ and $\alpha_5\beta_x\delta$) are activated by micromolar concentrations of GABA, mediating slower and prolonged inhibition known as 'tonic' inhibition (Farrant *et al.*, 2005). 'Phasic' and 'tonic' inhibition of $GABA_A$ receptors have distinct roles in the control of neuronal excitability, underlying different physiological importance in the brain (Farrant *et al.*, 2007). Therefore, the understanding of native $GABA_A$ receptor combinations and distribution of subunits in the brain is inevitable in order to understand the physiological roles of $GABA_A$ receptors and to develop agents with therapeutic potential.

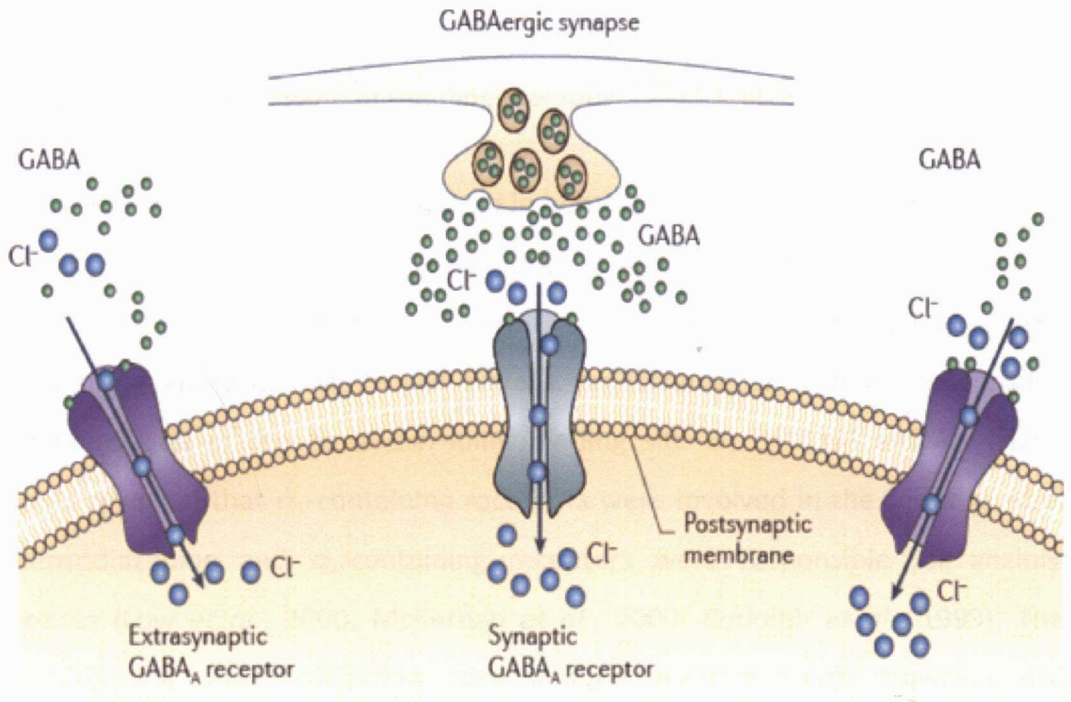

Figure 2.9 Synaptic and extrasynaptic $GABA_A$ receptors. *Synaptic $GABA_A$ receptors (green) are activated by GABA from the presynaptic vesicles mediating fast inhibitory postsynaptic potentials (phasic inhibition). Extrasynaptic $GABA_A$ receptors (purple) detect low concentration of GABA escaped from the synaptic cleft, mediating slow and prolonged inhibitory postsynaptic potentials (tonic inhibition). Figure adapted from reference (Rudolph et al., 2011).*

The high-affinity benzodiazepine binding site is believed to be located at the interface of the extracellular domain of α and γ_2 subunits. An *in vitro* study demonstrated a conserved histidine residue in α_1, α_2, α_3, and α_5 subunits to be a key benzodiazepine binding residue (Benson *et al.*, 1998). The α_1 subunit is located throughout the brain, especially in the cortex, thalamus, pallidum and hippocampus (Rudolph *et al.*, 2001). In contrast the α_2 and α_3 subunits are highly expressed in brain areas where the α_1 subunit is absent (Pirker *et al.*, 2000). Thus the α_2 subunit is expressed in the hippocampus, cortex, striatum and nucleus accumbens. Receptors containing the α_2 subunit are believed to be involved in anxiety, depression and cognitive impairments in schizophrenia (Rudolph *et al.*, 2011). The α_3 subunit is expressed in the cortex and the reticular nucleus of the thalamus, and α_3 knockout transgenic mice have the phenotype of deficit in sensorimotor information processing (Yee *et al.*, 2005), which is a common feature in schizophrenia patients. Therefore,

selective agents targeting α_3 containing receptors may be useful for treatments of sensorimotor gating deficits in psychiatric conditions. The α_5 subunit is expressed in deep layers of the cortex and in the hippocampus.

α subunits play an important role in benzodiazepine binding, and mutations at the conserved histidine residues to arginine (α_1 H101R) located in the extracellular domain, resulted in benzodiazepine insensitive receptors *in vitro* (Benson *et al.*, 1998). Studies using knock-in mice which have a point mutation within the conserved histidine residue in the benzodiazepine binding site α_1 (H101R) and α_2 (H101R) subunits revealed that α_1-containing receptors were involved in the sedative effects of benzodiazepine and α_2-containing receptors were responsible for anxiolytic responses (Low *et al.*, 2000; McKernan *et al.*, 2000; Rudolph *et al.*, 1999). These studies require further validation using subtype selective agents, however, drugs selective for α_2-containing receptors are expected to be anxiolytics with less side-effects associated with the clinically used non-selective benzodiazepine including sedative (Rudolph *et al.*, 2001).

Isoforms of β subunits are widely distributed in the brain (Pirker *et al.*, 2000) and surprisingly β_2 subunit knockout mice have no overt phenotype despite being the most abundant of the β subunits (Sur *et al.*, 2001). β_2 and β_3 subunits are involved in the action of the general anesthetic etomidate (Johnston, 2005). Mutating asparagine to serine residue at position 289 (N289S) located in the channel domain of β_3 subunit resulted in reducing etomidate activities *in vitro* (Belelli et al., 1997). In a study using knock-in mice containing a mutation in β_2 subunit (N265S which is the homologous residue in β_3) revealed that etomidate produces the sedation effect *via* β_2-containing receptors and the anaesthesic effect *via* β_3-containing receptors (Reynolds *et al.*, 2003). Improved recovery after etomidate anaesthesia was also observed, suggesting that β_3 subunit selective agents may result in anesthesics with an improved recovery profile (Reynolds *et al.*, 2003). β_3-containing receptors are also believed to be involved in sleep disorders, as a point mutation in β_3 subunit has been found in a patient with chronic insomnia (Johnston, 2005). In addition, the endogenous sleep

promoting fatty acid, oleamide was inactive in β_3 subunit knock out mice (Laposky *et al.*, 2001).

Amongst the three isoforms of γ subunits, it is the γ_2 subunit that is the most widely distributed and found throughout the brain, with the exception of the thalamus (Pirker *et al.*, 2000). Deletion of the γ_2 subunit appears to be lethal since almost all γ_2 homozygote knockout mice died in the first few days after birth (Gunther *et al.*, 1995). The γ_2 subunit contributes to the high affinity benzodiazepine binding site (Gunther *et al.*, 1995) and appears to play a role in synaptic clustering (Crestani *et al.*, 1999; Essrich *et al.*, 1998). The γ_1 subunit is expressed mainly in the bed nucleus of the stria terminalis and the γ_3 subunit is expressed throughout the brain with a low expression level (Pirker *et al.*, 2000). The physiological roles of γ_1 and γ_3 subunits are yet to be determined.

The δ subunit is expressed in the thalamus and cerebellum (Pirker *et al.*, 2000) and forms receptors specifically with α_4 and α_6 subunits (Jones *et al.*, 1997; Quirk *et al.*, 1995; Sur *et al.*, 1999). δ-containing $GABA_A$ receptors are also known as extrasynaptic receptors, which are activated by GABA which has escaped from the synaptic cleft to mediate tonic inhibition (Farrant *et al.*, 2005; Stell *et al.*, 2003; Wei *et al.*, 2003). δ subunit knockout mice are affected by occasional seizures and electroencephalographic abnormalities were found, implying the role of tonic inhibition in epilepsy (D'Hulst *et al.*, 2009; Mihalek *et al.*, 1999; Spigelman *et al.*, 2003).

The ε and θ subunits have been found in the hypothalamus, amygdala and thalamus (Sieghart *et al.*, 2002) and θ subunit co-assembles with $\alpha_2\beta_1\gamma_1$ receptors (Bonnert *et al.*, 1999). π subunit is mainly found in the peripheral tissues. Studies have implicated that the π subunit is involved in pregnancy (Hedblom *et al.*, 1997) and cancer (Takehara *et al.*, 2007).

2.2 $GABA_B$ receptors

GABA binding at $GABA_B$ receptors leads to the activation of $G_{i/o}$-proteins, a heterotrimeric protein structure comprised of: α, β and γ subunits. GDP/GTP exchange at $\alpha_{i/o}$ subunit results in dissociation of the $\beta\gamma$ dimer, triggering activation of various effectors including ion channels and enzymes (Figure 2.10) (Padgett *et al.*, 2010). There are two main important signalling cascades for the physiological roles of $GABA_B$ receptors. When GABA binds at $GABA_B$ receptors, they activate G-proteins (GDP/DTP exchange). The dissociation of the $\beta\gamma$ dimer stimulates the activation of K^+ channels, resulting in hyperpolarizing the neuron. At the same time α subunits inhibit the activity of adenyl cyclase which results in reduction of cAMP formation. cAMP is a secondly messenger used as intracellular signal transductions.

2.2.1 $GABA_B$ receptor structure

$GABA_B$ receptors belong to the class C of G-protein coupled receptors, which also includes metabotropic glutamate (mGlu) and Ca^{2+} sensing receptors (Pin *et al.*, 2003). There are three $GABA_B$ receptor subunits; $GABA_{B1a}$, $GABA_{B1b}$ and $GABA_{B2}$. Functional $GABA_B$ receptors are heterodimers formed from $GABA_{B1}$ and $GABA_{B2}$ subunits (Figure 2.11). $GABA_{B1}$ subunit cell surface expression is prevented through its C-terminal endoplasmic reticulum retention motif, so the interaction of $GABA_{B1}$ with $GABA_{B2}$ subunits via C-terminal coiled-coil α helices is essential to mask the retention signals to ensure surface expression (Margeta-Mitrovic *et al.*, 2000). It was found that $GABA_{B1}$ and $GABA_{B2}$ subunits have different properties in mobility and they dimerize primarily at the plasma membrane in hippocampal neurons (Ramirez *et al.*, 2009). A recent study using a new α-bungarotoxin binding site labeling technique reported $GABA_B$ receptor internalization was regulated by $GABA_{B2}$ subunits (Hannan *et al.*, 2011). Some $GABA_B$ receptors were found to form higher-order oligomeric assemblies, impacting on G-protein coupling efficacy (Maurel *et al.*, 2008). Pin and co-workers proposed the oligomerisation of $GABA_B$ receptors increases ways to modulate receptor signaling and activity, allowing $GABA_B$ receptors to have specific properties at different locations in the CNS (Pin *et al.*, 2009).

A single subunit structure contains, a large extracellular domain, known as Venus Flytrap domain (VFT) and seven transmembrane domain (Galvez *et al.*, 2000). The VFT from $GABA_{B1}$ subunit forms the orthosteric binding site (Galvez *et al.*, 2000; Malitschek *et al.*, 1999) and the transmembrane domain from $GABA_{B2}$ subunit is responsible for G-protein activation (Duthey *et al.*, 2002; Galvez *et al.*, 2001; Robbins *et al.*, 2001).

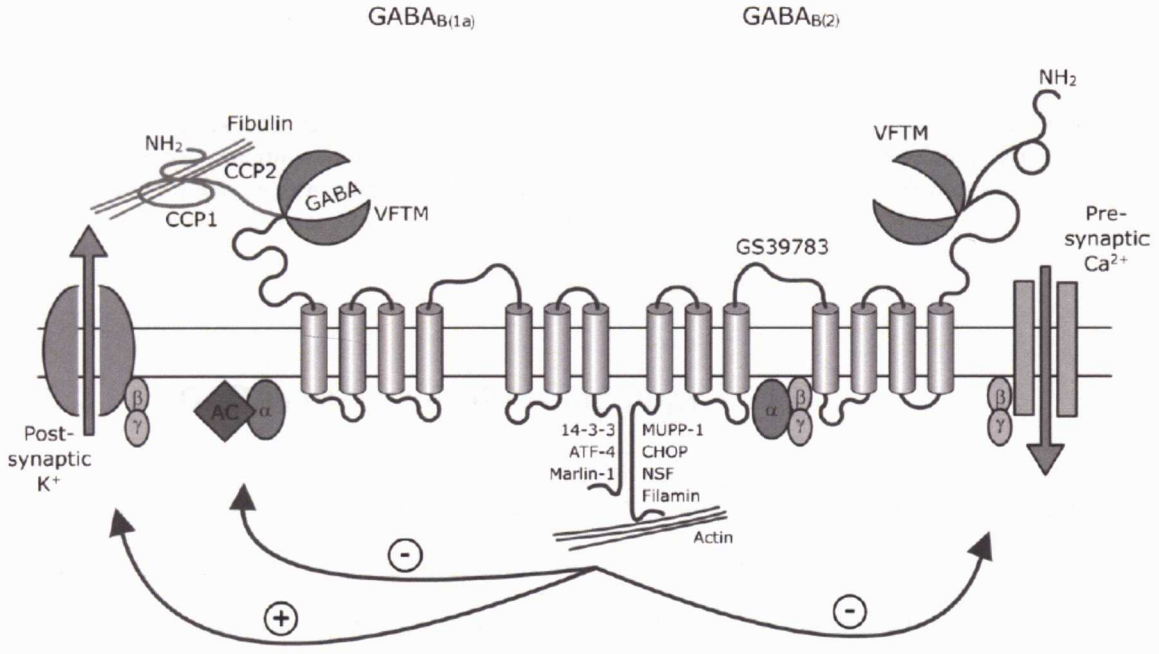

Figure 2.10 Schematic representation of the $GABA_B$ receptor and its primary signaling pathways. *Activation of $GABA_B$ receptor stimulates $G_{i/o}$ dissociation of $\alpha_{i/o}$ and $\beta\gamma$ dimer. $\alpha_{i/o}$ subunit inhibits adenylyl cyclase and $\beta\gamma$ dimer modulates volage-gated Ca^{2+} or G-protein gated inwardly rectifying K^+ (GIRK) channels. Figure adapted from reference (Emson, 2007).*

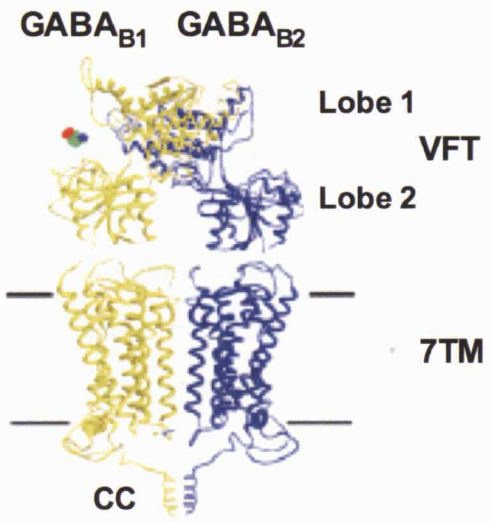

Figure 2.11 Structure of heteromeric GABA$_B$ receptor. *GABA$_{B1}$ (yellow) and GABA$_{B2}$ (blue) subunits are composed of a VFT domain and a 7TM domain. The C-terminal regions of the two subunits are joined via coiled-coil interaction. Abbreviations: VFT, venus flytrap; 7TM, seven transmembrane; CC, coiled-coil. Figure adapted from reference (Rondard et al., 2011).*

2.2.2 GABA$_B$ receptor pharmacology

GABA$_B$ receptors were first identified using the GABA analogue baclofen (Figure 2.12). Baclofen was identified as selective agonist inhibiting neurotransmitter release in the mammalian CNS (Bowery *et al.*, 1980). A number of analogues were developed based on the structure of baclofen, which led to the production of the first GABA$_B$ antagonist, phaclofen (Figure 2.12) (Kerr *et al.*, 1987).

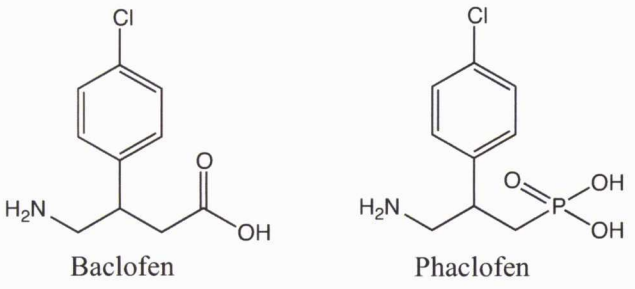

Figure 2.12 Structures of baclofen and phaclofen. *Baclofen is a selective GABA$_B$ agonist and phaclofen is a selective GABA$_B$ antagonist.*

2.2.3 $GABA_B$ receptors as therapeutic targets

$GABA_B$ receptors mediate slow and longer phase of pre- or post-synaptic inhibition in the CNS. They are found in many regions of the brain, and some of the highest regions of $GABA_B$ receptor expression include the hippocampus, thalamus, neocortex and cerebellum (Fernandez-Alacid *et al.*, 2009; Kulik *et al.*, 2006; Kulik *et al.*, 2003; Padgett *et al.*, 2010). $GABA_B$ receptors are implicated in a range of neuronal disorders including, sleep disorders, stress, epilepsy and substance abuse (Bettler *et al.*, 2004; Bowery, 2006; Enna *et al.*, 2004). The $GABA_B$ agonist, baclofen (Lioresal), is the only therapeutic agent that targets these receptors and is used as a muscle relaxant to treat spasticity in multiple sclerosis patients (Brogden *et al.*, 1974). $GABA_B$ antagonists also produce beneficial therapeutic effects, such as cognition improvement (Froestl *et al.*, 2004), models of absence epilepsy (Manning *et al.*, 2003) and antidepressant effects (Cryan *et al.*, 2005).

2.3 $GABA_C$ receptors

$GABA_C$ receptors were first described by Johnston and co-workers (1975) using the conformationally restricted analogue of GABA, *cis*-4-aminocrotonic acid (CACA, Figure 2.14). They discovered CACA depressed cat spinal interneurons, however, its effect was not blocked by bicuculline (Johnston *et al.*, 1975). In addition, the binding of radiolabelled baclofen was not affected by CACA on rat cerebellum (Drew *et al.*, 1984). This unique pharmacological profile of this receptor type was termed '$GABA_C$ receptors' or ' bicuculline- and baclofen-insensitive receptors'.

$GABA_C$ receptors have a higher affinity to GABA, a smaller chloride ion conductance and a longer mean channel opening time than the major $GABA_A$ receptors (Bormann *et al.*, 1995; Chebib *et al.*, 2000; Enz, 2001; Feigenspan *et al.*, 1994). In addition, $GABA_C$ receptors do not tend to desensitize as $GABA_A$ receptors do (Bormann, 2000; Enz *et al.*, 1998).

The International Union of Pharmacology (IUPHAR) has recently published a review on the classification of $GABA_A$ receptors, suggesting the usage of the term '$GABA_C$ receptor' should be avoided and re-classified as 'a subclass of the $GABA_A$ receptor' due to the sequence and structural similarities between ρ subunits that make up this receptor and $GABA_A$ receptor subunits (Barnard *et al.*, 1998; Olsen *et al.*, 2008). However, this nomenclature is still a matter of debate since their difference in pharmacology, structure, function and localization from other classes of GABA receptors (Bormann, 2000; Chebib *et al.*, 1999; Chebib *et al.*, 2000; Johnston, 2005; Johnston, 2002). For the purpose of this thesis, the term '$GABA_C$' has been used to describe ' bicuculline- and baclofen-insensitive receptors'.

2.3.1 $GABA_C$ receptor structure

$GABA_C$ receptors are structurally related to $GABA_A$ receptors, and also belong to Cys-loop LGIC family. $GABA_C$ receptors are pentameric assemblies of ρ subunits: In mammals, ρ_1-ρ_3 isoforms have been identified (Bailey *et al.*, 1999; Cutting *et al.*,

1992; Ogurusu *et al.*, 1999). The receptors are homomeric composed of only a single ρ-subunit or pseudo-homomeric receptors, composed of $\rho_1\rho_2$ or $\rho_2\rho_3$ subunit combinations (Chebib *et al.*, 2000; Enz *et al.*, 1998; Ogurusu *et al.*, 1999).

2.3.1.1 $GABA_C$ receptor orthosteric binding site

The orthosteric binding site of ρ_1 homomeric receptor is located at the interface of two subunits. The binding site is formed by residues drawn from five discontinuous stretches of amino acids from the N-terminal domain of each subunit. These stretches of residues are referred to as loops A-E (Figure 2.13). Loops A-C form the principle side of the binding site while loops D and E form the complementary side (Sedelnikova *et al.*, 2005).

A

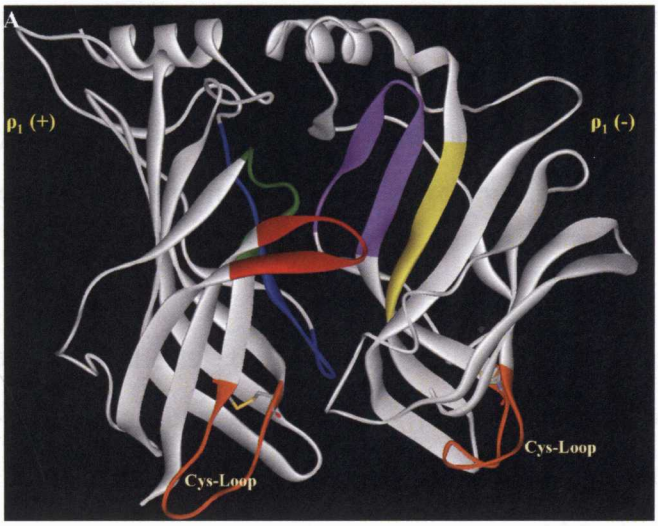

B

LYLRHYWKDE RLSFPSTNNL SMTFDGRLVK KI**WVPDMFFV** 140
Loop **D** Loop **A**

HSKRSFIHDT TTDN**VMLRVQ** **PDGKVLYSLR** VTVTAMCNMD 180
Loop **E**

FSRFPLDTQT CSLEI**ESYAY** TEDDLMLYWK KGNDSLKTDE 220
Loop **B**

RISLSQFLIQ EFHTTTKL**AF** **YSSTGWY**NRL YINFTLRRHI 260
Loop **C**

Figure 2.13 ρ_1 receptor orthosteric binding site. A *The orthosteric binding site is located at the interface of extracellular domain of ρ_1 subunit. Each loop is colour coded. The principle side loops (ρ_1 (+)): blue, loop A; green, loop B; red, loop C. The complementary side loops (ρ_1 (–)): yellow, loopD; purple, Loop E. Figure adapted from (Abdel-Halim et al., 2008).* ***B*** *Amino acid sequence of N-terminal of ρ_1 subunit. The amino acid sequences located at the orthosteric binding site are underlined. The Subunits sequence was taken from: Genbank®, Accession code: P24046 and reference (Sedelnikova et al., 2005).*

Homology models of $GABA_C$ receptor have been developed using the acetylcholine-binding protein (AChBP) crystal structure. This protein shares approximately 18% homology with the ρ subunit (Abdel-Halim *et al.*, 2008; Adamian *et al.*, 2009; Harrison *et al.*, 2006b; Osolodkin *et al.*, 2007; Sedelnikova *et al.*, 2005). Mutagenesis studies using natural and unnatural amino acids as well as the substituted cysteine accessibility method (SCAM) identified a number of residues that

are critical for GABA binding or channel gating at the ρ_1 receptor orthosteric binding site. These studies identified that an aromatic box located within the binding site play a role in ligand binding (Amin *et al.*, 1994; Harrison *et al.*, 2006a; Lummis *et al.*, 2011; Sedelnikova *et al.*, 2005; Torres *et al.*, 2002). The most important residues for GABA binding were; tyrosine at position 102 (Y102), tyrosine at position 198 (Y198), and arginine at position 104 (R104).

A series of mutagenesis studies were carried out to locate amino acids involved in GABA-evoked receptor activation (Amin *et al.*, 1994; Torres *et al.*, 2002). The studies found that a tyrosine at position 102 in loop D when mutated to cysteine (Y102C), serine (Y102S), tryptophan (Y102W) or glycine (Y102G) dramatically changed the GABA EC_{50} (Torres *et al.*, 2002). Furthermore, Y102C was accessible to modification by methanethisulfonate indicating the residue was water accessible. Furthermore co-application of GABA attenuated the modification by methanethisulfonate at Y102C mutant receptors, suggesting the tyrosine possibly involved in the GABA binding site.

Tyrosine at position 198 was identified as amino acid involved in GABA-mediated activation. Removal of benzene ring at this position has increased GABA EC_{50} value approximately 3000-fold (Amin *et al.*, 1994). Using the unnatural amino acid mutagenesis method, a series of tyrosine derivatives were incorporated at tyrosine position 198. The results indicated a cation-π interaction between the amino terminal of GABA and the tyrosine (Lummis *et al.*, 2005). Interestingly, the residues that forms the cation-π interaction is not conserved in $GABA_A$ and $GABA_C$ receptors (Lummis, 2009; Padgett *et al.*, 2007). These findings suggest that GABA binds subtly different locations and a different mode of GABA binding at these receptors is expected.

Homology model developed by Lummis and Harrison (Harrison *et al.*, 2006b) identified four arginine residues which were in close proximity to the carboxylic acid terminal of GABA. Mutagenesis and functional studies revealed that an arginine at position 158 (R158) was crucial for receptor function (Harrison *et al.*, 2006b). In

addition, mutating arginine at position 104 (R104) to either an alanine or glycine resulted in a 10000-fold increase in GABA EC_{50}. Their homology model indicates that this residue is important for GABA binding and in forming the structure of the binding pocket (Harrison *et al.*, 2006b).

2.3.2 $GABA_C$ receptor pharmacology

$GABA_C$ receptors are pharmacologically unique, as they are insensitive towards the classical $GABA_A$ receptor antagonist, bicuculline, and the $GABA_B$ selective agonist, baclofen (Drew *et al.*, 1984; Johnston *et al.*, 1975; Woodward *et al.*, 1993). They are also insensitive to benzodiazepines and other positive $GABA_A$ receptor modulators (Shimada *et al.*, 1992).

2.3.2.1 $GABA_C$ receptor agonists

GABA and conformationally restricted analogues of GABA, CACA and *trans*-4-aminocrotonic acid (TACA) activate recombinant $GABA_C$ receptors expressed in *Xenopus* oocytes (Figure 2.14) (Ng *et al.*, 2011). CACA is a partial agonist at homomeric ρ_1 and ρ_2 receptors and has weak agonist activity at ρ_3 receptors (Kusama *et al.*, 1993b; Vien *et al.*, 2002; Woodward *et al.*, 1993). TACA is a potent $GABA_C$ receptor agonist however it also activates $GABA_A$ receptors ($\alpha_1\beta_2\gamma_{2L}$) (Chebib *et al.*, 2000; Chebib *et al.*, 1998; Kusama *et al.*, 1993a; Vien *et al.*, 2002).

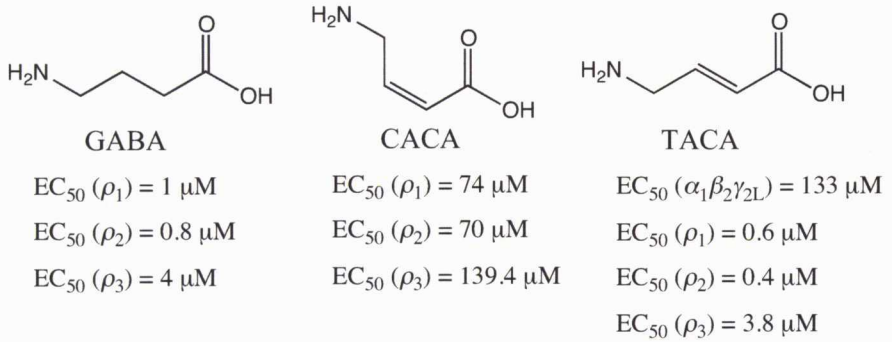

Figure 2.14 Structures of GABA, CACA and TACA.

GABOB is an endogenous derivative of GABA and the hydroxyl goup at third carbon of GABA creates a stereogenic centre, resulting in (*S*)-GABOB and (*R*)-GABOB (Figure 2.15). The enantioselective agonist actions of the (*S*)- and (*R*)- enantiomer of GABOB at ρ_1 receptors have been reported (Hinton et al., 2008). I-4AA (Figure 2.15) is a partial agonist at ρ_1 and ρ_2 homomeric receptors (Carland et al., 2004; Johnston, 2002) and acts as competitive antagonist at ρ_3 receptors (Johnston, 2002). Unlike I-4AA, muscimol (Figure 2.15) is a partial agonist at both human ρ_1 and ρ_2 and rat ρ_3 homomeric receptors expressed in *Xenopus* oocytes (Kusama et al., 1993a; Kusama et al., 1993b; Vien et al., 2002).

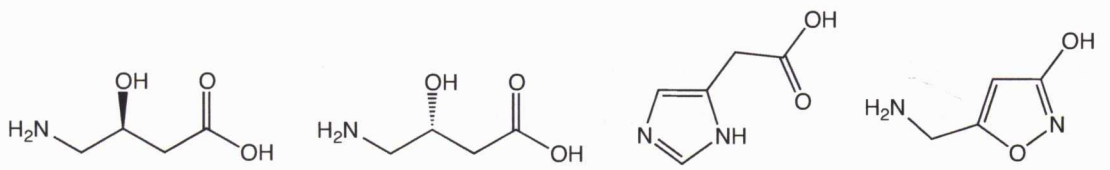

Figure 2.15 Structures of (S)-GABOB, (R)-GABOB, I-4AA and muscimol.

The conformationally restricted GABA analogues, (+)- and (–)-*cis*-2-(aminomethyl)cyclopropanecarboxylic acid ((+)- and (–)-CAMP) (Figure 2.16) exert opposite pharmacological effects at $GABA_C$ receptors (Crittenden *et al.*, 2006; Duke *et al.*, 2000). (+)-CAMP acts as a full agonist, while (–)-CAMP acts as antagonist (Duke *et al.*, 2000). (+)-CAMP acts as very weak antagonist at $GABA_A$ receptors and is inactive at $GABA_B$ receptors, indicating it is one of the most potent and selective $GABA_C$ receptor agonist known.

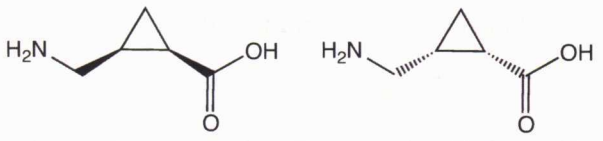

(+)-CAMP

EC_{50} (ρ_1) = 39.7 μM

EC_{50} (ρ_2) = 16.6 μM

EC_{50} (ρ_3) = 28.1 μM

(−)-CAMP

IC_{50} (ρ_1) = 890 μM

IC_{50} (ρ_2) = 400 μM

IC_{50} (ρ_3) = 178 μM

Figure 2.16 Structures of (+)-CAMP and (-)-CAMP

2.3.2.2 $GABA_C$ receptor antagonists

The phosphinic acid analogues of GABA (Figure 2.17), which were originally developed for $GABA_B$ receptors, were also found to be potent antagonists at $GABA_C$ receptors. 3-aminopropylphosphonic acid (3-APA), 3-aminopropylphosphinic acid (3-APPA) and 3-aminopropyl(methyl)phosphinic acid (3-APMPA) are potent competitive antagonists at ρ_1 homomeric receptors expressed in *Xenopus* oocytes (Woodward et al., 1993). CGP36742 (SGS742) (Figure 2.17) was developed as an orally active $GABA_B$ receptor antagonist with therapeutic potential for the treatment of cognitive deficits, absence seizures, epilepsy, and depression (Froestl et al., 2004). CGP36742 (SGS 742) also acts as a $GABA_C$ receptor antagonist with approximately half the potency as at $GABA_B$ receptors (Chebib *et al.*, 1997a; Ng *et al.*, 2011).

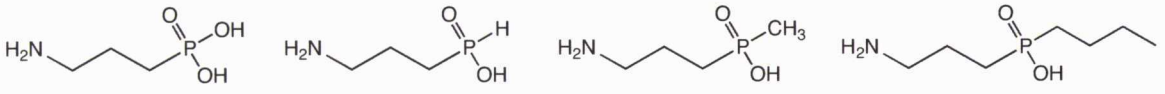

3-APA

K_B (ρ_1) = 10 μM

3-APPA

K_B (ρ_1) = 1.7 μM

3-APMPA

K_B (ρ_1) = 0.7 μM

CGP36742

IC_{50} ($GABA_B$) = 38 μM

IC_{50} (ρ_1) = 62.5 μM

Figure 2.17 Structures of 3-APA, 3-APPA, 3-APMPA and CGP36742.

(1,2,5,6-tetrahydropyridine-4-yl)methylphosphinic acid (TPMPA) (Figure 2.18) was the first selective $GABA_C$ receptor competitive antagonist (Murata et al., 1996), while ((S)-4-aminocyclopent-1-en-1-yl)(butyl)phosphinic acid ((S)-4-ACPBuPA) (Figure 2.18) is the most potent $GABA_C$ antagonist. (*S*)-4-ACPBuPA was developed based on a

series of conformationally restricted analogues of 4-aminocyclopentene carboxylic acids. Kumar and colleagues designed chimeric molecules composed of 4-aminocyclopentene moiety and alkylphosphinic acids (Kumar et al., 2008). It appears that the alkylphosphinic acid group helps to make the molecule more selective for the $GABA_C$ receptor while reducing activity for the $GABA_B$ receptor. Recently, the guanidine analogue, 3-[guanidino]-1-oxo-1-hydroxy-phospholane (3-GOHP) (Figure 2.18) was reported to be a potent selective $GABA_C$ competitive antagonist (Gavande et al., 2010b). In contrast, gabazine (SR-95531) (Figure 2.18) acts as an antagonist at both $GABA_A$ and $GABA_C$ receptors, with higher preference for the $GABA_A$ receptors (Zhang et al., 2008).

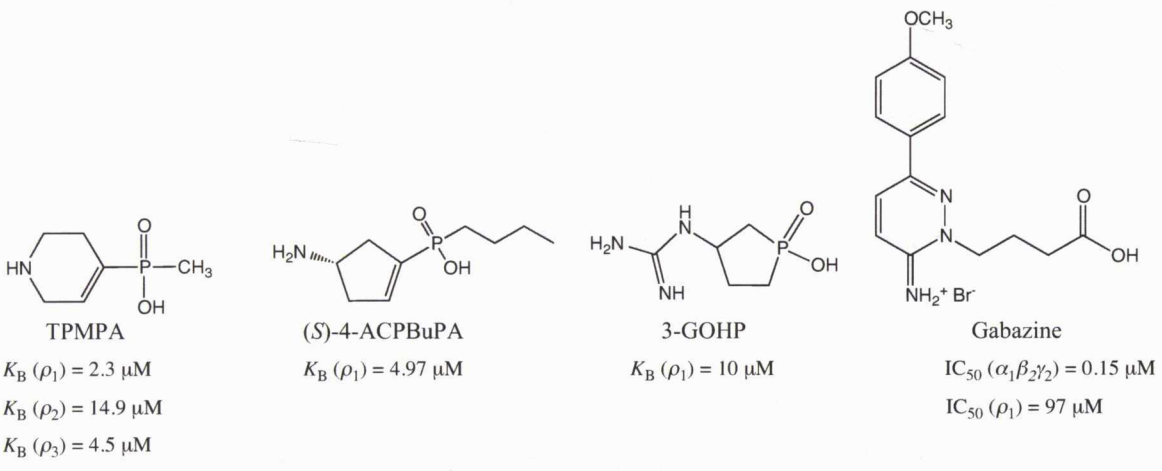

Figure 2.18 Structures of TPMPA, (S)-4-ACPBuPA, 3-GOHP and gabazine.

2.3.3 $GABA_C$ receptors as therapeutic targets

Unlike the $GABA_A$ receptor, the distribution of $GABA_C$ receptors in the CNS is restricted. ρ_1, ρ_2 and ρ_3 subunits are predominantly expressed in the retina (Qian *et al.*, 2009) and the superior colliculus (Boue-Grabot *et al.*, 1998; Clark *et al.*, 2001), indicating a role in visual processing. Indeed ρ_1 subunit knockout mice had defects in visual function by altering the signal from rod bipolar cells to third order cells (McCall *et al.*, 2002). In addition, $GABA_C$ receptor-mediated inhibition was not eliminated in

the superior colliculus in ρ_1 knockout mice, suggesting ρ_2 subunit has more functional role in this region (Schlicker *et al.*, 2009).

Experiments using $GABA_C$ selective antagonists, TPMPA and *cis*- and *trans*-(3-aminocyclopentanyl)methylphosphinic acid (*cis*- and *trans*-3-ACPBPA) on chick model of myopia showed that $GABA_C$ selective antagonists could be used to prevent the development of myopia (Chebib *et al.*, 2009b; Stone *et al.*, 2003). Although the ρ subunits dominate sites in the retina, they are also found throughout the brain. ρ_1 and ρ_2 subunits are localized in the cerebellum (Rozzo *et al.*, 2002), hippocampus (Alakuijala *et al.*, 2005) and lateral amygdala (Cunha *et al.*, 2010), while ρ_3 subunits are expressed in the hippocampus and cortex of the rat (Wegelius *et al.*, 1998). The expression of $GABA_C$ receptors in the hippocampus implies a role for the receptor in memory, and experiments using $GABA_C$ receptor selective antagonists, TPMPA, *cis*- and *trans*-3-ACPBPA were found to enhance memory in chicks and rats (Chebib *et al.*, 2009b; Gibbs *et al.*, 2005). Interestingly, reverse transcription-polymerase chain reaction (RT-PCR) studies observed a higher expression of ρ_2 subunit mRNA than ρ_1 and ρ_3 subunits mRNA in hippocampus, suggesting that the ρ_2 subunit may play the more dominant role in memory (Alakuijala *et al.*, 2005; Rozzo *et al.*, 2002).

$GABA_C$ receptors have also been shown to play an important role in sleep walking and fear and anxiety disorders (Cunha *et al.*, 2010; Johnston, 2002). Administration of TPMPA increases sleep walking behavior in rats, indicating $GABA_C$ receptors are also involved (Arnaud *et al.*, 2001). The lateral amygdala is associated with the fear learning memory (Blair *et al.*, 2001; LeDoux, 2000; Maren *et al.*, 2004), and the activation of $GABA_C$ receptors enhanced fear and learning, and it was attenuated by TPMPA *in vivo* (Cunha *et al.*, 2010). This study highlights that $GABA_C$ receptors are potential therapeutic targets for the treatment of fear and anxiety disorders.

2.4 Aims

The main aim of this thesis is to explore how ligands interact with their binding sites at $GABA_C$ receptors. Understanding of the interactions between ligands, especially endogenous molecules such as GABA, with their binding sites is important in developing potent and subtype-selective agents. The homology model of $GABA_C$ ρ_1 receptor ligand binding site (Abdel-Halim *et al.*, 2008) predicted amino acid residues that were involved in ligand binding. Receptor structure and function studies were also carried out using $GABA_C$ ρ_1 receptors. ρ_1 subunits form homomeric receptors and they express in recombinant systems making them a suitable model for carrying out receptor structure and function studies. A series of point mutations were introduced using molecular biology techniques and the effect of mutations were explored using structurally diverse GABA agonists and antagonists. The receptors were expressed in *Xenopus* oocytes and their functions were measured by two-electrode voltage clamp method.

Chapter 3:

Materials and Methods

Chapter 3: Materials and Methods

3.1 Materials

Human $GABA_C$ ρ_1 DNA cloned into the vector pcDNA3 was donated by Dr. David Weiss (The University of Alabama, Birmingham, AL). Human ρ_2 cloned into the pKS vector was donated by Dr. Garry Cutting. Human $GABA_A$ α_1, β_2 and γ_{2L} cDNAs cloned into pcDM8 were gifts from Dr. Paul Whiting (Merck Sharpe and Dohme, Harlow, UK). Rat GIRK4, human $GABA_{B(1b)}$ and $GABA_{B2}$ subcloned in pcDNA3.1(-), and rat GIRK1 subcloned in pBluescript were gifts from Drs. Fiona Marshall and Andrew Green (Glaxo Wellcome, UK). *Xenopus laevis* were obtained from South Africa and housed in the Department of Veterinary Science, University of Sydney.

GABA, muscimol, I-4AA, THIP and 5-aminovaleric acid (DAVA) were purchased from Sigma-Aldrich Chemical Co. (St Louis, MO, USA). 3-APMPA (3-Aminopropyl(methyl)phosphinic acid) was purchased from Tocris Bioscience (Bristol, UK). CGP-36742 or SGS-742 (3-aminopropyl-*n*-butylphosphinic acid), the enantiomers of 4-amino-3-hydroxybutanoic acid (GABOB) and (3-amino-2-hydroxypropyl)methylphosphinic acids (CGP44532 and CGP44533) were gifts from Dr. Wolfgang Froestl (formerly Novartis, Switzerland) and Prof. Povl Krogsgaard-Larsen (The University of Copenhagen, Denmark).

6-Imino-3-(4-methoxyphenyl)-1(6*H*)-pyridazinebutanoic acid (gabazine/SR-95531), (1,2,5,6-Tetrahydropyridin-4-yl)methylphosphinic acid (TPMPA), [(±)-*cis*-(3-aminocyclopentyl)butylphosphinic acid] ((±)-*cis*-3-ACPBPA), [(±)-*trans*-(3-aminocyclopentyl)butylphosphinic acid] ((±)-*trans*-3-ACPBPA), [(*S*)-4-amino-1-cyclopent-1-enyl(butyl)phosphinic acid] ((*S*)-4-ACPBPA), [(+)-4-aminocyclopent-1-ene-1-carboxylic acid] ((+)-4-ACPCA), 4-guanidinobutanoic acid (4-GBA), [(*Z*)-3-[(aminoiminomethyl)thio] prop-2-enoic acid] (ZAPA), (*R*)- and (*S*)-3F-GABA, enantiomers of *syn*- and *anti*-2,3-difluoro-4-aminobutyric acids were prepared according to previously published methods (Allan *et al.*, 1986; Deniau *et al.*, 2007;

Gavande *et al.*, 2010a; Hanrahan *et al.*, 2001; Hanrahan *et al.*, 2006; Hunter *et al.*, 2011; Kumar *et al.*, 2008) by Drs. Navnath Gavande from Faculty of Pharmacy, The University of Sydney, Sydney, Australia, Ken Mewett and Katherine Locock from Department of Pharmacology, The University of Sydney, Sydney, Australia, Luke Hunter from School of Chemistry, The University of New South Wales, Sydney, Australia, and Prof. David O'Hagan from School of Chemistry, The University of St Andrews, Scotland, United Kingdom.

(±)-4-aminocyclopent-1-enecarboxamide ((±)-4-ACPAM) and gabazine analogues (Table 8.1) were synthesized by Drs Katherine Locock and Navnath Gavande (affiliations as above) and the unpublished synthetic procedures are found in appendix.

3.2 Methods – Molecular Biology

3.2.1 Site-directed mutagenesis

Sense and antisense oligonucleotide primers were designed to introduce point mutations into the human $GABA_C$ (ρ_1) subunits and they were synthesized by Invitrogen (Invitrogen Australia Pty. Ltd. VIC, Australia). The QuickChange Site-directed Mutagenesis Kit II (Stratagene, CA, USA) was used to introduce mutations with accordance to the manufacturer's instructions. Briefly, the reaction mixture contained reaction buffer (5 μL; 100 mM KCl, 100 mM $(NH_4)2SO_4$, 200 mM Tris-HCl, pH 8.8, 20 mM $MgSO_4$, 1% Triton X100, 1mM/mL nuclease-free bovine serum albumin (BSA)), ρ_1 wild-type dsDNA template (5-50 ng), sense and antisense oligonucleotides (125 ng), dNTP (deoxynucleotide triphosphate) (1 μL) and sterile distilled water to make the final reaction volume of 49 μL. Then 1 μL of *Pfu* Turbo polymerase (2.5 U/μL) was added to the mix and a polymerase chain reaction (PCR) was performed using a thermal cycler (DNA Engine, MJ Research, Inc., MA, USA). The PCR cycle conditions were shown in Table 3.1, following the manufacture's instructions and the size of the plasmid DNA. After the PCR reaction, the mixture was

incubated with 1 μL of *Dpn* I (10U/μL) for 1 hour to digest parental dsDNA. The mixture was kept in the freezer (–20°C).

Table 3.1 PCR cycle conditions.

Segment	Number of Cycles	Temperature	Time
1	1	95 °C	30 s
2	18	95 °C	30 s
		55 °C	1 min
		68 °C	10 min
3		4 °C	∞

3.2.2 Transformation of DNA plasmids

Desired mutant or plasmid DNAs were transformed into XL 1-Blue supercompetent *E. coli* (Stratagene, CA, USA) for ρ_1, ρ_2, rat GIRK1, rat GIRK4, $GABA_{B(1b)}$ and $GABA_{B2}$ subunits or One Shot® TOP10/P3 competent cells (Invitrogen Australia Pty. Ltd. VIC, Australia) for α_1, β_2 and γ_{2L} subunits. Transformation was carried out according to the manufacture's instructions.

Briefly, for XL 1-blue supercompetent *E. coli*, plasmid DNA (1 μL; 100 ng/μL) and the supercompetent cells (30-50 μL) were combined in a microcentrifuge tube and incubate on ice for 10 minutes. Then the mixture was then heat shocked by placing the tube in a 42 °C water bath for 1 minute before returning on ice for further 5 minutes incubation. Transformed cells were then incubated in LB broth (500 μL; 10g/L typtone, 5 g/L yeast extract, 5 g/L NaCl; Sigma Chemical Co. Ltd) for ρ_1 and ρ_2 or NZYM broth (500 μL) (BIO 101, Inc., CA, USA) for GIRK1, rat GIRK4, $GABA_{B(1b)}$ and $GABA_{B2}$ at 37 °C for at least 30 minutes (Labec Incushaker, Crown Scientific, Sydney, Australia). Following incubation, the cultures were spread on LB agar (Sigma Chemical Co. Ltd) plates containing ampicillin (100 μg/ml). Plates were air dried then incubated at 37 °C for at least 16 hours.

For One Shot® TOP10/P3 competent cells, cells (50 μL) were thawed on ice and combined with plasmid DNA (1 μL; 100 ng/μL) and incubated on ice for 30 minutes. Then the mixture was heat shocked by placing the tube in a 42 °C water bath for 30 seconds. Transformed cells were then incubated in pre-warmed SOC medium (250 μL; 20g/L bacto-typtone, 5 g/L bacto-yeast extract, 0.5 g/L NaCl, 2.5 mM KCl, 10 mM $MgCl_2$, 20 mM glucose) (Invitrogen Australia Pty. Ltd. VIC, Australia) at 37 °C for exactly 1 hour at 225 rmp in a shaking incubator (Labec Incushaker, Crown Scientific, Sydney, Australia). Following incubation, the cultures were spread on LB agar (Sigma Chemical Co. Ltd) plates containing tetracycline (10 μg/ml) and ampicillin (50-100 μg/ml). Plates were air dried then incubated at 37 °C for at least 16 hours.

3.2.3 Growth of *E. coli.* containing DNA plasmids

Isolated bacterial colonies were picked and placed in 50 mL Falcon Tubes (Becton Dickinson, Sydney, Australia) containing LB broth (5 mL) with ampicillin (100 μg/ml) for ρ_1 and ρ_2, NZYM broth (5 mL) with ampicillin (100 μg/ml) for rat GIRK1, rat GIRK4, $GABA_{B(1b)}$ and $GABA_{B2}$ or LB broth (5 mL) with ampicillin (50-100 μg/mL) and tetracycline (10 μg/mL) for α_1, β_2 and γ_{2L} subunits. Inoculated media was then incubated for at least 16 hours at 37 °C in a shaking incubator (225 rpm). Glycerol stocks are made from the inoculated media, which contain 20 % glycerol. They were snapped frozen using dry ice and ethanol bath, and stored at -80°C.

3.2.4 Purification of plasmid DNA

Qiagen Spin Miniprep Kit (Qiagen, VIC, Australia) was used to purify wild-type and mutated plasmid DNA from *E. Coli* cells. Cells were harvested in a microcentrifuge tube by centrifugation (17900 x g; Eppendorf Centrifuge 5417R, Hamburg, Germany) for 2 minutes at room temperature. The supernatant was removed and the cell pellet was resuspended in Cell Resuspension Solution (250 μL; 50 mM Tris (pH 8), 10 mM EDTA, 100 μg/ml of RNase A), followed by Cell Lysis Solution (250 μL; 200 mM NaOH,

1 % SDS) to lyse the cell membrane. The mixture was thoroughly mixed and once the solution was clear Cell Neutralizing Solution (350 μL; 4.2 M Gu-HCl, 0.9 M CH_3COOK, pH 4.8) was added to precipitate chromosomal DNA and cell membranes. The precipitant was then pelleted by centrifugation for 10 minutes at 17900 x g. The clear supernatant containing plasmid DNA was retrieved and purified by QIAprep spin column and centrifuged for 1 minute (17900 x g). The flow-through was discarded and the column was subsequently washed by applying PB column washing buffer (500 μM; 5 M Gu-HCl, 10 mM Tris-HCl (pH 6.6) and 30 % ethanol), then it was centrifuged for 1 minute (17900 g). After discarding the flow-through the column was washed with PE washing buffer (750 μL; 10 mM Tris-HCl (pH 7.5) and 80 % ethanol) and it was centrifuged for 1 minute (17900 x g). Discard the flow-through and the column was spun for an additional minute (17900 x g) to remove the excess washing buffer trapped in the column. Plasmid DNA was eluted by the application of Elution buffer (50 μL; 10 mM Tris-HCl, pH 8.5) to the column and let stand for 1 minute before centrifuging (17900 x g) it over a microcentrifuge tube for 1 minute to collect the eluant.

The quantification and qualification of synthesized plasmid DNAs were determined absorbance at 260 nm and 280 nm using Nanodrop Spectrophotometer (Thermo Scientific, Wilmington, DE, USA). The purity of plasmid DNAs were accessed using the ratio of absorbance at 260 nm and 280 nm and a ratio of ~1.8 is generally accepted as pure (Thermo Scientific T042 technical Bulletin). For nucleic acid quantification, the Beer-Lambert equation was applied to use a factor with units of ng-cm/microliter (Equation 1).

$c = (A * \varepsilon) / b$ Equation 1

Where c is the nucleic acid concentration in ng/μl, A is the absorbance in AU, ε is the wavelenghth-dependent extinction coefficient in ng-cm/microliter and b is the pathlength in cm.

The presence of plasmid DNAs were also confirmed by agarose gel electrophoresis (0.9 %) using the GelDoc 1000 (Bio-Rad Laboratories, Hercules, CA, USA) and Molecular Analyst® (Bio-Rad Laboratories).

3.2.5 Mutation verification

Successful mutagenesis was confirmed by sequencing the whole gene of interest using appropriate primers. Samples of plasmid DNA were then sent to the Australian Genome Research Facility Ltd. (AGRF, Westmead Millennium Institute, Westmead, Australia). The samples typically contained, plasmid DNA (600-1000 ng), primer (0.8 pmol/ μL) and sterile distilled water to make the final reaction volume of 12 μL.

3.2.6 Linearization and purification of DNA

Plasmid DNA was linearized by incubation with *Xba*I enzyme for ρ_1 and rat GIRK4, *Eco*RI enzyme for $GABA_{B1b}$, $GABA_{B2}$, rat GIRK1, *Eco*RV enzyme for ρ_2, and *Not*I enzyme for α_1, β_2, and γ_{2L}, for 2 hours at 37 °C. Linearized DNA was purified by QIAquick PCR Purification Kit (Qiagen, VIC, Australia). Briefly, five volumes of buffer PB was added to the reaction mixture and mixed thoroughly. The mixture was then transferred to a QIAquick column and it was centrifuged (17900 x g) for 1 minute to bind the linearized DNA to the column. The flow-through was discarded and the column was washed by adding PE washing buffer (750 μL; 10 mM Tris-HCl (pH 7.5) and 80 % ethanol) and centrifuged (17900 x g) for 1 minute. After discarding the flow-through, the column was spun for an additional minute (17900 x g) to remove the excess washing buffer trapped in the column. Linearized DNA was eluted by the application of Elution buffer (30 μL; 10 mM Tris-HCl, pH 8.5) to the column and let stand for 1 minute before centrifuging (17900 x g) it over a microcentrifuge tube for 1 min to collect the eluant.

To ensure complete linearization of the plasmid DNA, agarose gel electrophoresis (0.9 %) using the GelDoc 1000 (Bio-Rad Laboratories, Hercules, CA, USA) and Molecular Analyst® (Bio-Rad Laboratories) was carried out.

3.2.7 cRNA synthesis

cRNA for ρ_1, ρ_2, α_1, β_2, γ_{2L}, rat GIRK1, rat GIRK4, $GABA_{B(1b)}$ and $GABA_{B2}$ were synthesized from linearized plasmid DNA using the T7 mMESSAGE mMACHINE kit (Ambion, Austin, TX, USA). The transcription reaction mixture contained linearized DNA (1 μg), reaction buffer (2 μL; salts, buffer, dithiothreitol and other ingredients), ribonucleotide mix (10 μL; 15 mM ATP, 15 mM CTP, 15 mM UTP, 2 mM GTP, 8 mM Cap Analog) and T7 enzyme mix (2 μL; T7 RNA polymerase and placental RNase inhibitor in 50% glycerol). The total reaction volume was kept at 20 μL. The reaction was incubated for 90 minutes at 37 °C. The RNA produced was purified by lithium chloride precipitation methods. Briefly, the reaction mixture was mixed thoroughly with 30 μL of Nuclease-free water and 30 μL of LiCl precipitation solution then it was chilled for at least 30 minutes at –20°C. Then, the mixture was centrifuged at 4 °C for 15 minutes (20817 x g; Eppendorf Centrifuge 5417R, Hamburg, Germany) to collect the RNA pellet. The supernatant was carefully removed and the RNA pellet was washed with 70 % ethanol (200 μL), then the mixture was centrifuged (15 minutes at 20817 x g) again to remove unincorporated nucleotides. 70 % ethanol was then carefully removed and the RNA pellet was incubated at 37 °C for 5 minutes to remove all ethanol. The RNA pellet was resuspended in Nuclease-free water (10-20 μL).

The quantification and qualification of synthesized cRNAs were determined absorbance at 260 nm and 280 nm using Nanodrop Spectrophotometer (Thermo Scientific, Wilmington, DE, USA). The purity of cRNAs were accessed using the ratio of absorbance at 260 nm and 280 nm and a ratio of ~2.0 is generally accepted as pure (Thermo Scientific T042 technical Bulletin). The presence of cRNAs were also confirmed by agarose gel electrophoresis (0.9 %) using the GelDoc 1000 (Bio-Rad Laboratories, Hercules, CA, USA) and Molecular Analyst® (Bio-Rad Laboratories).

3.3 Methods – Electrophysiology

3.3.1 Preparation and injection of *Xenopus laevis* oocytes

Xenopus laevis oocytes are widely used as a reliable expression system for LGICs receptors. For this work, the lack of endogenous GABA receptors allows us examine the expressed receptors in isolation.

Lobes of ovaries from Female *Xenopus laevis* (South Africa clawed frogs), which were anaesthetized with tricane (850 mg/500 mL), were harvested in accordance with the National Health and Medical Research Council (NHMRC) of Australia's ethical guidelines and approved by the University of Sydney Animal Ethics Committee. The lobes were rinsed with oocyte releasing buffer 2 (OR2: 82.5 mM NaCl, 2 mM KCl, 1 mM $MgCl_2.6H_2O$, 5 mM HEPES) and separated evenly by tweezers. The lobes were then incubated with collagenase A (Boehringer Manheim, Germany) (2 mg/mL in OR2) at 18 °C to release and defolliculate the oocytes. Stage V-VI oocytes were collected and stored in Frog Ringer buffer (ND96: 96 mM NaCl, 1 mM $MgCl_2.6H_2O$, 1.8 mM $CaCl_2.2H_2O$, 5 mM HEPES supplemented with 2.5 mM sodium pyruvate, 0.5 mM theophylline) with shaking at 18 °C.

Micropipettes were made using a microprocessor-controlled micropipette puller (PUL-100, World Precision Instruments, Inc., Sarasota, FL) and the tip was blunted to diameter 10-20 μm. They were filled with mineral oil (Sigma Chemical Co. Ltd) and cRNA solution was pulled into the micropipette using negative pressure. Stage V-VI oocytes were injected with 10-15 ng of cRNA. Mixtures of different cRNA were made for heteromeric receptor expressions. A mixture of α_1, β_2 and γ_{2L} cRNA at ratio of 1:1:10 was used for $\alpha_1\beta_2\gamma_{2L}$ receptor expression and a mixture of rat GIRK1, rat GIRK4, $GABA_{B(1b)}$ and $GABA_{B2}$ cRNA at the ratio of 1:1:1:2 was used to express $GABA_B$ (1b,2) receptors co-expressed with rat GIRK1 and 4 channels. After injection, the oocytes were stored at 18 °C with constant oscillation in ND 96 solution

supplemented with 2.5 mM sodium pyruvate, 0.5 mM theophylline, gentamycin (50 μg / ml) and tetracycline (2.5 mg/ml). Storage buffer was changed daily.

3.3.2 Two-electrode voltage-clamp methods

The two-electrode voltage clamp method was employed to assess GABA ligands activities at GABA receptors or the effect of mutations on the function of $GABA_C$ (ρ_1) receptors have been examined.

Two to eight days after injections, the activity was measured by two-electrode voltage clamp recording using Geneclamp 500 amplifier (Axon Instruments, Foster City, CA), a MacLab 2e recorder (AD Instruments, Sydney, NSW, Australia), and Chart version 5.5.6 program. Oocytes expressing receptors were placed in a cell bath and clamped at -60 mV with continuous flow of ND96 buffer. The recording microelectrodes were fabricated using PUL-100 micropipette puller (World Precision Instruments, Inc., FL, USA) and filled with 3 M KCl. The external bath reference electrode was a Ag^{2+}/AgCl electrode.

To collect pharmacological data, the cell bath was continuously perfused with ND96 and briefly switched to solutions containing drugs made with ND96 solution. Stock solutions of GABA ligands were prepared using MilliQ water or DMSO in the case of gabazine and its analogues. Drugs were stored at –20°C. During experiments, stock solutions were diluted as required with ND96. The concentrations of gabazine and its analogues were made with the total concentration of 0.8 % DMSO and not tested higher than 3 mM concentration due to the solubility concentrations above this. During the recording, the revel of receptor expression was determined by the application of maximum concentration GABA that produces maximum current (EC_{max}) (*e.g.* for $GABA_C$ ρ_1 wild-type receptors, EC_{max} = 100 μM). If EC_{max} GABA produced at least 100 nA of current receptor expression was considered sufficient. To construct agonist concentration-response curves, known concentrations of compounds were applied until maximum responses were obtained. In the case of inhibitory concentration response curves, antagonist effects were tested in the presence of

GABA concentration which effectively activates 50 % of the maximum response (EC_{50}). To examine the competitive nature of antagonists, a complete GABA concentration-response curve was obtained in the presence of a known concentration of antagonist.

When recording the function of $GABA_B$ (1b,2) receptors co-expressed with rat GIRK1 and 4 channels, the pharmacological measurement was performed after a two minute perfusion of ND96 and 45 mM K^+ buffer (45K; 45 mM NaCl, 45 mM KCl, 1 mM $MgCl_2$, 1.8 mM $CaCl_2$, 5 mM HEPES). Traces recorded in ND96 buffer were substracted offline from traces recorded in 45 mM K^+ buffer to correct the leak currents from endogenous oocyte. While recording, the oocytes were initially superfused with ND96 buffer until a stable baseline current was obtained, and then switched to 45 mM K^+ buffer.

Compounds were superfused till a steady baseline was achieved and the washing intervals were depending on the nature of receptors and compounds tested at the time. Typically, for ρ_1 and ρ_2 homomeric receptors, 5 minutes of washing interval was performed between doses. However, when testing SR-95531 and its analogues 10 minutes of washing interval was performed. When testing $\alpha_1\beta_2\gamma_{2L}$ heterometric receptors, 8 minutes of washing interval was performed between doses. At the beginning of the recording, each cell was tested by Zn^{2+} (100 μM) with the presence of GABA EC_{50} (30 μM) to ensure γ_{2L} incorporation. No GABA current inhibition by Zn^{2+} was considered to be the successful expression of $\alpha_1\beta_2\gamma_{2L}$ receptors. For $GABA_B$ receptors co-expressed with rat GIRK1 and rat GIRK4 channels, 6 minutes of washing interval was performed between does with 45 mM K^+ buffer.

3.4 Pharmacological data analysis

Current responses were normalized to the maximum GABA-activated current recorded in the same cell and expressed as a percentage of this maximum and fitted by least squares to Hill equation (Equation 2). GABA concentration response curves

were generated using GraphPad PRISM 5.02 (GraphPad software San Diego, CA). For other agonists tested at GABA receptors, the responses were normalized by GABA EC_{max} concentrations in order to construct their concentration response curves.

$$I = I_{max}[A]^{nH}/(EC_{50}{}^{nH} + [A]^{nH}) \qquad \text{Equation 2}$$

Where I is the current response to a known concentration of agonist, I_{max} is the maximum current obtained, [A] is the agonist concentration, EC_{50} is the concentration of agonist at which current response is half maximal and n_H is the Hill coefficient.

Dissociation equilibrium constants (K_B) were estimated *via* the Schild equation (Equation 3). Where [B] is the antagonist concentration, [A] is the EC_{50} of GABA in the presence of antagonist, [A*] is the EC_{50} of GABA in the absence of antagonist. The Schild plot of log([A]/[A*] – 1) versus log [B] was fitted and if the slope was sufficiently close to one indicated B was a competitive antagonist. The intercept on the x-axis provided an estimate of log K_B. Data are expressed as mean ± standard error of the mean (SEM).

$$K_B = [B]/([A]/[A^*] - 1) \qquad \text{Equation 3}$$

The inhibitory concentration curves were generated using GraphPad PRISM 5.02 and IC_{50} values were calculated using equation 4.

$$I = I_{max}[A]^{nH}/(IC_{50}{}^{nH} + [A]^{nH}) \qquad \text{Equation 4}$$

I is the peak current at a given concentration of agonist, I_{max} is the maximal current generated by the concentration of agonist, [A] is the concentration of GABA, IC_{50} is the antagonist concentration, which inhibits 50% of the maximum GABA response, and n_H is the Hill coefficient.

3.4.1 Estimating $\tau_{Deactivation}$ for the GABA deactivation phase

The deactivation phase of the currents produced by GABA EC_{50} concentrations were fitted with a monoexponential decay curve using GraphPad PRISM 5.02 (GraphPad software San Diego, CA) to estimate the $\tau_{Deactivation}$ for ρ_1 wild-type and mutant receptors.

3.5 Statistical analysis

Student's t-test was performed to determine the statistical significance of the change in EC_{50}, IC_{50} and $\tau_{Deactivation}$ values at $\rho_1$wild-type and $\rho_1$mutants. Two-tailed distributions, unequal variance and log of EC_{50}, IC_{50} or $\tau_{Deactivation}$ values from $\rho_1$wild-type and $\rho_1$mutants were used where appropriate.

Chapter 4:

GABA binding conformations

Chapter 4: GABA binding conformations

4.1 GABA binding conformations at GABA receptor ligand binding site

GABA **1** contains three rotatable carbon-carbon bonds that give rise to multiple configurations (Figure 4.1). The various low energy conformations of the molecule are important for its inhibitory effects in the central nervous system (CNS), as different conformations of GABA interact with different classes of GABA receptors, enzymes and transporters essential for developing potent and subtype selective agents.

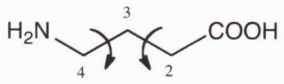

GABA **1**

Figure 4.1 Structure of GABA. *Rotatable carbon chain gives a rise to a number of different conformations of GABA.*

3-fluoro-GABA enantiomers (3F-GABA) were introduced as conformational probes by O'Hagan and co-workers (O'Hagan, 2011). They explored various GABA binding conformations at $GABA_A$ ($\alpha_1\beta_2\gamma_2$) receptors and GABA transaminase by comparing relative agonist activities of the enantiomers (Deniau et al., 2007). Introduction of fluorine at the third carbon of GABA creates a stereogenic centre, resulting in (*S*)-3F-GABA **2** and (*R*)-3F-GABA 3 (Figure 4.2). Fluorine has a partial negative charge due to its electonegativity. It forms a dipole of the C-F bond and it favours a close interaction with the protonated ammonium group (ie., F···N+ attraction), which provides up to 5.0 kcal mol^{-1} stability (Gooseman et al., 2007; O'Hagan, 2008; Sun et al., 2005). Newman projections of the three staggered conformations of the enantiomers of 3F-GABA (Figure 4.2) suggests that both enantiomers prefer the gauche conformations due to the interaction between the

fluorine and ammonium group. In addition, there are two disfavoured conformers, where the fluorine and ammonium group are anti to each other (Figure 4.2). Using this concept, the preferred chiral binding mode was assessed by comparing the activities of enantiomers of 3F-GABA at $GABA_A$ ($\alpha_1\beta_2\gamma_2$) receptors and GABA transaminase (Deniau et al., 2007). It was found that both enantiomers of 3F-GABA were partial agonists with similar I_{max} and EC_{50} values at recombinant $\alpha_1\beta_2\gamma_2$ receptors suggesting that they bind at the receptor in a similar conformation around C3 and C4 (Conformaer **B**) (Deniau et al., 2007).

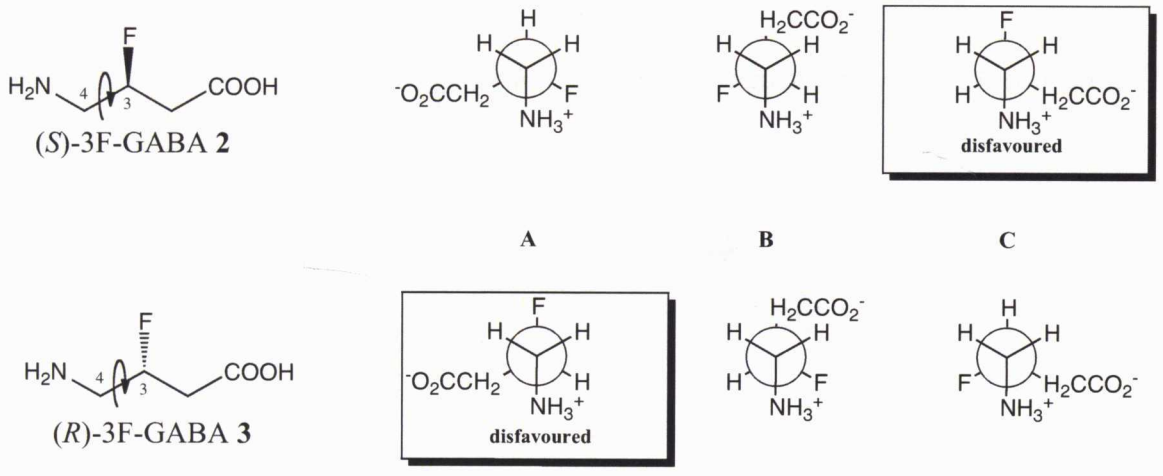

Figure 4.2 Newman projection showing staggered conformations. *Three staggered conformations **A**, **B** and **C** are shown after rotation around third and fourth carbons. Conformer **A** for (R)-3F-GABA and conformer **C** for (S)-3F-GABA are disfavoured, due to the fluorine and ammonium group are anti to each other. Figure adapted from reference (Deniau et al., 2007).*

4.2 Exploring GABA binding mode at $GABA_C$ receptor using conformational probes

Extensive mutagenesis studies and GABA analogue activities have contributed in developing homology models of the $GABA_C$ receptor binding site (Chebib et al., 2001; Chebib et al., 1997b; Crittenden et al., 2005; Harrison et al., 2006a; Lummis et al., 2005; Sedelnikova et al., 2005). However, the GABA binding mode at $GABA_C$

receptors is not yet clear. Several studies have hypothesized the binding mode of GABA using different homology models of the GABA binding site (Abdel-Halim et al., 2008; Adamian et al., 2009; Harrison et al., 2006b; Osolodkin et al., 2007; Sedelnikova et al., 2005), and each study proposes different amino-acid residues that make contacts with GABA, and their assessment of the conformation of the molecule on binding varies. One model (Harrison *et al.*, 2006b) predicts an extended structure for GABA binding whereas two of the models (Abdel-Halim *et al.*, 2008; Osolodkin *et al.*, 2007) predicted a similarly folded conformation, although they differ in the nature of the amino-acid residues contacted by the neurotransmitter. A quantitative structure-activity relationship model was constructed using conformationally restricted GABA analogues, and it was revealed that the putative optimal binding geometries of GABA at $GABA_C$ receptor binding site was similar to the biologically active TACA conformer (Figure 2.16) (Crittenden *et al.*, 2005).

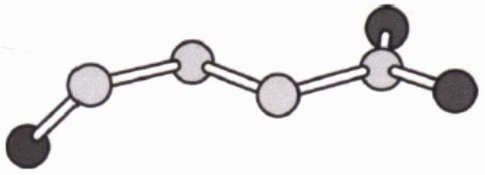

Figure 4.3 Proposed binding conformation of GABA at $GABA_C$ receptors. *Figure adapted from reference (Crittenden et al., 2005).*

Here, we investigated the binding mode of GABA at $GABA_C$ receptors using stereoisomers of 3F-GABA and new fluorinated GABA analogues, 2,3-difluoro-4-aminobutyric acids as conformational probes (Figure 4.4). GABA receptors were expressed on *Xenopus* oocytes and the activities of ligands were measured using two-electrode voltage clamp method.

The conformational probes were synthesized by Dr. Gildas Deniau, EASTChem School of Chemistry and Center of Biomolecular Sciences, The University of St. Andrews, United Kingdom and Dr. Luke Hunter, School of Chemistry, The University of New South Wales, Australia. Docking studies using the $GABA_C$ ρ_1 receptor

homology model (Abdel-Halim et al., 2008) were performed by Dr. Navnath Gavande and Dr. Munikumar Reddy Doddareddy, Faculty of Pharmacy, The University of Sydney, Australia. The conformational characteristics of compounds **4-7** (Figure 4.4) were probed using NMR simulation which was carried out by Dr. Luke Hunter, affiliation as above and Dr. Meredith Jordan, School of Chemistry, The University of Sydney, Australia.

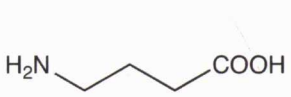

GABA **1**

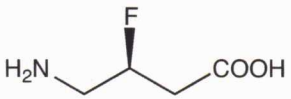

(*S*)-3F-GABA **2**

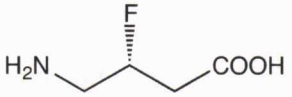

(*R*)-3F-GABA **3**

syn-Isomers

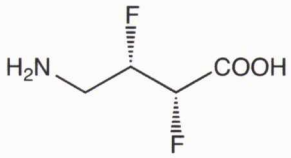

(2*S*,3*S*)-2,3-Difluoro-4-aminobutyric acid **4**

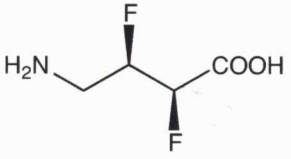

(2*R*,3*R*)-2,3-Difluoro-4-aminobutyric acid **5**

anti-Isomers

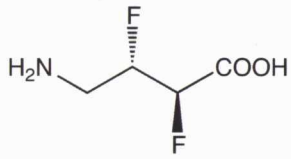

(2*R*,3*S*)-2,3-Difluoro-4-aminobutyric acid **6**

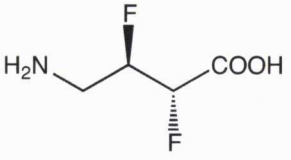

(2*S*,3*R*)-2,3-Difluoro-4-aminobutyric acid **7**

Figure 4.4 Structures of GABA 1, enantiomers of 3F-GABA 2,3 and stereoisomers of 2,3-difluoro-4-aminobutyric acid 4-5.

4.2.1 Results and discussion

4.2.1.1 Enantiomers of 3F-GABA at $GABA_C$ receptors

The activities of (*S*)-**2** and (*R*)-3F-GABA **3** were assessed at recombinant human $GABA_C$ (ρ_1 and ρ_2) receptors expressed in *Xenopus* oocytes, and the two-electrode voltage clamp was used to measure the response. GABA concentration response curves at (ρ_1) and (ρ_2) homomeric receptors revealed GABA being 2-fold more potent on (ρ_2) receptors (Table 4.1). Like GABA, compounds **2** and **3** displayed agonist activity without any antagonist effects. Both of the enantiomers were less potent agonists than GABA itself, by up to 10-fold for compound **2** and 20-fold for compound 3 (Figure 4.5, Table 4.1). This trend in potency was similar to what was observed previously with $GABA_A$ ($\alpha_1\beta_2\gamma_2$) receptors (Deniau *et al.*, 2007) and is probably due to fluorine reducing the pK_a of the amine (10.6 to 9.0), and thus weakening electrostatic interactions, such as hydrogen binding (H-bond) and cation-π interaction between the ligand carboxylate group and the arginine at position 104 (Arg104) and 158 (Arg158), to the surface of the receptors. This in turn suggests the folded binding conformation **C** (Figure 4.2) for GABA **1** best resemble the conformation of binding to the $GABA_C$ receptors. The data conflicts with one recent model (Harrison *et al.*, 2006b) which suggests a linear extended structure for GABA binding to $GABA_C$ receptors. The two studies (Abdel-Halim *et al.*, 2008; Osolodkin *et al.*, 2007) that propose a folded conformation for GABA binding to $GABA_C$ receptors, also predict the same chiral sense for binding *i.e.* conformation **C** (Figure 4.3) rather than conformation **A**, therefore this study which compares compounds **2** and **3** reinforces that developing hypothesis.

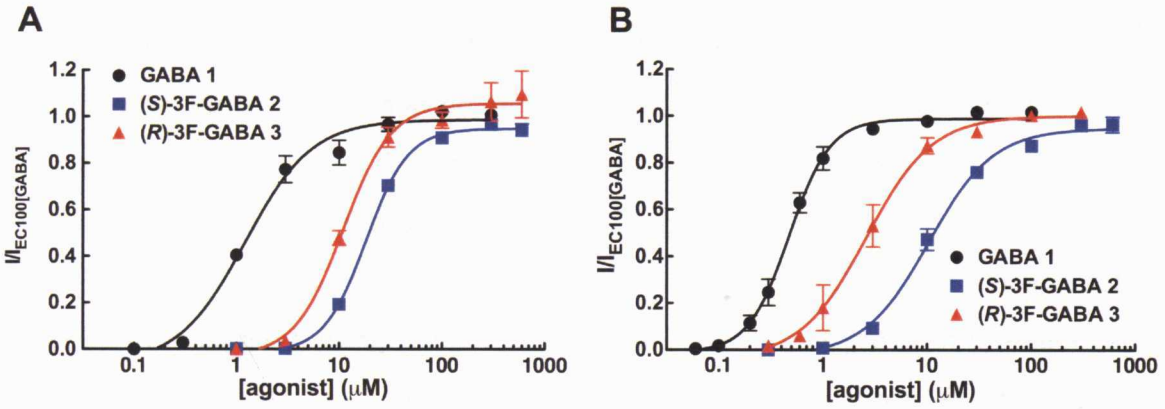

Figure 4.5 Concentration-response curves for GABA 1, (S)-3F-GABA 2 and (R)-3F-GABA 3 at $GABA_C$ receptors. ***A*** *at human (ρ_1) receptors and* ***B*** *at human (ρ_2) receptors expressed in Xenopus oocytes. Data are the mean ± SEM (n = 3-4 oocytes). Figure adapted from reference (Yamamoto et al., 2011a).*

Table 4.1 Pharmacological evaluation of compounds 1-3 at human human (ρ_1) and (ρ_2) receptors expressed in Xenopus oocytes.

	ρ_1 [a]	ρ_2 [a]
GABA **1**	EC_{50} = 0.81 ± 0.07 μM	EC_{50} = 0.48 ± 0.05 μM
(*S*)-3F-GABA **2**	EC_{50} = 18.72 ± 0.60 μM	EC_{50} = 10.76 ± 1.90 μM
(*R*)-3F-GABA **3**	EC_{50} = 11.10 ± 1.24 μM	EC_{50} = 2.92 ± 0.66 μM

[a] All data are the mean ± SEM (n = 3-4 oocytes).

To delineate the key interactions responsible for differences in potency, the structures of compounds **1-3** were flexibly docked into the ligand-binding site of a homology model of $GABA_C$ (ρ_1) receptor ligand binding site (Abdel-Halim et al., 2008) (Figure 4.6). Both ligands docked in the more favourable gauche conformation (O'Hagan, 2011), with the dipole of the C-F bond pointing towards the positively charged amino group of the ligands. The acidic groups of the ligands were flanked between the guanidium groups of arginine at position 104 (Arg104) and position 158 (Arg158) forming a salt bridges and H-bonds with the hydroxyl group of threonine at position 244 (Thr244). The basic amine group oriented towards the acidic amino acid, gulutamate at position 196 (Glu196), forming an H-bond. Additionally, the amino group of the ligands was shown to be making an H-bond with tyrosine at position 198 (Tyr198) and serine at position 168 (Ser168), which may be important for the shape and stability of the active site.

For both isomers the orientation of the C-F bond was examined for its interaction with other groups which may contributing their stability or instability in the binding site. There were no obvious short contacts to F in the case of (*S*)-3F-GABA **2**. In the case of (*R*)-3F-GABA **3**, the C-F bond is located 3.5 Å from a guanidium hydrogen of Arg104 (Figure 4.6). This is beyond a reasonable H-bonding distance for organic bound fluorine (Howard *et al.*, 1996), and the C-F to H-N angle is rather acute, however this interaction may contribute additional stabilisation for that isomer.

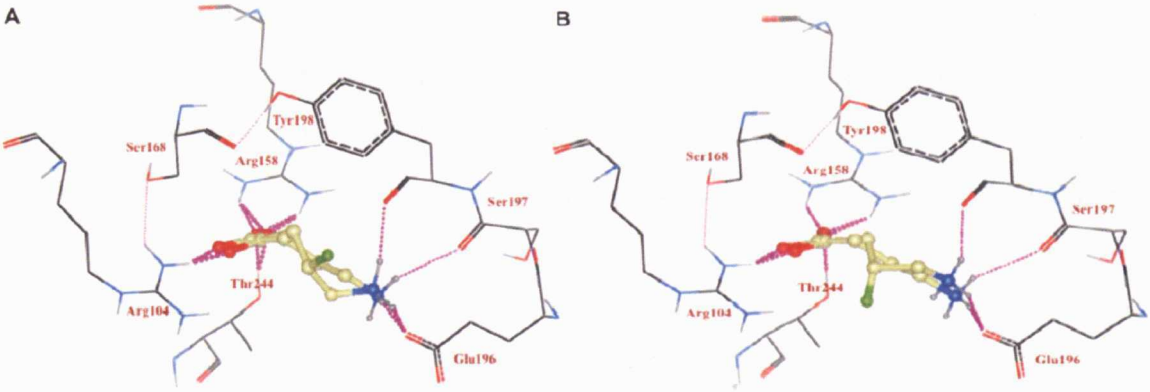

Figure 4.6 Enantiomers of 3F-GABA docked into the homology model of (ρ_1) receptor GABA binding site. ***A*** *GABA* ***1*** *and (S)-3F-GABA* ***2*** *docked in the binding site. Selected H-bonds are depicted with dashed pink lines.* ***B*** *GABA* ***1*** *and (R)-3F-GABA* ***3*** *docked in the binding site. Selected H-bonds are depicted with dashed pink lines. Figure adapted from reference (Yamamoto et al., 2011a).*

4.2.1.2 Stereoisomers of 2,3-difluoro-4-aminobutyric acids at GABA receptors

The introduction of fluorines at C2 and C3 positions lead to four stereoisomers of 2,3-difluoro-4-aminobutyric acids (**4-7**) (Figure 4.4). The highly polarized C-F bond participates in a variety of stereoelectronic interactions with neighbouring functional groups in ways that affect the molecular conformation. Therefore, compounds **4-7** were expected to form different preferred conformations leading to different binding properties at GABA receptors.

The pharmacology of compounds **4-7** was investigated at $GABA_A$ ($\alpha_1\beta_2\gamma_{2L}$), $GABA_B$ (1b,2) co-expressed with rat GIRK1 and rat GIRK4, and $GABA_C$ (ρ_1) receptors (Table 4.2). In the case of $GABA_A$ ($\alpha_1\beta_2\gamma_{2L}$) receptors, the *syn*-isomers **4** and **5** are inactive at 100 μM whereas the *anti*-isomers **6** and **7** exhibited modest antagonist activities (Figure 4.7). The higher $GABA_A$ activity of the *anti*-isomers **6** and **7** relative to the *syn*-isomers **4** and **5** is consistent with a folded binding conformation as predicted by previous studies (Deniau *et al.*, 2007; Dickenson *et al.*, 1990). However, the fluorine substituents of **4-7** were expected to lower the pK_a of the amino group, substantially decreasing the potency. Hence the magnitude of the activities at $GABA_A$ receptors is very small so this conclusion is rather tentative.

At the $GABA_B$ (1b,2) receptors, compound **4** was inactive, while **5**-**7** exhibited varying degrees of agonist activity with **5** being the most potent agonist (Figure 4.8). To our knowledge, no detailed model of the binding geometry of GABA at $GABA_B$ receptors has been created, so this result may be relevant to future endeavours in this regard.

At the $GABA_C$ (ρ_1) receptor some intriguing trends were observed (Figure 4.9 and Table 4.2). The *syn*-isomers **4** and **5** were more potent at $GABA_C$ receptors than the *anti*-isomers **6** and **7**, and this is consistent with a binding mode in which the GABA carbon chain adopts a *trans* conformation (Crittenden *et al.*, 2005). The high selectivity of compound **4** for $GABA_C$ over both $GABA_A$ and $GABA_B$ receptors is striking, and it is also interesting that compound **5** exhibited dual $GABA_B$/$GABA_C$ receptor selectivity despite the closer structural relationship between $GABA_A$ and $GABA_C$ receptors. Of particular note is the observation that compound **4** is an agonist at $GABA_C$ (ρ_1) receptors while compound **5** is an antagonist (Figure 4.10 and Table 4.2).

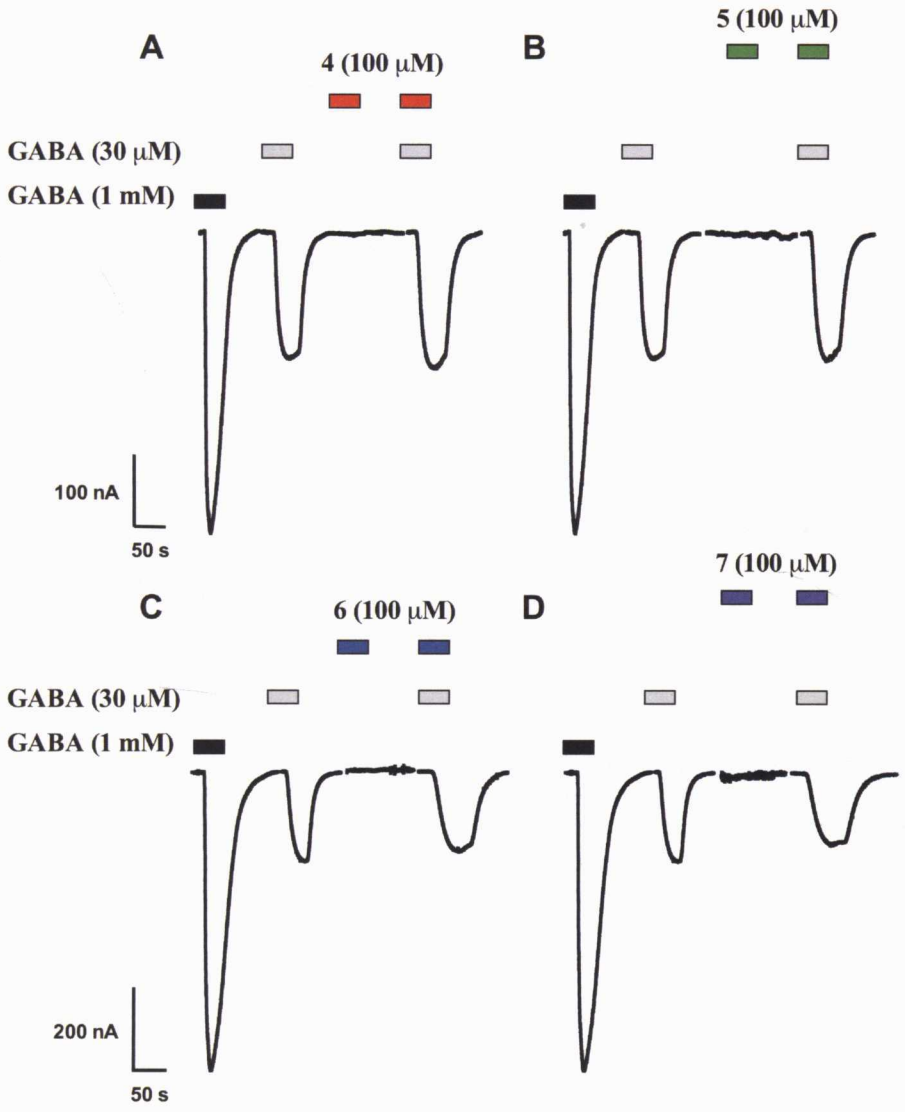

Figure 4.7 Sample current trace (nA vs sec) showing the effect of compounds 4-7 at GABA$_A$ ($\alpha_1\beta_2\gamma_{2L}$) receptors expressed in Xenopus oocytes. ***A 4*** *had no agonist effect at 100 μM (red bar), and did not inhibit the current produced by GABA (30 μM) (grey bar).* ***B 5*** *had no agonist effect at 100 μM (green bar), and did not inhibit the current produced by GABA (30 μM) (grey bar).* ***C 6*** *had no agonist effect at 100 μM (blue bar). However the current produced by GABA (30 μM) (grey bar) was inhibited by 5.3 % in the presence of* ***6*** *(100 μM) (blue bar).* ***D 7*** *had no agonist effect at 100 μM (purple bar). However the current produced by GABA (30 μM) (grey bar) was inhibited by 8.3 % in the presence of* ***7*** *(100 μM) (purple bar). Figure adapted from reference (Yamamoto et al., 2011b).*

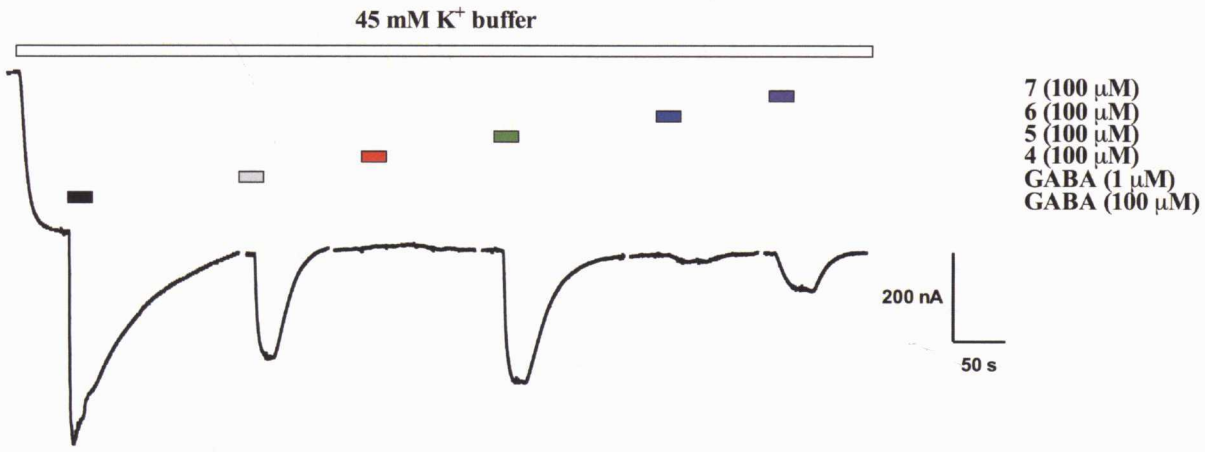

Figure 4.8 Sample current trace (nA vs sec) showing the effects 4-7 at human $GABA_B$ (1b/2) receptors co-expressed with GIRK1/4 channels in Xenopus oocytes. *In the presence of 45 mM K+ buffer (open bar),* ***4*** *had no effect as agonist or antagonist when tested at 100 μM (red bar).* ***5*** *(100 μM) activated the receptor by 106.4 % compared to the current produced by GABA EC_{50} (grey bar).* ***6*** *(100 μM; blue bar) and* ***7*** *(100 μM; purple bar) produced weak agonist responses alone (4.6 % and 23 %, respectively) without inhibiting the response produced by GABA (1 μM). Figure adapted from reference (Yamamoto et al., 2011b).*

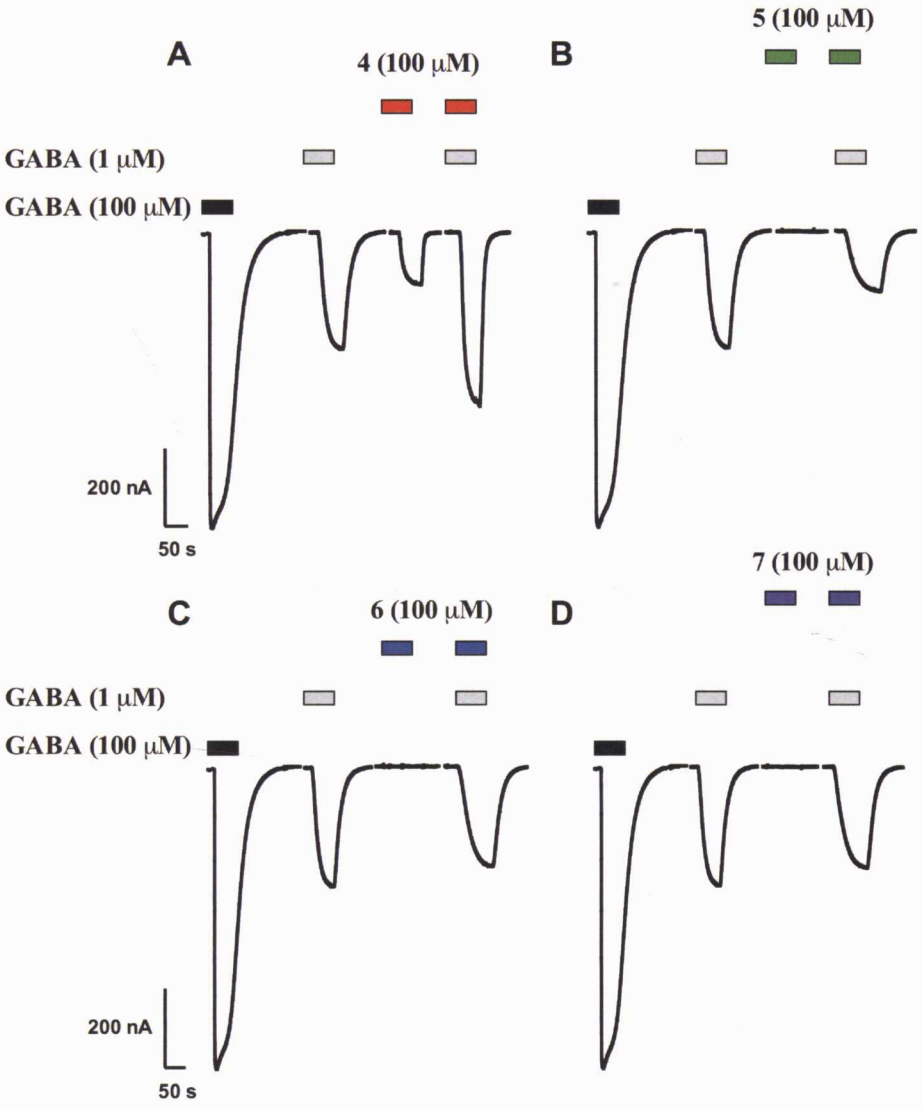

Figure 4.9 Sample current trace (nA vs sec) showing the effect of 4-7 at $GABA_C$ (ρ_1) receptors expressed in Xenopus oocytes. ***A*** *Sample current trace showing weak agonist effect of* ***4*** *at 100 μM (red bar).* ***4*** *had additive effects in the presence of GABA (1 μM) (grey bar) indicating no antagonist properties.* ***B 5*** *had no agonist effect at 100 μM (green bar) but inhibited the current produced by GABA (1 μM) (grey bar) by 50.2 %.* ***C 6*** *had no agonist effect at 100 μM (blue bar). However the current produced by GABA (1 μM) (grey bar) was inhibited by 14.8 % in the presence of* ***6*** *(100 μM) (blue bar).* ***D 7*** *had no agonist effect at 100 μM (purple bar). However the current produced by GABA (1 μM) (grey bar) was inhibited by 15.4 % in the presence of* ***7*** *(100 μM) (purple bar). Figure adapted from reference (Yamamoto et al., 2011b).*

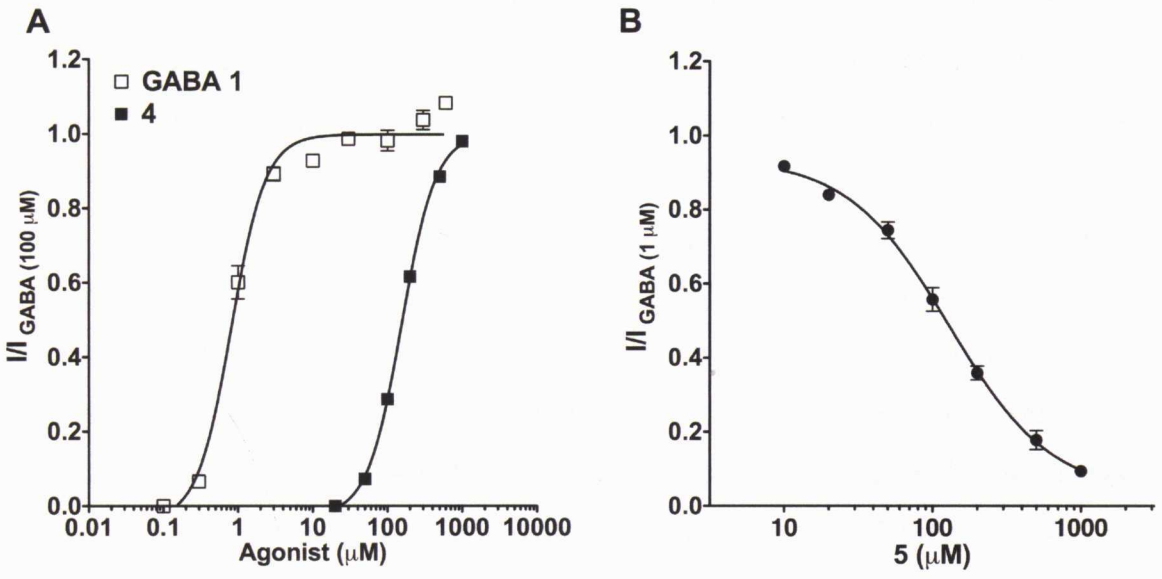

Figure 4.10 Pharmacology of compound 4 and 5 at human $GABA_C$ (ρ_1) receptors expressed in Xenopus oocytes. ***A*** *Concentration response curves for GABA* ***1*** *and compound* ***4****. Each data point represents the mean ± SEM (n = 4 oocytes). All data are normalized with $I_{GABA\ (100\ \mu M)}$.* ***B*** *Inhibitory concentration response curve for compound* ***5****. Each data point represents the mean ± SEM (n = 4 oocytes). All data are normalized with $I_{GABA\ (1\ \mu M)}$. Figure adapted from reference (Yamamoto et al., 2011b).*

Table 4.2 Pharmacological evaluation of compounds 4-7 at GABA receptors expressed in Xenopus oocytes.

	$GABA_A$ ($\alpha_1\beta_2\gamma_{2L}$) [a]	$GABA_B$ (1b,2) [a]	$GABA_C$ (ρ_1) [a]
4	0 % [b]	0 % [c]	EC_{50} = 154.7 ± 5.4 μM [d]
5	0 % [b]	106.4 ± 2.8 % [c]	IC_{50} = 128.4 ± 8.2 μM [e]
6	5.3 ± 3.4 % [b]	4.6 ± 2.0 % [c]	14.8 ± 1.2 % [f]
7	8.3 ± 2.2 % [b]	23.0 ± 2.5 % [c]	15.4 ± 3.6 % [f]

[a] All data are the mean ± SEM (n = 3-4 oocytes). [b] Percent inhibition of 100 μM compound in presence of EC_{50} GABA **1** (30 μM). [c] Percent activation by 100 μM compound compared to the response produced by EC_{50} GABA **1** (1 μM). [d] Agonist activity (Figure 4.10**A**). [e] Antagonist activity (Figure 4.10**B**). [f] Percent inhibition of 100 μM compound in presence of EC_{50} GABA **1** (1 μM).

The conformational characteristics of compounds **4** and **5** were probed by NMR and molecular modelling studies. The lowest-energy geometries were found to be **4a** and **4b** (Figure 4.11). The *syn*-isomer **4** was found to have a strong preference for the fully extended conformation **4a** (Figure 4.11**A**) in aqueous solution. This conformation gives *gauche* alignment between C3-C4 bond due to the charge-dipole interaction ($F\cdots N^+$ attraction). Rotation about C3-C4 bond of conformer **4b** leads to the next higher energy conformer **4b** (Figure 4.11**A**), which also benefits from $F\cdots N^+$ proximity and the fluorine *gauche* effect. Both low-energy geometries of **4** contain a *trans* arrangement of the carbon atoms, and notably, the slightly higher-energy conformer **4b** closely resembles the proposed active geometry of GABA at $GABA_C$ (ρ_1) receptors (Figure 4.3) (Crittenden *et al.*, 2005).

In the case of the *syn*-isomer **5**, the minimum energy conformer was **5a** and this geometry has the same N-C-C-C-C arrangement as **4a** (Figure 4.11**B**). However, the next higher energy conformer was **5b** and contains a non-superimposable N-C-C-C-C arrangement compared with **4b**, so compound **5** cannot readily access the proposed GABA binding geometry at $GABA_C$ (ρ_1) receptors.

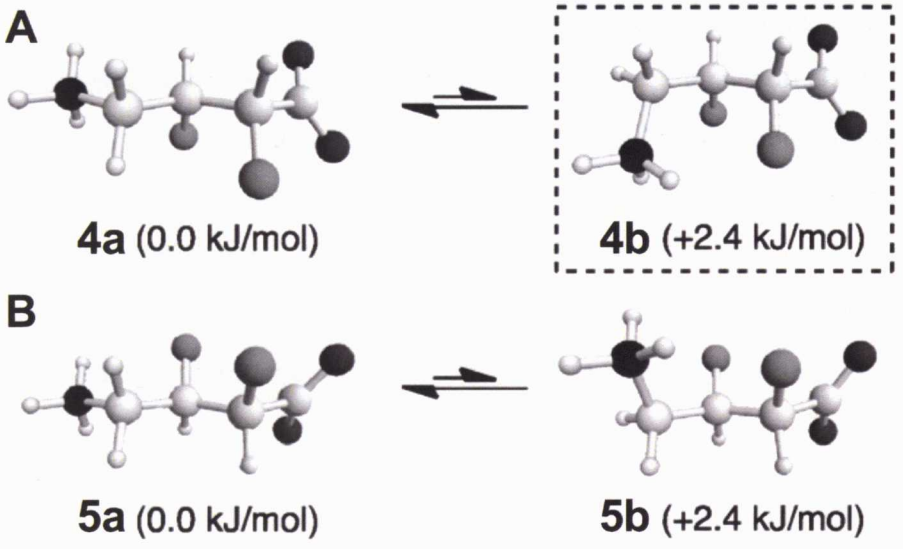

Figure 4.11 Lowest-energy conformations of compounds 4 and 5. *Structures resembling to the proposed $GABA_C$ receptor binding mode (4b) is highlighted. Figure adapted from reference (Yamamoto et al., 2011b).*

In an attempt to gain further information about the molecular interactions governing agonist *vs.* antagonist activity in this system, docking studies were performed using a homology model of the $GABA_C$ (ρ_1) receptor ligand binding site (Abdel-Halim *et al.*, 2008). The two lowest-energy conformers of **4** and **5** were rigidly docked in separate experiments (Figure 4.12). Previous studies identified several amino acid residues that are critical for binding, including Arg158 and Arg104 which form salt bridges with the GABA carboxylate group, and Tyr198 which forms a hydrogen bond and a cation-π interaction with the GABA ammonium group (Abdel-Halim *et al.*, 2008; Lummis *et al.*, 2005). When the fully extended conformer of **4a** is docked into the model of the receptor, no hydrogen bonding contact with Tyr198 was observed (Figure 4.12**A**), and so it was concluded that the fully extended conformer is unlikely to be the bioactive geometry. In contrast, when the next higher-energy conformer of **4b** is docked, the contact with Tyr198 is restored (Figure 4.12**A**). This next-higher energy conformer of **4** is close to the proposed $GABA_C$-active geometry (Figure 4.3) (Crittenden *et al.*, 2005).

When the enantiomeric ligand **5** was docked, both the fully extended and the next-higher energy conformers (**5a** and **5b**, respectively) made contacts with Arg158, Arg 104 and Tyr198 (Figure 4.12**B**). However, in both cases this entails a significantly altered docking pose that involves substantial deviation of the carbon chain from the alignment previously described by the proposed putative optimal binding geometries of GABA and in the study using compounds **2** and **3** (Figure 4.3, Figure 4.6) (Abdel-Halim *et al.*, 2008; Crittenden *et al.*, 2005). This deviation could lead to additional steric interactions with other binding site residues such as Thr244, possibly leading to a more open binding site and, hence, antagonist activity (Abdel-Halim *et al.*, 2008).

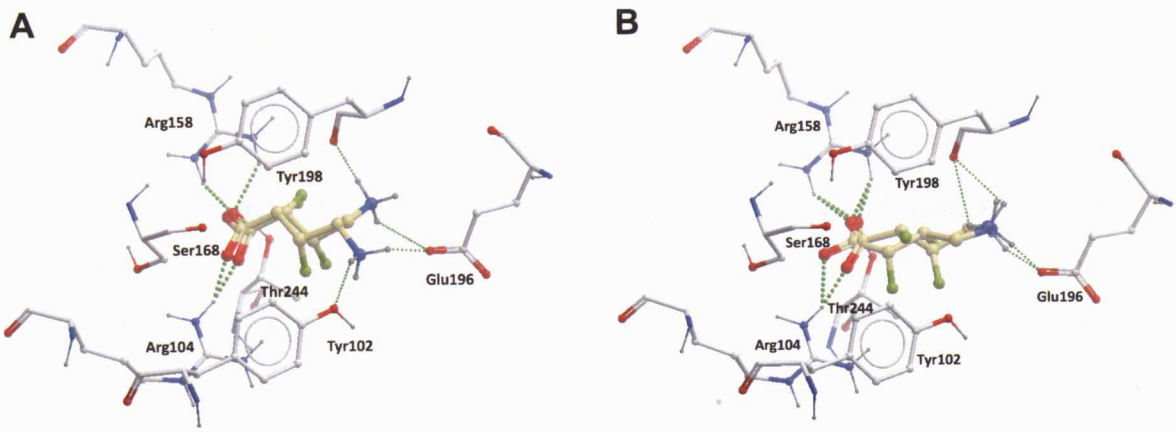

Figure 4.12 Compounds 4 and 5 docked into the homology model of (ρ_1) receptor GABA binding site. A *Overlay image of conformers* ***4a*** *and* ***4b*** *docked in the binding site. Selected H-bonds are depicted with dashed green lines.* ***B*** *Overlay image of conformers* ***5a*** *and* ***5b*** *docked in the binding site. Selected H-bonds are depicted with dashed green lines. Figure adapted from reference (Yamamoto et al., 2011b).*

4.3 Conclusion

In summary, the studies suggest a different mode of GABA binding at $GABA_A$ and $GABA_C$ receptors (Figure 4.13). The proposed mode of GABA binding at $GABA_C$ receptors provided by enantiomers of 3F-GABA and the stereoisomers of 2,3-difluoro-4-aminobutyric acids support the putative optimal binding geometries of GABA at $GABA_C$ receptors predicted by a quantitative structure-activity relationship model and the ρ_1 homology modelling study (Abdel-Halim *et al.*, 2008; Crittenden *et al.*, 2005). Furthermore it was found that the *syn*-isomers of 2,3-difluoro-4-aminobutyric acids (**4** and **5**) have opposite pharmacology at $GABA_C$ (ρ_1) receptors. These studies contribute to understanding the binding mode of GABA and to the pharmacology of GABAergic compounds at $GABA_C$ receptors. The findings will give insight into the design and development of new ligands with therapeutic values at GABA receptors.

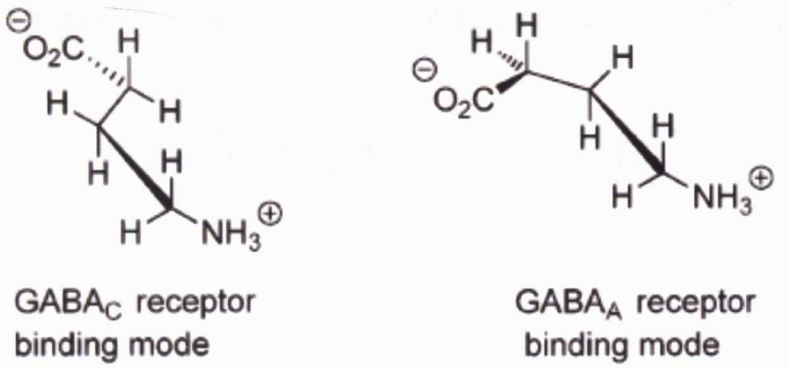

Figure 4.13 Proposed binding conformations of GABA 1 at $GABA_A$ and $GABA_C$ receptors. *Figure adapted from reference (Yamamoto et al., 2011a).*

Chapter 5:

Differentiating enantioselective actions of GABOB

Chapter 5: Differentiating enantioselective actions of GABOB

4-Amino-3-hydroxybutanoic acid (GABOB) is an endogenous molecule found within the central nervous system (CNS), possessing anticonvulsant properties (Johnston, 1996a). It is formed by two metabolic pathways: Either the metabolism of putrescine to γ-aminobutyric acid (GABA) and then hydroxylation of GABA at the third carbon (C3) (Nakao et al., 1991; Noto et al., 1988), or by the hydroxylation of putrescine to 2-hydroxyputrescine and then oxidative N-dealkylation to GABOB (Noto et al., 1988). Introducing a hydroxyl group at the C3 position of GABA generates a stereogenic centre, thus producing the enantiomers *R*-(–)-GABOB and *S*-(+)-GABOB (Figure 5.1). Of the two enantiomers, *R*-(–)-GABOB is the more potent anticonvulsant (Nakao et al., 1991) and has been shown to have a greater inhibitory effect on induced seizures in cat brain and rabbit motor cortex (Aishita et al., 1978; Katayama et al., 1977).

Like GABA, GABOB mediates its inhibitory effects by activating ionotropic ($GABA_A$ and $GABA_C$) and metabotropic ($GABA_B$) receptors. Both isomers of GABOB act as agonists at all three classes of GABA receptors. However there are differences in their potencies: The affinity of *S*-(+)-GABOB is higher than *R*-(–)-GABOB at $GABA_A$ receptors (Krogsgaard-Larsen et al., 1985; Roberts et al., 1981). In contrast, *R*-(–)-GABOB is the more potent agonist at $GABA_B$ and $GABA_C$ receptors (Falch et al., 1986; Hinton et al., 2008). While *S*-(+)-GABOB shows similar efficacy for $GABA_C$ receptors, it acts as a partial agonist at $GABA_B$ receptors (Ong et al., 2001).

Of particular interest to this study is the ionotropic $GABA_C$ receptor. $GABA_C$ receptors are members of the Cys-loop superfamily of ligand-gated which include nicotinic acetylcholine (nACh), serotonin type-3A ($5\text{-}HT_{3A}$), strychnine-sensitive glycine, $GABA_A$ receptors and invertebrate glutamate-gated chloride channels (GluCl) (Corringer et al., 2010; Hilf et al., 2009a; Miller et al., 2010; Thompson et al., 2010) and share a similar tertiary and identical quaternary pentameric structure (Ortells et

al., 1995). $GABA_C$ receptors are formed by ρ subunits (ρ_1-ρ_3) and exist as homopentameric receptors with distinct pharmacology compared to that of $GABA_A$ and $GABA_B$ receptors (Chebib et al., 2000; Zhang et al., 2008). They are highly expressed in retina and in distinct areas of the brain; cerebellum (Rozzo et al., 2002), hippocampus (Alakuijala et al., 2005), superior colliculus (Boue-Grabot et al., 1998) and lateral amygdala (Cunha et al., 2010). Experimental evidence suggests that $GABA_C$ receptors are potential therapeutic targets for the treatment of myopia (Stone et al., 2003), anxiety (Cunha et al., 2010), memory (Johnston, 2002) and sleep-related disorders (Arnaud et al., 2001).

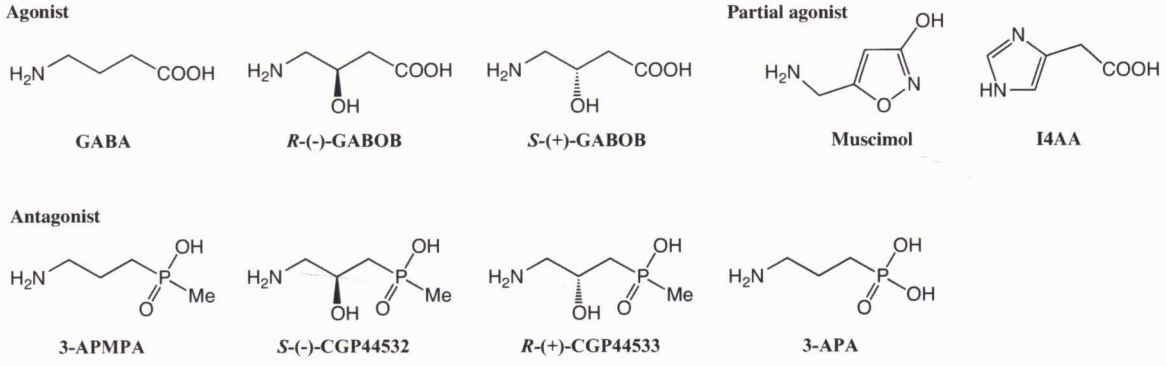

Figure 5.1 Structures of agonists; GABA, R-(−)-GABOB, S-(+)-GABOB, partial agonists; muscimol, I4AA and antagonists; 3-APMPA, S-(−)-CGP44532, R-(+)-CGP44533, 3-APA. *Figure adapted from reference (Yamamoto et al., 2012a)*

In this study, we docked the enantiomers of GABOB in our previously reported homology model of the ρ_1 receptor binding site (Abdel-Halim et al., 2008) (Figure 5.2) in order to elucidate the key interactions between the receptor and ligands. Threonine at position 244 (T244) in the ρ_1 subunit is located in loop C of the ligand binding site. This residue is highly conserved in chloride selective Cys-loop receptors, such as the $GABA_{A/C}$ and glycine receptors (Amin et al., 1994; Brejc et al., 2001). Our homology model predicts a possible hydrogen-bond (H-bond) formation between the acidic group of GABA and the hydroxyl group of T244 (Yamamoto *et al.*, 2011a) and a possible H-bond between the C3-hydroxyl group of GABOB and T244 (Figure 5.2). In addition, the model predicts there are no H-bonds between the C3-hydroxyl group of the phosphinic analogue of GABOB, *S*- and *R*-(3-amino-2-

hydroxypropyl)methylphosphinic acid (*S*-(–)-CGP44532 and *R*-(+)-CGP44533) and T244 (Figure 5.2). However, a possible H-bond was predicted with methyl phosphonate analogues of GABA, possibly as a result of the extra oxygen in the compound (Xie et al., 2011). To validate these predictions, we mutated T244 to explore the effect on affinity and efficacy of these ligands using molecular biology and electrophysiology techniques. Partial agonists were also examined to explore the effect of the mutation on channel gating.

Docking studies using the $GABA_C$ ρ_1 receptor homology model (Abdel-Halim et al., 2008) were performed by Dr. Munikumar Reddy Doddareddy, Faculty of Pharmacy, The University of Sydney, Australia.

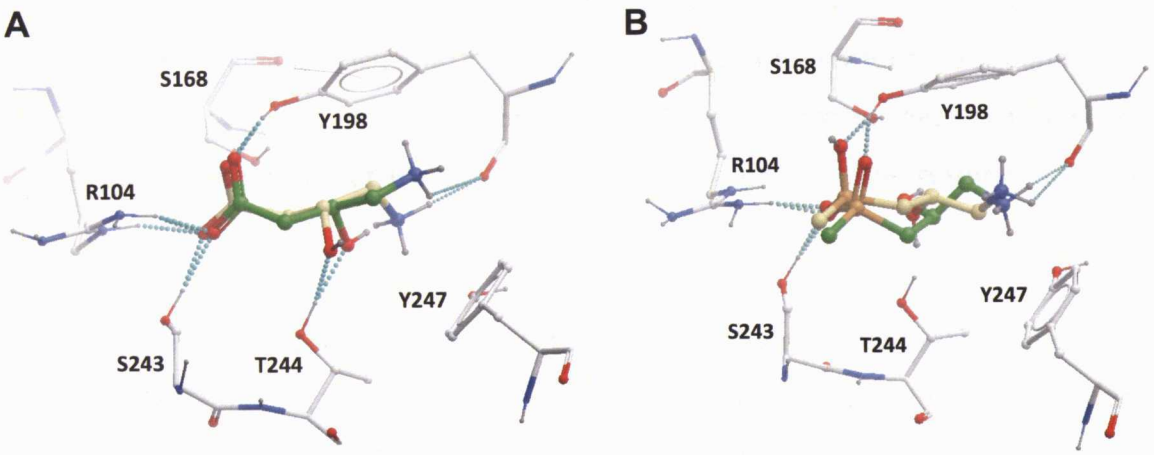

Figure 5.2 Ligands docked into the ρ_1 receptor GABA binding site. ***A*** *The hydroxyl group of R-(–)-GABOB (yellow) and S-(+)-GABOB (green) forming H-bond with the hydroxyl group of T244. Selected H-bonds are depicted with dashed cyan lines.* ***B*** *The hydroxyl group of R-(+)-CGP44533 (yellow) and S-(–)-CGP44532 (green) not interacting with T244. Selected H-bonds are depicted with dashed cyan lines. Figure adapted from reference (Yamamoto et al., 2012a).*

5.1 Results and discussion

5.1.1 Mutation at threonine 244

The role of the hydroxyl group on the side-chain of the threonine residue at position 244 (T244) was explored by mutating T244 to alanine (T244A), glycine (T244G), serine (T244S), valine (T244V), isoleucine (T244I), leucine (T244L) and phenylalanine (T244F). As previously reported, only the serine mutant (T244S) produced receptors that elicited a chloride current in response to GABA (Amin et al., 1994). The observed GABA EC_{50} value at ρ_1T244S mutant receptors was increased by 39-fold compared to ρ_1 wild-type receptors (Table 5.1), indicating that GABA has reduced potency for the mutant receptor. This is consistent with previous findings (Figure 5.3) (Amin et al., 1994). Altered GABA sensitivity indicates either a change in GABA binding for the orthosteric binding site or a change in receptor gating. Homology modelling predicts that the acidic group of GABA may form an H-bond with the hydroxyl group of T244 (Yamamoto *et al.*, 2011a), indicating that the change in GABA potency observed at the ρ_1T244S mutant is most likely the result of altered binding and/or gating.

Mutation of T244 to amino acids that lack a hydroxyl group in their side chain (T244A, T244G, T244V, T244I, T244L and T244F) resulted in a lack of GABA-mediated responses, even when GABA was tested at a concentration of 30 mM (n = 9-15). This suggests that a hydroxyl group at position 244 in $GABA_C$ ρ_1 receptors is important for GABA induced receptor activation. To assess the effect of the T244 mutation on receptor gating, we examined the activity of the partial agonists, muscimol and imidazole-4-acidic acid (I4AA), at ρ_1T244S mutant receptors. The intrinsic efficacy of muscimol at 100 μM produced 2.4 ± 0.8 % (n = 5) of the maximum response of GABA (1 mM) at ρ_1T244S mutant receptors, and it was reported that muscimol at 100 μM produce 79 % of the maximum response of GABA at ρ_1 wild-type receptors (Carland et al., 2004) (Figure 5.4**A**). We did not observe I4AA (1 mM, n = 4) acting as an agonist at ρ_1T244S mutant receptors (Figure 5.4**B**). However, at the concentrations we tested, muscimol and I4AA acted as antagonists (Muscimol; IC_{50} = 32.8 ± 2.2 μM, n =

6, I4AA; IC_{50} = 21.4 ± 1.7 μM, n = 4) (Figure 5.4**C**, **D** and **E**, Table 5.1). The conversion of a partial agonist to antagonist at mutant receptors infers that while the compound still binds to the receptor, they are unable to activate or gate the receptor. Thus, our results demonstrate that mutation of T244 alters receptor gating.

Interestingly, we and others (Amin *et al.*, 1994) showed that mutating T244 has a much more dramatic effect on GABA potency compared to mutating the adjacent serine residue (S243) of the ρ_1 subunit (Harrison et al., 2006a). Mutation of serine 243 to alanine (S243A) afforded mutant receptors that were functional, with GABA potency reduced only by approximately 2-fold compared to ρ_1 wild-type (Harrison et al., 2006a). The lack of a hydroxyl group in the residue at 243 did not strongly change the potency of GABA. However, our results confirm the fact that removal of the hydroxyl group at T244 was not tolerated (Amin et al., 1994), indicating that the T244 has a more important role in ρ_1 receptor GABA mediated channel gating than S243.

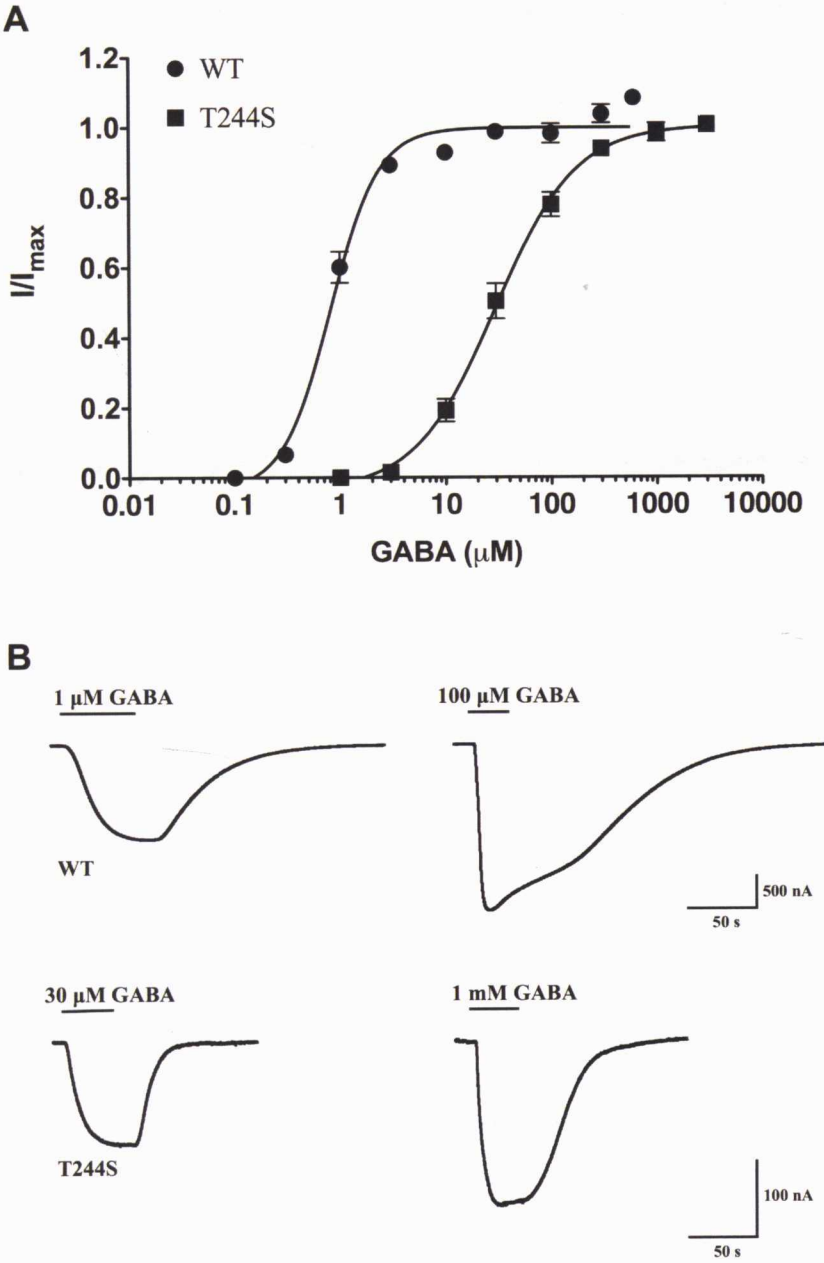

Figure 5.3 Effect of mutation at threonine 244. ***A*** *Normalized concentration-response curves from responses to GABA for ρ_1 wild-type and ρ_1T244S mutant receptors expressed in Xenopus oocytes. Each data point represents the mean ± SEM (n = 4-7). All data are normalized with I_{max}, which refers to their maximum current.* ***B*** *Example of responses for GABA at ρ_1 wild-type and ρ_1T244S receptors at approximately EC_{50} and I_{max} GABA concentrations. Figure adapted from reference (Yamamoto et al., 2012a).*

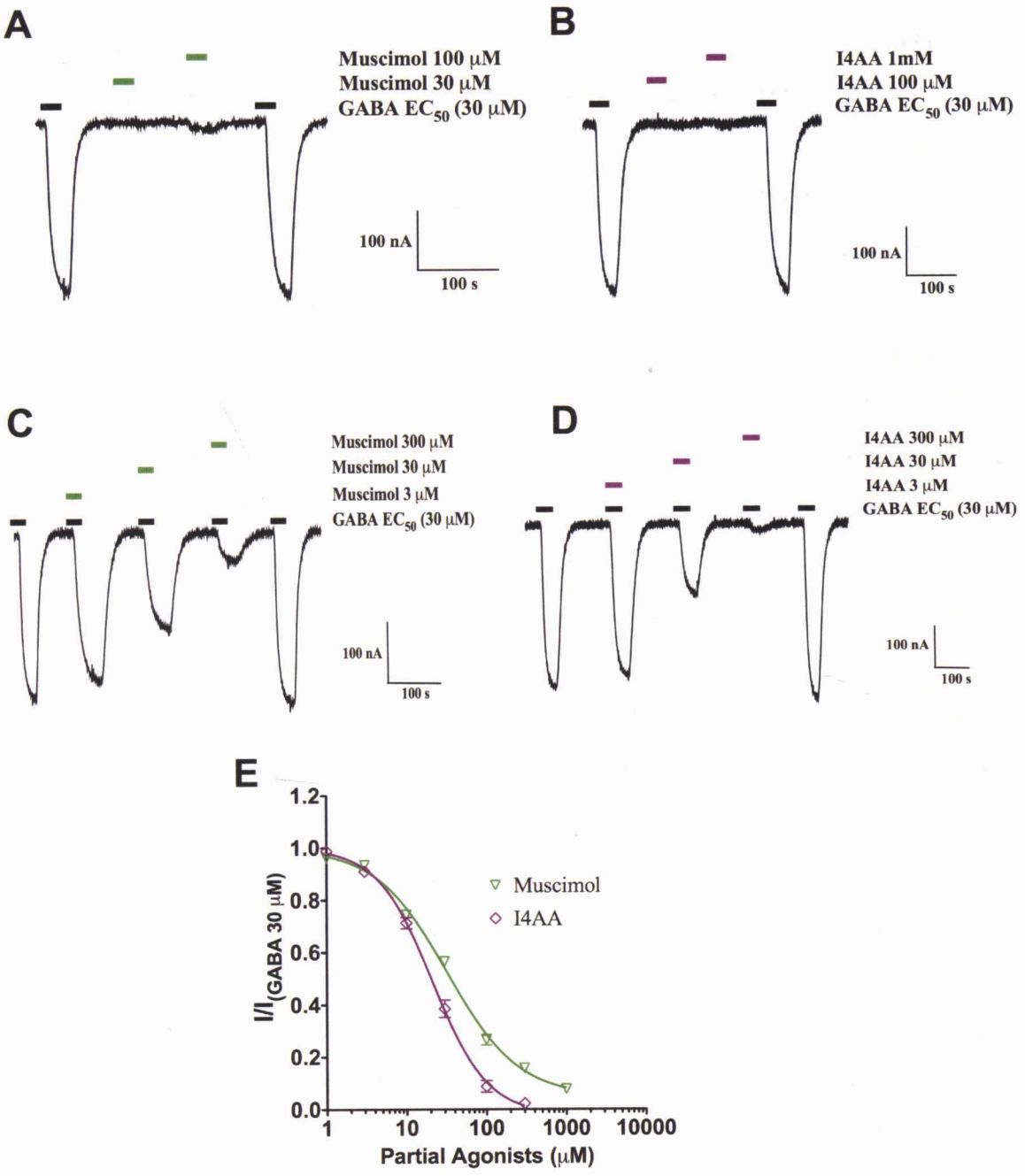

Figure 5.4 Effect of partial agonists at ρ_1T244S mutant receptor expressed in Xenopus oocytes. ***A*** *Sample current trace showing the effect of muscimol (green) (30 μM and 100 μM) at ρ_1T244S mutant receptors.* ***B*** *Sample current trace showing the effect of I4AA (purple) (100 μM and 1 mM) at ρ_1T244S mutant receptors.* ***C*** *Sample current trace showing inhibition of GABA EC_{50} 30 μM (black) by muscimol concentrations, 3 μM, 30 μM and 300 μM (green).* ***D*** *Sample current trace showing inhibition of GABA EC_{50} 30 μM (black) by I4AA concentrations, 3 μM, 30 μM and 300 μM (purple).* ***E*** *Inhibitory concentration response curves for muscimol (green) and I4AA (purple) at ρ_1T244S mutant receptors. Data are the mean ± SEM (n = 4-6 oocytes). All data are normalized with $I_{(GABA\ 30\ \mu M)}$ concentrations. Figure adapted from reference (Yamamoto et al., 2012a).*

T244 is located in loop C within the orthosteric binding site. Studies using crystal structures of the related acetylcholine binding protein (AChBP) have shown that upon agonist binding, loop C undergoes a distinctive binding conformation, resulting in constriction of the binding site (Celie et al., 2004; Hansen et al., 2005). Loop C directly interacts with ligands, suggesting that a conformational change in loop C is one of the first steps which contributes to the channel gating. Other studies using rate-equilibrium free energy relationships (REFER) (Purohit *et al.*, 2007c) examined the sequence of conformational changes during nACh receptor channel gating and found the conformational changes at the extracellular domain of the receptor before the channel gating. In another study using REFER (Purohit *et al.*, 2007b), it was found that residues in loop C of the mouse ACh receptor α-subunit and the surrounding area undergo initial stages of gating motion upon changes in receptor conformation. Taken together, these studies provide strong evidence that loop C is involved in agonist-mediated channel gating. Our homology modelling of the ρ_1 subunit predicts that T244 may be involved in GABA binding and/or gating (Yamamoto *et al.*, 2011a). In agreement with this prediction, introduction of the T244S mutation into ρ_1 resulted in an approximately 39-fold change in GABA affinity, which is consistent with that previously reported (Amin *et al.*, 1994). In addition, changes in the efficacy of the partial agonists muscimol and I4AA were observed. The partial agonists acted as antagonists at the mutant receptors. These findings, along with data from other groups (Celie et al., 2004; Hansen et al., 2005; Purohit et al., 2007b) strongly suggests that mutation of T244 predominantly alters receptor gating as well as GABA binding.

Table 5.1 Pharmacological data for agonists and antagonists at ρ_1 wild-type and ρ_1T244S mutant receptors expressed in Xenopus oocytes.

	$\rho_1$wild-type receptors	ρ_1T244S mutant receptors
GABA	EC_{50} = 0.8 ± 0.1 μM	EC_{50} = 31.5 ± 4.5 μM
Muscimol	EC_{50} = 1.4 ± 0.2 μM [a]	IC_{50} = 32.8 ± 2.2 μM
I4AA	EC_{50} = 8.6 ± 1.0 μM [a]	IC_{50} = 21.4 ± 1.7 μM
R-(–)-GABOB	EC_{50} = 19 μM [b]	1mM activates 26.0 ± 0.8 % [d]
S-(+)-GABOB	EC_{50} = 45 μM [b]	IC_{50} = 417.4 ± 7.0 μM
		K_B = 204.0 ± 14.3 μM [e]
3-APMPA	IC_{50} = 0.75 μM [c]	IC_{50} = 0.64 ± 0.03 μM
S-(–)-CGP44532	IC_{50} = 17 μM [b]	IC_{50} = 16.6 ± 1.0 μM
R-(+)-CGP44533	IC_{50} = 5 μM [b]	IC_{50} = 28.8 ± 2.4 μM
3-APA	IC_{50} = 20.8 ± 3.3 μM	IC_{50} = 33.1 ± 2.0 μM

[a] Data from (Carland et al., 2004) [b] Data from (Hinton et al., 2008) [c] Data from (Chebib et al., 1997a). All Data are the mean ± SEM (n = 4-13 oocytes). [d] Percentage activation by *R*-(–)-GABOB (1 mM) compared to the current produced by a submaximal concentration of GABA (30 μM, EC_{50}). Data are the mean ± SEM (n = 3 oocytes). [e] The K_B value is the mean ± SEM (n = 4).

5.1.2 Effect of GABOB at ρ_1T244S receptors

The enantiomers of GABOB are full agonists at ρ_1 receptors (Hinton et al., 2008), but at ρ_1T244S receptors it was found that *R*-(–)-GABOB and *S*-(+)-GABOB exert opposite pharmacological effects; *R*-(–)-GABOB is a weak partial agonist (1 mM activates 26 % of the current produced by GABA EC_{50}; n = 3), while *S*-(+)-GABOB is a competitive antagonist (K_B = 204.0 ± 14.3 μM, n = 4.) (Figure 5.5, Figure 5.6, Table 5.1). The change in GABOB pharmacology observed with the introduction of the T244S mutation infers that the interaction between the enantiomers and the hydroxyl group of T244 differs. Threonine possesses two chiral centres and it is L-threonine that is naturally found in proteins. In contrast, L-serine has only one chiral centre. The major differences between L-threonine and L-serine lie in their side chain volume and the rotational freedom of the hydroxyl group. Specifically, the position of the hydroxyl group of threonine is restricted due to the additional methyl group in the side chain. This restriction and added volume appears to stabilize T244 in a conformation that is optimal for agonist interaction. Indeed, our experimental data suggests that L-threonine at the position 244 in the ρ_1 ligand binding site is preferred in the agonist induced activation compared to serine (Table 5.1).

The weak partial agonist activity of *R*-(–)-GABOB at ρ_1T244S receptors suggests that *R*-(–)-GABOB can interact with the serine hydroxyl group, but not as strongly as with the hydroxyl group of the original threonine residue. Thus, the increased rotational freedom of serine may allow the amino acid residue side chain to adopt conformations that are unable to interact with *R*-(–)-GABOB. In contrast, *S*-(+)-GABOB, like muscimol and I4AA, acts as a competitive antagonist at ρ_1T244S receptors. This implies that *S*-(+)-GABOB can still bind but it is unable to facilitate activation, suggesting that the mutation has removed the ability of the molecule to gate the receptor, possibly due to a lack of interaction between the serine hydroxyl and *S*-(+)-GABOB.

An alternative explanation may be postulated from our homology modelling studies and the role of loop C in the active conformation of the receptor. Our

previous homology modelling studies (Abdel-Halim *et al.*, 2008; Yamamoto *et al.*, 2011a) have shown the possible formation of H-bonds between S243 or T244 with the carboxylate group of GABA. Modelling studies with GABOB show the possible formation of an H-bond with the hydroxyl group of GABOB (Figure 5.2). Upon ligand binding, loop C is thought to close over or engulf the agonist, and with this movement coupling agonist binding to channel gating (Celie et al., 2004; Hansen et al., 2005). It is possible that T244 initially forms an H-bond with the hydroxyl group of GABOB and that gating of the receptor may require the H-bond to break and make an alternative H-bond with the carboxylate group in order to stabilize the subsequent conformational change of loop C. The hydroxyl group of the serine side chain has more rotational freedom than threonine and may therefore adopt conformations that do not interact with the hydroxyl of *S*-(+)-GABOB and interact only weakly with *R*-(–)-GABOB. Thus *S*-(+)-GABOB is a competitive antagonist at the mutant. On the other hand, while serine may preferentially interact with the hydroxyl group of *R*-(–)-GABOB, it may also be capable of forming a H-bond with the carboxylate group. Therefore, *R*-(–)-GABOB is a very weak partial agonist at the ρ_1T244S receptors.

Insertion of a methyl at the C2 position of *trans*-4-aminocrotonic acid (TACA) to give *trans*-4-amino-2-methylbut-2-enoic acid (2-MeTACA) results in a similar change in activity (Chebib *et al.*, 1997b). TACA is a full agonist at ρ_1 receptors, however, 2-MeTACA is an antagonist. Initial studies suggested that this change in activity was due to steric factors. However, we now speculate that the methyl group at the C2 position may interact unfavourably with T244 and interrupt any possible H-bond with carboxylate group of 2-MeTACA, preventing gating of the receptor and therefore 2-MeTACA acts as an antagonist at ρ_1 wild-type receptors.

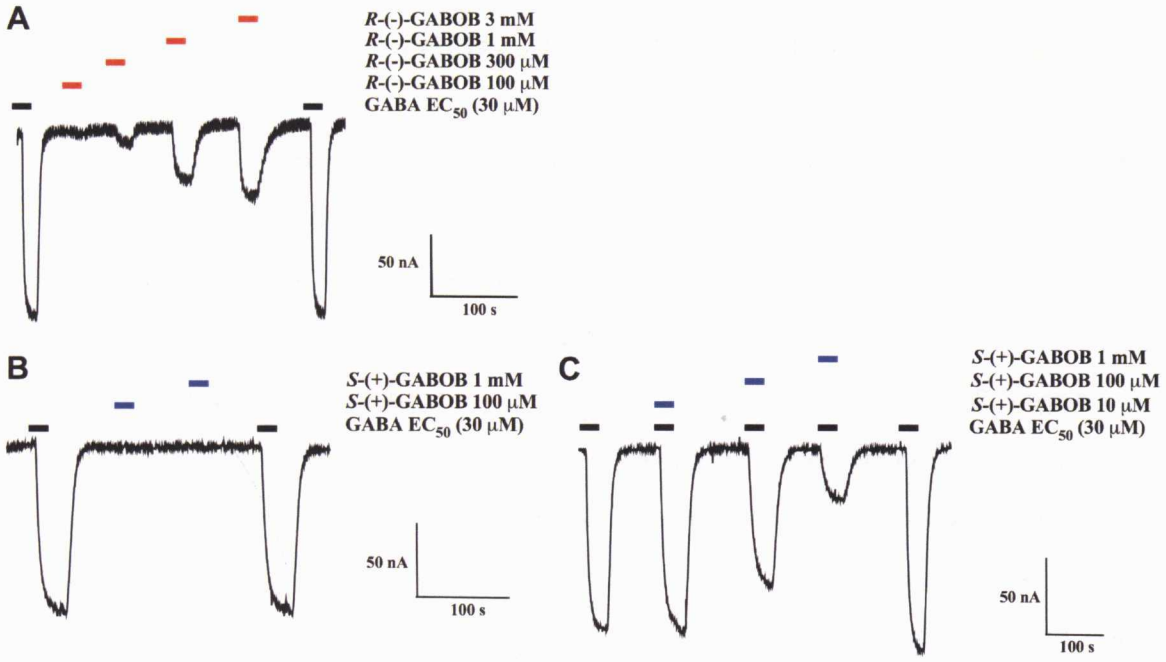

Figure 5.5 Effect of the enantiomers of GABOB at ρ_1T244S mutant receptor expressed in Xenopus oocytes. ***A*** *Sample current trace showing weak agonist effect of R-(–)-GABOB on ρ_1T244S mutant receptor. GABA EC_{50} 30 μM (black) activates the receptor, allowing Cl- ions to pass through the pore. Application of R-(–)-GABOB (red), 100 μM, 300 μM, 1 mM and 3mM concentrations activates the receptor in concentration dependent manner.* ***B*** *Sample current trace showing the effect of S-(+)-GABOB (blue) at ρ_1T244S mutant receptor. S-(+)-GABOB did not exhibit agonist effects at concentration 100 μM and 1 mM.* ***C*** *Sample current trace showing inhibition of GABA EC_{50} 30 μM (black) by S-(+)-GABOB (blue) concentrations, 10 μM, 100 μM and 1 mM. Figure adapted from reference (Yamamoto et al., 2012a).*

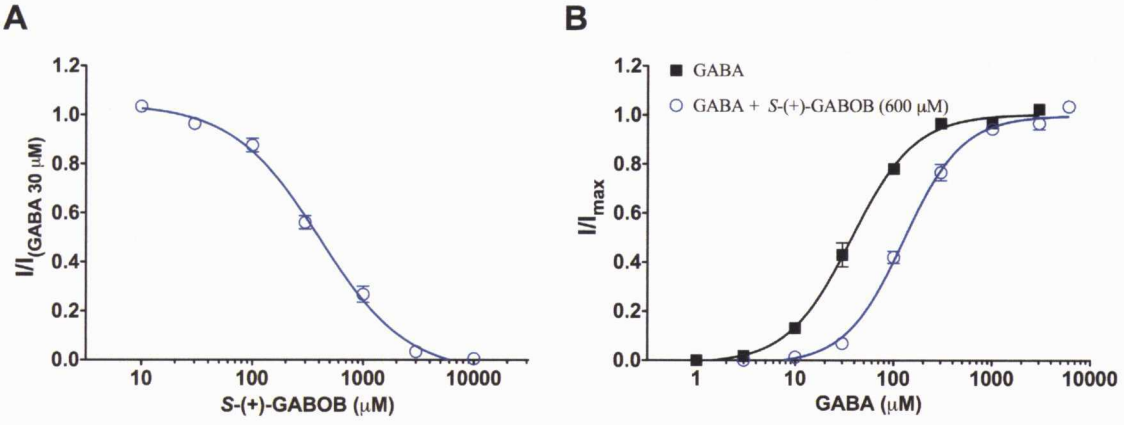

Figure 5.6 Pharmacology of S-(+)-GABOB at ρ_1T244S mutant receptor expressed in Xenopus oocytes. ***A*** *Inhibitory concentration-response curve for S-(+)-GABOB at ρ_1T244S mutant receptors. Each data point represents the mean ± SEM (n = 6). All data are normalized with $I_{(GABA\ 30\ \mu M)}$.* ***B*** *Concentration-response curves of GABA alone (black, n = 4) and GABA in the presence of S-(+)-GABOB 600 μM (blue, n = 4) at ρ_1T244S mutant receptor. Each data point represents the mean ± SEM (n = 4). All data are normalized with I_{max}. Figure adapted from reference (Yamamoto et al., 2012a).*

5.1.3 Antagonist activity at ρ_1T244S receptors

We further investigated the role of T244 on ρ_1 receptor antagonists. The methylphosphinic and phosphonic acid analogues of GABA, 3-aminopropyl(methyl)phosphinic acid (3-APMPA) and 3-aminopropylphosphonic acid (3-APA), respectively, and the methylphosphinic acid analogues of GABOB, *S*-3-amino-2-hydroxypropyl)methylphosphinic acid (*S*-(–)-CGP44532), *R*-3-amino-2-hydroxypropyl)methylphosphinic acid (*R*-(+)-CGP44533), showed no agonist activity (100 μM, n = 5) at ρ_1T244S receptors. This is consistent with the compounds acting as antagonists at ρ_1 wild-type receptors (Chebib et al., 1997a; Hinton et al., 2008; Johnston, 1996b). Our homology model does not predict any H-bonds between T244 and the hydroxyl group of the GABOB analogues, *R*-(+)-CGP44533 and *S*-(–)-CGP44533 (Figure 5.2). In addition, no H-bond was predicted for 3-APMPA, while an H-bond was observed between the phosphonic acid group of 3-APA and T244 in the model (Figure 5.7), similar to what was observed with the methylphosphonate (Xie et al., 2011). Electrophysiological data demonstrated that the IC_{50} values observed at ρ_1T244S mutant receptors for 3-APMPA and *S*-(–)-CGP44533 were unchanged compared to ρ_1 wild-type receptors (Figure 5.8, Table 5.1). In contrast, the IC_{50} values for *R*-(+)-CGP44533 and 3-APA were increased by approximately 6-fold and 2-fold, respectively, at ρ_1T244S receptors (Table 5.1). These subtle changes in IC_{50} values suggest T244 is not important for antagonist affinity, as predicted by the homology model and therefore the effect of the T244S mutation on antagonist activity was not as drastic as that observed for the agonists.

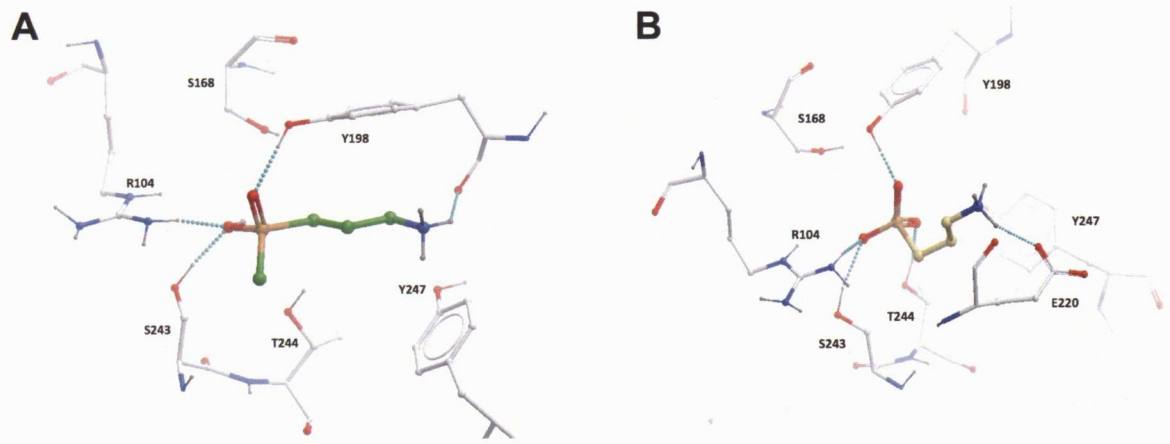

Figure 5.7 3-APMPA and 3-APA docked into the ρ_1 receptor GABA binding site. A *3-APMPA docked into the ρ_1 receptor GABA binding site. Selected H-bonds are depicted with dashed green lines.* ***B*** *3-APA docked into the ρ_1 receptor GABA binding site. Selected H-bonds are depicted with dashed green lines. Figure adapted from reference (Yamamoto et al., 2012a).*

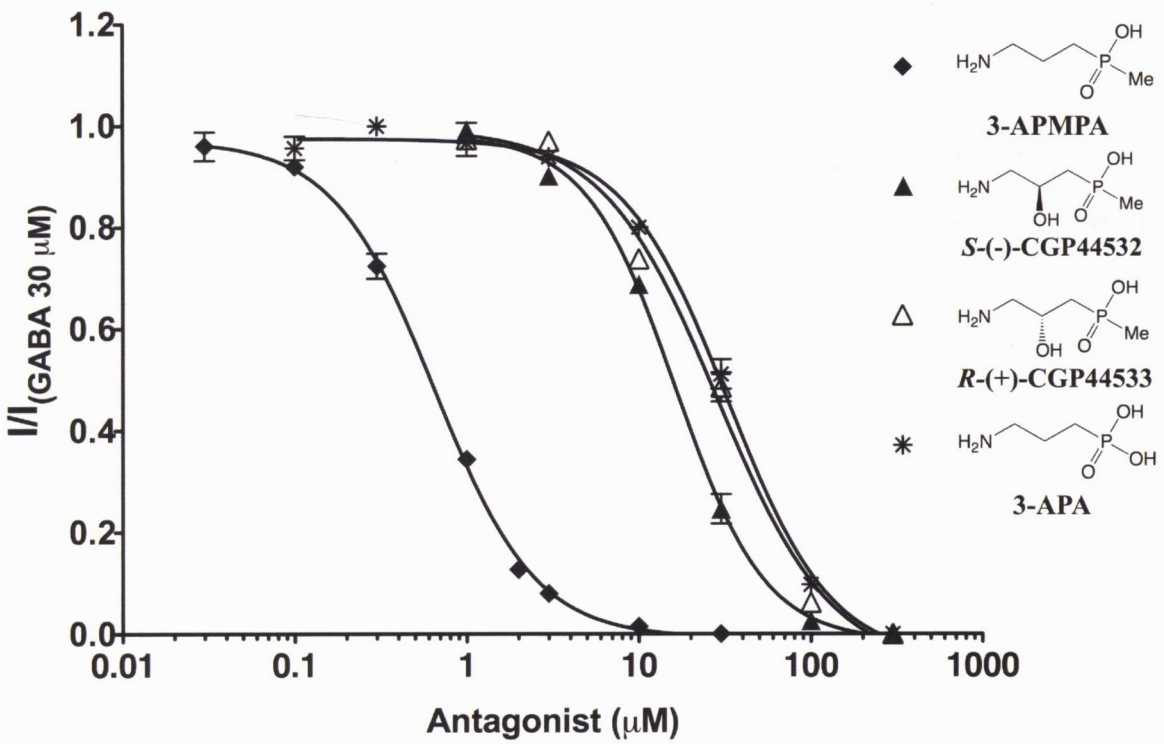

Figure 5.8 Inhibitory concentration response curves for 3-APMPA, S-(−)-CGP44532, R-(+)-CGP44533 and 3-APA at ρ_1T244S receptors expressed in Xenopus oocytes. *Each data point represents the mean ± SEM (n = 5-13 oocytes). All antagonists were tested with the presence of GABA EC_{50} (30 μM). All data are normalized with $I_{(GABA\ 30\ \mu M)}$. Figure adapted from reference (Yamamoto et al., 2012a).*

5.2 Conclusion

Threonine at position 244 is critical for ρ_1 receptor pharmacology. A hydroxyl group on the side chain of the amino acid at position 244 in ρ_1 receptors is crucial for agonist-mediated activation. This is consistent with previous findings (Amin *et al.*, 1994). In addition, T244 plays an important role for the enantioselective actions of GABOB, with *S*-(+)-GABOB converted to a competitive antagonist, while *R*-(–)-GABOB acts as a weak partial agonist at ρ_1T244S mutant receptors.

While mutating T244 had a significant effect on agonist activity, antagonist activity remained similar to ρ_1 wild-type. Studies using the crystal structure of AChBP from *Aplysia Californica* reported that loop C did not exhibit significant changes in conformational change upon antagonist binding (Hansen et al., 2005). However, the interaction between T244 and antagonists may have minor effects on the stability of antagonist binding, resulting in the small changes in affinity of *R*-(+)-CGP44533 and 3-APA at ρ_1T244S receptors. In contrast, T244 in loop C is involved in receptor gating upon agonist binding. Thus, this study confirms that mutation of T244 has a significant influence on agonist potency and efficacy and highlights the dynamic role of loop C in channel gating with T244 playing a critical role in agonist-evoked receptor activation.

Chapter 6:

Ligand interactions at different conformations of GABA receptors

Chapter 6: Ligand interactions at different conformations of GABA receptors

γ-Aminobutyric acid (GABA) is the major inhibitory neurotransmitter in the mammalian central nervous system (CNS), activating three receptors termed $GABA_A$, $GABA_B$ and $GABA_C$. The $GABA_C$ receptor is found on the retina and at distinct anatomical areas within the CNS, including the superior colliculus (Boue-Grabot *et al.*, 1998), cerebellum (Rozzo *et al.*, 2002), hippocampus (Alakuijala *et al.*, 2005) and lateral amygdala (Cunha *et al.*, 2010), and have been shown to play an important role in the onset of myopia (Stone *et al.*, 2003), the sleep-waking process (Arnaud *et al.*, 2001), memory enhancement (Johnston, 2002) and in fear and anxiety disorders (Cunha *et al.*, 2010). The design of potent and selective $GABA_C$ receptor antagonists, along with understanding how these agents modulate the receptor, will help characterize of these receptors and establish whether $GABA_C$ receptors play a major role in various CNS disorders (Chebib et al., 2009b; Gavande et al., 2010b).

$GABA_C$ receptors belong to the Cys-loop ligand-gated ion channel (LGIC) superfamily (Ortells *et al.*, 1995). All members of this superfamily require five subunits to form functional receptors. In mammals, $GABA_C$ receptors are composed of three ρ subunits, ρ_1-ρ_3, which form homomeric receptors or pseudo-homomeric receptors, composed of $\rho_1\rho_2$ or $\rho_2\rho_3$ subunit combinations (Chebib *et al.*, 2000; Enz *et al.*, 1998; Ogurusu *et al.*, 1999). The orthosteric binding site of the Cys-loop receptors is located at the interface of two subunits, formed by residues drawn from five discontinuous stretches of amino acids from the N-terminal domain of each subunit. These stretches of residues are referred to as loops A-E. Loops A-C form the principle side of the binding site and loops D and E form the complementary side (Sedelnikova *et al.*, 2005). $GABA_C$ receptors potentially have five orthosteric or GABA binding sites; GABA binding to these sites induce conformational changes within the receptor that subsequently lead to the opening of the pore, allowing Cl^- ions to pass through.

X-ray crystal structures of related prokaryotic proton-gated ion channels have provided some insights into the structural rearrangement that can occur during receptor gating (Cederholm *et al.*, 2009). ELIC (*Erwinia chrysanthem* ligand-gated ion channel) represents an inactive receptor conformation and GLIC (*Gloebacter violaceus* ligand-gated ion channels) represents a desensitized receptor conformation (Hilf *et al.*, 2009b; Hilf *et al.*, 2008). Despite a lack of mammalian crystal structures, there is strong evidence that structural changes occur within the orthosteric binding site upon activation of the receptor by GABA (Kash *et al.*, 2004) and that the binding site is constricted in the active conformation (Wagner *et al.*, 2001).

Tyrosine at position 102 (Y102) is located on loop D of the ρ_1 subunit within the GABA binding site. This residue has been proposed to be associated with agonist binding and channel gating (Torres *et al.*, 2002). Recently, this residue was demonstrated not to form a cation-π interaction with GABA (Lummis *et al.*, 2011) and in an alternative homology model of the ρ_1 GABA binding site implicates that this residue does not directly bind GABA (Abdel-Halim *et al.*, 2008). Mutation of Y102 to serine (ρ_1Y102S) in the ρ_1 subunit shifts the equilibrium of the receptor towards the open conformation, producing a constitutively active form of the receptor (Torres *et al.*, 2002). The competitive antagonist 3-aminopropyl-methyl-phosphinic acid (3-APMPA) inhibits the spontaneous current of ρ_1Y102S receptors in a concentration-dependent manner (Torres *et al.*, 2002), demonstrating that 3-APMPA acts as an inverse agonist, inducing a conformational change which shifts the equilibrium of the receptor towards the closed conformation.

In this study, the role of Y102 in antagonist activity was assessed. Y102 was mutated to serine (ρ_1Y102S), cysteine (ρ_1Y102C) and alanine (ρ_1Y102A), and the resulting mutant receptors represent channels with a proportion in the open conformational state (ρ_1Y102S) and almost entirely in the closed conformational state (ρ_1Y102C, ρ_1Y102A) of the channel. Twelve known antagonists (**1**-**7** and **9**-**13**) and two novel antagonists (**8** and **14**) were evaluated at ρ_1 wild-type and mutant receptors to investigate if antagonist activity was altered with receptor conformation.

6.1 Results and discussion

The mechanism by which an agonist binds and subsequently opens the channel of Cys-loop receptors is complex and involves many structural changes throughout the receptor, including changes within the orthosteric binding site. Ligands, for example 3-APMPA (**2**), have different affinities for the open or closed conformational states of the receptor, as the conformation of the binding site differs between the two conformational states (Torres *et al.*, 2002). Constitutively active receptors, such as the ρ_1Y102S receptor, provide an opportunity to assess the activity of antagonists on receptors in equilibrium between the open or closed conformational states of the receptor.

6.1.1 ρ_1Y102S receptors are constitutively active

Consistent with previous studies (Torres *et al.*, 2002) the EC_{50} values for GABA increased by 21-, 233- and 196-fold when ρ_1 Y102 was mutated to cysteine, serine or alanine, respectively (Figure 6.1, Table 6.1). This change in GABA sensitivity suggests that mutation of Y102 on the ρ_1 subunit results in a change in GABA affinity or altered receptor gating. Of the three mutant receptors evaluated, ρ_1Y102S receptors were constitutively active. When clamped at -60 mV, the holding current for cells expressing ρ_1Y102S (-200.3 ± 20.1 nA, n = 11) was greater than that in cells expressing ρ_1 wild-type (-15.2 ± 4.0 nA, n = 11), ρ_1Y102A (-0.2 ± 1.7 nA, n = 11), and ρ_1Y102C (-5.6 ± 4.1 nA, n = 11) mutant receptors. This suggests that ρ_1Y102S receptors exist in equilibrium between the open and closed conformational states, while ρ_1 wild-type, ρ_1Y102A and ρ_1Y102C receptors predominantly prefer the closed conformational state.

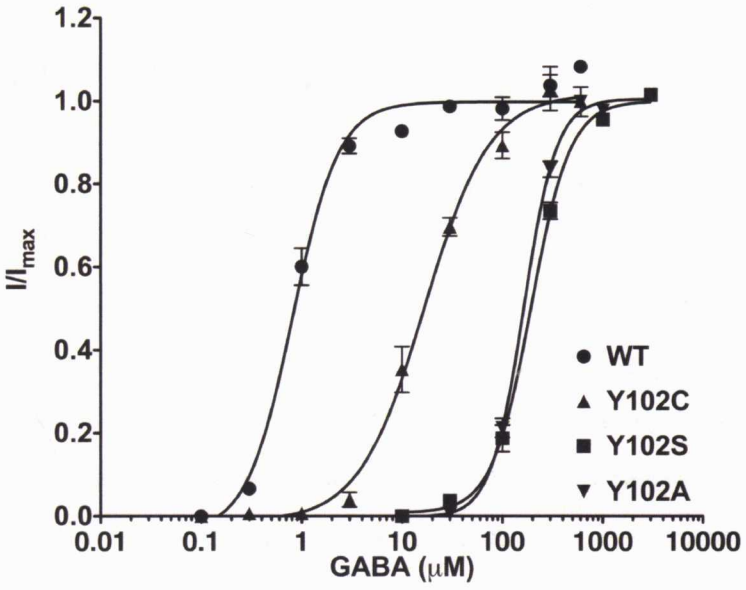

Figure 6.1 GABA concentration response curves for human ρ_1 wild-type (WT) and ρ_1Y102C, ρ_1Y102S and ρ_1Y102A receptors expressed in Xenopus oocytes. *Each data point represents the mean ± SEM (n = 3-4). All data are normalized with I_{max}, which refers to their maximum current. EC_{50} values are listed in* ***Table 6.1****. Figure adapted from reference (Yamamoto et al., 2012b).*

Table 6.1 EC_{50} values for GABA at ρ_1 wild-type and ρ_1Y102 mutant receptors.

ρ_1 Y102 mutation	EC_{50} (μM)
Wild-Type	0.8 ± 0.1
Y102C	17.6 ± 1.2
Y102S	193.7 ± 9.7
Y102A	163.1± 2.0
All data are the means ± SEMs (n = 3-4 oocytes).	

6.1.2 (±)-4-ACPAM (8) and SR-95813 (14) are potent antagonists at ρ_1 receptors

In this study, a total of twelve known and two novel agents were evaluated at ρ_1 receptors. TPMPA (**1**), 3-APMPA (**2**) SGS-742/CGP-36742 (**3**), (±)-*cis*-3-ACPBPA (**4**), (±)-3-*trans*-ACPBPA (**5**), *S*-4-ACPBPA (**6**), (+)-*S*-4-ACPCA (**7**), THIP (**9**), DAVA (**10**), 4-GBA (**11**), ZAPA (**12**) and SR-93351/Gabazine (**13**) (Figure 6.2, Figure 6.4, Table 6.2) have been shown previously to act as competitive antagonists at ρ_1 wild-type receptors, indicating that they bind to the GABA binding site. The activities of two novel ligands, (±)-4-ACPAM (**8**) and SR-95813 (**14**), were characterized at ρ_1 wild-type receptors recombinantly expressed in *Xenopus* oocytes (Figure 6.3). These novel compounds are interesting in that they do not possess an acid moiety (carboxylic or phosphinic acid), a feature common to all ligands that bind to the GABA binding site. Instead of the usual acid moiety, (±)-4-ACPAM (**8**) has an amide group, while SR-95813 (**14**) has a nitrile group. To our surprise, these compounds were found to be potent ρ_1 receptor competitive antagonists. Figure 6.3**A** demonstrates that (±)-4-ACPAM (**8**) inhibits the EC_{50} of GABA (1 μM) in a concentration-dependent manner (Figure 6.3**A**, IC_{50} = 9.6 ± 0.9 μM, n = 4). Schild plot analysis demonstrates that in the presence of increasing concentrations of (±)-4-ACPAM (**8**) (30, 100 and 300 μM; n = 3-4 oocytes per antagonist concentration), the concentration response curve for GABA is shifted to the right in a parallel manner (Figure 6.3**B**, K_B = 30.3 ± 3.1 μM, slope did not differ from 1, see Figure 6.4), indicating that (±)-4-ACPAM (**8**) is a competitive antagonist at ρ_1 wild-type receptors.

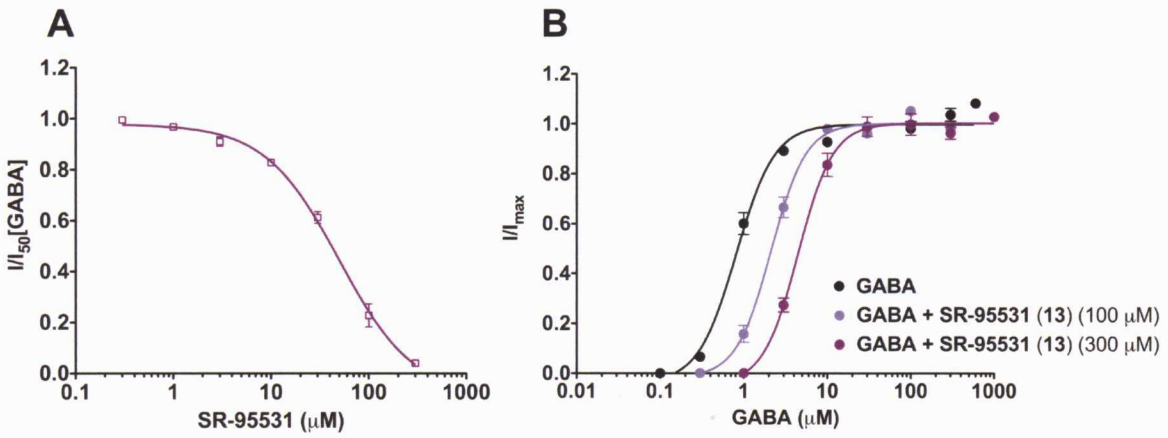

Figure 6.2 Pharmacology of SR-95531 (13). ***A*** *Inhibitory concentration response curve for SR-95531 (**13**) against GABA (1 μM) at ρ_1 wild-type receptors. Each data point represents the mean ± SEM (n = 4).* ***B*** *Concentration response curves of GABA alone (black dot, n = 3) and in the presence of SR-95531 (**13**) at 100 (light purple dot, n = 3) and 300 μM (dark purple dot, n = 4). Each data point represents the mean ± SEM (n = 3-4). All data are normalized with I_{max}, which refers to their maximum current. Figure adapted from reference (Yamamoto et al., 2012b).*

Similarly, SR-95813 (**14**) inhibits the response produced by GABA (1 μM) in a concentration-dependent manner (Figure 6.3**C**, IC_{50} = 8.0 ± 0.8 μM, n = 4). Schild plot analysis shows that in the presence of increasing concentrations of SR-95813 (**14**) (30 100 and 300 μM; n = 3-4 oocytes per antagonist concentration), the GABA concentration response curve is shifted to the right in a parallel manner (Figure 6.3**D**, K_B = 12.4 ± 0.4 μM, slope did not differ from 1, see Figure 6.4), indicating that SR-95813 (**14**) blocks ρ_1 wild-type receptors in a competitive manner.

Mutagenesis studies of the ρ_1 receptor identified arginine 104 (R104) as important for GABA binding and this residue is thought to interact via a salt bridge with the carboxylate group of GABA (Harrison et al., 2006a). Homology models of the ρ_1 receptor support this observation (Abdel-Halim *et al.*, 2008). As (±)-4-ACPAM (**8**) and SR-95813 (**14**) do not possess a carboxylate group, it would be interesting to evaluate R104 in the binding of these ligands.

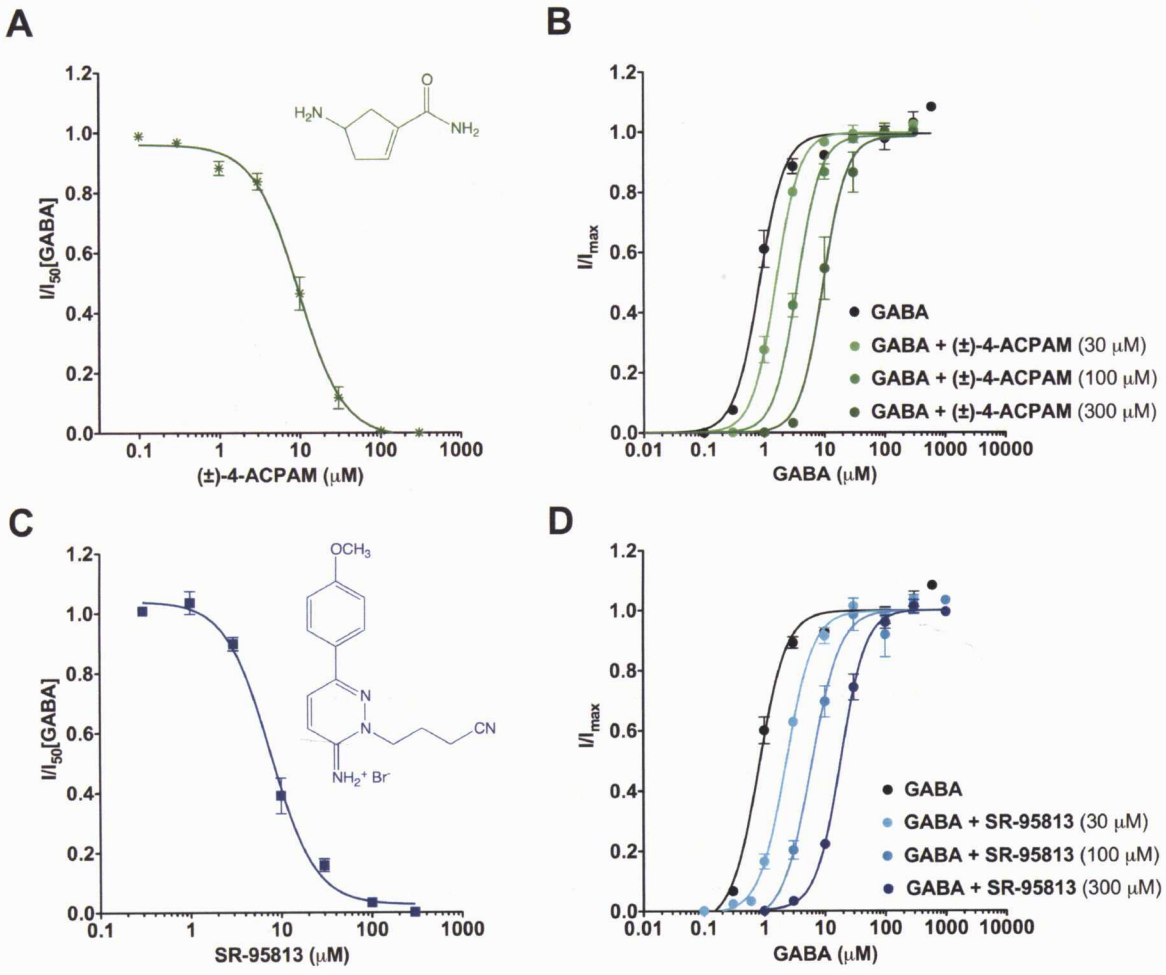

Figure 6.3 Pharmacology of (±)-4-ACPAM (8) and SR-95813 (14) at human ρ_1 wild-type receptors expressed in Xenopus oocytes. ***A*** *Inhibitory concentration response curve for (±)-4-ACPAM (**8**) against GABA (1 μM) at ρ_1 wild-type receptors. Each data point represents the mean ± SEM (n = 4).* ***B*** *Concentration response curves of GABA alone (black dot, n = 3) and in the presence of (±)-4-ACPAM (**8**) at 30 (light green dot, n = 3), 100 (green dot, n = 4) and 300 μM (dark green dot, n = 3). Each data point represents the mean ± SEM (n = 3-4). All data are normalized with I_{max}, which refers to their maximum current.* ***C*** *Inhibitory concentration response curve for SR-95813 (**14**) against GABA (1 μM) at ρ_1 wild-type receptors. Each data point represents the mean ± SEM (n = 4).* ***D*** *Concentration response curves of GABA alone (black dot, n = 4) and in the presence of SR-95813 (**14**) at 30 (light blue dot, n = 3), 100 (blue dot, n = 4) and 300 μM (dark blue dot, n = 3). Each data point represents the mean ± SEM (n = 3-4). All data are normalized with I_{max}, which refers to their maximum current. Figure adapted from reference (Yamamoto et al., 2012b).*

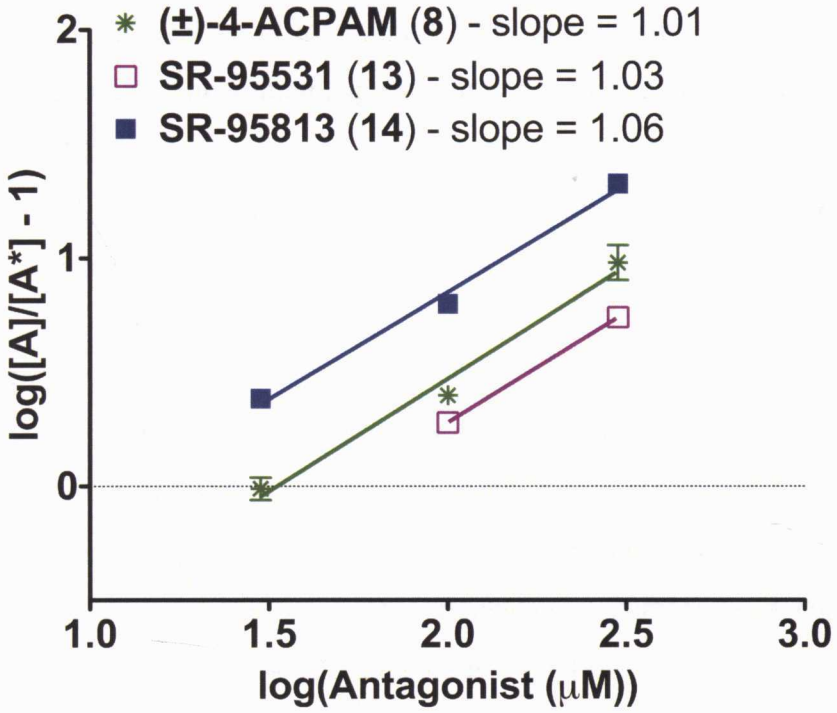

Figure 6.4 Schild plot analysis for (±)-4-ACPAM (8), SR-95531 (13) and SR-95813 (14). *The action of (±)-4-ACPAM (**8**) (green), SR-95531 (**13**) (purple) and SR-95813 (**14**) (blue) in antagonizing the effect of GABA at ρ_1 wild-type receptors. Each data point represents the mean ± SEM (n = 3-4). Figure adapted from reference (Yamamoto et al., 2012b).*

6.1.3 Assessing the activity of antagonists at a proportion of receptors in the open conformational state

The activities of fourteen GABA antagonists (**1-14**) were evaluated using the constitutively active ρ_1Y102S receptors. Antagonists were tested at 100 μM and 300 μM in the absence of GABA. The percentage inhibition of the spontaneous current was measured and normalized to the initial resting current for each cell. All antagonists tested inhibited the spontaneous current of ρ_1Y102S receptors to a various extent when evaluated at 300 μM, with the exception of (±)-4-ACPAM (**8**). (±)-

4-ACPAM (**8**), at either 100 μM or 300 μM, failed to inhibit the spontaneous current at these receptors (Figure 6.5**B**).

Of the compounds tested, SGS-742 (**3**), *S*-4-ACPCA (**7**), (±)-4-ACPAM (**8**) and DAVA (**10**) were the weakest at inhibiting (0-9 %) the constitutive current produced by ρ_1Y102S receptors. The remaining antagonists inhibited the current by 10-87 % (Table 6.2). 3-APMPA (**2**) was the most effective inhibitor of the constitutive current, while TPMPA (**1**), (±)-*cis*-3-ACPBPA (**4**), 4-GBA (**11**), SR-95331 (**13**) and SR-95813 (**14**) displayed moderate inhibition of the constitutive current.

To explore the relative activity of antagonists on the open conformational state of the ρ_1 receptor, we focused on five structurally different GABA antagonists, TPMPA (**1**), (±)-*cis*-3-ACPBPA (**4**), (±)-4-ACPAM (**8**), 4-GBA (**11**), SR-95531 (**13**) and SR-95813 (**14**) (Table 6.2, Table 6.3). Application of the competitive antagonist, TPMPA (**1**), to ρ_1Y102S receptors inhibited the spontaneous current in a concentration-dependent manner (Figure 6.5**A**). This indicates that TPMPA shifts the equilibrium of ρ_1Y102S receptors from the open to the closed conformational state, thus acting as an inverse agonist (Table 6.3). However TPMPA is weak exhibiting a 600-fold decrease in potency.

Figure 6.5**C** shows the concentration response curves for TPMPA (**1**), (±)-*cis*-3-ACPBPA (**4**), (±)-4-ACPAM (**8**), 4-GBA (**11**) SR-95531 (**13**) and SR-95813 (**14**) inhibiting the spontaneous current of ρ_1Y102S receptors. The affinities of the compounds against the spontaneous current were lower compared to the ρ_1 wild-type (Table 6.2, Table 6.3). The order of potency of the compounds at ρ_1Y102S receptors was SR-95813 (**14**) > SR-95531 (**13**) > (±)-*cis*-3-ACPBPA (**4**) > 4-GBA (**11**) > TPMPA (**1**) (Table 6.3). (±)-4-ACPAM (**8**) had a very small effect on the constitutive activity of ρ_1Y102S receptors even at the 1 mM concentration (Figure 6.5**C**) and failed to significantly inhibit GABA (EC_{50}; 180 μM) at this mutant receptor (Figure 6.5**D**).

Interestingly, both SR-95531 (**13**) and SR-95813 (**14**) could not completely block the spontaneous current of ρ_1Y102S receptors (Figure 6.5**C**), indicating they

may act as partial inverse agonists at the mutant receptor. Furthermore, in the presence of GABA, both SR-95531 (**13**) and SR-95813 (**14**) inhibited GABA with IC_{50} values approximately 2-fold weaker than the EC_{50} value that inhibits the constitutive activity (Table 6.3, Table 6.4, Figure 6.6) suggesting the binding affinity of these compounds are similar in the presence or absence of GABA at ρ_1Y102S receptors.

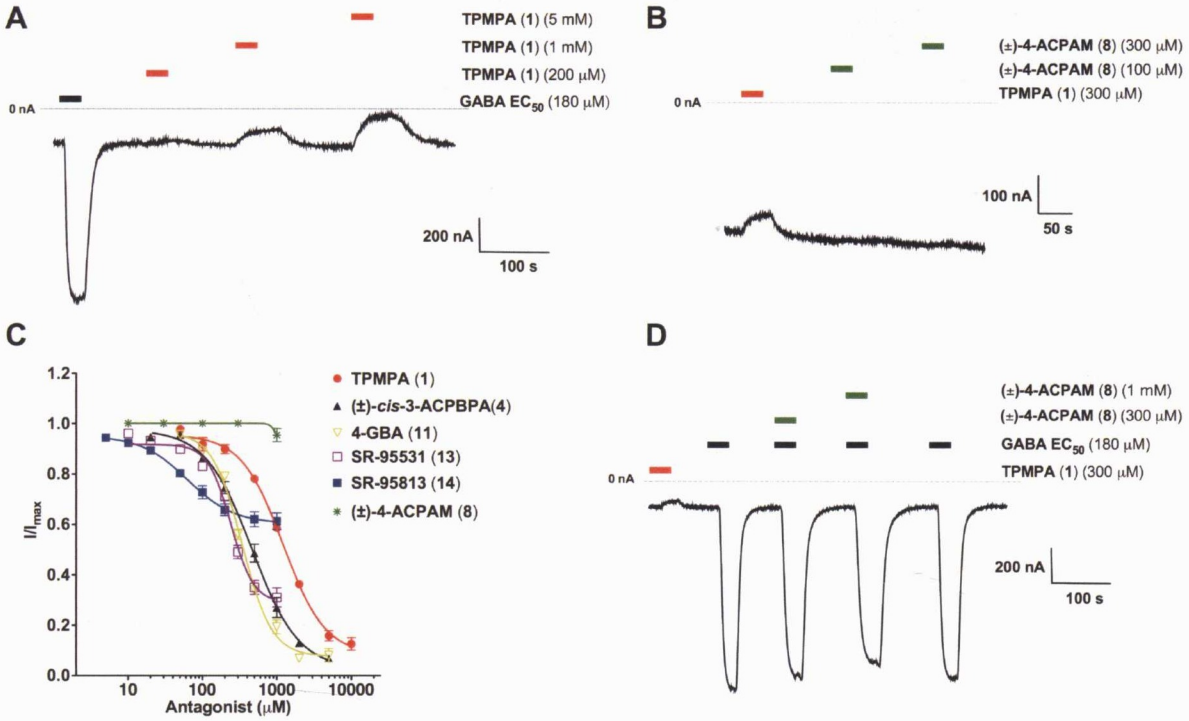

Figure 6.5 Effect of GABA antagonists at ρ_1Y102S receptor spontaneous currents. ***A*** *A sample current traces showing inverse agonist effects of TPMPA (**1**) at ρ_1Y102S receptors expressed in Xenopus oocytes. GABA EC_{50} (180 μM) activates the receptor (black bar), allowing the flow of Cl^- ions. Application of TPMPA (**1**) (200 μM, 1 mM and 5 mM) alone inhibited the resting conductance in a concentration dependent manner (red bar).* ***B*** *A sample current trace showing the effect of (±)-4-ACPAM (**8**) at ρ_1Y102S receptor spontaneous current. (±)-4-ACPAM (**8**) did not exhibit inverse agonist effects at 100 μM and 300 μM (green bar).* ***C*** *Inhibitory concentration-response curves for TPMPA (**1**) (red), SR-95531 (**13**) (purple), SR-95813 (**14**) (blue), (±)-cis-3-ACPBPA (**4**) (black) and 4-GBA (**11**) (yellow) at ρ_1Y102S receptors expressed in Xenopus oocytes. All data are normalized with I_{max}, which refers to the initial resting conductance. Each data point represents the mean ± SEM (n = 3-5).* ***D*** *A sample current trace showing weak inhibitions of GABA EC_{50} (180 μM) (black bar) by (±)-4-ACPAM (**8**) (300 μM and 1mM) (green bar) at ρ_1Y102S receptors. Figure adapted from reference (Yamamoto et al., 2012b).*

Table 6.2 Effects of structurally diverse antagonists at ρ_1 wild-type and ρ_1Y102S receptors.

Compound	Antagonist activity at human ρ_1 wild-type receptors	% inhibition of spontaneous current at ρ_1Y102S receptors [a]	
		100 μM	300 μM
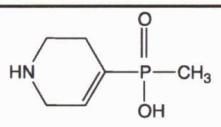 TPMPA (**1**)	IC_{50} = 2.22 μM [b]	8.7 ± 0.3	22.3 ± 2.7
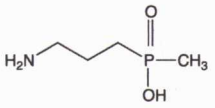 3-APMPA (**2**)	IC_{50} = 0.75 μM [c]	47.9 ± 4.7	87.6 ± 6.7
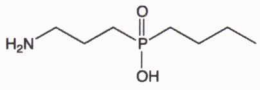 SGS-742/CGP-36742 (**3**)	IC_{50} = 62.5 μM [c]	1.4 ± 0.5	4.7 ± 0.3
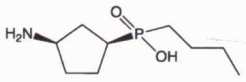 (±)-*cis*-3-ACPBPA (**4**)	IC_{50} = 5.06 μM [d]	13.8± 0.7	33.7 ± 0.4
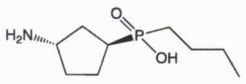 (±)-3-*trans*-ACPBPA (**5**)	IC_{50} = 72.58 μM [d]	NA [l]	6.6 ± 1.6
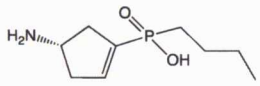 *S*-4-ACPBPA (**6**)	IC_{50} = 4.97 μM [e]	5.7 ± 0.6	17.5 ± 0.9
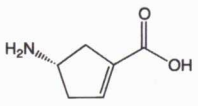 (+)-*S*-4-ACPCA (**7**)	K_i = 6.0 μM [f]	0.3 ± 0.2	2.0 ± 0.6
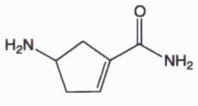 (±)-4-ACPAM (**8**)	IC_{50} = 9.6 ± 0.9 μM K_B = 30.3 ± 3.1 μM	NA [l]	NA [l]

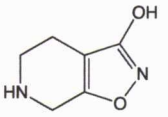 THIP (**9**)	IC_{50}= 10 μM [g]	1.3 ± 0.7	10.7 ± 0.3
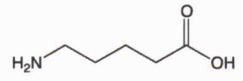 DAVA (**10**)	K_B = 20 μM [h]	2.2 ± 0.5	5.5 ± 0.2
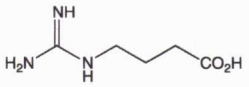 4-GBA (**11**)	IC_{50} = 18.75 μM [i]	13.5 ± 1.3	37.8 ± 3.1
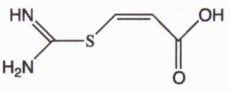 ZAPA (**12**)	IC_{50}= 11 μM [g]	3.2 ± 1.1	9.9 ± 0.8
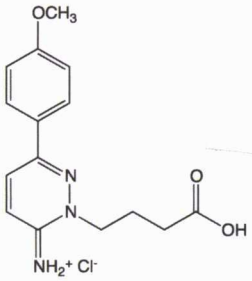 SR-95531/Gabazine (**13**)	IC_{50} = 60.7 ± 12.6 μM [j] K_B = 51.2 ± 2.9 μM [k]	16.4 ± 1.3	28.8 ± 5.9
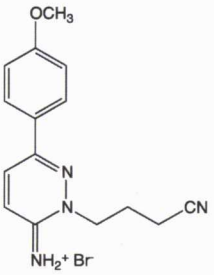 SR-95813 (**14**)	IC_{50} = 8.0 ± 0.8 μM K_B = 12.4 ± 0.4 μM	25.0 ± 2.0	33.3 ± 1.7

[a] Percentage inhibitions of ρ_1Y102S receptor spontaneous currents by compounds (100 μM and 300 μM), which were normalized by initial resting conductance. All data are the mean ± SEMs (n = 3-12 oocytes). [b] Data from reference (Gavande et al., 2010b). [c] Data from reference (Chebib *et al.*, 1997a). [d] Data from reference (Ng et al., 2011). [e] Data from reference (Kumar et al., 2008). [f] Data from reference (Chebib et al., 2001). [g] Data from reference (Woodward et al., 1993). [h] Data from reference (Chebib et al., 2000). [i] Data from reference (Chebib et al., 2009a). [j] see Figure 6.2. [k] see Figure 6.4.[l] NA stands for not active at the concentration.

Table 6.3 EC_{50} values of TPMPA (1), (±)-cis-3-ACPBPA (4), 4-GBA (11), SR-95531 (13), SR-95813 (14) at ρ_1Y102S receptors.

Compound	EC_{50} (μM) [a]
TPMPA (**1**)	1234.3 ± 57.7
(±)-*cis*-3-ACPBPA (**4**)	488.3 ± 60.5
4-GBA (**11**)	568.7 ± 25.3
SR-95531 (**13**)	312.9 ± 15.1
SR-95813 (**14**)	64.3 ± 2.8

[a] Concentration which inhibits 50% of the maximum spontaneous current of ρ_1Y102S receptor. Data are the mean ± SEM (n = 4-5 oocytes).

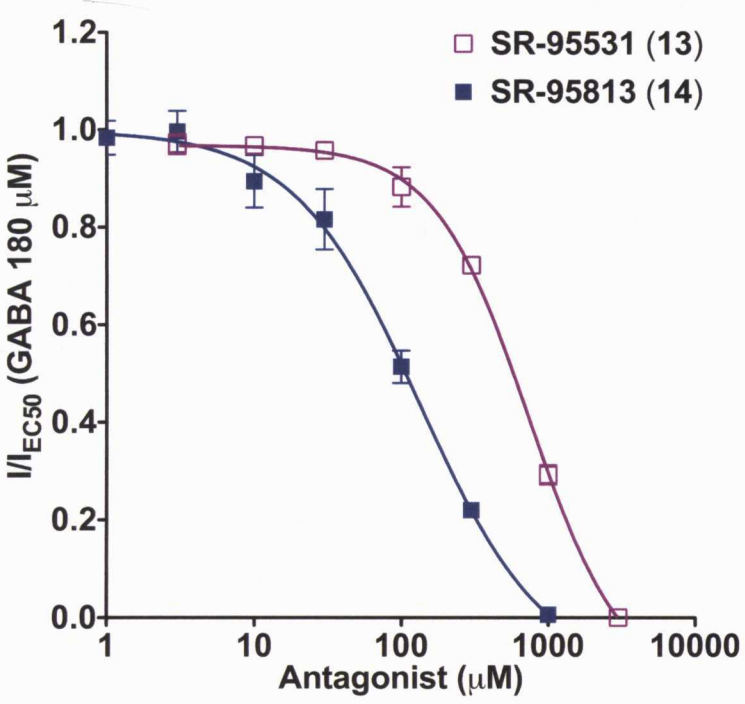

Figure 6.6 Inhibitory concentration-response curves for SR-95531 (13) and SR-95813 (14) at ρ_1Y102S receptors. *Each data point represents the mean ± SEM (n = 3-5). All antagonists were tested in the presence of GABA EC_{50} (180 μM). All data are normalized with I_{EC50}[GABA]. Figure adapted from reference (Yamamoto et al., 2012b).*

6.1.4 Assessing the activity of antagonists at receptors in the closed conformational state

The activities of the five antagonists were examined at ρ_1Y102C and ρ_1Y102A receptors (Table 6.4, Figure 6.7). In contrast to ρ_1Y102S receptors, ρ_1Y102C and ρ_1Y102A receptors were not constitutively active, thus existing predominantly in the closed conformational state. Interestingly, (±)-4-ACPAM (**8**) at a concentration of 300 μM regained some of its antagonist activity for the ρ_1Y102C and ρ_1Y102A mutant receptors (Table 6.4). At ρ_1Y102C receptors, (±)-4-ACPAM (**8**) displayed a 25-fold increase in IC_{50} compared to ρ_1 wild-type (At ρ_1 wild-type; IC_{50} = 9.6 ± 0.9 μM: at ρ_1Y102C; IC_{50} = 241.8 ± 17.2 μM). As (±)-4-ACPAM (**8**) did not inhibit the constitutive activity of ρ_1Y102S mutant receptors, nor did it inhibit GABA (Figure 6.5**B** and Figure 6.5**D**) or the inverse agonist effects of SR-95531 (**13**) (Figure 6.8, n = 3) at this receptor, we can infer that either tyrosine is crucial for the binding of (±)-4-ACPAM (**8**) or that (±)-4-ACPAM (**8**) acts at receptors existing predominantly in the closed over the open conformational state.

At ρ_1Y102C receptors, the IC_{50} values for TPMPA (**1**), (±)-*cis*-3-ACPBPA (**4**) and 4-GBA (**11**) were also increased by 200-, 22- and 25-fold, respectively, compared to ρ_1 wild-type receptors (Table 6.4). As the cysteine and alanine mutations did not affect potency of the antagonists to the same extent as the serine mutation, indicating that these compounds have the ability to preferentially bind to the closed conformational state of the receptor. A similar phenomenon is observed with tetracaine at nicotinic acetylcholine (nACh) receptors (Gallagher *et al.*, 1999). Tetracaine has a 100 fold higher affinity for the closed conformation compared the desensitized conformation of the *Torpedo* nACh receptor, implicating tetracaine is a closed conformation channel blocker.

In contrast to what was observed at ρ_1Y102S receptors, the inhibitory activity of SR-95531 (**13**) and its analogue SR-95813 (**14**) was significantly reduced at both ρ_1Y102C and ρ_1Y102A receptors. SR-95531 (**13**) (300 μM) inhibited only 7.5 % of the current elicited by GABA EC_{50} (20 μM) at ρ_1Y102C receptors and was inactive at

ρ_1Y102A receptors (Figure 6.9, Table 6.4). Furthermore, SR-95813 (**14**) (300 μM) did not inhibit the current elicited by GABA EC_{50} (20 μM) at both ρ_1Y102C and ρ_1Y102A receptors (Figure 6.9, Table 6.4). Thus, the order of potency of the compounds tested at ρ_1Y102C receptors was (±)-*cis*-3-ACPBPA (**4**) > 4-GBA (**11**) ≅ TPMPA (**1**) >> SR-95531 (**13**) ≅ SR-95318 (**14**). As SR-95531 (**13**) and its analogue SR-95813 (**14**) are more potent at ρ_1Y102S than ρ_1Y102C receptors, may indicate that the compounds are more likely to bind to the open over the closed conformational state of the receptor. While we cannot rule out the possibility of direct interaction between the introduced residues and the antagonists tested, there is no clear structure activity relationship to suggest that either possibility may be the case.

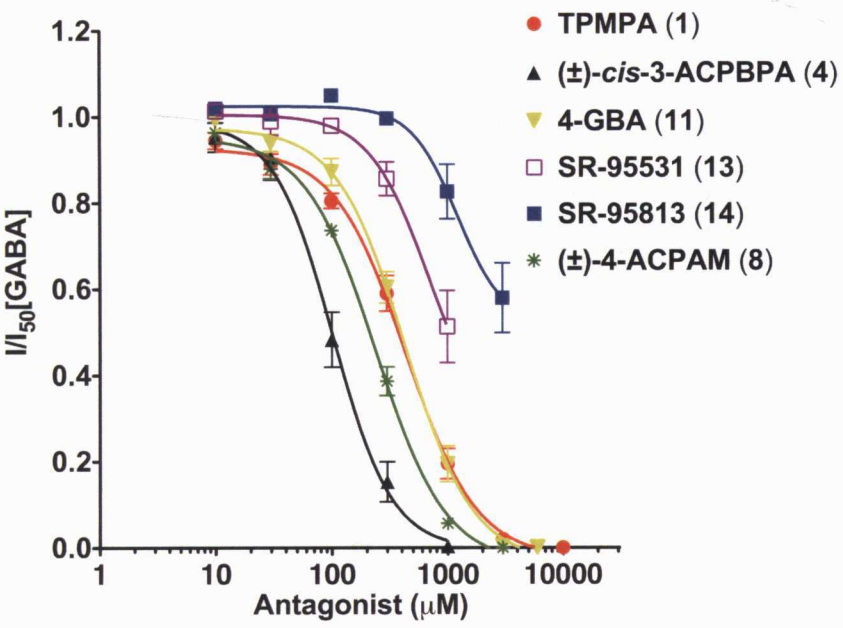

Figure 6.7 Inhibitory concentration-response curves for TPMPA (1), (±)-cis-3-ACPBPA (4), (±)-4-ACPAM (8), 4-GBA (11), SR-95531 (13) and SR-95813 (14) at ρ_1Y102C receptors expressed in Xenopus oocytes. *Each data point represents the mean ± SEM (n = 3-5). All antagonists were tested in the presence of GABA EC_{50} (20 μM). All data are normalized with I_{EC50}[GABA]. Figure adapted from reference (Yamamoto et al., 2012b).*

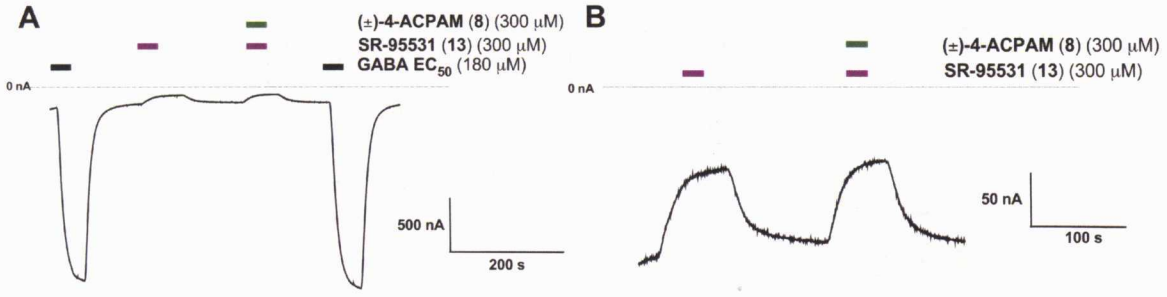

Figure 6.8 Effect of (±)-4-ACPAM (8) on inverse agonist activity of SR-95531 (13). A *A sample current traces showing inverse agonist effects of SR-95531 (**13**) at ρ_1Y102S receptors expressed in Xenopus oocytes. GABA EC_{50} (180 μM) activates the receptor (black bar), allowing flow of Cl^- ions. Application of SR-95531 (**13**) (purple bar, 300 μM) shifts the equilibrium of ρ_1Y102S receptors. Co-application of (±)-4-ACPAM (**8**) (green bar, 300 μM) has no effect on the inverse agonist activity of SR-95531 (**13**) (purple bar, 300 μM).* ***B*** *Magnified view of the effects of SR-95531 (**13**) (purple bar, 300 μM) alone and with the presence of (±)-4-ACPAM (**8**) (green bar, 300 μM) at ρ_1Y102S receptors. Figure adapted from reference (Yamamoto et al., 2012b).*

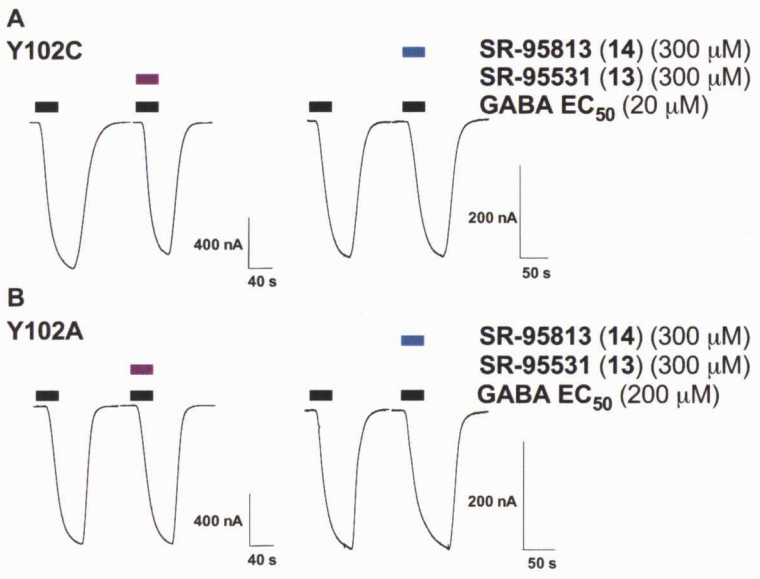

Figure 6.9 Sample current trace showing the effect of SR-95531 (13) and SR-95813 (14) at ρ_1Y102C and ρ_1Y102A receptors in Xenopus oocytes. A. *The current produced by GABA (20 μM) (black bar) was inhibited by 7.5 % in the presence of SR-95531 (**13**) (300 μM, purple bar), and SR-95813 (**14**) (300 μM, dark blue) did not inhibit the current produced by GABA (20 μM, black bar) at ρ_1Y102C mutated receptors.* ***B.*** *SR-95531 (**13**) (300 μM, purple bar), and SR-95813 (**14**) (300 μM, dark blue) did not inhibit the current produced by GABA (200 μM, black bar) at ρ_1Y102A mutated receptor. Figure adapted from reference (Yamamoto et al., 2012b).*

Table 6.4 Effect of ρ_1Y102 mutations on the activity of selected antagonists in the presence of GABA EC_{50}.

	% inhibition of GABA EC_{50} by selected compounds				
	WT	Y102S	Y102C		Y102A
Compound	300 μM [a]	300 μM [a]	300 μM [a]	IC_{50} (μM) [b]	300 μM [a]
TPMPA (**1**)	100.0 ± 0.0 %	13.0 ± 1.5 %	49.7 ± 5.5 %	447.2 ± 50.9	25.1 ± 4.4 %
(±)-*cis*-3-ACPBPA (**4**)	100.0 ± 0.0 %	22.5 ± 2.4 %	90.8 ± 2.6 %	110.7 ± 22.6	74.1 ± 11.5 %
(±)-4-ACPAM (**8**)	100.0 ± 0.0 %	Inactive at 300 μM	68.5 ± 2.1 %	241.8 ± 17.2	21.0 ± 1.0 %
4-GBA (**11**)	98.9 ± 0.6 %	9.8 ± 2.8 %	50.6 ± 7.1 %	460.1 ± 58.1	47.9 ± 7.1 %
SR-95531 (**13**)	96.0 ± 0.9 %	775.7 ± 54.9 μM [c]	7.5 ± 4.1 %	50.7 ± 6.4 % [d]	Inactive at 300 μM
SR-95813 (**14**)	98.8 ± 1.2 %	135.2 ± 16.0 μM [c]	Inactive at 300 μM	17.3 ± 6.4 % [d]	Inactive at 300 μM

[a] Data are percentage inhibition of the current produced by EC_{50} (submaximal concentration) of GABA by selected compounds (300 μM). EC_{50} (submaximal concentration) values for GABA at ρ_1 wild-type, ρ_1Y102S, ρ_1Y102C and ρ_1Y102A mutant receptors are, 1 μM, 180 μM, 20 μM and 200 μM respectively. All data are the mean ± SEM (n = 3-6 oocytes) [b] Compound concentrations of which inhibits EC_{50} of GABA (20 μM) on ρ_1Y102C receptors. [c] IC_{50} values against EC_{50} of GABA (180 μM) at ρ_1Y102S receptors. [d] Data are percentage inhibition of the current produced by EC_{50} of GABA (20 μM) by SR-95531 (**13**) and SR-95813 (**14**) (1 mM). All data are the mean ± SEM (n = 3 oocytes).

Previous studies have shown that mutating Y102 of the ρ_1 subunit to phenylalanine alters the effect of SR-95531 (**13**) (Zhang *et al.*, 2008) and that the mutation of the homologous residue in the $GABA_A$ receptor α_1-subunit (phenylalanine at position 64) to cysteine dramatically changes the affinity of SR-95531 (Holden *et al.*, 2002). The data presented in this study using SR-95531 (**13**), SR-95813 (**14**), (±)-*cis*-3-ACPBPA (**4**), 4-GBA (**11**) and TPMPA (**1**) provides further support that Y102 plays a key role in binding/gating. However, the activity of SR-95531 (**13**) and its analogue SR-95813 (**14**) is not dramatically changed when ρ_1 Y102 is mutated to serine. This indicates that, at least with the gabazine analogues, π-π interactions are not the main interactions affecting the activity of these compounds at ρ_1 receptors, despite an improved affinity of SR-95531 (**13**) when Y102 is mutated to phenylalanine (Zhang *et al.*, 2008). This supports the homology model which infers that Y102 does not directly interact with GABA (Abdel-Halim *et al.*, 2008) and is most likely a residue involved in channel gating. In support of this conclusion, the partial agonist imidazole-4-acetic acid (I4AA) activated the ρ_1Y102C mutant receptor with high efficacy and lower potency compared to ρ_1 wild-type (Torres *et al.*, 2002), consistent with Y102 being a residue involved in gating.

6.2 Conclusion

In conclusion, the affinity of ρ_1 receptor antagonists is dependent on the receptor conformation as a result of the introduced mutations. In this study we investigated the potencies of a range of antagonists at ρ_1 wild-type, ρ_1Y102S, ρ_1Y102C, and ρ_1Y102A mutant receptors. It was found that the acid moiety that is a common feature of most ρ_1 antagonists was not found to be critical for antagonist activity, as demonstrated with (±)-4-ACPAM (**8**) and SR-95813 (**14**). We also confirmed that Y102 plays an important role in the potency of (±)-4-ACPAM (**8**), SR-95531 (**13**) and SR-95813 (**14**). In addition, (±)-4-ACPAM (**8**) is more potent for closed conformational state of the ρ_1 receptor, while SR-95531 (**13**) and its analogue SR-95813 (**14**) are more potent where there are receptors in the open conformational state.

Chapter 7:

Role of phenylalanine 124 located within a novel hydrophobic cavity

Chapter 7: Role of phenylalanine 124 located within a novel hydrophobic cavity

The orthosteric binding site of the $GABA_C$ ρ_1 receptor is located at the interface of extracellular N-terminal domain of two subunits. The N-terminal domain is made of β-strands (1-10) (Cederholm *et al.*, 2009). The inner β-sheet (β-strands 1, 2, 3, 5, 6 and 8) interacts with the outer β-sheet (β-strands 4, 7, 9 and 10) forming a β-sandwich core. The residues forming the GABA binding site of ρ_1 receptors are located on five discontinuous regions of the N-terminal, referred to as loops (A-E). Loops A, B and C form the principal side and Loops D and E form the complementary side of the binding pocket (Figure 7.1**B**) (Sedelnikova *et al.*, 2005). There is evidence indicating that aromatic residues typically play key roles in ligand binding (Amin et al., 1994; Harrison et al., 2006a; Lummis et al., 2011; Sedelnikova et al., 2005; Torres et al., 2002).

Due to the lack of high-resolution structural data of $GABA_C$ ρ_1 receptors, homology models of the $GABA_C$ ρ_1 receptor ligand binding site have been developed based on a protein isolated from *Lymnaea stagnalis*, the acetylcholine binding protein (AChBP). This protein is pentameric, binds acetylcholine (ACh) and has 24% sequence homology to the N-terminal domain of nicotinic acetylcholine (nACh) α_7 Cys-loop receptors (Abdel-Halim *et al.*, 2008; Adamian *et al.*, 2009; Brejc *et al.*, 2001; Harrison *et al.*, 2006b; Osolodkin *et al.*, 2007). Modelling studies of the ρ_1 receptor identified a novel hydrophobic cavity which extended beyond the GABA binding site, located between loops A and E (Abdel-Halim *et al.*, 2008). It was found that the cavity accommodated the aromatic ring of the 5-substituted-imidazole-4-acetic acid agonists, 5-Ph-I4AA, 5-*p*-Me-Ph-I4AA and 5-*p*-F-Ph-I4AA (Figure 7.1**A**) (Abdel-Halim *et al.*, 2008; Madsen *et al.*, 2007). This cavity was composed of the loop B residues on one side and the opposing side was formed by a non-characterized part of the $GABA_C$ ρ_1 receptor sequence (Figure 7.1**B**). The model also predicted that the phenylalanine 124 (F124) pointed toward the vicinity of the cavity and docking studies suggested F124 was located within 2.3 Å of the aromatic ring of 5-Ph-I4AA (Figure 7.1**A**). F124 is

located on the β3-strand of the ρ_1 receptor (Figure 7.1**B**) and the role of this residue or the β3-strand of the ρ_1 receptor has not been established.

To investigate the role of F124 in ρ_1 receptor activity, F124 was mutated to alanine (F124A), valine (F124V), leucine (F124L), tyrosine (F124Y) and tryptophan (F124W). The purpose of mutating F124 into alanine, valine, leucine, tyrosine and tryptophan were to explore role of side-chain volume in receptor function. Mutant receptors were expressed in *Xenopus* oocytes and receptor function was assessed using the two-electrode voltage clamp method. Competitive antagonists were examined to explore the effect of the mutations within the orthosteric binding site. The kinetic properties of ρ_1F124Y mutant receptors expressed on HEK-293 cells were also examined using the outside out patch clamp method by Dr. Jane Carland, School of Medicine, The University of New South Wales. Docking studies using the $GABA_C$ ρ_1 receptor homology model (Abdel-Halim *et al.*, 2008) were performed by Dr. Heba Abdel-Halim, Faculty of Pharmacy, The University of Sydney.

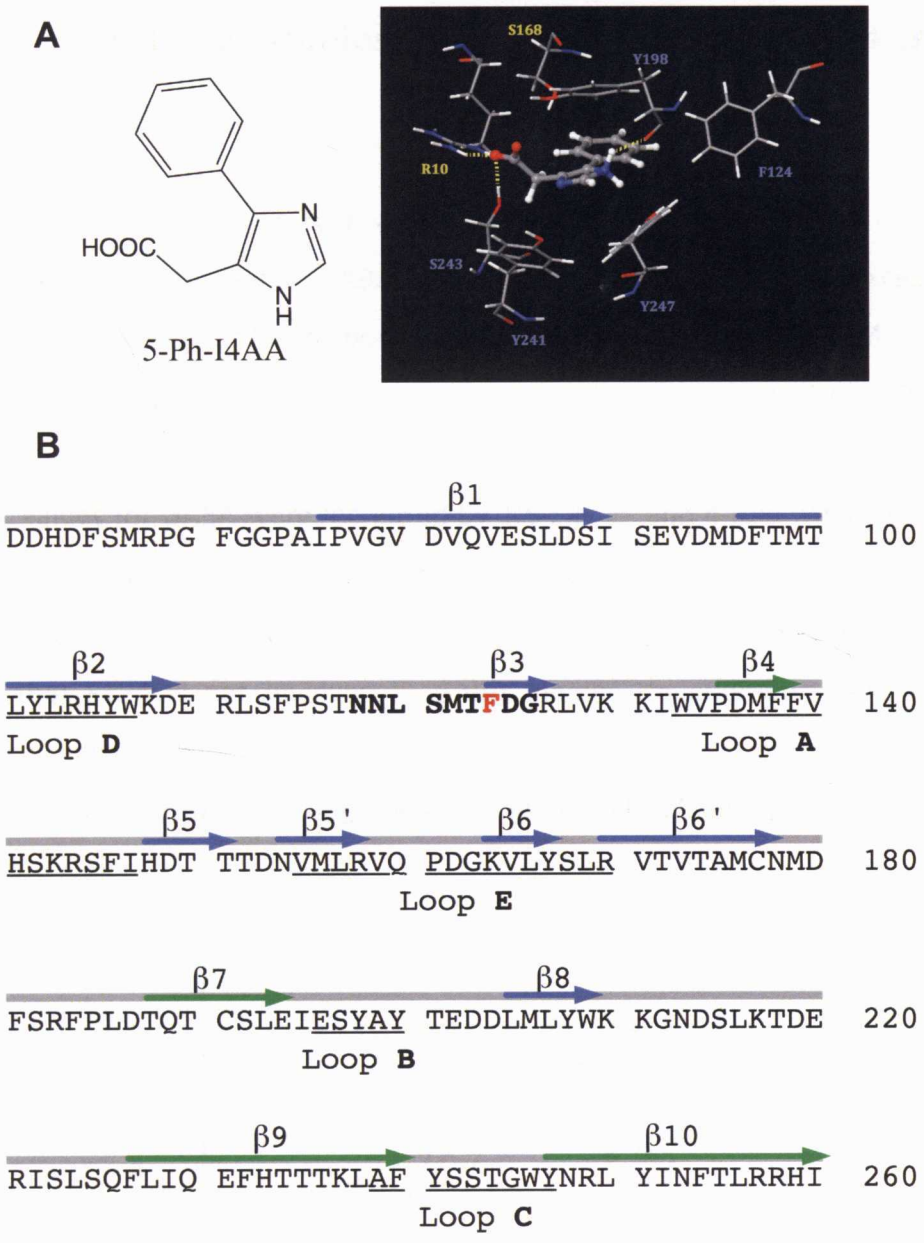

Figure 7.1 The GABA$_C$ ρ_1 receptor homology model. ***A*** *5-Ph-I4AA (Ball and Stick) docked into the homology model of GABA$_C$ ρ_1 receptor GABA binding site (Abdel-Halim et al., 2008), highlighting binding residues and F124. Selected hydrogen bonds are depicted with dashed yellow lines.* ***B*** *The amino acid sequence of the N-terminal of ρ_1 subunit. β-strands are blue (inner sheet) or green (outer sheet) arrows and connecting loops are gray lines which are indicated above the sequence labelled in Greek letters as predicted in the homology model of GABA$_C$ ρ_1 receptor (Abdel-Halim et al., 2008). The non-characterized part of sequence is in bold and F124 is highlighted in red. The amino acid sequences located at the orthosteric binding site are underlined according to the reference (Sedelnikova et al., 2005). The sequence was taken from: Genbank®, Accession code: P24046.*

7.1 Results and discussion

7.1.1 Functional studies of ρ_1 wild-type and ρ_1F124 mutant receptors

Expression of ρ_1 wild-type and ρ_1F124 mutant subunit cRNAs in *Xenopus* oocytes produced functional GABA activated receptors, with the exception of ρ_1F124A mutant receptor (no response was observed with GABA (30 mM, n = 7). At all functional ρ_1F124 mutant receptors GABA potency was reduced. This was observed as rightward shifts in the GABA concentration response curves (Figure 7.2). The EC_{50} values for GABA were increased by 1.5-, 2-, 3- and 4-fold when ρ_1F124 was mutated to tryptophan, tyrosine, leucine and valine respectively (Table 7.1; $p<0.05$, using Student's t-test). These subtle changes in GABA EC_{50} values at mutant receptors suggest that F124 is not involved in GABA binding. In addition, there were no significant changes to the Hill slopes ($p>0.05$, using Student's t-test), suggesting that the mutations were not affecting cooperatively effects of multiple agonist binding sites (Table 7.1).

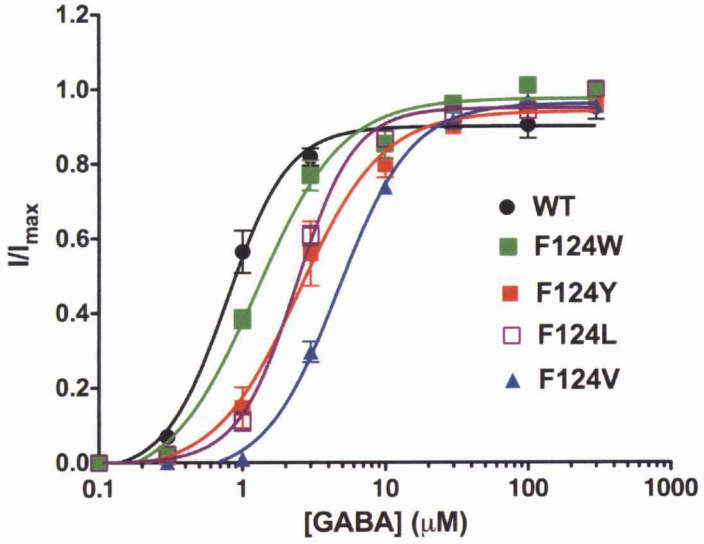

Figure 7.2 GABA concentration response curved for ρ_1 wild-type and ρ_1F124 mutant receptors. *Normalized concentration-response curves from responses to GABA for ρ_1 wild-type (black), ρ_1F124W (green), ρ_1F124Y (red), ρ_1F124L (purple) and ρ_1F124V (blue) mutant receptors expressed in Xenopus oocytes. Each data point represents the mean ± SEM (n = 3-6). All data are normalized with I_{max}, which refers to their maximum current.*

7.1.2 Kinetic properties of ρ_1 wild-type and ρ_1F124Y mutant receptors expressed in *Xenopus* oocytes and HEK-293 cells

In this study, we found that GABA evoked macroscopic deactivation rates of ρ_1F124 mutant receptors were different to ρ_1 wild-type receptors (Figure 7.3) when expressed in *Xenopus* oocytes. The deactivation phase of the currents produced by GABA EC_{50} concentrations were fitted with a monoexponential decay curve to estimate the $\tau_{Deactivation}$ for ρ_1 wild-type and ρ_1F124 mutant receptors (Table 7.1). For ρ_1 wild-type receptors, the current deactivation rate was consistent with previous findings ($\tau_{Deactivation}$ = 22.7 ± 1.4 s, n = 4) (Chang *et al.*, 1999). At mutant receptors, the current deactivation rates were significantly faster ($p<0.05$, using Student's t-test). The mutant receptors, ρ_1F124W, ρ_1F124Y, ρ_1F124L and ρ_1F124V, deactivated approximately 1.6-, 3-, 3.5- and 2.5-fold faster than $\rho_1$wild-type receptors respectively.

The mechanism of agonist-evoked receptor activation is complex and three independent steps are involved, agonist binding, sequential conformational change in the extracellular domain then lead to channel gating (Chang *et al.*, 2009). Our electrophysiological data and modelling study (Abdel-Halim *et al.*, 2008) suggest that F124 is unlikely to be involved directly in GABA binding. Interestingly, ρ_1 homomeric receptors are not prone to desensitization (Amin *et al.*, 1994; Bormann *et al.*, 1995; Chebib *et al.*, 2000) and a study performed by Chang and Weiss found channel opening locked agonist onto ρ_1 receptors (Chang *et al.*, 1999). Thus, it is possible that the change in deactivation kinetics observed at mutant receptors is due to a change/alteration of the GABA-off rate.

The ρ_1 wild-type and ρ_1F124Y mutant receptors were also expressed on HEK-293 cells to characterize the kinetic properties of the receptors using a piezoelectric driver-based rapid solution exchange system. The ρ_1 wild-type and ρ_1F124Y mutant receptor kinetic properties expressed in HEK-293 cells were quantitatively

characterized using outside-out patch configuration. At both ρ_1 wild-type and ρ_1F124Y mutant receptors the activation rate increased with increasing concentrations of GABA, while the deactivation rate was concentration independent (Table 7.2). The findings for ρ_1 wild-type receptor are consistent with previous reports (Yang *et al.*, 2006). The current decay rate was approximately 5-fold faster at ρ_1F124Y mutant than ρ_1 wild-type receptors (Table 7.2), consistent with our findings from receptors expressed in oocytes (Table 7.1).

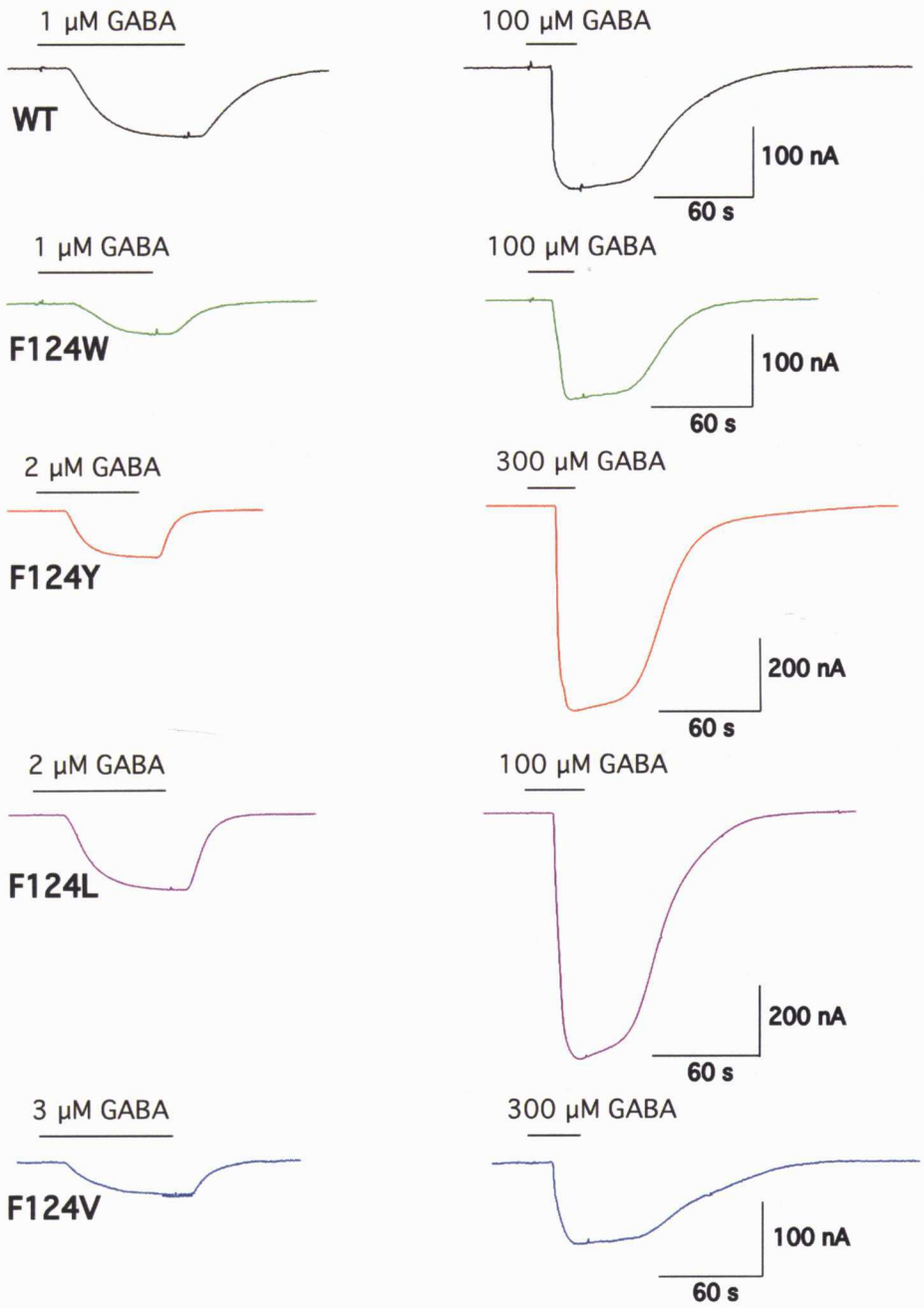

Figure 7.3 Sample current trace (nA vs sec) showing the effect of GABA at ρ_1 wild-type and ρ_1F124 mutants expressed in Xenopus oocytes. *Example of responses for GABA at ρ_1 wild-type (black), ρ_1F124W (green), ρ_1F124Y (red), ρ_1F124L (purple) and ρ_1F124V (blue) mutant receptors at approximately EC_{50} and I_{max} GABA concentrations.*

Table 7.1 A comparison of intrinsic efficacy of GABA, Hill coefficient and $\tau_{Deactivation}$ at ρ_1 wild-type and ρ_1F124 mutant receptors expressed in Xenopus oocytes.

ρ_1 F124 mutation	EC_{50} (μM)	Hill coefficient (n_H)	$\tau_{Deactivation}$ [c] (s) at GABA EC_{50} concentration
WT	0.83 ± 0.05	1.96 ± 0.22	22.70 ± 1.36
F124W	1.24 ± 0.08 [a]	1.42 ± 0.25	13.81 ± 0.95 [a]
F124Y	1.98 ± 0.15 [a]	1.60 ± 0.08	7.28 ± 0.89 [a]
F124L	2.37 ± 0.21 [a]	2.17 ± 0.07	6.53 ± 0.32 [a]
F124V	3.44 ± 0.71 [a]	1.46 ± 0.21	9.17 ± 0.51 [a]
F124A	NR [b]	-	-

All Data are the mean ± SEM (n = 3-6 oocytes). [a] Significantly different from wild-type (WT) (p<0.05, using Student's t-test). [b] NR, no response was detected at GABA 30 mM concentration (n = 4). [c] The deactivation phase of the current was approximated by a monoexponential function.

Table 7.2 Kinetic properties of ρ_1 wild-type and ρ_1F124Y mutant receptors expressed in HEK-293 cells.

	WT		
GABA (μM)	$\tau_{Activation}$ (ms) [a]	Rise time (s)	$\tau_{Deactivation}$ (ms) [b]
3	2240 ± 153	7.4 ± 0.5	6518 ± 972
10	910 ± 170	2.4 ± 0.4	3943 ± 856
30	215 ± 80	0.9 ± 0.4	5157 ± 730
100	39 ± 6	0.12 ± 0.03	3512 ± 981
	F124Y		
10	633 ± 66	1.4 ± 0.2	774 ± 135 [c]
30	193 ± 30	0.45 ± 0.04	900 ± 400 [c]
100	126 ± 13	0.4 ± 0.08	663 ± 178 [c]

All recordings were made at a pipette potential of -40 mV. Data are mean ± SEM (n = 3-8). [a] The activation phase of the current was approximated by a monoexponential function. [b] The deactivation phase of the current was approximated by two exponentials. Data are presented as the weight average mean of $\tau_{Deactivation}$ 1 and $\tau_{Deactivation}$ 2. [c] Significantly different from wild-type (WT) (p<0.05, using Student's t-test).

For Cys-loop receptor activation, agonist binding initiates a series of conformational changes within the N-terminal domain, resulting in a constriction of the binding pocket to gate the channel pore (Celie *et al.*, 2004; Hansen *et al.*, 2005; Wagner *et al.*, 2001). This structural rearrangement at the binding site during channel gating may be involved in slowing agonist release at ρ_1 wild-type receptors (Chang *et al.*, 1999). If that is the case, mutations at F124 may influence the open conformation of the N-terminal domain. Therefore, these findings infer that by altering the size or polarity of amino acid side-chain decreases $\tau_{Deactivation}$ by influencing the GABA-off rate. F124 may stabilise the protein backbone around the GABA binding site. Thus mutations at this position may have an effect on sustaining the channel open conformation or they may influence the mechanism of constriction of the binding site upon GABA binding, resulting reduction in $\tau_{Deactivation}$.

Cys-loop receptors are conformationally dynamic, and when an agonist binds triggers rapid structural rearrangements in the millisecond time frame leading to channel opening. Stability and flexibility of proteins are interdependent and hydrophobic cores usually achieve protein stability. Amino acids with bulky side chains are usually found at protein cores to fill the space (Chothia, 1984; Sandberg *et al.*, 1989) and any mutations which loosen the packing of these cores can decrease thermodynamic stability (Eriksson *et al.*, 1992; Kellis *et al.*, 1988; Pakula *et al.*, 1989; Sonavane *et al.*, 2008). The recent work by Czajkowski and co-workers proposed the loose packing of the extracellular domain hydrophobic core influences the function of Cys-loop receptors (Dellisanti *et al.*, 2011). They introduced mutations at β2- and β6'-strands to disrupt the loose packing and found that interruption of β-core packing influenced receptor function. As F124 is located in the inner β-sheet (β3-strand) (Figure 7.1), it is possible that the mutations affect protein stability and flexibility, thus affecting the receptor $\tau_{Deactivation}$ rate.

7.1.3 Activities of competitive antagonists at ρ_1 wild-type and ρ_1F124 mutant receptors

The activities of the competitive antagonists TPMPA and gabazine (SR-95531) were measured to assess the effect of F124 mutations upon antagonist binding (Figure 7.4). TPMPA and gabazine maintained their antagonist activity at F124 mutant receptors (Table 5.3). However there was a significant change in the apparent K_B values for the competitive antagonist TPMPA at ρ_1F124W and ρ_1F124V mutant compared to ρ_1 wild-type receptors. No significant change in the apparent K_B values was observed at ρ_1F124Y and ρ_1F124L receptors (p>0.05, using Student's t-test). In addition, a significant change in gabazine activity was found at ρ_1F124Y and ρ_1F124V receptors (p<0.05, using Student's t-test), but not at ρ_1F124W and ρ_1F124L receptors (p>0.05, using Student's t-test). Although there were significant changes in antagonist activities at some mutants, the changes were subtle, suggesting it is unlikely that F124 is forming part of the binding site for TPMPA and gabazine.

The change in the observed antagonists affinities may relate to the size of amino acid side chain volume at the position 124. Phenylalanine contains a large side-chain and mutation of this residue to amino acids with a similar side-chain volume, tryprophan and tyrosine (the apparent volumes of phenylalanine, tryptophan and tyrosine in solution are, 121.3, 144.1 and 123.6 ml/mole respectively.), has relatively small impact on agonist/competitive antagonist binding site(s). On the other hand, the side-chain volume of valine (91.3 ml/mole) is reduced compared to phenylalanine (121.3 ml/mole) (Zamyatnin, 1972). ρ_1F124V receptors were functional and exhibited significant changes in the agonist/competitive affinities. At ρ_1F124V mutant receptors, TPMPA and gabazine affinities were altered (Table 7.3), and also the affinity of GABA was reduced up to 4-fold suggesting the structure of agonist/competitive antagonist binding site(s) were affected by the insertion of smaller amino acids at position 124. It appears that the side-chain volume is important at the position 124 to stabilize the structure of agonist/competitive antagonist binding site(s).

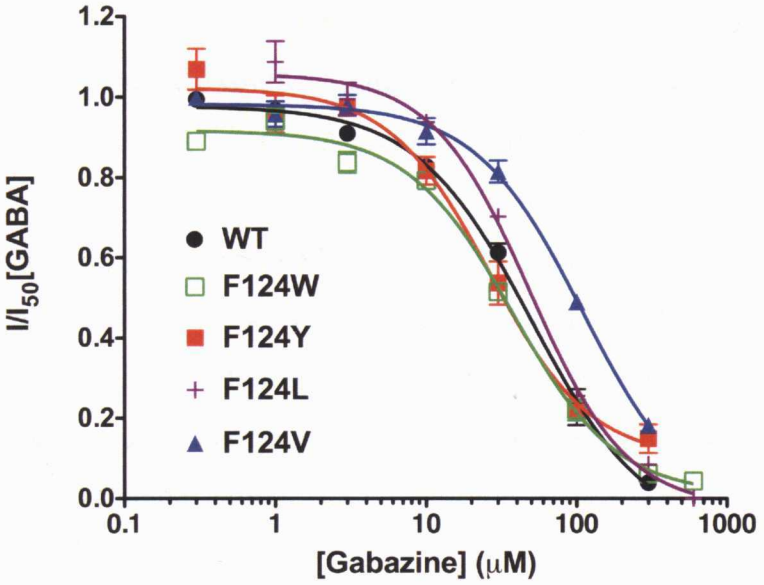

Figure 7.4 Inhibitory concentration-response curves for gabazine at ρ_1 wild-type and ρ_1F124 mutants. *ρ_1 wild-type (black), ρ_1F124W (green), ρ_1F124Y (red), ρ_1F124L (purple) and ρ_1F124V (blue) mutant receptors expressed in Xenopus oocytes. Each data point represents the mean ± SEM (n = 3-4). All data are normalized with $I_{50\,[GABA]}$.*

Table 7.3 Activities of competitive antagonists at ρ_1 wild-type and ρ_1F124 mutant receptors expressed in Xenopus oocytes.

ρ_1 F124 mutation	TPMPA (μM)	SR-95531 (μM)
WT	K_B = 1.89 ± 0.04	IC_{50} = 60.66 ± 12.55
F124W	K_B = 3.05 ± 0.21 [a]	IC_{50} = 36.83 ± 1.86
F124Y	K_B = 2.50 ± 0.24	IC_{50} = 29.40 ± 4.79 [a]
F124L	K_B = 2.16 ± 0.30	IC_{50} = 48.69 ± 2.56
F124V	K_B = 4.2 ± 1.01 [a]	IC_{50} = 127.30 ± 19.57 [a]

Data are the mean ± SEM (n = 3-4 oocytes). [a] Significantly different from wild-type (WT) (p<0.05, using Student's t-test).

7.2 Conclusion

Mutations at F124 had a modest effect on receptor pharmacology but had significant effect on the deactivation rate ($\tau_{Deactivation}$) when expressed in *Xenopus* oocytes and HEK-293 cells. The activities for TPMPA and gabazine were not greatly

affected by the mutations suggesting that F124 is unlikely to be involved in antagonist binding. At ρ_1F124V receptors, GABA affinity was shifted approximately 4-fold with significant but minor changes in TPMPA and gabazine potency suggesting that the removal of an aromatic ring at position 124 could influence the stability of the overall structure of the agonist/antagonist binding site(s). The amino acid side chain volume and its polarity appear to be important at the position 124, influencing the GABA deactivation current at ρ_1 wild-type receptors. We hypothesize that F124 may be involved in channel gating or contributing in sustaining the open conformation of N-terminal domain upon channel gating.

Chapter 8:

The effect of novel gabazine analogues at GABA receptors

Chapter 8: The effect of novel gabazine analogues at GABA receptors

Gabazine **1** (Figure 8.1), also known as SR-95531, is a potent and selective $GABA_A$ receptor antagonist, widely used as a pharmacological tool when studying $GABA_A$ receptors *in vitro* and *ex vivo*. Intravenous administration of gabazine (**1**) elicits tonic-clonic seizures in mice, indicating its ability to cross the blood brain barrier (Heaulme *et al.*, 1986).

Gabazine **1** contains a butyric acid and an aminopyridazine moiety, which have some chemical characteristics similar to GABA, implicating a possible interaction with GABA recognition sites. However, it is not necessary to have compounds that strictly resemblance GABA in order to displace [^{3}H]GABA from its binding site (Wermuth *et al.*, 1987). Gabazine was identified from a series of aminopyridazine derivatives that were synthesized to conduct structure-activity relationship studies at $GABA_A$ receptors (Heaulme *et al.*, 1986; Iqbal *et al.*, 2011; Wermuth *et al.*, 1987). It was shown that the presence of an aromatic ring at the 6-position of the pyridazine ring and an extended aminobutyric acid side-chain were important for antagonist activity (Wermuth *et al.*, 1987). In addition, the substituents attached to the aromatic ring were found to be important for potency (Heaulme *et al.*, 1986; Iqbal *et al.*, 2011).

$GABA_C$ receptors are another class of ionotropic GABA receptors (Ortells *et al.*, 1995) found at distinct anatomical areas within the central nervous system (CNS) including the superior colliculus (Boue-Grabot *et al.*, 1998), cerebellum (Rozzo *et al.*, 2002), hippocampus (Alakuijala *et al.*, 2005) and lateral amygdala (Cunha *et al.*, 2010). $GABA_C$ receptors have been shown to play an important role in the onset of myopia (Stone *et al.*, 2003), in the sleep-waking process (Arnaud *et al.*, 2001), memory enhancement (Johnston, 2002) and in fear and anxiety disorders (Cunha *et al.*, 2010). Therefore, designing potent $GABA_C$ receptor selective agents, that cross the blood brain barrier, will help establish the physiological importance of these receptors in these processes.

Gabazine **1** is known to inhibit current elicited by GABA at $GABA_C$ receptors, however the inhibitory effect is weaker than at $GABA_A$ receptors (Zhang *et al.*, 2008). Previously we found that substituting the carboxylic acid group of gabazine with a nitrile improved its activity at $GABA_C$ (ρ_1) receptors (Yamamoto *et al.*, 2012b). Therefore, designing agents based on the core structure of gabazine with the knowledge of $GABA_C$ receptor antagonists may lead to more potent and selective agents that act on $GABA_C$ receptors. In this study, the pharmacological characterization of a series of novel 6-aryl-3-aminopyridazine derivatives (Gavande *et al.*, 2010a) were performed to establish a structure-activity relationship profile.

The series of 6-aryl-3-aminopyridazine analogues were designed and synthesized by Dr. Navnath Gavande, Faculty of Pharmacy, The University of Sydney, Australia.

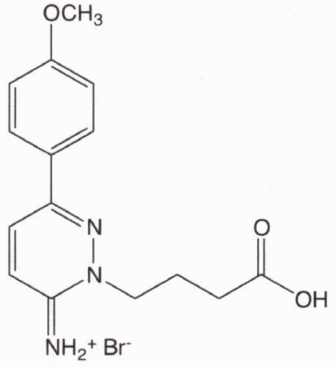

Gabazine (SR-95531) **1**

Figure 8.1 Structure of gabazine

8.1 Results and discussion

8.1.1 Antagonist activities at GABA receptors

We evaluated 14 novel 6-aryl-3-aminopyridazine derivatives (Table 8.1) at recombinant $GABA_A$ ($\alpha_1\beta_2\gamma_{2L}$) and $GABA_C$ (ρ_1) receptors expressed in *Xenopus* oocytes and the activities of the analogues were measured using the two-electrode voltage clamp methods. All gabazine analogues **2-15** had no agonist effects at $GABA_A$ or $GABA_C$ receptors when tested at 100 μM (n = 3). Consistent with previous findings (Zhang *et al.*, 2008), it was found that gabazine **1** was an antagonist, inhibiting the effect of GABA at both receptor combinations, and it was found that gabazine was approximately 200-fold more potent at $GABA_A$ ($\alpha_1\beta_2\gamma_{2L}$) than $GABA_C$ (ρ_1) receptors (IC_{50} ($\alpha_1\beta_2\gamma_{2L}$) = 0.3 ± 0.0 μM, IC_{50} (ρ_1) = 60.7 ± 12.5 μM) (Table 8.2).

The inhibitory activities of the remaining 14 novel gabazine analogues **2-15** were then evaluated in the presence of the GABA EC_{50} concentration at $GABA_A$ and $GABA_C$ receptors (EC_{50} values for GABA at $GABA_A$ and $GABA_C$ receptors were 30 μM and 1 μM, respectively). Compounds were initially tested using two concentrations, 0.1 μM and 1 μM at $GABA_A$ receptors, and 30 μM and 100 μM at $GABA_C$ receptors in the presence of their respective GABA EC_{50} concentrations. The percentage inhibition of the GABA current by compounds **2-15** was measured and normalized to the current obtained by GABA alone (Table 8.2). If the activity of analogues were higher or similar to gabazine **1**, then full inhibitory concentration response curves were generated and IC_{50} values were calculated (Table 8.2, Figure 8.2, Figure 8.3).

Table 8.1 Structures of gabazine analogues.

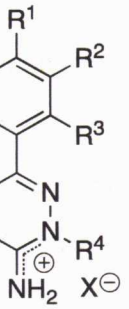

Compound	R^1	R^2	R^3	R^4	X
2	H	OCH_3	H	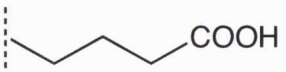	Br
3	H	H	OCH_3		
4	H	H	H		
5	OH	H	H		
6	OCH_3	H	H	-	-
7	H			-	-
8	OCH_3	H	H		Cl
9	OCH_3	H	H	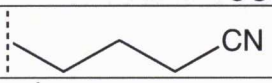	Br
10	OCH_3	H	H	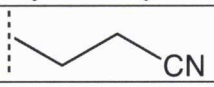	Br
11	OCH_3	H	H		Cl
12	OCH_3	H	H		Cl
13	OCH_3	H	H	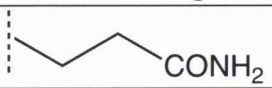	Cl
14	OCH_3	H	H	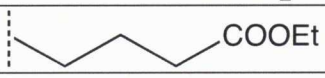	Cl
15	OCH_3	H	H	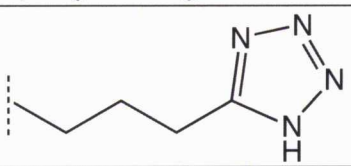	Cl

8.1.1.1 *Antagonist activities at $GABA_A$ receptors*

All tested compounds **2-15** inhibited the current produced by GABA (30 μM) at $GABA_A$ receptors. It was found that a *para* (*p*)-methoxy group as in gabazine **1** is approximately 2 fold more potent than when the methoxy group is either in the *ortho* (*o*)-**2** or *meta* (*m*)-position **3** (Table 8.2). Hydrogen bond donor groups such as the (*p*)-hydroxy group, as found on analogue **5**, reduced the potency by approximately 4 fold at $GABA_A$ receptors (Table 8.2). In addition, removal of the substituent on the aromatic ring as shown in analogue **4** resulted in a decrease in potency at $GABA_A$ receptors. Removing the butyric acid side-chain to generate analogue **6** and replacing the (*p*)-methoxyphenyl by the bicyclic aromatic quinolin ring **7** also reduced the potency at $GABA_A$ receptors (Table 8.2, Figure 8.2).

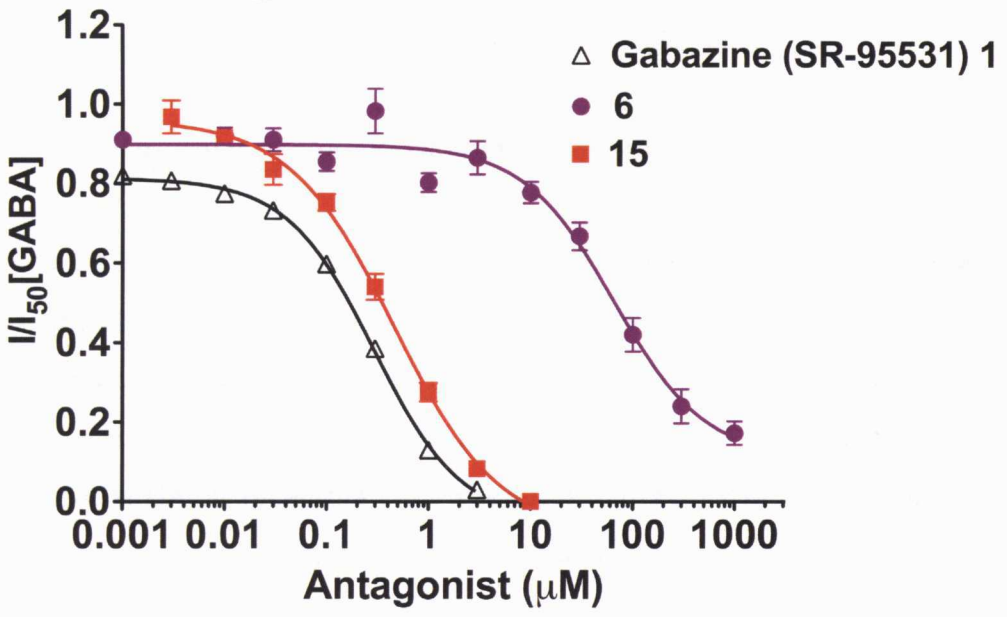

Figure 8.2 Inhibitory concentration-response curves for gabazine 1, compounds 6 and 15 at $GABA_A$ ($\alpha_1\beta_2\gamma_{2L}$) receptors. *Gabazine **1**, compounds **6** and **15** are shown in black, purple and red respectively. Each data point represents the mean ± SEM (n = 3-4).*

The effect of modifying the butyric acid side-chain of gabazine on the antagonist activity was also studied. The resulting compounds **8-15** were found to be antagonists with varying potency at $GABA_A$ receptors. Increasing the length of the side-chain to generate analogue **8** or substituting the carboxylic acid with a nitrile group to generate **9** and **10**, an amide group **13** or an ethyl ester group to give **14** resulted in compounds with weaker inhibitory effects than gabazine **1** at $GABA_A$ receptors (Table 8.2). Similar results were reported in a previous gabazine structure-activity relationship study for $GABA_A$ receptors (Wermuth *et al.*, 1987). In their study, lengthening the butyric side chain or substituting with nitriles or ethyl ester groups resulted in weaker displacements of [^{3}H]GABA binding at rat whole brain membranes (Wermuth *et al.*, 1987). Replacing the carboxylic acid moiety of the butyric acid chain with either a phosphonic **11** or phosphinic acid group **12** also reduced the potency by approximately 4-fold as compared to gabazine **1** at $GABA_A$ receptors. The only analogue that showed similar potency to gabazine was **15**, the 5-substituted-1*H*-tetrazole analogue (IC_{50} ($\alpha_1\beta_2\gamma_{2L}$) = 0.5 ± 0.1 μM). This was not surprising as tetrazoles are well known to act as carboxylic acid bioisosteres (Herr, 2002).

8.1.1.2 Antagonist activities at $GABA_C$ receptors

At $GABA_C$ receptors, compounds **9**, **10**, **13-15** inhibited currents produced by GABA (1 μM) (Figure 8.3) while compounds **8**, **11** and **12**, at either 30 μM or 100 μM, failed to inhibit the GABA current (Table 8.2). Similar to what was found for the $GABA_A$ receptor, the methoxy group in the (*p*)-position **1** was approximately 2-4 fold more potent at $GABA_C$ receptors than when it is in the (*o*)-**2** or (*m*)-position **3** (Table 8.2). In addition, the (*p*)-hydroxy analogue **5** was approximately 4 fold less potent than gabazine **1** while the removing the substitution **4** also resulted in a decrease in potency at $GABA_C$ receptors (Table 8.2).

Unlike what was found at the $GABA_A$ receptor however, removing the butyric acid side-chain produced some interesting and unexpected findings. Compound **6** (IC_{50} (ρ_1) = 4.3 ± 0.4 μM) was approximately 15-fold more potent as an antagonist at $GABA_C$ receptors as compared to gabazine **1** (IC_{50} (ρ_1) = 60.7 ± 12.5 μM) and

approximately 20-fold more potent at $GABA_C$ as compared to $GABA_A$ receptors (IC_{50} ($\alpha_1\beta_2\gamma_{2L}$) = 67.8 ± 9.7 μM). However, modification at the phenyl ring **7** reduced antagonist potency at $GABA_C$ receptors (Table 8.2).

Modifications of the butyric acid side-chain of gabazine **8-15** altered activity at $GABA_C$ receptors (Table 8.2). Lengthening the butyric acid side-chain **8** or substituting the carboxylic acid group with a phosphonic **11** or phosphinic acid **12** resulted in compounds, which were practically inactive at $GABA_C$ receptors (Table 8.2). Substituting the carboxylic acid with a nitrile (compounds **9** and **10,** IC_{50} (ρ_1) = 8.0 ± 0.8 and 3.4 ± 0.6 μM, respectively) or an amide group **13** (IC_{50} (ρ_1) = 14.3 ± 3.4 μM) also resulted in a compound with improved inhibitory effects compared to gabazine **1** (IC_{50} (ρ_1) = 60.7 ± 12.5 μM) at $GABA_C$ receptors (Table 8.2, Figure 8.3). Substituting the carboxylic acid group with an ethyl ester group **14** did not significantly change the potency of the compound at $GABA_C$ receptors (Table 8.2; $p>0.05$, using Student's t-test). The 5-substituted-1*H*-tetrazole analogue **15** (IC_{50} (ρ_1) = 3.4 ± 0.6 μM) had improved antagonist potency, being 20-fold more potent than gabazine **1** at $GABA_C$ receptors. Our findings indicate that the carboxylic acid moiety is not necessary for antagonist activity at $GABA_C$ receptors consistent with our previous study (Yamamoto *et al.*, 2012b) while it is critical for potency at $GABA_A$ receptors, suggesting that selective $GABA_C$ receptor antagonists can be designed with reduced $GABA_A$ receptor effects.

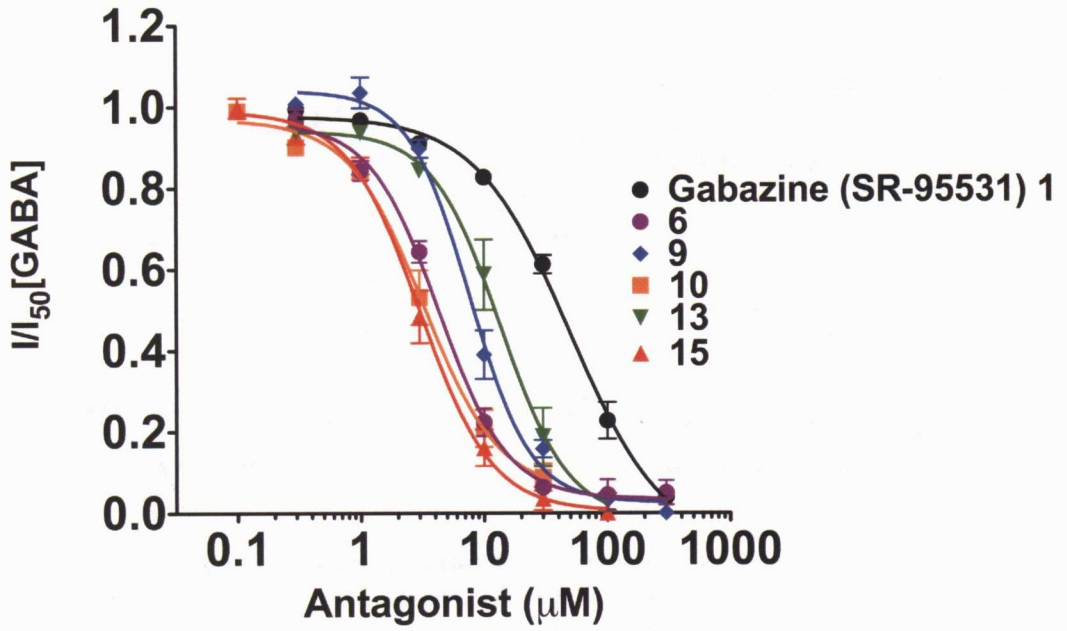

Figure 8.3 Inhibitory concentration-response curves for gabazine 1, compounds 6, 9, 10, 13 and 15 at $GABA_C$ (ρ_1) receptors. *Gabazine **1**, compounds **6**, **9**, **10**, **13** and **15** are shown in black, purple, blue, orange, green and red respectively. Each data point represents the mean ± SEM (n = 3-4).*

*8.1.1.3 Compound **6** is a competitive antagonist at $GABA_C$ receptors*

Removal of the butyric acid side-chain and the resulting (*p*)-methoxy compound **6** showed weak inhibitory effects at $GABA_A$ receptors as compared to gabazine **1** (Figure 8.2, Table 8.2). As previously reported, gabazine **1** and compound **9** are competitive antagonists at $GABA_C$ receptors (Yamamoto *et al.*, 2012b). In order to determine whether the compound **6** is a competitive antagonist at $GABA_C$ receptors, we constructed a Schild plot to determine the dissociation constants (K_B) for **6** and compared K_B values with gabazine **1** and compound **9** at $GABA_C$ receptors (Figure 8.4, Table 8.2). It was found that all three compounds inhibited $GABA_C$ receptors in a competitive manner as the Schild slopes did not differ from 1 (Figure 8.4**B**).

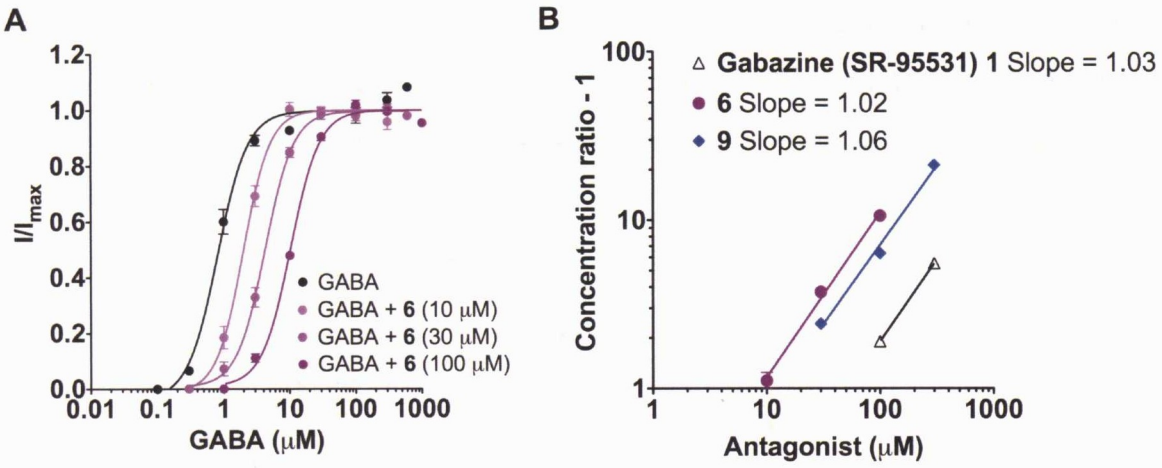

Figure 8.4 Pharmacology of compound 6 at $GABA_C$ (ρ_1) receptors. ***A*** *Concentration response curves of GABA alone (black dot, n = 4) and in the presence of compound* ***6*** *at 10 (light purple dot, n = 4), 30 (purple dot, n = 3) and 100 μM (dark purple dot, n = 3). Each data point represents the mean ± SEM (n = 3-4). All data are normalized with I_{max}, which refers to their maximum GABA current.* ***B*** *Schild plot analysis for gabazine* ***1****, compounds* ***6*** *and* ***9*** *at $GABA_C$ (ρ_1) receptors. The action of gabazine* ***1*** *(black), compounds* ***6*** *(purple) and* ***9*** *(blue) in antagonizing the effect of GABA at ρ_1 receptors. Each data point represents the mean ± SEM (n = 3-4).*

These data are interesting as they show that it is not necessary to possess an acid moiety to attain compounds that are potent and selective for $GABA_C$ receptors. To date most compounds reported to be potent at $GABA_C$ receptors contain a carboxylic acid or bioisostere (Ng *et al.*, 2011) in order to act as a competitive antagonist at $GABA_C$ receptors. However, our previous study in Chapter 6, we discovered two antagonists which did not possess acid moiety, SR-95813 and (±)-4-ACPAM, and they were both competitive antagonists at $GABA_C$ (ρ_1) receptors (Yamamoto *et al.*, 2012b). In contrast, previous reports indicated that the butyric acid side-chain in gabazine **1** is important to retain/improve antagonist potency at GABA sites (Wermuth *et al.*, 1987). Consistent with our previous study, this study suggests it is not the case for $GABA_C$ receptors. Therefore, current studies are underway to develop non-zwitterionic selective $GABA_C$ antagonists that can probe the binding site at $GABA_C$ receptors.

Gabazine **1** and compound **6** were docked into our homology model of the $GABA_C$ receptor ligand binding site (Abdel-Halim *et al.*, 2008) (Figure 8.5). The model predicts that the pyridazine ring is orientated in the opposite direction to gabazine **1**

and in the case of compound **6**, the nitrogens are interacting with arginine at position 104 making direct interactions through hydrogen bonds. The difference in the binding mode of the pyridazine ring may contribute to the differences in the activities of the two compounds at $GABA_C$ receptors.

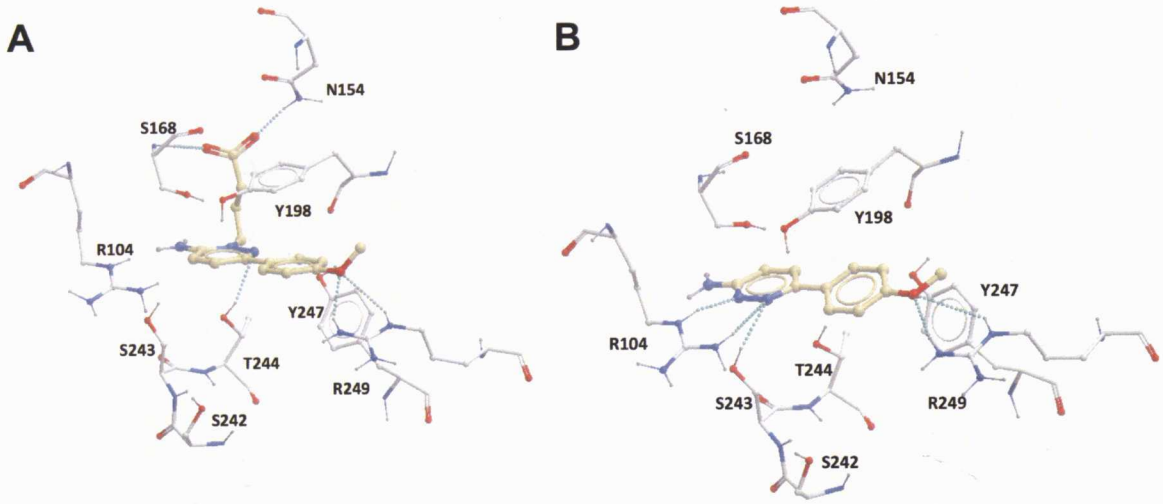

Figure 8.5 Gabazine 1 and compound 6 docked into the homology model of (ρ_1) receptor GABA binding site. ***A*** *Image of gabazine* ***1*** *docked in the binding site. Selected H-bonds are depicted with dashed green lines.* ***B*** *Image of compound* ***6*** *docked in the binding site. Selected H-bonds are depicted with dashed green lines.*

Table 8.2 Activities of gabazine 1 and its analogues 2-15 at GABA receptors.

Compound	% Inhibition of GABA EC_{50} at $GABA_A$ ($\alpha_1\beta_2\gamma_{2L}$) receptor [a]			% Inhibition of GABA EC_{50} at $GABA_C$ (ρ_1) receptor [b]		
	0.1 μM [c]	1 μM [c]	IC_{50} (μM) [d]	30 μM [c]	100 μM [c]	IC_{50} [d] / K_B [e] (μM)
1	40.3 ± 1.3	87.0 ± 0.8	IC_{50} = 0.3 ± 0.0	44.5 ± 4.0	83.0 ± 5.0	IC_{50} = 60.7 ± 12.5 K_B = 51.2 ± 2.9
2	30.3 ± 3.1	68.8 ± 0.3		15.9 ± 0.9	52.6 ± 5.4	
3	20.2 ± 3.0	24.3 ± 2.3		10.6 ± 1.6	16.2 ± 4.4	
4	20.7 ± 2.8	33.1 ± 3.1		13.2 ± 2.3	35.8 ± 3.9	
5	4.3 ± 2.3	21.0 ± 3.0		13.3 ± 5.6	22.1 ± 2.5	
6	13.5 ± 2.0	20.9 ± 1.7	IC_{50} = 67.8 ± 9.7	94.5 ± 1.3	95.4 ± 2.7	IC_{50} = 4.3 ± 0.4 K_B = 8.6 ± 0.7
7	13.6 ± 0.5	17.0 ± 0.9		10.8 ± 1.1	15.6 ± 3.8	
8	20.7 ± 1.8	23.7 ± 1.9		NA	NA	
9	16.4 ± 3.4	31.9 ± 1.7		84.3 ± 2.1	96.8 ± 0.5	IC_{50} = 8.0 ± 0.8 K_B = 12.4 ± 0.4
10	28.4 ± 0.8	55.2 ± 2.1		91.3 ± 3.4	100. 0 ± 0.0	IC_{50} = 3.4 ± 0.6
11	8.9 ± 2.7	22.4 ± 2.0		NA	NA	
12	19.9 ± 1.4	24.5 ± 1.6		NA	NA	
13	21.8 ± 1.0	37.7 ± 1.1		81.3 ± 7.2	97.3 ± 2.2	IC_{50} = 14.3 ± 3.4
14	7.7 ± 2.8	27.0 ± 1.6		68.2 ± 3.5	88.3 ± 2.0	
15	58.7 ± 1.9	93.2 ± 0.5	IC_{50} = 0.5 ± 0.1	96.5 ± 2.9	100. 0 ± 0.0	IC_{50} = 3.4 ± 0.6

Determined electrophysiologically in *Xenopus* oocytes expressing $GABA_A$ ($\alpha_1\beta_2\gamma_{2L}$) or $GABA_C$ (ρ_1) receptors. Data are the mean ± SEM of inhibition in 3-4 different cells. [a] Percent inhibition of the chloride ion flow triggered by GABA EC_{50} concentration (30 μM) and test compound. [b] Percent inhibition of the chloride ion flow triggered by GABA EC_{50} concentration (1 μM) and test compound. [c] Concentration of test compound. NA: no activity was observed at the tested concentration. [d] Data are the mean ± SEM (n = 3-4). [e] Data are the mean ± SEM (n = 3). Structures are given in Table 8.1.

8.2 Conclusion

In this chapter the effect of a variety of gabazine analogues (**2-15**) were studied at recombinant $GABA_A$ and $GABA_C$ receptors. It was found that the (*p*)-methoxy substitutuent of gabazine **1** is crucial for potency at both $GABA_A$ and $GABA_C$ receptors which is consistent with previous findings (Wermuth *et al.*, 1987). The chemical modifications at the butyric acid moiety, resulted in improved antagonist potency at $GABA_C$ but not at $GABA_A$ receptors (Table 8.2). On the other hand, lengthening of the side chain **8** was disfavored at both receptors. Improved activities at $GABA_C$ receptors were observed when the carboxylic acid group of gabazine is replaced with either a nitrile **9** and **10**, an amide **13** or an ethyl ester **14**. (+)-4-ACPCA is a potent competitive antagonist at $GABA_C$ receptors and it posses a carboxylic acid moiety (Chebib *et al.*, 2001). We found that substitution of the carboxylic acid with an amide group did not affect the antagonist activity of (±)-4-ACPAM (Yamamoto *et al.*, 2012b). It appears the carboxylic acid moiety is not necessary for antagonist activity at $GABA_C$ receptors. It will be interesting to explore the binding sites of non-zwitterionic selective $GABA_C$ antagonists.

To our surprise, the phosphonic **11** and phosphinic acid **12** analogues had no inhibitory effects at $GABA_C$ receptors. Phosphonic or phosphinic acids are known to enhance the selectivity of compounds for $GABA_C$ receptors over $GABA_A$ receptors (Chebib *et al.*, 2007; Kumar *et al.*, 2008; Murata *et al.*, 1996) but this was not found to be the case for these analogues (Table 8.2).

The 5-substituted-1*H*-tetrazole analogue **15** had similar potency to gabazine **1** at $GABA_A$ while it had improved potency at $GABA_C$ receptors. 5-Substituted-1*H*-tetrazole is often used as a metabolism-resistant isosteric replacement for carboxylic acids, improving pharmacokinetics of medicinally active compounds (Herr, 2002). It will be interesting to design analogues based on the structure of 5-substituted-1*H*-tetrazole analogue **15** for animal models in the future.

Finally, the removal of the butyric side-chain **6** improved antagonist potency for $GABA_C$ but not for $GABA_A$ receptors (Figure 8.2 and Figure 8.3). It appears that the butyric acid side-chain of gabazine **1** is not important for its potency and its competitive nature at $GABA_C$ receptors. In addition, this compound was approximately 20-fold weaker at $GABA_A$ receptors, indicating it is selective for $GABA_C$ over $GABA_A$ receptors. Our findings suggest that compound **6** may have potential physiological effects such as memory improving effects *in vivo* targeting primarily at $GABA_C$ receptors. This hypothesis could be tested using behavioural experiments on a mouse model.

Chapter 9:

General Discussion

Chapter 9: General Discussion

The Cys-loop superfamily of LGICs is critical for mediating the inter-cellular communication of neurons in the CNS. All members of the family, including $GABA_C$ receptors, share significant amino-acid sequence homology and have an identical quaternary pentameric structure. The extracellular N-terminal domain contains the signature motif, a conserved pair of cysteine residues that bond together to form a loop along with the orthosteric ligand binding site that is located at the interface between two subunits. This thesis focused on how ligands interact within their binding site and their relationship with receptor function.

During channel gating, signals are mediated from the extracellular domain to the transmembrane domain *via* coupling regions. As shown by the REFER approach and kinetic studies, sequential conformational changes at the N-terminal domain occur upon agonist binding to gate the channel pore. However, detailed molecular knowledge of the ligand binding site and the gating mechanism across Cys-loop receptors is not fully understood. The observations made in this thesis serve to emphasize that upon agonist or antagonist binding, the conformation of the receptor changes and at the same time, the open or closed conformational states influence the conformation of the binding site. We observed that a series of point mutations at the binding site influences receptor gating, highlighting the dynamic nature of these receptors. These findings draw attention to the relationship between ligand binding and receptor gating, and also the relationship between receptor structure and function.

We employed pharmacological tools, partial agonists and competitive antagonists to assess the effect of mutations on receptor function. Changes in GABA activity at mutant receptors imply GABA binding and/or receptor function have been compromised. Usually changes in the potency and efficacy of partial agonists against GABA indicate that the mutations have altered receptor gating (Chapter 5 and Chapter 6). Changes in competitive antagonist activities imply structural changes to the agonist binding site by the mutations (Chapter 6 and Chapter 7). Thus, partial

agonists and competitive antagonists give us insights into the effects of mutations, which could not be revealed by full agonists alone.

Xenopus oocytes are very useful when studying $GABA_C$ receptor ligands, however it is not a suitable assay to use when aiming to address questions related to neurological disorders. It is important to understand how $GABA_C$ receptor behaves in mammals to discuss and implication the therapeutic potential of results. Receptors usually exist with associated proteins and the potential partner proteins differ between the expressing systems. It is important to use mammalian expression systems such as HEK293 cells, since it is likely that important associated proteins exist in mammalian cells but not in *Xenopus* oocytes. The work using mouse L929 fibroblasts by Everitt and his co-workers showed the co-expression of GABARAP specially is important in $GABA_A$ receptor functions (Everitt *et al.*, 2004). This implicates that the use of neuronal cells, either primary or immortal cultures, we may be able to observe unknown receptor functions due to the unidentified associated proteins. This allows us to yield information that oocytes and transfected cell lines cannot.

GABA is a major inhibitory neurotransmitter in the mammalian CNS. It has three rotatable bonds that give rise to multiple conformations, and the different binding modes of GABA interact with different effector systems. A large number of conformationally constricted GABA analogues have been developed, however the GABA binding conformation at $GABA_A$, $GABA_B$ and $GABA_C$ receptors has not been defined completely (Deniau *et al.*, 2007). Chapter 4 of this thesis described the binding conformation of GABA at $GABA_C$ ρ_1 receptor 'orthosteric' binding site by employing mono-fluoro-γ-aminobutyric acids; (*S*)- and (*R*)-3-fluoro-γ-aminobutyric acids and the stereoisomers of di-fluoro-γ-aminobutyric acids; *syn*- and *anti*-2,3-difluoro-4-aminobutyric acids, as conformational probes to explore the GABA binding conformational modes at $GABA_C$ receptors. Our study suggested that the binding mode of GABA at the $GABA_C$ receptor was different to that found at $GABA_A$ receptors. Our results also correlate with the proposed $GABA_C$ receptor binding geometry (Crittenden *et al.*, 2005) and expand the library of known GABAergic compounds that

act on $GABA_C$ receptors to inform the ongoing development of new ligands for the various potential therapeutic applications.

To our knowledge, no detailed model of the binding geometry of GABA at $GABA_B$ receptors has been established. The activation mechanisms for class C G-protein-coupled receptors, including metabotropic glutamate (mGlu) and $GABA_B$ receptors are complex (Rondard *et al.*, 2011). Like Cys-loop receptors, agonist binding induces conformational changes at the venus flytrap (VFT) domain to initiate intramolecular signal transduction *via* the heptahelical domain which activates G-proteins (Kunishima *et al.*, 2000; Matsushita *et al.*, 2010). $GABA_B$ receptors are known to activate the Gαi and Gαo-protein family (Menon-Johansson *et al.*, 1993) and they regulate many aspects of synaptic transmission (Chalifoux *et al.*, 2011). GABA activates G-protein-regulated inward-rectifying K^+-channels (GIRK) *via* postsynaptic $GABA_B$ receptors (Kulik *et al.*, 2006) and the activation of receptors also limits presynaptic neurotransmitter release by inhibiting Ca^{2+}-channel opening (Dolphin, 2003; Tatebayashi *et al.*, 1992). In this study, we co-expressed $GABA_{B(1b,2)}$ with rat GIRK 1 and rat GIRK4, and we found one of the *syn*-2,3-difluoro-4-aminobutyric acid isomers failed to activate the GIRK channels. It has been proposed that the types of mGlu receptor activated signaling pathway are determined by ligand-specific conformational changes at the VFT dimer (Tateyama *et al.*, 2004; Tateyama *et al.*, 2006). If the same applies for $GABA_B$ receptors, it is possible that the different GABA binding modes induce different signaling cascades. It will be interesting to try our GABA conformational probes in native cells to explore the relationship between GABA binding mode and the $GABA_B$ receptor mediated signaling cascades.

GABOB is an endogenous ligand found in the CNS. Homology modelling of the $GABA_C$ ρ_1 receptor revealed that a potential hydrogen bond (H-bond) interaction occurs between the hydroxyl group of GABOB and the loop C residue, threonine 244 (T244) of the ligand binding site of the ρ_1 subunit. Using site-directed mutagenesis, the effect of mutating T244 on the efficacy and pharmacology of GABOB and various other related ligands were examined (Chapter 5). It was found that mutating T244 to small neutral amino acids produced GABA-insensitive receptors. Only by mutating

ρ_1T244 to serine (ρ_1T244S) a GABA-responsive receptor was produced, albeit with 39-fold less sensitivity to GABA than wild-type receptors. We also observed that the partial agonists, muscimol and I4AA were converted to antagonists at ρ_1T244S mutant receptors, indicating that T244 is predominantly involved in channel gating. Interestingly, the potencies of antagonists were not altered suggesting that T244 is not critical for their binding. Therefore, this study highlighted the dynamic nature of receptor gating and the role of loop C in agonist induced receptor activation.

Agonist binding induces conformational changes within the N-terminal domain to transmit signals to the transmembrane domains to gate the channel. Understanding the dynamic nature of receptor gating is currently limited by the present reported models for LGICs. Furthermore, there is no crystal structure of the $GABA_C$ ρ_1 receptor and thus not much is known about the receptor structure and function in channel gating. Our homology model of the $GABA_C$ ρ_1 receptor is based on acetylcholine-binding protein (AChBP), which is a soluble protein isolated from *Lymnaea stagnalis* ($_L$-AChBP) (Brejc et al., 2001). The model was optimized to predict loop C conformations at open or closed conformations by performing a combination of quantum mechanics/molecular mechanics (QM/MM) simulation (Abdel-Halim et al., 2008). The model predicted conformational changes at loop C after agonists or antagonists binding, consisting with the findings observed using crystal structures of *Aplysia Californica* AChBP, which was co-crystalized with a number of nicotinic agonists and antagonists (Hansen et al., 2005). One of the problems with homology modelling studies is that it can only produce a snap shot of ligand interactions at a particular moment of a predicted conformation of the receptor (e.g. resting, open or closed states). Although our model was optimized, it most likely resembles the ligand-bound state because the template used contains the ligand HEPES and was neither in the open or desensitized state (Brejc et al., 2001). Therefore, it is simply a model and does not predict the intermediate interactions that occur when the ligand binds to gate the channel. As previously described, we can define the role of amino acid residues by using partial agonists if full agonists can activate the mutant receptors (Chapter 5 and Chapter 6). In addition, the AChBP has no structural features required for ion channel functions (e.g. the transmembrane domain), so it is not an ideal

candidate to use if we want to understand how channel gating is regulated by ligand binding. Recently a glutamate-gated chloride channels (GluCl) has been crystallized and the receptor has a higher homology (33%) to $GABA_C$ ρ_1 receptor than $_L$-AChBP (18%) (Hibbs et al., 2011). Therefore, it is preferable to use the GluCl crystal structure ($GluCl_{cryst}$) as a template for homology model of $GABA_C$ ρ_1 receptor. The limitations to using this crystal structure is that, the receptor was co-crystallized with an antibacterial agent Fab, and that receptors can rapidly undergo conformational changes to gate the channels indicating the energy transfer from closed to open states occurs in subtle manner that are not accounted for with crystal structures. Therefore, any changes in the receptor environment can interfere with receptor function. As such, we do not know how much the structural information obtained from $GluCl_{cryst}$-Fab resembles the native receptors.

The crystal structure of the extracellular N-terminal domain of the mouse nACh α_1 subunit (α211) at 1.94 Å resolution has also been reported (Dellisanti *et al.*, 2007a). It was co-crystallized with α-bungarotoxin and provided key structural elements of nACh receptors including the main immunogenic region (MIR), which had not been observed by previous studies using AChBP. Lin and his colleagues have compared the structural differences and similarities between the AChBP and α211 and they revealed many receptor-specific structural features important at the atomic level (Chen, 2010; Dellisanti *et al.*, 2007b). One of their findings is the identification of hydration cavities in the hydrophobic core of N-terminal domain. These hydration cavities do not exist or occur less frequently at AChBP sequences. It was subsequently proposed that the loose packing of N-terminal domain was developed through evolution for channel functions (Dellisanti *et al.*, 2011). Their study showed that changes in Cys-loop receptor function occurs by mutating the hydrophilic residues into bulky or hydrophobic residues suggesting the flexibility of N-terminal domain contributes to receptor gating.

We also observed changes in receptor function when a conserved hydrophobic residue, phenylalanine 124 (F124) located at β3-strand of the ρ_1 receptor was mutated to various amino acids (Chapter 7). F124 is located on the non-

characterized part of the $GABA_C$ ρ_1 receptor sequence and our homology modelling studies predicted it contributed to a novel hydrophobic cavity. Mutation studies at F124 revealed that the residue was unlikely to be involved directly in ligand binding. However the amino acid side chain volume and its polarity appeared to be important for receptor function and the stability of the overall structure of the agonist/antagonist binding site. Altering the amino acid side chain volume or its polarity also influenced the gating kinetics of the receptor. From this study, it is hypothesized that F124 may be involved in channel gating or contributing to the stabilization of the open conformation of N-terminal domain upon channel gating. Further studies are required to elucidate the role of F124 and the novel hydrophobic cavity.

Overall, at present the use of homology models remain at best as 'a representation' due to the challenges raised by the limited sequence identity and the number of available crystal structures. Detailed structural receptor information with high resolution is still necessary for drug design and development studies (Taly *et al.*, 2009). Nonetheless, homology models offer initial ideas of how ligands interact with their binding site (Abdel-Halim *et al.*, 2008; Yamamoto *et al.*, 2012a; Yamamoto *et al.*, 2012b; Yamamoto *et al.*, 2011a; Yamamoto *et al.*, 2011b, Chapter 8), and homologues of the Cys-loop LGICs found in bacteria provide some insight into receptor gating (Hilf *et al.*, 2009b; Hilf *et al.*, 2008; Pan *et al.*, 2012).

In Chapter 6, we employed a range of structurally diverse GABA antagonists to explore their effects on two conformations of the ρ_1 receptor; the open and closed conformational states. The different conformational states were achieved by mutating tyrosine at position 102 (Y102) to serine (ρ_1Y102S), cysteine (ρ_1Y102C) and alanine (ρ_1Y102A). ρ_1Y102S receptors were constitutively active indicating that a proportion of receptors exist in the open conformational state. This receptor characteristic enabled one to assess the activity of antagonists in the absence of an agonist (ρ_1Y102S) compared to those receptors existing predominantly in the closed conformational state (ρ_1 wild-type, ρ_1Y102C and ρ_1Y102A).

It was found that all $GABA_C$ antagonists studied were inverse agonists at ρ_1Y102S receptors with the exception of (±)-4-ACPAM. However, (±)-4-ACPAM inhibited GABA-evoked current at ρ_1Y102C and ρ_1Y102A, suggesting that (±)-4-ACPAM preferred binding to the closed over the open conformational state of the receptor. We also found that GABA antagonists were more potent at the closed compared to the open conformation states suggesting that the antagonists act by stabilizing the closed state and thus reducing activation by agonists in addition to competing for the binding site.

Gabazine (SR-95531) is a potent $GABA_A$ receptor competitive antagonist and it is known to cross the blood brain barrier. Gabazine also inhibits GABA-evoked currents at $GABA_C$ receptors, however the inhibitory effect is weaker. A series of novel 6-aryl-3-aminopyridazine derivatives were designed to establish a structure-activity relationship profile and develop more potent and selective $GABA_C$ receptor antagonists (Chapter 8). We identified one analogue lacking the butyric acid side-chain that was approximately 20-fold more potent at $GABA_C$ over $GABA_A$ receptors. Designing chemical structures based on this analogue may serve to develop selective $GABA_C$ receptor antagonists with possible physiological effects including memory enhancing effects.

9.1 Future direction

9.1.1 Ligand specific conformational changes

The findings in this thesis emphasize that upon agonist or antagonist binding, the conformation of the receptor changes. It will be interesting to explore the difference between agonist and antagonist induced signal transduction mechanisms. Antagonist induced conformational change in the receptor is difficult to detect since we cannot observe the change unless the receptors are constitutively active. Lynch and co-workers have used the voltage-clamp fluorometry (VCF) technique to explore ligand specific glycine receptor conformational changes with interesting results (Pless *et al.*, 2009; Wang *et al.*, 2010). They labeled the region of interest with an

environmentally sensitive fluorophore. This technique allows us to simultaneously monitor current changes and changes in fluorescence intensity (ΔF) during ligand application and detect antagonist induced electrophysiologically silent conformational changes (Pless *et al.*, 2008). They found one residue in loop C responded differently to glycine and strychnine, indicating its importance in ligand discrimination (Pless *et al.*, 2009). They have also found three residues in inner beta sheets which discriminated between agonists and antagonists. Strychnine is a competitive antagonist at glycine receptors, and it only induced local conformational changes which do not occur at the interface of the transmembrane domain (Pless *et al.*, 2009).

Chang and Weiss have also explored agonist/antagonist induced conformational changes at $GABA_C$ ρ_1 receptors using VCF (Chang et al., 2002; Li et al., 2010; Zhang et al., 2009). They saw changes in ΔF upon 3-APMPA and 3-APA application, which were less than GABA, and also that the changes were opposite to that of GABA at the regions in N-terminal domain (Chang *et al.*, 2002). Their findings indicate that the inhibitory effect of 3-APMPA is not by simply competing with GABA at the binding site, but to also stabilize the receptor in a unique closed conformation. TPMPA is a competitive antagonist at $GABA_C$ receptors and it is also an inverse agonist (Chapter 6). It also inhibited the spontaneous current produced by the mutation in the pore region of $GABA_C$ ρ_1 receptors (Carland *et al.*, 2004). It will be interesting to use the VCF technique or other fluorescence methods to explore how $GABA_C$ antagonists evoke conformational changes at the transmembrane domain *via* coupling regions and explore the difference in the energy transfer occurring during conformational changes upon agonist or antagonist binding.

9.1.2 $GABA_C$ ρ_1 receptor orthosteric binding site

Mutating threonine at position 244 (T244) influenced ρ_1 receptor gating, and having a hydroxyl group at the position was critical for agonist induced receptor activation (Yamamoto *et al.*, 2012a). As the ρ_1 receptor is a homomeric receptor containing five identical binding sites, we can vary the number and positioning of the

binding sites within the pentamer by co-expressing wild-type subunits with subunits mutated to form a disabled binding site (*e.g.* the non-functional ρ_1T244A). Mutating T244 into alanine (ρ_1T244A) disables GABA binding site. Here we can explore the number of active binding site by co-expressing experiments of WT and mutants by changing the concentration ratio of ρ_1 WT and T244A cRNA mixtures. This way we can explore the number of active binding sites required for agonist induced $GABA_C$ ρ_1 receptor channel opening.

9.1.3 Role of F124

Our $GABA_C$ ρ_1 receptor homology model identified a novel hydrophobic cavity and predicted the side chain of F124 points towards the cavity. By mutating F124, we observed changes in whole cell deactivation currents using both two-electrode voltage clamp and patch clamp methods (Chapter 7). We hypothesized that the residue was involved in receptor gating or contributing in stabilizing the open conformation of N-terminal domain upon channel gating. Activation of $GABA_C$ ρ_1 receptor locks the agonist in the binding site (Chang *et al.*, 1999), thus changes in deactivation rate imply that the GABA dissociation equilibrium constant may have been altered at mutant receptors. Radioligand-binding experiments using ρ_1 wild-type and mutant receptors can give us insights into whether the mutations at F124 influence the receptor by detaining the agonist upon binding or not. However, changes in receptor activation by these mutations indicate not only what influences ligand binding but also receptor gating and differentiating between these can be difficult. However employing partial agonists as pharmacological tools to explore the effect of a mutation on receptor gating as shown in Chapter 6 can provide insights into whether an amino acid is involved in binding or gating. Furthermore, single-channel recordings can also be used to provide ways to explore the effect of a mutation on receptor gating by comparing bursts of channel opening. Altering the mean number of openings per burst between ρ_1 wild-type and mutant receptors may imply that the residue is involved in stabilizing the open conformation.

9.2 Conclusion

This thesis describes how ligand binding and receptor gating are closely related and explores the effect of receptor conformational changes on receptor pharmacology. We also achieved to facilitate the understanding of the relationship between the ligand chemical structures and their activities at GABA receptors. It is one of the important aspects in drug discovery to understand how ligands interact with their binding sites.

Appendices

Appendix 1 Synthetic procedures and characterization data for (±)-4-ACPAM

Methyl 4-*tert*-butoxycarbonylaminocyclopent-1-enecarboxylate (Locock *et al.*, 2009) (2.90 g, 12 mmol) was added to an aqueous solution of 0.5 M sodium hydroxide (80 mL) and tetrahydrofuran (40 mL) and allowed to stir overnight at room temperature. Excess tetrahydrofuran was removed from this solution under reduced pressure followed by extraction with dichloromethane (60 mL). The remaining aqueous fraction was acidified to pH 3 with 10% aqueous citric acid in the presence of dichloromethane (180 mL). The combined organic phases were dried over magnesium sulphate and evaporated to give 4-*tert*-butoxycarbonylaminocyclopent-1-enecarboxylic acid (2.59 g, 95% yield). R_f = 0.35 (4:1 ethyl acetate/petroleum ether). ^{1}H NMR (300 MHz, $CDCl_3$): δ 6.86 (1H, s, *H*C=), 4.75 (1H, br s, N*H*), 4.39 (1H, bs, C(4)*H*), 2.97 (2H, bt, *J* = 9 Hz, C(3)*H* and C(5)*H*), 2.49 – 2.39 (2H, m, C(3)*H* and C(5)*H*), 1.45 (9H, s, Boc). ^{13}C NMR (300 MHz, $CDCl_3$): δ 168.96 (C=O), 143.94 (=C), 134.27 (HC=), 79.80 (*C*$(CH_3)_3$), 50.40 (CHNHBoc), 41.57 (cyclopentene CH_2), 39.03 (cyclopentene CH_2), 28.60 (C(*C*$H_3)_3$). CI-MS *m/z* 154 (52%, MH^+-C_4H_8O), 126 (100, MH^+-Boc), 93 (14, MH^+-Boc-H_2O), 82 (45, MH^+-Boc-CO_2).

Triethylamine (304 mg, 3 mmol) was added to a solution of 4-*tert*-butoxycarbonylaminocyclopent-1-enecarboxylic acid (341 mg, 1.5 mmol) in tetrahydrofuran (30 mL) at 0°C. *iso*-Butylchoroformate (338 mg, 2.5 mmol) was added dropwise, and the solution left to stir for 15 minutes. Gaseous ammonia was bubbled through the solution for 20 minutes and the reaction left to stir at 0°C for a further 2 hours. The reaction was concentrated *in vacuo*, diluted with ethyl acetate (30 mL) and washed with aqueous sodium hydroxide (1M, 10 mL), saturated citric acid (10 mL) and brine (10 mL). The organic fraction was dried over sodium sulphate and solvent was removed under reduced pressure. The product was isolated using flash chromatography, eluting with ethyl acetate/dichloromethane (10:1) to give *tert*-butyl 3-carbamoylcyclopent-3-enylcarbamate (315 mg, 92% yield). R_f = 0.47 (ethyl acetate). ^{1}H NMR (300 MHz, $CDCl_3$): δ 6.52 (1H, s, *H*C=), 5.72-5.18 (2H, br d, NH_2), 4.85-4.64

(1H, m, C(4)*H*), 4.40 (1H, br s, N*H*Boc), 3.04-2.84 (2H, m, C(3)*H* and C(5)*H*), 2.52-2.33 (2H, m, C(3)*H* and C(5)*H*), 1.45 (9H, s, Boc). ^{13}C NMR (300 MHz, $CDCl_3$): δ 166.76 ((C=O)NH_2), 155.57 ((C=O)O*t*-Bu), 137.01 (HC=), 136.91 (=C), 79.80 *C*(CH_3)), 50.65 (CHNHBoc), 41.14 (cyclopentene CH_2), 39.64 (cyclopentene CH_2), 28.60 C(*C*H_3)). *tert*-Butyl 3-carbamoylcyclopent-3-enylcarbamate (315 mg, 1.39 mmol) was dissolved in a saturated solution of hydrochloric acid in ethyl acetate and the resulting solution allowed to stir for 4 hours. Solvent was removed *in vacuo*, and the product isolated using an ion-exchange column of Dowex 50W (H^+) (10 mL), eluting the amino amide with ammonia (2M). This gave 4-aminocyclopent-1-enecarboxamide (156 mg, 89% yield). R_f = 0.27 (4:1:1 *n*-butanol/acetic acid/water). ^{1}H NMR (300 MHz, D_2O): δ 6.32 (1H, s, *H*C=), 4.03-3.93 (1H, m, C*H*NH_2), 3.01-2.84 (2H, m, C(3)*H* and C(5)*H*), 2.56-2.43 (2H, m, C(3)*H* and C(5)*H*). ^{13}C NMR (300 MHz, D_2O): δ 171.13 (C=O), 140.23 (HC=), 136.08 (=C), 50.91 ($CHNH_2$), 42.31 (cyclopentene CH_2), 40.52 (cyclopentene CH_2). ESI-MS m/*z* positive ion mode: 127 (55%, MH^+), 110 (5%, MH^+-NH_3); negative ion mode: 126 (20%, M^+-H).

Appendix 2 Synthetic procedues for novel gabazine analogues

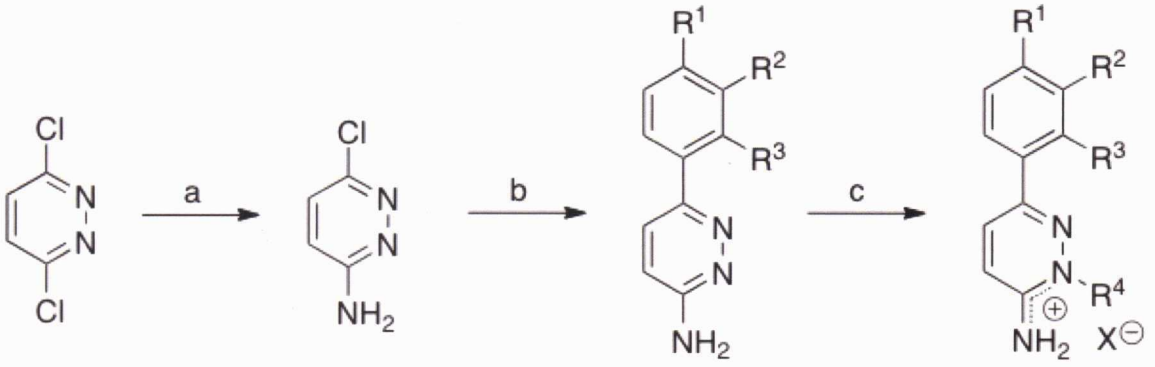

Scheme 1 *Reagents and Conditions: a) 28-30% NH_4OH, MW, 120°C, 30 min., 87%; b) aryl/heteroaryl boronic acid, 5 mol% $Pd(PPh_3)_4$, K_2CO_3 (1.5 equiv.), EtOH:water (4:1), MW, 120°C, 10 min., 75-94%; c) alkyl halide, MW, 80°C, 15 min., 84-96%.*

The initial step of the synthesis involved the monoamination of 3,6-dichlorpyridazine using 28-30% aq. ammonium hydroxide as the source for the amine functionality of 3-amino-6-chloropyridazine under microwave irradiation (Scheme 1) (Gavande *et al.*, 2010a). After optimization of Suzuki coupling reaction, we coupled various aryl/heteroaryl boronic acids with unprotected 3-amino-6-chloropyridazine under microwave irradiation (CEM Discover S-Class microwave reactor: equipped with single mode reactor and fiber optic temperature control; method: dynamic mode at power 300W) at 120 °C with stirring for 10 min afforded the corresponding 3-amino-6-arylpyridazines in moderate to good yield. The *N*-alkylation of the *endo* amidinic system of 3-amino-6-arylpyridazines with alkyl halides under microwave irradiation yielded desired compounds (**1-5** and **8-15**) in good yield.

References

References

Abdel-Halim H, Hanrahan JR, Hibbs DE, Johnston GA, Chebib M (2008). A molecular basis for agonist and antagonist actions at GABA(C) receptors. *Chem Biol Drug Des* **71**(4): 306-327.

Absalom NL, Lewis TM, Kaplan W, Pierce KD, Schofield PR (2003). Role of charged residues in coupling ligand binding and channel activation in the extracellular domain of the glycine receptor. *J Biol Chem* **278**(50): 50151-50157.

Absalom NL, Schofield PR, Lewis TM (2009). Pore structure of the Cys-loop ligand-gated ion channels. *Neurochem Res* **34**(10): 1805-1815.

Adamian L, Gussin HA, Tseng YY, Muni NJ, Feng F, Qian H, *et al.* (2009). Structural model of rho1 $GABA_C$ receptor based on evolutionary analysis: Testing of predicted protein-protein interactions involved in receptor assembly and function. *Protein Sci* **18**(11): 2371-2383.

Aishita H, Akimoto A, Makita T (1978). Comparison of the inhibitory effects of GABOB optical isomers on seizure discharges elicited by electrical stimulation of the motor cortex in rabbits. *IRCS Med Sci Nerv Syst Pharmacol Physiol* **6**: 115.

Akk G, Steinbach JH (2000). Activation and block of recombinant GABA(A) receptors by pentobarbitone: a single-channel study. *Br J Pharmacol* **130**(2): 249-258.

Alakuijala A, Palgi M, Wegelius K, Schmidt M, Enz R, Paulin L, *et al.* (2005). GABA receptor rho subunit expression in the developing rat brain. *Brain Res Dev Brain Res* **154**(1): 15-23.

Allan RD, Dickenson HW, Fong J (1986). Structure-activity studies on the activity of a series of cyclopentane GABA analogues on $GABA_A$ receptors and GABA uptake. *Eur J Pharmacol* **122**(3): 339-348.

Amin J, Weiss DS (1993). GABAA receptor needs two homologous domains of the beta-subunit for activation by GABA but not by pentobarbital. *Nature* **366**(6455): 565-569.

Amin J, Weiss DS (1994). Homomeric rho 1 GABA channels: activation properties and domains. *Receptors Channels* **2**(3): 227-236.

Andersen N, Corradi J, Bartos M, Sine SM, Bouzat C (2011). Functional relationships between agonist binding sites and coupling regions of homomeric Cys-loop receptors. *J Neurosci* **31**(10): 3662-3669.

Arnaud C, Gauthier P, Gottesmann C (2001). Study of a $GABA_C$ receptor antagonist on sleep-waking behavior in rats. *Psychopharmacology (Berl)* **154**(4): 415-419.

Awapara J, Landua AJ, Fuerst R, Seale B (1950). Free gamma-aminobutyric acid in brain. *J Biol Chem* **187**(1): 35-39.

Bailey ME, Albrecht BE, Johnson KJ, Darlison MG (1999). Genetic linkage and radiation hybrid mapping of the three human GABA(C) receptor rho subunit genes: GABRR1, GABRR2 and GABRR3. *Biochim Biophys Acta* **1447**(2-3): 307-312.

Barnard EA, Skolnick P, Olsen RW, Mohler H, Sieghart W, Biggio G, *et al.* (1998). International Union of Pharmacology. XV. Subtypes of gamma-aminobutyric acidA receptors: classification on the basis of subunit structure and receptor function. *Pharmacol Rev* **50**(2): 291-313.

Belelli D, Casula A, Ling A, Lambert JJ (2002). The influence of subunit composition on the interaction of neurosteroids with GABA(A) receptors. *Neuropharmacology* **43**(4): 651-661.

Belelli D, Lambert JJ, Peters JA, Wafford K, Whiting PJ (1997). The interaction of the general anesthetic etomidate with the gamma-aminobutyric acid type A receptor is influenced by a single amino acid. *Proc Natl Acad Sci U S A* **94**(20): 11031-11036.

Ben-Ari Y (2001). Developing networks play a similar melody. *Trends Neurosci* **24**(6): 353-360.

Benson JA, Low K, Keist R, Mohler H, Rudolph U (1998). Pharmacology of recombinant gamma-aminobutyric acidA receptors rendered diazepam-insensitive by point-mutated alpha-subunits. *FEBS Lett* **431**(3): 400-404.

Bettler B, Kaupmann K, Mosbacher J, Gassmann M (2004). Molecular structure and physiological functions of GABA(B) receptors. *Physiol Rev* **84**(3): 835-867.

Bianchi MT, Botzolakis EJ, Lagrange AH, Macdonald RL (2009). Benzodiazepine modulation of GABA(A) receptor opening frequency depends on activation context: a patch clamp and simulation study. *Epilepsy Res* **85**(2-3): 212-220.

Blair HT, Schafe GE, Bauer EP, Rodrigues SM, LeDoux JE (2001). Synaptic plasticity in the lateral amygdala: a cellular hypothesis of fear conditioning. *Learn Mem* **8**(5): 229-242.

Bocquet N, Nury H, Baaden M, Le Poupon C, Changeux JP, Delarue M, *et al.* (2009). X-ray structure of a pentameric ligand-gated ion channel in an apparently open conformation. *Nature* **457**(7225): 111-114.

Boehm SL, 2nd, Homanics GE, Blednov YA, Harris RA (2006). delta-Subunit containing GABAA receptor knockout mice are less sensitive to the actions of 4,5,6,7-tetrahydroisoxazolo-[5,4-c]pyridin-3-ol. *Eur J Pharmacol* **541**(3): 158-162.

Bonnert TP, McKernan RM, Farrar S, le Bourdelles B, Heavens RP, Smith DW, *et al.* (1999). theta, a novel gamma-aminobutyric acid type A receptor subunit. *Proc Natl Acad Sci U S A* **96**(17): 9891-9896.

Bormann J (2000). The 'ABC' of GABA receptors. *Trends Pharmacol Sci* **21**(1): 16-19.

Bormann J, Feigenspan A (1995). $GABA_C$ receptors. *Trends Neurosci* **18**(12): 515-519.

Boue-Grabot E, Roudbaraki M, Bascles L, Tramu G, Bloch B, Garret M (1998). Expression of GABA receptor rho subunits in rat brain. *J Neurochem* **70**(3): 899-907.

Bouzat C (2011). New insights into the structural bases of activation of Cys-loop receptors. *J Physiol Paris*.

Bouzat C, Bartos M, Corradi J, Sine SM (2008). The interface between extracellular and transmembrane domains of homomeric Cys-loop receptors governs open-channel lifetime and rate of desensitization. *J Neurosci* **28**(31): 7808-7819.

Bouzat C, Gumilar F, Spitzmaul G, Wang HL, Rayes D, Hansen SB, *et al.* (2004). Coupling of agonist binding to channel gating in an ACh-binding protein linked to an ion channel. *Nature* **430**(7002): 896-900.

Bowery N (1989). $GABA_B$ receptors and their significance in mammalian pharmacology. *Trends Pharmacol Sci* **10**(10): 401-407.

Bowery NG (2006). $GABA_B$ receptor: a site of therapeutic benefit. *Curr Opin Pharmacol* **6**(1): 37-43.

Bowery NG, Hill DR, Hudson AL, Doble A, Middlemiss DN, Shaw J, *et al.* (1980). (-)Baclofen decreases neurotransmitter release in the mammalian CNS by an action at a novel GABA receptor. *Nature* **283**(5742): 92-94.

Brehm L, Hjeds H, Krogsgaard-Larsen P (1972). The structure of muscimol, a GABA analogue of restricted conformation. *Acta Chem Scand* **26**(3): 1298-1299.

Brejc K, van Dijk WJ, Klaassen RV, Schuurmans M, van Der Oost J, Smit AB, *et al.* (2001). Crystal structure of an ACh-binding protein reveals the ligand-binding domain of nicotinic receptors. *Nature* **411**(6835): 269-276.

Brogden RN, Speight TM, Avery GS (1974). Baclofen: a preliminary report of its pharmacological properties and therapeutic efficacy in spasticity. *Drugs* **8**(1): 1-14.

Butler AS, Lindesay SA, Dover TJ, Kennedy MD, Patchell VB, Levine BA, *et al.* (2009). Importance of the C-terminus of the human 5-HT_{3A} receptor subunit. *Neuropharmacology* **56**(1): 292-302.

Carland JE, Cooper MA, Sugiharto S, Jeong HJ, Lewis TM, Barry PH, *et al.* (2009). Characterization of the effects of charged residues in the intracellular loop on ion permeation in alpha1 glycine receptor channels. *J Biol Chem* **284**(4): 2023-2030.

Carland JE, Moorhouse AJ, Barry PH, Johnston GA, Chebib M (2004). Charged residues at the 2' position of human $GABA_C$ rho 1 receptors invert ion selectivity and influence open state probability. *J Biol Chem* **279**(52): 54153-54160.

Cederholm JM, Schofield PR, Lewis TM (2009). Gating mechanisms in Cys-loop receptors. *Eur Biophys J* **39**(1): 37-49.

Celie PH, van Rossum-Fikkert SE, van Dijk WJ, Brejc K, Smit AB, Sixma TK (2004). Nicotine and carbamylcholine binding to nicotinic acetylcholine receptors as studied in AChBP crystal structures. *Neuron* **41**(6): 907-914.

Chakrapani S, Auerbach A (2005). A speed limit for conformational change of an allosteric membrane protein. *Proc Natl Acad Sci U S A* **102**(1): 87-92.

Chakrapani S, Bailey TD, Auerbach A (2004). Gating dynamics of the acetylcholine receptor extracellular domain. *J Gen Physiol* **123**(4): 341-356.

Chakrapani S, Bailey TD, Auerbach A (2003). The role of loop 5 in acetylcholine receptor channel gating. *J Gen Physiol* **122**(5): 521-539.

Chalifoux JR, Carter AG (2011). $GABA_B$ receptor modulation of synaptic function. *Curr Opin Neurobiol* **21**(2): 339-344.

Chang Y, Wang R, Barot S, Weiss DS (1996). Stoichiometry of a recombinant $GABA_A$ receptor. *J Neurosci* **16**(17): 5415-5424.

Chang Y, Weiss DS (1999). Channel opening locks agonist onto the $GABA_C$ receptor. *Nat Neurosci* **2**(3): 219-225.

Chang Y, Weiss DS (2002). Site-specific fluorescence reveals distinct structural changes with GABA receptor activation and antagonism. *Nat Neurosci* **5**(11): 1163-1168.

Chang YC, Wu W, Zhang JL, Huang Y (2009). Allosteric activation mechanism of the cys-loop receptors. *Acta Pharmacol Sin* **30**(6): 663-672.

Chebib M, Duke RK, Allan RD, Johnston GA (2001). The effects of cyclopentane and cyclopentene analogues of GABA at recombinant GABA(C) receptors. *Eur J Pharmacol* **430**(2-3): 185-192.

Chebib M, Gavande N, Wong KY, Park A, Premoli I, Mewett KN, *et al.* (2009a). Guanidino acids act as rho1 GABA(C) receptor antagonists. *Neurochem Res* **34**(10): 1704-1711.

Chebib M, Hanrahan JR, Kumar RJ, Mewett KN, Morriss G, Wooller S, *et al.* (2007). (3-Aminocyclopentyl)methylphosphinic acids: novel GABA(C) receptor antagonists. *Neuropharmacology* **52**(3): 779-787.

Chebib M, Hinton T, Schmid KL, Brinkworth D, Qian H, Matos S, *et al.* (2009b). Novel, potent, and selective GABAC antagonists inhibit myopia development and facilitate learning and memory. *J Pharmacol Exp Ther* **328**(2): 448-457.

Chebib M, Johnston GA (1999). The 'ABC' of GABA receptors: a brief review. *Clin Exp Pharmacol Physiol* **26**(11): 937-940.

Chebib M, Johnston GA (2000). GABA-Activated ligand gated ion channels: medicinal chemistry and molecular biology. *J Med Chem* **43**(8): 1427-1447.

Chebib M, Mewett KN, Johnston GA (1998). GABA(C) receptor antagonists differentiate between human rho1 and rho2 receptors expressed in Xenopus oocytes. *Eur J Pharmacol* **357**(2-3): 227-234.

Chebib M, Vandenberg RJ, Froestl W, Johnston GA (1997a). Unsaturated phosphinic analogues of gamma-aminobutyric acid as GABA(C) receptor antagonists. *Eur J Pharmacol* **329**(2-3): 223-229.

Chebib M, Vandenberg RJ, Johnston GA (1997b). Analogues of gamma-aminobutyric acid (GABA) and trans-4-aminocrotonic acid (TACA) substituted in the 2 position as $GABA_C$ receptor antagonists. *Br J Pharmacol* **122**(8): 1551-1560.

Chen L (2010). In pursuit of the high-resolution structure of nicotinic acetylcholine receptors. *J Physiol* **588**(Pt 4): 557-564.

Cherubini E, Gaiarsa JL, Ben-Ari Y (1991). GABA: an excitatory transmitter in early postnatal life. *Trends Neurosci* **14**(12): 515-519.

Chothia C (1984). Principles that determine the structure of proteins. *Annu Rev Biochem* **53:** 537-572.

Clark SE, Garret M, Platt B (2001). Postnatal alterations of GABA receptor profiles in the rat superior colliculus. *Neuroscience* **104**(2): 441-454.

Colquhoun D (1998). Binding, gating, affinity and efficacy: the interpretation of structure-activity relationships for agonists and of the effects of mutating receptors. *Br J Pharmacol* **125**(5): 924-947.

Corringer PJ, Baaden M, Bocquet N, Delarue M, Dufresne V, Nury H, *et al.* (2010). Atomic structure and dynamics of pentameric ligand-gated ion channels: new insight from bacterial homologues. *J Physiol* **588**(Pt 4): 565-572.

Costa E, Guidotti A (1979). Molecular mechanisms in the receptor action of benzodiazepines. *Annu Rev Pharmacol Toxicol* **19:** 531-545.

Crestani F, Lorez M, Baer K, Essrich C, Benke D, Laurent JP, *et al.* (1999). Decreased GABAA-receptor clustering results in enhanced anxiety and a bias for threat cues. *Nat Neurosci* **2**(9): 833-839.

Crittenden DL, Chebib M, Jordan MJT (2005). A quantitative structure-activity relationship investigation into agonist binding at GABAC receptors. *J. Mol. Struct.: THEOCHEM* **755**(Copyright (C) 2012 American Chemical Society (ACS). All Rights Reserved.): 81-89.

Crittenden DL, Park A, Qiu J, Silverman RB, Duke RK, Johnston GA, *et al.* (2006). Enantiomers of cis-constrained and flexible 2-substituted GABA analogues exert opposite effects at recombinant GABA(C) receptors. *Bioorg Med Chem* **14**(2): 447-455.

Cryan JF, Kaupmann K (2005). Don't worry 'B' happy!: a role for GABA(B) receptors in anxiety and depression. *Trends Pharmacol Sci* **26**(1): 36-43.

Cunha C, Monfils MH, Ledoux JE (2010). GABA(C) Receptors in the Lateral Amygdala: A Possible Novel Target for the Treatment of Fear and Anxiety Disorders? *Front Behav Neurosci* **4**: 6.

Curtis DR, Duggan AW, Felix D, Johnston GA (1970). GABA, bicuculline and central inhibition. *Nature* **226**(5252): 1222-1224.

Curtis DR, Duggan AW, Felix D, Johnston GA, McLennan H (1971a). Antagonism between bicuculline and GABA in the cat brain. *Brain Res* **33**(1): 57-73.

Curtis DR, Felix D (1971b). The effect of bicuculline upon synaptic inhibition in the cerebral and cerebellar corticles of the cat. *Brain Res* **34**(2): 301-321.

Cutting GR, Curristin S, Zoghbi H, O'Hara B, Seldin MF, Uhl GR (1992). Identification of a putative gamma-aminobutyric acid (GABA) receptor subunit rho2 cDNA and colocalization of the genes encoding rho2 (GABRR2) and rho1 (GABRR1) to human chromosome 6q14-q21 and mouse chromosome 4. *Genomics* **12**(4): 801-806.

Cymes GD, Grosman C, Auerbach A (2002). Structure of the transition state of gating in the acetylcholine receptor channel pore: a phi-value analysis. *Biochemistry* **41**(17): 5548-5555.

Cymes GD, Ni Y, Grosman C (2005). Probing ion-channel pores one proton at a time. *Nature* **438**(7070): 975-980.

D'Hulst C, Atack JR, Kooy RF (2009). The complexity of the $GABA_A$ receptor shapes unique pharmacological profiles. *Drug Discov Today* **14**(17-18): 866-875.

Davies PA, Kirkness EF, Hales TG (1997). Modulation by general anaesthetics of rat $GABA_A$ receptors comprised of alpha 1 beta 3 and beta 3 subunits expressed in human embryonic kidney 293 cells. *Br J Pharmacol* **120**(5): 899-909.

Del Castillo J, Katz B (1957). Interaction at end-plate receptors between different choline derivatives. *Proc R Soc Lond B Biol Sci* **146**(924): 369-381.

Dellisanti CD, Hanson SM, Chen L, Czajkowski C (2011). Packing of the extracellular domain hydrophobic core has evolved to facilitate pentameric ligand-gated ion channel function. *J Biol Chem* **286**(5): 3658-3670.

Dellisanti CD, Yao Y, Stroud JC, Wang ZZ, Chen L (2007a). Crystal structure of the extracellular domain of nAChR alpha1 bound to alpha-bungarotoxin at 1.94 A resolution. *Nat Neurosci* **10**(8): 953-962.

Dellisanti CD, Yao Y, Stroud JC, Wang ZZ, Chen L (2007b). Structural determinants for alpha-neurotoxin sensitivity in muscle nAChR and their implications for the gating mechanism. *Channels (Austin)* **1**(4): 234-237.

Deniau G, Slawin AM, Lebl T, Chorki F, Issberner JP, van Mourik T, *et al.* (2007). Synthesis, conformation and biological evaluation of the enantiomers of 3-fluoro-gamma-aminobutyric acid ((R)- and (S)-3F-GABA): an analogue of the neurotransmitter GABA. *Chembiochem* **8**(18): 2265-2274.

Dickenson HW, Duke RK, Balcar VJ, Allan RD, Johnston GAR (1990). Binding to rat brain membranes of (+)-trans-(1S,3S)-3-aminocyclopentane-1-carboxylic acid, (+)-TACP, a selective $GABA_A$ receptor agonist. *Mol. Neuropharmacol.* **1**(Copyright (C) 2012 American Chemical Society (ACS). All Rights Reserved.): 1-6.

Dolphin AC (2003). G protein modulation of voltage-gated calcium channels. *Pharmacol Rev* **55**(4)**:** 607-627.

Drew CA, Johnston GA, Weatherby RP (1984). Bicuculline-insensitive GABA receptors: studies on the binding of (-)-baclofen to rat cerebellar membranes. *Neurosci Lett* **52**(3)**:** 317-321.

Duke RK, Chebib M, Balcar VJ, Allan RD, Mewett KN, Johnston GA (2000). (+)- and (-)-cis-2-aminomethylcyclopropanecarboxylic acids show opposite pharmacology at recombinant rho(1) and rho(2) GABA(C) receptors. *J Neurochem* **75**(6)**:** 2602-2610.

Duthey B, Caudron S, Perroy J, Bettler B, Fagni L, Pin JP*, et al.* (2002). A single subunit (GB2) is required for G-protein activation by the heterodimeric GABA(B) receptor. *J Biol Chem* **277**(5)**:** 3236-3241.

Emson PC (2007). GABA(B) receptors: structure and function. *Prog Brain Res* **160:** 43-57.

Enna SJ, Bowery NG (2004). GABA(B) receptor alterations as indicators of physiological and pharmacological function. *Biochem Pharmacol* **68**(8)**:** 1541-1548.

Enz R (2001). GABA(C) receptors: a molecular view. *Biol Chem* **382**(8)**:** 1111-1122.

Enz R, Cutting GR (1998). Molecular composition of $GABA_C$ receptors. *Vision Res* **38**(10)**:** 1431-1441.

Eriksson AE, Baase WA, Zhang XJ, Heinz DW, Blaber M, Baldwin EP*, et al.* (1992). Response of a protein structure to cavity-creating mutations and its relation to the hydrophobic effect. *Science* **255**(5041)**:** 178-183.

Essrich C, Lorez M, Benson JA, Fritschy JM, Luscher B (1998). Postsynaptic clustering of major $GABA_A$ receptor subtypes requires the gamma 2 subunit and gephyrin. *Nat Neurosci* **1**(7): 563-571.

Everitt AB, Luu T, Cromer B, Tierney ML, Birnir B, Olsen RW, *et al.* (2004). Conductance of recombinant GABA (A) channels is increased in cells co-expressing GABA(A) receptor-associated protein. *J Biol Chem* **279**(21): 21701-21706.

Falch E, Hedegaard A, Nielsen L, Jensen BR, Hjeds H, Krogsgaard-Larsen P (1986). Comparative stereostructure-activity studies on $GABA_A$ and $GABA_B$ receptor sites and GABA uptake using rat brain membrane preparations. *J Neurochem* **47**(3): 898-903.

Farrant M, Kaila K (2007). The cellular, molecular and ionic basis of GABA(A) receptor signalling. *Prog Brain Res* **160:** 59-87.

Farrant M, Nusser Z (2005). Variations on an inhibitory theme: phasic and tonic activation of GABA(A) receptors. *Nat Rev Neurosci* **6**(3): 215-229.

Farrar SJ, Whiting PJ, Bonnert TP, McKernan RM (1999). Stoichiometry of a ligand-gated ion channel determined by fluorescence energy transfer. *J Biol Chem* **274**(15): 10100-10104.

Feigenspan A, Bormann J (1994). Differential pharmacology of $GABA_A$ and $GABA_C$ receptors on rat retinal bipolar cells. *Eur J Pharmacol* **288**(1): 97-104.

Fernandez-Alacid L, Aguado C, Ciruela F, Martin R, Colon J, Cabanero MJ, *et al.* (2009). Subcellular compartment-specific molecular diversity of pre- and post-synaptic GABA-activated GIRK channels in Purkinje cells. *J Neurochem* **110**(4): 1363-1376.

Filippova N, Wotring VE, Weiss DS (2004). Evidence that the TM1-TM2 loop contributes to the rho1 GABA receptor pore. *J Biol Chem* **279**(20): 20906-20914.

Fritschy JM, Benke D, Mertens S, Oertel WH, Bachi T, Mohler H (1992). Five subtypes of type A gamma-aminobutyric acid receptors identified in neurons by double and triple immunofluorescence staining with subunit-specific antibodies. *Proc Natl Acad Sci U S A* **89**(15): 6726-6730.

Froestl W, Gallagher M, Jenkins H, Madrid A, Melcher T, Teichman S, *et al.* (2004). SGS742: the first GABA(B) receptor antagonist in clinical trials. *Biochem Pharmacol* **68**(8): 1479-1487.

Gallagher MJ, Cohen JB (1999). Identification of amino acids of the torpedo nicotinic acetylcholine receptor contributing to the binding site for the noncompetitive antagonist [(3)H]tetracaine. *Mol Pharmacol* **56**(2): 300-307.

Galvez T, Duthey B, Kniazeff J, Blahos J, Rovelli G, Bettler B, *et al.* (2001). Allosteric interactions between GB1 and GB2 subunits are required for optimal GABA(B) receptor function. *EMBO J* **20**(9): 2152-2159.

Galvez T, Prezeau L, Milioti G, Franek M, Joly C, Froestl W, *et al.* (2000). Mapping the agonist-binding site of $GABA_B$ type 1 subunit sheds light on the activation process of GABAB receptors. *J Biol Chem* **275**(52): 41166-41174.

Gavande N, Johnston GA, Hanrahan JR, Chebib M (2010a). Microwave-enhanced synthesis of 2,3,6-trisubstituted pyridazines: application to four-step synthesis of gabazine (SR-95531). *Org Biomol Chem* **8**(18): 4131-4136.

Gavande N, Karim N, Johnston GA, Hanrahan JR, Chebib M (2011). Identification of Benzopyran-4-one Derivatives (Isoflavones) as Positive Modulators of GABA(A) Receptors. *ChemMedChem*.

Gavande N, Yamamoto I, Salam NK, Ai T-H, Burden PM, Johnston GAR, *et al.* (2010b). Novel Cyclic Phosphinic Acids as $GABA_C$ ρ Receptor Antagonists: Design, Synthesis, and Pharmacology. *ACS Medicinal Chemistry Letters* **2**(1): 11-16.

Gee VJ, Kracun S, Cooper ST, Gibb AJ, Millar NS (2007). Identification of domains influencing assembly and ion channel properties in alpha 7 nicotinic receptor and 5-HT3 receptor subunit chimaeras. *Br J Pharmacol* **152**(4): 501-512.

Gibbs ME, Johnston GA (2005). Opposing roles for GABAA and GABAC receptors in short-term memory formation in young chicks. *Neuroscience* **131**(3): 567-576.

Gleitsman KR, Kedrowski SM, Lester HA, Dougherty DA (2008). An intersubunit hydrogen bond in the nicotinic acetylcholine receptor that contributes to channel gating. *J Biol Chem* **283**(51): 35638-35643.

Gooseman NE, O'Hagan D, Peach MJ, Slawin AM, Tozer DJ, Young RJ (2007). An electrostatic gauche effect in beta-fluoro- and beta-hydroxy-N-ethylpyridinium cations. *Angew Chem Int Ed Engl* **46**(31): 5904-5908.

Grosman C, Salamone FN, Sine SM, Auerbach A (2000a). The extracellular linker of muscle acetylcholine receptor channels is a gating control element. *J Gen Physiol* **116**(3): 327-340.

Grosman C, Zhou M, Auerbach A (2000b). Mapping the conformational wave of acetylcholine receptor channel gating. *Nature* **403**(6771): 773-776.

Gunther U, Benson J, Benke D, Fritschy JM, Reyes G, Knoflach F, *et al.* (1995). Benzodiazepine-insensitive mice generated by targeted disruption of the gamma 2 subunit gene of gamma-aminobutyric acid type A receptors. *Proc Natl Acad Sci U S A* **92**(17): 7749-7753.

Haeger S, Kuzmin D, Detro-Dassen S, Lang N, Kilb M, Tsetlin V, *et al.* (2010). An intramembrane aromatic network determines pentameric assembly of Cys-loop receptors. *Nat Struct Mol Biol* **17**(1): 90-98.

Hales TG, Dunlop JI, Deeb TZ, Carland JE, Kelley SP, Lambert JJ, *et al.* (2006). Common determinants of single channel conductance within the large cytoplasmic loop of 5-hydroxytryptamine type 3 and alpha4beta2 nicotinic acetylcholine receptors. *J Biol Chem* **281**(12): 8062-8071.

Hannan S, Wilkins ME, Dehghani-Tafti E, Thomas P, Baddeley SM, Smart TG (2011). GABAB receptor internalisation is regulated by the R2 subunit. *J Biol Chem*.

Hanrahan JR, Chebib M, Johnston GA (2011). Flavonoid modulation of GABA(A) receptors. *Br J Pharmacol* **163**(2): 234-245.

Hanrahan JR, Mewett KN, Chebib M, Burden PM, Johnston GAR (2001). An improved, versatile synthesis of the GABAC antagonists (1,2,5,6-tetrahydropyridin-4-yl)methylphosphinic acid (TPMPA) and (piperidin-4-yl)methylphosphinic acid (P4MPA). *Journal of the Chemical Society, Perkin Transactions 1*(19): 2389-2392.

Hanrahan JR, Mewett KN, Chebib M, Matos S, Eliopoulos CT, Crean C, *et al.* (2006). Diastereoselective synthesis of (+/-)-(3-aminocyclopentane)alkylphosphinic acids, conformationally restricted analogues of GABA. *Org Biomol Chem* **4**(13): 2642-2649.

Hansen SB, Sulzenbacher G, Huxford T, Marchot P, Taylor P, Bourne Y (2005). Structures of Aplysia AChBP complexes with nicotinic agonists and antagonists reveal distinctive binding interfaces and conformations. *EMBO J* **24**(20): 3635-3646.

Harrison NJ, Lummis SC (2006a). Locating the carboxylate group of GABA in the homomeric rho GABA(A) receptor ligand-binding pocket. *J Biol Chem* **281**(34): 24455-24461.

Harrison NJ, Lummis SC (2006b). Molecular modeling of the GABA(C) receptor ligand-binding domain. *J Mol Model* **12**(3): 317-324.

Heaulme M, Chambon JP, Leyris R, Molimard JC, Wermuth CG, Biziere K (1986). Biochemical characterization of the interaction of three pyridazinyl-GABA derivatives with the $GABA_A$ receptor site. *Brain Res* **384**(2): 224-231.

Hedblom E, Kirkness EF (1997). A novel class of $GABA_A$ receptor subunit in tissues of the reproductive system. *J Biol Chem* **272**(24): 15346-15350.

Herr RJ (2002). 5-Substituted-1H-tetrazoles as carboxylic acid isosteres: medicinal chemistry and synthetic methods. *Bioorganic & Medicinal Chemistry* **10**(11): 3379-3393.

Hibbs RE, Gouaux E (2011). Principles of activation and permeation in an anion-selective Cys-loop receptor. *Nature* **474**(7349): 54-60.

Hibbs RE, Sulzenbacher G, Shi J, Talley TT, Conrod S, Kem WR, *et al.* (2009). Structural determinants for interaction of partial agonists with acetylcholine binding protein and neuronal alpha7 nicotinic acetylcholine receptor. *EMBO J* **28**(19): 3040-3051.

Hilf RJ, Dutzler R (2009a). A prokaryotic perspective on pentameric ligand-gated ion channel structure. *Curr Opin Struct Biol* **19**(4): 418-424.

Hilf RJ, Dutzler R (2009b). Structure of a potentially open state of a proton-activated pentameric ligand-gated ion channel. *Nature* **457**(7225): 115-118.

Hilf RJ, Dutzler R (2008). X-ray structure of a prokaryotic pentameric ligand-gated ion channel. *Nature* **452**(7185): 375-379.

Hinton T, Chebib M, Johnston GA (2008). Enantioselective actions of 4-amino-3-hydroxybutanoic acid and (3-amino-2-hydroxypropyl)methylphosphinic acid at recombinant GABA(C) receptors. *Bioorg Med Chem Lett* **18**(1): 402-404.

Holden JH, Czajkowski C (2002). Different residues in the GABA(A) receptor alpha 1T60-alpha 1K70 region mediate GABA and SR-95531 actions. *J Biol Chem* **277**(21): 18785-18792.

Hosie AM, Wilkins ME, Smart TG (2007). Neurosteroid binding sites on GABA(A) receptors. *Pharmacol Ther* **116**(1): 7-19.

Howard JAK, Hoy VJ, O'Hagan D, Smith GT (1996). How good is fluorine as a hydrogen bond acceptor? *Tetrahedron* **52**(Copyright (C) 2012 American Chemical Society (ACS). All Rights Reserved.): 12613-12622.

Huebsch KA, Maimone MM (2003). Rapsyn-mediated clustering of acetylcholine receptor subunits requires the major cytoplasmic loop of the receptor subunits. *J Neurobiol* **54**(3): 486-501.

Hunter L, Jolliffe KA, Jordan MJ, Jensen P, Macquart RB (2011). Synthesis and conformational analysis of alpha,beta-difluoro-gamma-amino acid derivatives. *Chemistry* **17**(8): 2340-2343.

Im WB, Pregenzer JF, Binder JA, Dillon GH, Alberts GL (1995). Chloride channel expression with the tandem construct of alpha 6-beta 2 GABAA receptor subunit requires a monomeric subunit of alpha 6 or gamma 2. *J Biol Chem* **270**(44): 26063-26066.

Iqbal F, Ellwood R, Mortensen M, Smart TG, Baker JR (2011). Synthesis and evaluation of highly potent GABA(A) receptor antagonists based on gabazine (SR-95531). *Bioorg Med Chem Lett* **21**(14): 4252-4254.

Jackel C, Kleinz R, Makela R, Hevers W, Jezequel S, Korpi ER, *et al.* (1998). The main determinant of furosemide inhibition on GABA(A) receptors is located close to the first transmembrane domain. *Eur J Pharmacol* **357**(2-3): 251-256.

Jeanclos EM, Lin L, Treuil MW, Rao J, DeCoster MA, Anand R (2001). The chaperone protein 14-3-3eta interacts with the nicotinic acetylcholine receptor alpha 4 subunit. Evidence for a dynamic role in subunit stabilization. *J Biol Chem* **276**(30): 28281-28290.

Jha A, Auerbach A (2010). Acetylcholine receptor channels activated by a single agonist molecule. *Biophys J* **98**(9): 1840-1846.

Jha A, Cadugan DJ, Purohit P, Auerbach A (2007). Acetylcholine receptor gating at extracellular transmembrane domain interface: the cys-loop and M2-M3 linker. *J Gen Physiol* **130**(6): 547-558.

Johnston GA (2005). GABA(A) receptor channel pharmacology. *Curr Pharm Des* **11**(15): 1867-1885.

Johnston GA (1996a). $GABA_A$ receptor pharmacology. *Pharmacol Ther* **69**(3): 173-198.

Johnston GA (1996b). GABAc receptors: relatively simple transmitter -gated ion channels? *Trends Pharmacol Sci* **17**(9): 319-323.

Johnston GA (2002). Medicinal chemistry and molecular pharmacology of GABA(C) receptors. *Curr Top Med Chem* **2**(8): 903-913.

Johnston GA, Curtis DR, Beart PM, Game CJ, McCulloch RM, Twitchin B (1975). Cis- and trans-4-aminocrotonic acid as GABA analogues of restricted conformation. *J Neurochem* **24**(1): 157-160.

Johnston GA, Curtis DR, De Groat WC, Duggan AW (1968). Central actions of ibotenic acid and muscimol. *Biochem Pharmacol* **17**(12): 2488-2489.

Jones A, Korpi ER, McKernan RM, Pelz R, Nusser Z, Makela R, *et al.* (1997). Ligand-gated ion channel subunit partnerships: $GABA_A$ receptor alpha6 subunit gene inactivation inhibits delta subunit expression. *J Neurosci* **17**(4): 1350-1362.

Kao PN, Karlin A (1986). Acetylcholine receptor binding site contains a disulfide cross-link between adjacent half-cystinyl residues. *J Biol Chem* **261**(18): 8085-8088.

Karim N, Curmi J, Gavande N, Johnston GA, Hanrahan JR, Tierney ML, *et al.* (2011a). 2'-Methoxy-6-methylflavone: A novel anxiolytic and sedative with subtype selective activating and modulating actions at GABA(A) receptors. *Br J Pharmacol.*

Karim N, Gavande N, Wellendorph P, Johnston GA, Hanrahan JR, Chebib M (2011b). 3-Hydroxy-2'-methoxy-6-methylflavone: a potent anxiolytic with a unique selectivity profile at GABA(A) receptor subtypes. *Biochem Pharmacol* **82**(12): 1971-1983.

Kash TL, Jenkins A, Kelley JC, Trudell JR, Harrison NL (2003). Coupling of agonist binding to channel gating in the GABA(A) receptor. *Nature* **421**(6920): 272-275.

Kash TL, Trudell JR, Harrison NL (2004). Structural elements involved in activation of the gamma-aminobutyric acid type A ($GABA_A$) receptor. *Biochem Soc Trans* **32**(Pt3): 540-546.

Katayama Y, Mori A (1977). Inhibitory action of (3*R*)-(−)-4-amino-3-hydroxybutanoic acid on *N*-amidinobenzamide induced seizure activity in cat brain. *IRCS Med Sci Nerv Syst Pharmacol Physiol* **5**: 437.

Kelley SP, Dunlop JI, Kirkness EF, Lambert JJ, Peters JA (2003). A cytoplasmic region determines single-channel conductance in 5-HT_3 receptors. *Nature* **424**(6946): 321-324.

Kellis JT, Jr., Nyberg K, Sali D, Fersht AR (1988). Contribution of hydrophobic interactions to protein stability. *Nature* **333**(6175): 784-786.

Keramidas A, Moorhouse AJ, Schofield PR, Barry PH (2004). Ligand-gated ion channels: mechanisms underlying ion selectivity. *Prog Biophys Mol Biol* **86**(2): 161-204.

Kerr DI, Ong J, Prager RH, Gynther BD, Curtis DR (1987). Phaclofen: a peripheral and central baclofen antagonist. *Brain Res* **405**(1): 150-154.

Kitamura K, Hausser M (2011). Dendritic calcium signaling triggered by spontaneous and sensory-evoked climbing fiber input to cerebellar Purkinje cells in vivo. *J Neurosci* **31**(30): 10847-10858.

Kjaer M, Nielsen H (1983). The analgesic effect of the GABA-agonist THIP in patients with chronic pain of malignant origin. A phase-1-2 study. *Br J Clin Pharmacol* **16**(5): 477-485.

Konno T, Busch C, Von Kitzing E, Imoto K, Wang F, Nakai J, *et al.* (1991). Rings of anionic amino acids as structural determinants of ion selectivity in the acetylcholine receptor channel. *Proc Biol Sci* **244**(1310): 69-79.

Kopp Lugli A, Yost CS, Kindler CH (2009). Anaesthetic mechanisms: update on the challenge of unravelling the mystery of anaesthesia. *Eur J Anaesthesiol* **26**(10): 807-820.

Kracun S, Harkness PC, Gibb AJ, Millar NS (2008). Influence of the M3-M4 intracellular domain upon nicotinic acetylcholine receptor assembly, targeting and function. *Br J Pharmacol* **153**(7): 1474-1484.

Krasowski MD, Koltchine VV, Rick CE, Ye Q, Finn SE, Harrison NL (1998). Propofol and other intravenous anesthetics have sites of action on the gamma-aminobutyric acid type A receptor distinct from that for isoflurane. *Mol Pharmacol* **53**(3): 530-538.

Krogsgaard-Larsen P, Frolund B, Jorgensen FS, Schousboe A (1994). $GABA_A$ receptor agonists, partial agonists, and antagonists. Design and therapeutic prospects. *J Med Chem* **37**(16): 2489-2505.

Krogsgaard-Larsen P, Frolund B, Liljefors T (2006). GABA(A) agonists and partial agonists: THIP (Gaboxadol) as a non-opioid analgesic and a novel type of hypnotic. *Adv Pharmacol* **54:** 53-71.

Krogsgaard-Larsen P, Nielsen L, Falch E, Curtis DR (1985). GABA agonists. Resolution, absolute stereochemistry, and enantioselectivity of (S)-(+)- and (R)-(-)-dihydromuscimol. *J Med Chem* **28**(11): 1612-1617.

Kulik A, Vida I, Fukazawa Y, Guetg N, Kasugai Y, Marker CL, *et al.* (2006). Compartment-dependent colocalization of Kir3.2-containing K+ channels and $GABA_B$ receptors in hippocampal pyramidal cells. *J Neurosci* **26**(16): 4289-4297.

Kulik A, Vida I, Lujan R, Haas CA, Lopez-Bendito G, Shigemoto R, *et al.* (2003). Subcellular localization of metabotropic GABA(B) receptor subunits GABA(B1a/b) and GABA(B2) in the rat hippocampus. *J Neurosci* **23**(35): 11026-11035.

Kumar RJ, Chebib M, Hibbs DE, Kim HL, Johnston GA, Salam NK, *et al.* (2008). Novel gamma-aminobutyric acid rho1 receptor antagonists; synthesis, pharmacological activity and structure-activity relationships. *J Med Chem* **51**(13): 3825-3840.

Kunishima N, Shimada Y, Tsuji Y, Sato T, Yamamoto M, Kumasaka T, *et al.* (2000). Structural basis of glutamate recognition by a dimeric metabotropic glutamate receptor. *Nature* **407**(6807): 971-977.

Kusama T, Spivak CE, Whiting P, Dawson VL, Schaeffer JC, Uhl GR (1993a). Pharmacology of GABA rho 1 and GABA alpha/beta receptors expressed in Xenopus oocytes and COS cells. *Br J Pharmacol* **109**(1): 200-206.

Kusama T, Wang TL, Guggino WB, Cutting GR, Uhl GR (1993b). GABA rho 2 receptor pharmacological profile: GABA recognition site similarities to rho 1. *Eur J Pharmacol* **245**(1): 83-84.

Lambert JJ, Belelli D, Hill-Venning C, Peters JA (1995). Neurosteroids and $GABA_A$ receptor function. *Trends Pharmacol Sci* **16**(9): 295-303.

Langosch D, Thomas L, Betz H (1988). Conserved quaternary structure of ligand-gated ion channels: the postsynaptic glycine receptor is a pentamer. *Proc Natl Acad Sci U S A* **85**(19): 7394-7398.

Lape R, Colquhoun D, Sivilotti LG (2008). On the nature of partial agonism in the nicotinic receptor superfamily. *Nature* **454**(7205): 722-727.

Laposky AD, Homanics GE, Basile A, Mendelson WB (2001). Deletion of the GABA(A) receptor beta 3 subunit eliminates the hypnotic actions of oleamide in mice. *Neuroreport* **12**(18): 4143-4147.

Laurie DJ, Seeburg PH, Wisden W (1992). The distribution of 13 GABAA receptor subunit mRNAs in the rat brain. II. Olfactory bulb and cerebellum. *J Neurosci* **12**(3): 1063-1076.

LeDoux JE (2000). Emotion circuits in the brain. *Annu Rev Neurosci* **23**: 155-184.

Lee DJ, Keramidas A, Moorhouse AJ, Schofield PR, Barry PH (2003). The contribution of proline 250 (P-2') to pore diameter and ion selectivity in the human glycine receptor channel. *Neurosci Lett* **351**(3): 196-200.

Li P, Khatri A, Bracamontes J, Weiss DS, Steinbach JH, Akk G (2010). Site-specific fluorescence reveals distinct structural changes induced in the human rho 1 GABA receptor by inhibitory neurosteroids. *Mol Pharmacol* **77**(4): 539-546.

Locock KE, Johnston GA, Allan RD (2009). GABA analogues derived from 4-aminocyclopent-1-enecarboxylic acid. *Neurochem Res* **34**(10): 1698-1703.

Low K, Crestani F, Keist R, Benke D, Brunig I, Benson JA, *et al.* (2000). Molecular and neuronal substrate for the selective attenuation of anxiety. *Science* **290**(5489): 131-134.

Lummis SC (2009). Locating GABA in GABA receptor binding sites. *Biochem Soc Trans* **37**(Pt 6): 1343-1346.

Lummis SC, D LB, Harrison NJ, Lester HA, Dougherty DA (2005). A cation-pi binding interaction with a tyrosine in the binding site of the $GABA_C$ receptor. *Chem Biol* **12**(9): 993-997.

Lummis SCR, Harrison NJ, Wang J, Ashby JA, Millen KS, Beene DL, *et al.* (2011). Multiple Tyrosine Residues Contribute to GABA Binding in the $GABA_C$ Receptor Binding Pocket. *ACS Chemical Neuroscience*. DOI: 10.1021/cn200103n

Madsen C, Jensen AA, Liljefors T, Kristiansen U, Nielsen B, Hansen CP, *et al.* (2007). 5-Substituted imidazole-4-acetic acid analogues: synthesis, modeling, and pharmacological characterization of a series of novel gamma-aminobutyric acid(C) receptor agonists. *J Med Chem* **50**(17): 4147-4161.

Malitschek B, Schweizer C, Keir M, Heid J, Froestl W, Mosbacher J, *et al.* (1999). The N-terminal domain of gamma-aminobutyric Acid(B) receptors is sufficient to specify agonist and antagonist binding. *Mol Pharmacol* **56**(2): 448-454.

Manach C, Scalbert A, Morand C, Remesy C, Jimenez L (2004). Polyphenols: food sources and bioavailability. *Am J Clin Nutr* **79**(5): 727-747.

Manning JP, Richards DA, Bowery NG (2003). Pharmacology of absence epilepsy. *Trends Pharmacol Sci* **24**(10): 542-549.

Maren S, Quirk GJ (2004). Neuronal signalling of fear memory. *Nat Rev Neurosci* **5**(11): 844-852.

Margeta-Mitrovic M, Jan YN, Jan LY (2000). A trafficking checkpoint controls GABA(B) receptor heterodimerization. *Neuron* **27**(1): 97-106.

Martin IL, Lattmann E (1999). Benzodiazepine recognition site ligands and $GABA_A$ receptors. *Expert Opin. Ther. Pat.* **9**(Copyright (C) 2012 American Chemical Society (ACS). All Rights Reserved.): 1347-1358.

Mathers DA, Barker JL (1980). (-)Pentobarbital opens ion channels of long duration in cultured mouse spinal neurons. *Science* **209**(4455): 507-509.

Matsushita S, Nakata H, Kubo Y, Tateyama M (2010). Ligand-induced rearrangements of the GABA(B) receptor revealed by fluorescence resonance energy transfer. *J Biol Chem* **285**(14): 10291-10299.

Maurel D, Comps-Agrar L, Brock C, Rives ML, Bourrier E, Ayoub MA, *et al.* (2008). Cell-surface protein-protein interaction analysis with time-resolved FRET and snap-tag technologies: application to GPCR oligomerization. *Nat Methods* **5**(6): 561-567.

McCall MA, Lukasiewicz PD, Gregg RG, Peachey NS (2002). Elimination of the rho1 subunit abolishes GABA(C) receptor expression and alters visual processing in the mouse retina. *J Neurosci* **22**(10): 4163-4174.

McKernan RM, Rosahl TW, Reynolds DS, Sur C, Wafford KA, Atack JR, *et al.* (2000). Sedative but not anxiolytic properties of benzodiazepines are mediated by the GABA(A) receptor alpha1 subtype. *Nat Neurosci* **3**(6): 587-592.

Meeks JP, Holy TE (2009). An ex vivo preparation of the intact mouse vomeronasal organ and accessory olfactory bulb. *J Neurosci Methods* **177**(2): 440-447.

Menon-Johansson AS, Berrow N, Dolphin AC (1993). G(o) transduces $GABA_B$-receptor modulation of N-type calcium channels in cultured dorsal root ganglion neurons. *Pflugers Arch* **425**(3-4): 335-343.

Mercado J, Czajkowski C (2006). Charged residues in the alpha1 and beta2 pre-M1 regions involved in $GABA_A$ receptor activation. *J Neurosci* **26**(7): 2031-2040.

Mewett KN, Fernandez SP, Pasricha AK, Pong A, Devenish SO, Hibbs DE, *et al.* (2009). Synthesis and biological evaluation of flavan-3-ol derivatives as positive modulators of $GABA_A$ receptors. *Bioorg Med Chem* **17**(20): 7156-7173.

Mihalek RM, Banerjee PK, Korpi ER, Quinlan JJ, Firestone LL, Mi ZP, *et al.* (1999). Attenuated sensitivity to neuroactive steroids in gamma-aminobutyrate type A receptor delta subunit knockout mice. *Proc Natl Acad Sci U S A* **96**(22): 12905-12910.

Mihic SJ, Ye Q, Wick MJ, Koltchine VV, Krasowski MD, Finn SE, *et al.* (1997). Sites of alcohol and volatile anaesthetic action on GABA(A) and glycine receptors. *Nature* **389**(6649): 385-389.

Miller PS, Smart TG (2010). Binding, activation and modulation of Cys-loop receptors. *Trends Pharmacol Sci* **31**(4): 161-174.

Miyazawa A, Fujiyoshi Y, Stowell M, Unwin N (1999). Nicotinic acetylcholine receptor at 4.6 A resolution: transverse tunnels in the channel wall. *J Mol Biol* **288**(4): 765-786.

Miyazawa A, Fujiyoshi Y, Unwin N (2003). Structure and gating mechanism of the acetylcholine receptor pore. *Nature* **423**(6943): 949-955.

Mody I, Pearce RA (2004). Diversity of inhibitory neurotransmission through GABA(A) receptors. *Trends Neurosci* **27**(9): 569-575.

Murata Y, Woodward RM, Miledi R, Overman LE (1996). The first selective antagonist for a $GABA_C$ receptor. *Bioorganic & Medicinal Chemistry Letters* **6**(17): 2073-2076.

Nakao J, Hasegawa T, Hashimoto H, Noto T, Nakajima T (1991). Formation of GABOB from 2-hydroxyputrescine and its anticonvulsant effect. *Pharmacol Biochem Behav* **40**(2): 359-366.

Nayeem N, Green TP, Martin IL, Barnard EA (1994). Quaternary structure of the native GABAA receptor determined by electron microscopic image analysis. *J Neurochem* **62**(2): 815-818.

Ng CK, Kim HL, Gavande N, Yamamoto I, Kumar RJ, Mewett KN, *et al.* (2011). Medicinal chemistry of rho GABA(C) receptors. *Future Med Chem* **3**(2): 197-209.

Noto T, Hasegawa T, Nakao J, Kamimura H, Harada H, Nakajima T (1988). Formation of gamma-amino-beta-hydroxybutyric acid from 2-hydroxyputrescine in rat brain. *J Neurochem* **51**(2): 548-551.

Nusser Z, Roberts JD, Baude A, Richards JG, Somogyi P (1995). Relative densities of synaptic and extrasynaptic $GABA_A$ receptors on cerebellar granule cells as determined by a quantitative immunogold method. *J Neurosci* **15**(4): 2948-2960.

Nusser Z, Sieghart W, Somogyi P (1998). Segregation of different $GABA_A$ receptors to synaptic and extrasynaptic membranes of cerebellar granule cells. *J Neurosci* **18**(5): 1693-1703.

O'Hagan D (2011). 3-fluoro-GABA enantiomers: exploring the conformation of GABA binding to $GABA_A$ receptors and GABA aminotransferase. *Future Med Chem* **3**(2): 189-195.

O'Hagan D (2008). Understanding organofluorine chemistry. An introduction to the C-F bond. *Chem Soc Rev* **37**(2): 308-319.

Ogurusu T, Yanagi K, Watanabe M, Fukaya M, Shingai R (1999). Localization of GABA receptor rho 2 and rho 3 subunits in rat brain and functional expression of homooligomeric rho 3 receptors and heterooligomeric rho 2 rho 3 receptors. *Receptors Channels* **6**(6): 463-475.

Olsen RW, Sieghart W (2008). International Union of Pharmacology. LXX. Subtypes of gamma-aminobutyric acid(A) receptors: classification on the basis of subunit composition, pharmacology, and function. Update. *Pharmacol Rev* **60**(3): 243-260.

Ong J, Bexis S, Marino V, Parker DA, Kerr DI, Froestl W (2001). Comparative activities of the enantiomeric GABA(B) receptor agonists CGP 44532 and 44533 in central and peripheral tissues. *Eur J Pharmacol* **412**(1): 27-37.

Ortells MO, Lunt GG (1995). Evolutionary history of the ligand-gated ion-channel superfamily of receptors. *Trends Neurosci* **18**(3): 121-127.

Osolodkin DI, Chupakhin VI, Palyulin VA, Zefirov NS (2007). Modeling and analysis of ligand-receptor interactions in the GABAc receptor. *Dokl Biochem Biophys* **412:** 25-28.

Padgett CL, Hanek AP, Lester HA, Dougherty DA, Lummis SC (2007). Unnatural amino acid mutagenesis of the GABA(A) receptor binding site residues reveals a novel cation-pi interaction between GABA and beta 2Tyr97. *J Neurosci* **27**(4)**:** 886-892.

Padgett CL, Slesinger PA (2010). $GABA_B$ receptor coupling to G-proteins and ion channels. *Adv Pharmacol* **58:** 123-147.

Pakula AA, Sauer RT (1989). Genetic analysis of protein stability and function. *Annu Rev Genet* **23:** 289-310.

Pan J, Chen Q, Willenbring D, Yoshida K, Tillman T, Kashlan OB*, et al.* (2012). Structure of the pentameric ligand-gated ion channel ELIC cocrystallized with its competitive antagonist acetylcholine. *Nat Commun* **3:** 714.

Parker I, Gundersen CB, Miledi R (1986). Actions of pentobarbital on rat brain receptors expressed in *Xenopus* oocytes. *J Neurosci* **6**(8)**:** 2290-2297.

Persohn E, Malherbe P, Richards JG (1992). Comparative molecular neuroanatomy of cloned $GABA_A$ receptor subunits in the rat CNS. *J Comp Neurol* **326**(2)**:** 193-216.

Peters JA, Cooper MA, Carland JE, Livesey MR, Hales TG, Lambert JJ (2010). Novel structural determinants of single channel conductance and ion selectivity in 5-hydroxytryptamine type 3 and nicotinic acetylcholine receptors. *J Physiol* **588**(Pt 4)**:** 587-596.

Pin JP, Comps-Agrar L, Maurel D, Monnier C, Rives ML, Trinquet E*, et al.* (2009). G-protein-coupled receptor oligomers: two or more for what? Lessons from mGlu and GABAB receptors. *J Physiol* **587**(Pt 22)**:** 5337-5344.

Pin JP, Galvez T, Prezeau L (2003). Evolution, structure, and activation mechanism of family 3/C G-protein-coupled receptors. *Pharmacol Ther* **98**(3)**:** 325-354.

Pirker S, Schwarzer C, Wieselthaler A, Sieghart W, Sperk G (2000). GABA(A) receptors: immunocytochemical distribution of 13 subunits in the adult rat brain. *Neuroscience* **101**(4): 815-850.

Pistis M, Belelli D, Peters JA, Lambert JJ (1997). The interaction of general anaesthetics with recombinant $GABA_A$ and glycine receptors expressed in *Xenopus* laevis oocytes: a comparative study. *Br J Pharmacol* **122**(8): 1707-1719.

Pless SA, Lynch JW (2008). Illuminating the structure and function of Cys-loop receptors. *Clin Exp Pharmacol Physiol* **35**(10): 1137-1142.

Pless SA, Lynch JW (2009). Ligand-specific conformational changes in the alpha1 glycine receptor ligand-binding domain. *J Biol Chem* **284**(23): 15847-15856.

Popot JL, Changeux JP (1984). Nicotinic receptor of acetylcholine: structure of an oligomeric integral membrane protein. *Physiol Rev* **64**(4): 1162-1239.

Purohit P, Auerbach A (2007a). Acetylcholine receptor gating at extracellular transmembrane domain interface: the "pre-M1" linker. *J Gen Physiol* **130**(6): 559-568.

Purohit P, Auerbach A (2007b). Acetylcholine receptor gating: movement in the alpha-subunit extracellular domain. *J Gen Physiol* **130**(6): 569-579.

Purohit P, Mitra A, Auerbach A (2007c). A stepwise mechanism for acetylcholine receptor channel gating. *Nature* **446**(7138): 930-933.

Qian H, Ripps H (2009). Focus on molecules: the $GABA_C$ receptor. *Exp Eye Res* **88**(6): 1002-1003.

Quirk K, Whiting PJ, Ragan CI, McKernan RM (1995). Characterisation of delta-subunit containing $GABA_A$ receptors from rat brain. *Eur J Pharmacol* **290**(3): 175-181.

Ramirez OA, Vidal RL, Tello JA, Vargas KJ, Kindler S, Hartel S, *et al.* (2009). Dendritic assembly of heteromeric gamma-aminobutyric acid type B receptor subunits in hippocampal neurons. *J Biol Chem* **284**(19): 13077-13085.

Rayes D, De Rosa MJ, Sine SM, Bouzat C (2009). Number and locations of agonist binding sites required to activate homomeric Cys-loop receptors. *J Neurosci* **29**(18): 6022-6032.

Reyes-Ruiz JM, Ochoa-de la Paz LD, Martinez-Torres A, Miledi R (2010). Functional impact of serial deletions at the C-terminus of the human GABArho1 receptor. *Biochim Biophys Acta* **1798**(5): 1002-1007.

Reynolds DS, Rosahl TW, Cirone J, O'Meara GF, Haythornthwaite A, Newman RJ, *et al.* (2003). Sedation and anesthesia mediated by distinct GABA(A) receptor isoforms. *J Neurosci* **23**(24): 8608-8617.

Robbins MJ, Calver AR, Filippov AK, Hirst WD, Russell RB, Wood MD, *et al.* (2001). GABA(B2) is essential for g-protein coupling of the GABA(B) receptor heterodimer. *J Neurosci* **21**(20): 8043-8052.

Roberts E, Frankel S (1950). gamma-Aminobutyric acid in brain: its formation from glutamic acid. *J Biol Chem* **187**(1): 55-63.

Roberts E, Krause DN, Wong E, Mori A (1981). Different efficacies of d- and l-gamma-amino-beta-hydroxybutyric acids in GABA receptor and transport test systems. *J Neurosci* **1**(2): 132-140.

Rondard P, Goudet C, Kniazeff J, Pin JP, Prezeau L (2011). The complexity of their activation mechanism opens new possibilities for the modulation of mGlu and $GABA_B$ class C G protein-coupled receptors. *Neuropharmacology* **60**(1): 82-92.

Rozzo A, Armellin M, Franzot J, Chiaruttini C, Nistri A, Tongiorgi E (2002). Expression and dendritic mRNA localization of $GABA_C$ receptor rho1 and rho2 subunits in developing rat brain and spinal cord. *Eur J Neurosci* **15**(11): 1747-1758.

Rudolph U, Crestani F, Benke D, Brunig I, Benson JA, Fritschy JM, *et al.* (1999). Benzodiazepine actions mediated by specific gamma-aminobutyric acid(A) receptor subtypes. *Nature* **401**(6755): 796-800.

Rudolph U, Crestani F, Mohler H (2001). GABA(A) receptor subtypes: dissecting their pharmacological functions. *Trends Pharmacol Sci* **22**(4): 188-194.

Rudolph U, Knoflach F (2011). Beyond classical benzodiazepines: novel therapeutic potential of $GABA_A$ receptor subtypes. *Nat Rev Drug Discov* **10**(9): 685-697.

Rudolph U, Mohler H (2004). Analysis of $GABA_A$ receptor function and dissection of the pharmacology of benzodiazepines and general anesthetics through mouse genetics. *Annu Rev Pharmacol Toxicol* **44**: 475-498.

Sandberg WS, Terwilliger TC (1989). Influence of interior packing and hydrophobicity on the stability of a protein. *Science* **245**(4913): 54-57.

Schlicker K, McCall MA, Schmidt M (2009). GABAC receptor-mediated inhibition is altered but not eliminated in the superior colliculus of GABAC rho1 knockout mice. *J Neurophysiol* **101**(6): 2974-2983.

Schofield PR, Darlison MG, Fujita N, Burt DR, Stephenson FA, Rodriguez H, *et al.* (1987). Sequence and functional expression of the GABA A receptor shows a ligand-gated receptor super-family. *Nature* **328**(6127): 221-227.

Sedelnikova A, Smith CD, Zakharkin SO, Davis D, Weiss DS, Chang Y (2005). Mapping the rho1 GABA(C) receptor agonist binding pocket. Constructing a complete model. *J Biol Chem* **280**(2): 1535-1542.

Shimada S, Cutting G, Uhl GR (1992). gamma-Aminobutyric acid A or C receptor? gamma-Aminobutyric acid rho 1 receptor RNA induces bicuculline-, barbiturate-, and benzodiazepine-insensitive gamma-aminobutyric acid responses in Xenopus oocytes. *Mol Pharmacol* **41**(4): 683-687.

Sieghart W (2006). Structure, pharmacology, and function of $GABA_A$ receptor subtypes. *Adv Pharmacol* **54:** 231-263.

Sieghart W, Sperk G (2002). Subunit composition, distribution and function of GABA(A) receptor subtypes. *Curr Top Med Chem* **2**(8): 795-816.

Siegwart R, Jurd R, Rudolph U (2002). Molecular determinants for the action of general anesthetics at recombinant alpha(2)beta(3)gamma(2)gamma-aminobutyric acid(A) receptors. *J Neurochem* **80**(1): 140-148.

Smit AB, Syed NI, Schaap D, van Minnen J, Klumperman J, Kits KS, *et al.* (2001). A glia-derived acetylcholine-binding protein that modulates synaptic transmission. *Nature* **411**(6835): 261-268.

Smith GB, Olsen RW (1995). Functional domains of $GABA_A$ receptors. *Trends Pharmacol Sci* **16**(5): 162-168.

Somogyi P, Tamas G, Lujan R, Buhl EH (1998). Salient features of synaptic organisation in the cerebral cortex. *Brain Res Brain Res Rev* **26**(2-3): 113-135.

Sonavane S, Chakrabarti P (2008). Cavities and atomic packing in protein structures and interfaces. *PLoS Comput Biol* **4**(9): e1000188.

Sperk G, Schwarzer C, Tsunashima K, Fuchs K, Sieghart W (1997). GABA(A) receptor subunits in the rat hippocampus I: immunocytochemical distribution of 13 subunits. *Neuroscience* **80**(4): 987-1000.

Spigelman I, Li Z, Liang J, Cagetti E, Samzadeh S, Mihalek RM, *et al.* (2003). Reduced inhibition and sensitivity to neurosteroids in hippocampus of mice lacking the GABA(A) receptor delta subunit. *J Neurophysiol* **90**(2): 903-910.

Stell BM, Brickley SG, Tang CY, Farrant M, Mody I (2003). Neuroactive steroids reduce neuronal excitability by selectively enhancing tonic inhibition mediated by delta subunit-containing $GABA_A$ receptors. *Proc Natl Acad Sci U S A* **100**(24): 14439-14444.

Stone RA, Liu J, Sugimoto R, Capehart C, Zhu X, Pendrak K (2003). GABA, experimental myopia, and ocular growth in chick. *Invest Ophthalmol Vis Sci* **44**(9): 3933-3946.

Sun A, Lankin DC, Hardcastle K, Snyder JP (2005). 3-Fluoropiperidines and N-methyl-3-fluoropiperidinium salts: the persistence of axial fluorine. *Chemistry* **11**(Copyright (C) 2012 U.S. National Library of Medicine.): 1579-1591.

Sur C, Farrar SJ, Kerby J, Whiting PJ, Atack JR, McKernan RM (1999). Preferential coassembly of alpha4 and delta subunits of the gamma-aminobutyric acidA receptor in rat thalamus. *Mol Pharmacol* **56**(1): 110-115.

Sur C, Wafford KA, Reynolds DS, Hadingham KL, Bromidge F, Macaulay A, *et al.* (2001). Loss of the major GABA(A) receptor subtype in the brain is not lethal in mice. *J Neurosci* **21**(10): 3409-3418.

Takehara A, Hosokawa M, Eguchi H, Ohigashi H, Ishikawa O, Nakamura Y, *et al.* (2007). Gamma-aminobutyric acid (GABA) stimulates pancreatic cancer growth through overexpressing $GABA_A$ receptor pi subunit. *Cancer Res* **67**(20): 9704-9712.

Taly A, Corringer PJ, Guedin D, Lestage P, Changeux JP (2009). Nicotinic receptors: allosteric transitions and therapeutic targets in the nervous system. *Nat Rev Drug Discov* **8**(9): 733-750.

Tatebayashi H, Ogata N (1992). GABAB-mediated modulation of the voltage-gated Ca2+ channels. *Gen Pharmacol* **23**(3): 309-316.

Tateyama M, Abe H, Nakata H, Saito O, Kubo Y (2004). Ligand-induced rearrangement of the dimeric metabotropic glutamate receptor 1alpha. *Nat Struct Mol Biol* **11**(7): 637-642.

Tateyama M, Kubo Y (2006). Dual signaling is differentially activated by different active states of the metabotropic glutamate receptor 1alpha. *Proc Natl Acad Sci U S A* **103**(4): 1124-1128.

Thompson AJ, Lester HA, Lummis SC (2010). The structural basis of function in Cys-loop receptors. *Q Rev Biophys* **43**(4): 449-499.

Torres VI, Weiss DS (2002). Identification of a tyrosine in the agonist binding site of the homomeric rho1 gamma-aminobutyric acid (GABA) receptor that, when mutated, produces spontaneous opening. *J Biol Chem* **277**(46): 43741-43748.

Tretter V, Ehya N, Fuchs K, Sieghart W (1997). Stoichiometry and assembly of a recombinant GABAA receptor subtype. *J Neurosci* **17**(8): 2728-2737.

Unwin N (1993). Nicotinic acetylcholine receptor at 9 A resolution. *J Mol Biol* **229**(4): 1101-1124.

Unwin N (2005). Refined structure of the nicotinic acetylcholine receptor at 4A resolution. *J Mol Biol* **346**(4): 967-989.

Vien J, Duke RK, Mewett KN, Johnston GA, Shingai R, Chebib M (2002). trans-4-Amino-2-methylbut-2-enoic acid (2-MeTACA) and (+/-)-trans-2-aminomethylcyclopropanecarboxylic acid ((+/-)-TAMP) can differentiate rat rho3 from human rho1 and rho2 recombinant GABA(C) receptors. *Br J Pharmacol* **135**(4): 883-890.

Vigh J, Vickers E, von Gersdorff H (2011). Light-evoked lateral GABAergic inhibition at single bipolar cell synaptic terminals is driven by distinct retinal microcircuits. *J Neurosci* **31**(44): 15884-15893.

Villmann C, Oertel J, Ma-Hogemeier ZL, Hollmann M, Sprengel R, Becker K, *et al.* (2009). Functional complementation of Glra1(spd-ot), a glycine receptor subunit mutant, by independently expressed C-terminal domains. *J Neurosci* **29**(8): 2440-2452.

Wagner DA, Czajkowski C (2001). Structure and dynamics of the GABA binding pocket: A narrowing cleft that constricts during activation. *J Neurosci* **21**(1): 67-74.

Wang DT, Hill AP, Mann SA, Tan PS, Vandenberg JI (2011). Mapping the sequence of conformational changes underlying selectivity filter gating in the K(v)11.1 potassium channel. *Nat Struct Mol Biol* **18**(1): 35-41.

Wang Q, Pless SA, Lynch JW (2010). Ligand- and subunit-specific conformational changes in the ligand-binding domain and the TM2-TM3 linker of $\alpha1$ $\beta2$ $\gamma2$ $GABA_A$ receptors. *J Biol Chem* **285**(51): 40373-40386.

Wegelius K, Pasternack M, Hiltunen JO, Rivera C, Kaila K, Saarma M, *et al.* (1998). Distribution of GABA receptor rho subunit transcripts in the rat brain. *Eur J Neurosci* **10**(1): 350-357.

Wei W, Zhang N, Peng Z, Houser CR, Mody I (2003). Perisynaptic localization of delta subunit-containing GABA(A) receptors and their activation by GABA spillover in the mouse dentate gyrus. *J Neurosci* **23**(33): 10650-10661.

Wermuth CG, Bourguignon JJ, Schlewer G, Gies JP, Schoenfelder A, Melikian A, *et al.* (1987). Synthesis and structure-activity relationships of a series of aminopyridazine derivatives of gamma-aminobutyric acid acting as selective GABA-A antagonists. *J Med Chem* **30**(2): 239-249.

Whiting PJ (2003). GABA-A receptor subtypes in the brain: a paradigm for CNS drug discovery? *Drug Discov Today* **8**(10): 445-450.

Williams BM, Temburni MK, Levey MS, Bertrand S, Bertrand D, Jacob MH (1998). The long internal loop of the alpha 3 subunit targets nAChRs to subdomains within individual synapses on neurons in vivo. *Nat Neurosci* **1**(7): 557-562.

Wisden W, Laurie DJ, Monyer H, Seeburg PH (1992). The distribution of 13 $GABA_A$ receptor subunit mRNAs in the rat brain. I. Telencephalon, diencephalon, mesencephalon. *J Neurosci* **12**(3): 1040-1062.

Woodward RM, Polenzani L, Miledi R (1993). Characterization of bicuculline/baclofen-insensitive (rho-like) gamma-aminobutyric acid receptors expressed in Xenopus oocytes. II. Pharmacology of gamma-aminobutyric acidA and gamma-aminobutyric acidB receptor agonists and antagonists. *Mol Pharmacol* **43**(4): 609-625.

Xie A, Yan J, Yue L, Feng F, Mir F, Abdel-Halim H, *et al.* (2011). 2-Aminoethyl methylphosphonate, a potent and rapidly acting antagonist of GABA(A)-rho1 receptors. *Mol Pharmacol* **80**(6): 965-978.

Yamamoto I, Absalom N, Carland JE, Doddareddy MR, Gavande N, Johnston GAR, *et al.* (2012a). Differentiating Enantioselective Actions of GABOB: A Possible Role for

Threonine 244 in the Binding Site of $GABA_C$ ρ_1 Receptors. *ACS Chemical Neuroscience* DOI: 10.1021/cn3000229.

Yamamoto I, Carland JE, Locock K, Gavande N, Absalom N, Hanrahan JR, *et al.* (2012b). Structurally Diverse GABA Antagonists Interact Differently with Open and Closed Conformational States of the ρ_1 Receptor. *ACS Chemical Neuroscience* DOI: 10.1021/cn200121r.

Yamamoto I, Deniau GP, Gavande N, Chebib M, Johnston GA, O'Hagan D (2011a). Agonist responses of (R)- and (S)-3-fluoro-gamma-aminobutyric acids suggest an enantiomeric fold for GABA binding to GABA(C) receptors. *Chem Commun (Camb)* **47**(28): 7956-7958.

Yamamoto I, Jordan MJ, Gavande N, Doddareddy MR, Chebib M, Hunter L (2011b). The enantiomers of syn-2,3-difluoro-4-aminobutyric acid elicit opposite responses at the GABA(C) receptor. *Chem Commun (Camb)* **48**: 829-931.

Yang J, Cheng Q, Takahashi A, Goubaeva F (2006). Kinetic properties of GABA rho1 homomeric receptors expressed in HEK293 cells. *Biophys J* **91**(6): 2155-2162.

Yee BK, Keist R, von Boehmer L, Studer R, Benke D, Hagenbuch N, *et al.* (2005). A schizophrenia-related sensorimotor deficit links alpha 3-containing $GABA_A$ receptors to a dopamine hyperfunction. *Proc Natl Acad Sci U S A* **102**(47): 17154-17159.

Zamyatnin AA (1972). Protein volume in solution. *Prog Biophys Mol Biol* **24:** 107-123.

Zhang J, Xue F, Chang Y (2009). Agonist- and antagonist-induced conformational changes of loop F and their contributions to the rho1 GABA receptor function. *J Physiol* **587**(Pt 1): 139-153.

Zhang J, Xue F, Chang Y (2008). Structural determinants for antagonist pharmacology that distinguish the rho1 GABAC receptor from $GABA_A$ receptors. *Mol Pharmacol* **74**(4): 941-951.

Zhang J, Xue F, Whiteaker P, Li C, Wu W, Shen B, *et al.* (2011). Desensitization of α7 Nicotinic Receptor Is Governed by Coupling Strength Relative to Gate Tightness. *J Biol Chem* **286**(28): 25331-25340.

Zhou Y, Pearson JE, Auerbach A (2005). Phi-value analysis of a linear, sequential reaction mechanism: theory and application to ion channel gating. *Biophys J* **89**(6): 3680-3685.